Congenital Disorders of Glycosylation and TMEM165 : A new player in proteoglycan synthesis

Sajida Khan

University of Lorraine- Faculty of Sciences and Technology

Doctoral School BioSE (Biology-Health-Environment)

Thesis

Presented for the title of

Doctor of Life and Health Sciences

from the University of Lorraine

By

Sajida Khan

Congenital Disorders of Glycosylation and TMEM165: A new player in proteoglycan synthesis

Public defence on 16th October 2020

Jury members:

Reviewers :	**Dr. Franck Verrecchia**	Director of Research INSERM, University of Nantes
	Dr. Catherine Baugé	MC-University of Caen Normandie
Examiners :	**Dr. François Foulquier**	Director of Research CNRS, University of Lille
	Dr. Lydia Barré	Ingénieur d'Etude, University of Lorraine (co supervisor)
	Dr. Mohamed Ouzzine	Director of Research INSERM (Supervisor)

Laboratory : IMoPA (Ingénierie Moléculaire et Physiopathologie Articulaire) *UMR 7365 CNRS-Université de Lorraine ; 9, Avenue de la Forêt de Haye, CS 50184, 54505 Vandœuvre-lès-Nancy, FRANCE*

Université de Lorraine- Faculté des sciences et technologies

École doctorale BioSE

Thèse

Présenté pour l'obtention du titre de

DOCTEUR DE L'UNIVERSITE DE LORRAINE

Mention : 《Science de la Vie et de la Santé》

Par

Sajida Khan

Troubles Congénitaux de la Glycosylation et TMEM165 : un nouvel acteur dans la biosynthèse des protéoglycanes

Soutenue publiquement le 16 Octobre 2020

Membres du jury :

Rapporteurs :	**Dr. Franck Verrecchia**	Directeur de Recherche INSERM, Université de Nantes
	Dr. Catherine Baugé	MC Université de Caen, Normandie
Examinateurs :	**Dr. François Foulquier**	Directeur de Recherche CNRS, Université de Lille
	Dr. Lydia Barré	IE-Université de Lorraine, (Co-Directeur de thèse)
	Dr. Mohamed Ouzzine	Directeur de Recherche INSERM Université de Lorraine (Directeur de thèse)

Laboratoire : IMoPA (Ingénierie Moléculaire et Physiopathologie Articulaire), *UMR 7365 CNRS-Université de Lorraine ; 9, Avenue de la Forêt de Haye, CS 50184, 54505 Vandœuvre-lès-Nancy, FRANCE*

To my Parents, Husband, Shahwaiz, Bhaiyya, siblings, and extended family.

Acknowledgments

First and foremost, I would like to pay sincere gratitude to my thesis director **Dr. Mohamed Ouzzine** for accepting me in his group, continuous support, patience, vast knowledge and guidance throughout my maters and PhD thesis. Special thanks to co-director of my thesis **Dr. Lydia Barré** for having faith in me and teaching me different research techniques. Without help; discussions, patience, and ideas from my thesis director and codirector of the thesis, this piece of work would not have been possible. Their guidance has helped me a lot throughout my research and stay in France.

I would also like to thank members of jury for the thesis defence **Dr. Franck Verrecchia, Dr. Catherine Baugé** and **Dr. François Foulquier** for taking time out of their busy schedules to evaluate my research work. Their suggestions and critical opinions will help me to improve quality of this work.

I express my deepest gratitude and appreciation for brother like **Irfan shaukat**, in helping me manage and settle in early days when I could not speak a single word of French. My sincere thanks to the other members of **MolCelTEG TEAM.** I will not forget the nice company of **Dima, Mahdia** and recently **Malak** especially during late hours, weekends, and holidays. We are like battle companion supporting each other. I would like to convey my gratitude and best wishes to **Xie Zhe** who has helped me learn and understand research during my master's internship. Many thanks to **Sylvie, Nick, Catherine** and **Sandrine** for helpful discussions, exchanging the smiles and offering help generously. To my office mates **Defné, Benjamin, Elise, Anne, Océane and Paul** thank you for your cheerful talks, productive discussions and for keeping the office lively.

I thank my lab fellows **Meriam, Fatouma, Reine, Maroua, David, Fréd, Alex, Stefania, Anne-Bé and Adriene** for making my stay memorable. I would also like to thank all the people of lab, who have helped me either way specially **Cecile, Marie-Hélèn, Jean Baptiste** and **Laurent**. I extend my regards to **Karine** and **Florence** for help and support in administrative tasks. I would like to thank my friends in Nancy specially **Samina**, my first ever friend in Nancy **Anaya**, **Maimuna** and my friends back in Pakistan for their love, encouragement, and generous prayers.

Special thanks are due to **Higher Education Commission (HEC) of Pakistan** for funding my PhD studies and **Campus France** for managing me during my stay in France.

I would also like to say a heartfelt thanks to my **parents, siblings, nieces,** and **my extended family** for their endless prayers, love, and utmost support through thick and thin despite the geographical distance. A simple thanks is not enough for **my eldest brother (Bhaiyya)** who has contributed a lot to where I am today, because of him I did not give up thank you **bhaiyya** for always being on my side and for your guidance throughout. I am grateful to all the praying hands for making me do it.

Finally, to my husband **Tauqir** for his unconditional love, understanding and support. I cannot thank him enough for always being by my side throughout this PhD, living every single minute of it, and without whom, I would not have had the courage to embark on this journey in the first place. I am grateful to him for taking care of Shahwaiz throughout. To my son **Shahwaiz,** I am sorry for all your sufferings and sacrifices due to my late stays at lab even on the weekends I was not available for you. Thank you, my son for welcoming me with your smile after long tiring day, your smile and hugs have been the beacon and have helped me stay strong and motivated, to me, you will always be the Centre of my world for the rest of my life.

Sajida Khan

Nancy, France

TABLE OF CONTENTS

LIST OF FIGURES

LIST OF TABLES

1 INTRODUCTION

1.1 Skeletal Development

1.1.1 Elements of Human skeletal System

Human skeleton is a highly complex, customized, and dynamic organ that serves as a body frame. The skeleton in vertebrates undergoes constant changes and regeneration. Skeletal system constitutes 15% of total body mass and preforms several structural and metabolic functions; this complex system not only provides morphological features to the body but also protects vital organs, helps controlled postures and movements, serves as house of haematopoiesis, stores minerals, and adsorbs toxins. (Lefebvre and Bhattaram 2010a)**.** In an adult skeleton there are 206 individual bones arranged in two divisions; one is axial skeleton that runs along the body's midline axis forming central core of the body consisting of 80 bones arranged in skull, hyoid, auditory ossicles, ribs, sternum and vertebral column. Whereas the second division is appendicular skeleton that forms the extremities of the arms and legs, this division is made up of 126 bones arranged in upper limbs, lower limbs, pelvic and pectoral girdle **(Figure1.1)** (Clarke 2008)

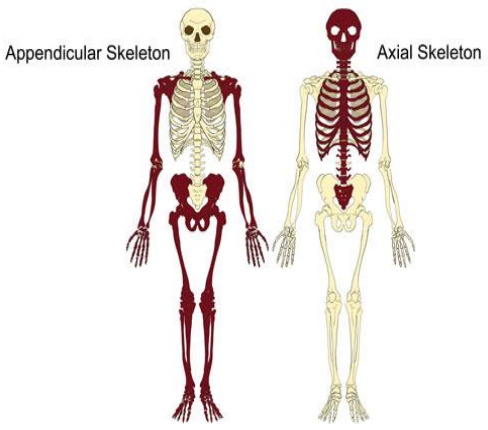

Figure 1. 1 : *Divisions of the Human skeleton: Appendicular skeleton forms extremities and axial skeleton forms central core of the body. (Adapted from: http://www.teachpe.com/anatomy/skeleton_axial.php).*

There are four (some includes joint as fifth component) basic components of skeleton in vertebrates including bones (constitute a major proportion of total mass of skeletal system), cartilage (provides strength and support), ligaments (connect bones to bones) and tendons (connect muscles to bones).

Bones and cartilage provide the framework of the skeletal system while interacting with other types of tissues during development (Kobayashi and Kronenberg 2014). Skeletogenesis or skeletal development begins at the early days of the vertebrate embryo with evolution of multipotent mesenchymal cells from ectoderm and mesoderm that migrate to specific locations in the body and undergoes skeletal fate. Most of these multipotent mesenchymal cells develop into chondrocytes (that form cartilage) and osteoblasts (bone cells), whereas some remain as mesenchymal stem cells throughout life.

1.1.1.1 Osteogenesis and Skeletal Development

The initiation of skeletal formation begins with the migration of mesenchymal cells derived from these embryonic lines to the sites of future bone development. At these sites, the cells form a condensate of high cell density which gives the shape and size of the future bone. During condensation, the mesenchymal cells differentiate either into osteoblasts to form bone directly *(intramembranous ossification)* or into chondrocytes and form a cartilage model called cartilage anlage which will be at the basis of the formation of the future bone *(endochondral ossification)* (Gentili et al., 2009)

1.1.1.2 Intramembranous ossification

Intramembranous ossification is a process that forms flat and irregular bones directly without cartilage intermediate (Lefebvre and Bhattaram 2010a)**.** Bones formed through this process include the craniofacial bones, ribs, scapula, and medial clavicles. Natural healing of bone fractures is another important role of intramembranous ossification. This is a chondrocytes-independent process in which mesenchymal cells condense and differentiate directly into osteoblasts (Kobayashi and Kronenberg 2014). The deposit of extracellular matrix (ECM) by osteoblast forms ossification centres to establish bone plates. These bone plates are not fused at the junctions (a functional structure between skull bones is called suture) (Development et al. 2016; Hall and Miyake 2000)**.** The suture is responsible for maintenance and separation of

membrane bones as well as regulation of skull growth. A minority of osteogenic mesenchymal cells near suture differentiate into osteoprogenitor cells and later to osteoblasts expressing type 1 collagen, bone sialoprotein and osteocalcin forming the bone matrix along the bone margin (Ornitz and Marie, 2002)**. Figure 1.2** illustrates intramembranous bone formation.

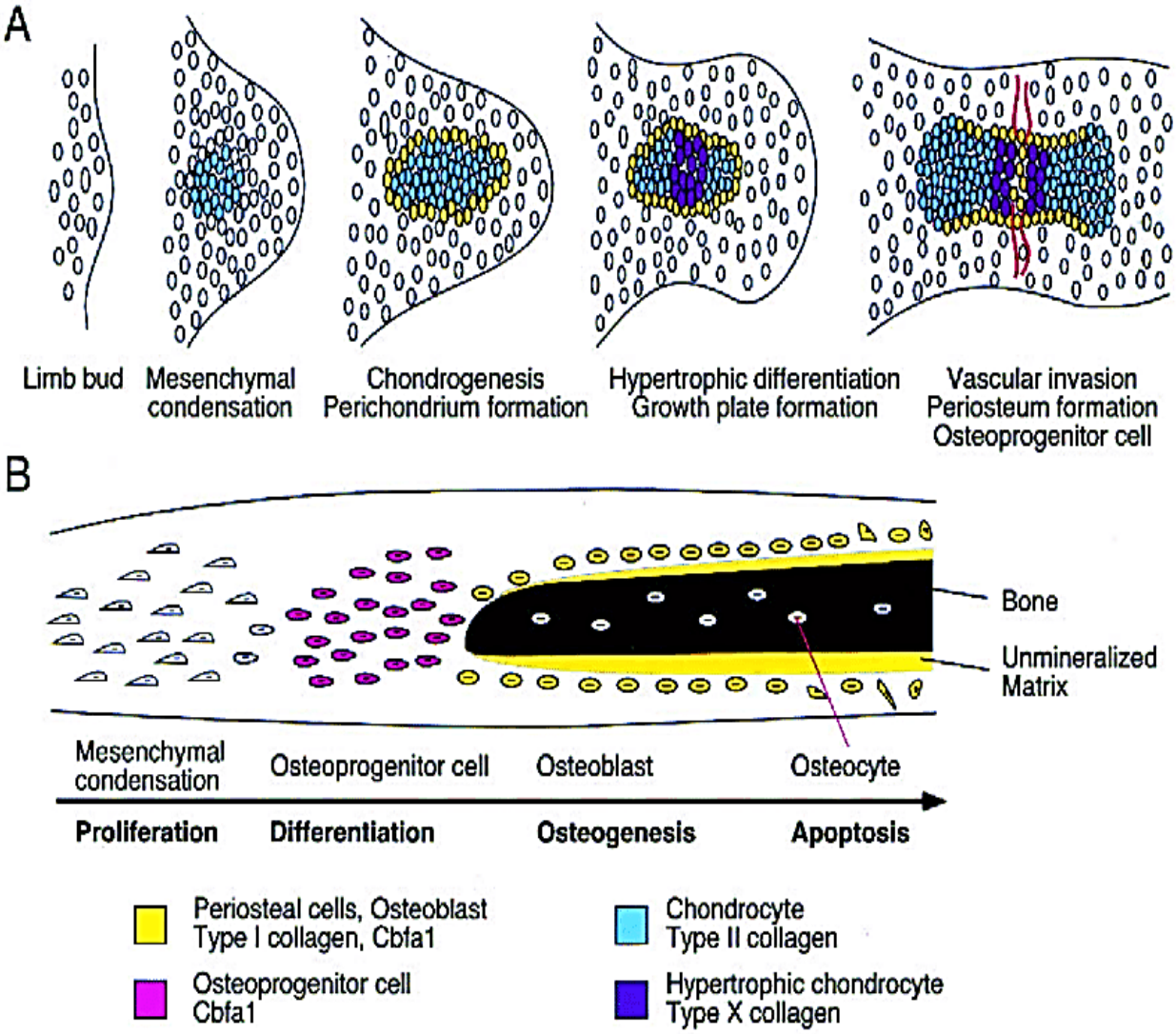

Figure 1. 2: *Schematic representation of intramembranous bone formation:* ***(A)*** *Development of endochondral bone begins with mesenchymal condensation expresses collagen type II (blue). From the centre, cells differentiate to chondrocytes followed by hypertrophy and expression of collagen type X (royal blue), development of perichondrium (yellow), vascular invasion and ossification centre containing osteoblasts expressing collagen type I (yellow).* ***(B)*** *Development of intramembranous bone. The mesenchymal cells condense and differentiate into osteoprogenitors (purple), the osteoprogenitors mature to osteoblasts (yellow) and deposit the bone matrix. Osteoblasts either become osteocytes and get into the matrix or die via apoptosis* (Ornitz and Marie, 2002)

1.1.1.3 Endochondral ossification

The process responsible for the genesis and growth in length of long bones, vertebral column, and bone of skull base is named endochondral ossification (Dao et al. 2012). Primary skeleton is completely cartilaginous and grows rapidly, then replaced by bone during foetal and post-natal development. Most of the bone tissues develop through well organised endochondral ossification (Lefebvre and Bhattaram, 2010a; Mackie et al., 2008). The first and the foremost step in the formation of these cartilage templates is proliferation and condensation of mesenchymal cells that is followed by differentiation into chondrocytes. Chondrocytes secrete a matrix rich in collagen type II and proteoglycans (PGs) mainly aggrecan and express transcription factors (mainly Sox9) leading a characteristic genetic program. Chondrocytes maturate and produce cartilaginous matrix that is gradually replaced by bone. The distinct steps of endochondral ossification are presented in **figure 1.3.**

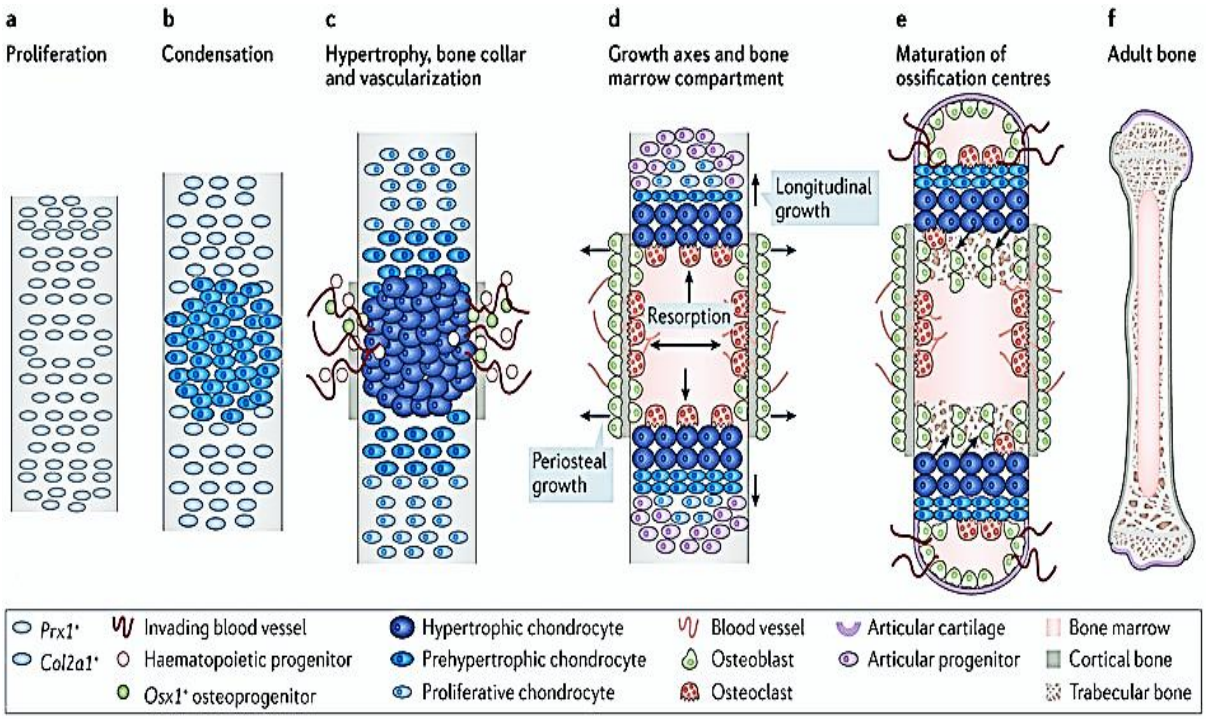

Figure 1. 3: *Endochondral ossification in long bone:* ***(a)*** *Proliferation of mesenchymal progenitor cells to populate the centre of limb bud.* ***(b)*** *Condensation of mesenchymal stem cells* ***(c)*** *Hypertrophy of cells and neovascularization* ***(d)*** *Formation of the primary ossification centre, bone marrow compartment, followed by longitudinal and periosteal (width) growth* ***(e)*** *Maturation and appearance of the secondary ossification centre at epiphysis.* ***(f)*** *Mature adult bone* (Salazar, Gamer, and Rosen 2016a).

The engagement of mesenchymal cells to form chondrocytes progenitor cells is also induced by paracrine factors that influence mesodermal cell to express transcriptional factors Pax1 (Paired box 1) and Scleraxis (Cserjesi et al. 1995; Šošić et al. 1997)**.** Proliferation of progenitor cells is followed by condensation of mesenchymal cells into nodules, differentiation into chondrocytes that produce ECM rich in collagen type II and aggrecan. To varying degrees, and depending on the bone involved, proliferative chondrocytes acquires a flattened discoid shape and form columns with an orientation that directs the prolongation of the bone (Abad et al. 2002; Kuss et al. 2014)**.** Following proliferation, chondrocytes start getting bigger in size (this is called cellular hypertrophy) and modify their genetic program to synthesize collagen type X. The capability of chondrocyte to modify their size and become hypertrophic is essential for bone growth (Chung 2004). The hypertrophic chondrocytes direct the mineralization of the surrounding matrix and the ossification process, via the production of vascular endothelium growth factors (VEGFs) to attract blood vessels and osteoblasts and production of MMP13 and osteocalcin (Berendsen and Olsen, 2015). In addition, prehypertrophic cells direct the adjacent perichondral cells (osteoblast progenitor cells) to differentiate into osteoblasts to form the bone collar (Maeda et al. 2007). Hypertrophic chondrocytes then undergo apoptotic cell death or converted into osteoblasts (Tsang, Chan, and Cheah 2015). The cartilage matrix left behind provides scaffolding for the osteoblasts that invade the rest of the cartilage tissue with the blood vessels and deposit bone matrix, this process takes place during the formation of the diaphysis and the epiphysis, as well as during the growth phase of long bones and is called *primary ossification*. Bone extension is rapid during foetal life due to the rate of formation of hypertrophic chondrocytes from proliferative chondrocytes. Therefore, hypertrophic cells play a crucial role in the coordination of chondrogenesis and osteogenesis.

As the bone grows, secondary ossification centres are established at the murine age of about 5 to 7 days of postnatal life (Dao et al. 2012). In long bones of the limbs, chondrocytes continue to proliferate between the bone regions of the primary and secondary ossification centres (Shim 2015). The growth plate forms a separate plate of cells between the secondary and primary ossification centres. At the top of the growth plate, round chondrocytes do not proliferate quickly and are called resting or reserve chondrocytes. They serve as precursors

for proliferating chondrocytes. In men, growth plates disappear during adolescence after a surge in pubertal activity (Benyi and Sävendahl, 2017; Shim, 2015)

1.1.1.4 Extracellular Matrix

ECM is an active network of molecules secreted by resident cells in each tissue and organ. It is a set of structural and functional proteins arranged in a 3D ultra-structure (Velleman 2000)**.** In the growth plate, the ECM is organised in three different areas pericellular, territorial and interterritorial based on their distance from chondrocyte cells **(Figure 1.4)** (Silva-Almeida et al. 2012).

Pericellular matrix (PM) is the area around the cells, this matrix is made up of collagens and PGs, specially syndecan but also contains decorin, biglycan and matrilin (Bhosale and Richardson, 2008; Cancedda et al., 2000; Gentili et al., 2009)**.** In addition to type II collagen and PGs, type VI collagen is a major structural element of this matrix (Kolb et al. 2001; Theocharis et al. 2016). PM links cells to its surrounding matrix and differs from the rest of the matrix because it channels the communication between the chondrocytes and the ECM and transduces biomechanical and biochemical signals to chondrocytes. It is also considered as a regulatory field for growth factors, where they are activated, degraded, or transported.

Territorial matrix (TM) is present just after PM and is present throughout the cartilage (Buckwalter, 1997; Buckwalter and Mankin, 1998). It is mainly composed of collagen fibrils and PGs (aggrecan, biglycans and decorin) (to regulate the bioavailability of growth factors). Another important role of TM is protection of chondrocytes from mechanical stress (Heinegård and Saxne, 2011)(Bhosale and Richardson, 2008).

Interterritorial matrix (ITM) is far most and largest area having abundance of PGs and oriented bundles of collagen fibrils mainly type II collagen (Bhosale and Richardson, 2008; Heinegård and Saxne, 2011)

The ECM of bone is made up of a mineralized ECM and an organic matrix consisting of 90% of type I collagen secreted by osteoblasts and other matrix components including non-collagenous proteins, osteocalcin, osteopontin, osteonectin, fibronectin, bone sialoprotein type II, bone morphogenetic proteins (BMPs) and growth factors (Hay 1991)**.** This matrix also

contains small leucine-rich PGs (SLRPs) including decorin, biglycan, lumicane, osteoadherin and serum proteins (Roughley and Lee, 1994; Velleman, 2000)

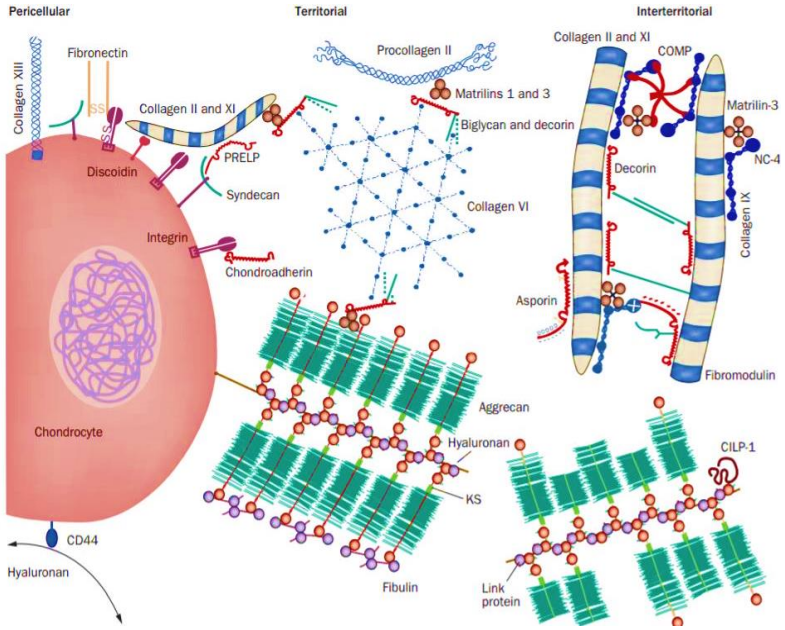

Figure 1. 4 : *Organisation and composition of Extracellular Matrix of cartilage: Matrix is organised into three areas. The pericellular matrix is located immediately around the cell and contains molecules that interact with receptors on the surface of the cells. Slightly far from cell just after PM is the territorial matrix and at the maximum distance from cell lies interterritorial matrix* (Heinegård and Saxne, 2011)

1.1.1.5 Composition of the extracellular matrix

The ECM of both cartilage and bone is made up of mostly collagen, PGs, and small quantities of other non-collagenous glycoprotein and hyaluronan (Gao et al. 2014). Various reports have shown the presence of different types of collagens and PGs expressed differently in the mature cartilage, in the transition zone from cartilage to bone, and in the ECM of mature bone (Catistagnola et al. 1988).

Water

Cartilage has a very large proportion of water both in its free form or linked to PGs. Interaction between water and macromolecules of the matrix influences the mechanical properties of

the tissue. Under the effect of a load, water is driven into the regions of the cartilage without load and towards the articular cavity, carrying outside the tissue the metabolic waste of the chondrocytes, lactic acid. The phenomenon being reversible, when the load ceases, a reverse flow is created from the joint cavity to the cartilage, bringing the cartilage back to its basal hydration, and bringing with it the nutrients necessary for cellular functioning, glucose. A continuous exchange takes place between the water molecules fixed by the negative charges of PGs and the free phase circulating outside the field of attraction of PGs, which contributes to its regeneration.

Type II collagen

Type II collagen is a secreted homotrimeric protein composed of three α1 helices (Col2a1). It is the main component of hyaline cartilage and one of the markers of the chondrocyte phenotype. During development of the growth plate, type II collagen is abundantly expressed in immature chondrocytes and its expression decreases in mature or hypertrophic chondrocytes (Iyama et al. 1991; Manduca, Castagnola, and Cancedda 1988). Type II collagen represents 90% of the collagens (of which ten types are currently identified) present in cartilage. Collagens type IX and XI interact with collagen type II and control its fibrillation and diameter of fibres. Thus, a deletion in the α1 chain of collagen XI in mice leads to the formation of type II collagen fibres of abnormally large diameter and consequently to brittleness of the cartilage (Catistagnola et al. 1988; Hu et al. 2006). The Col2a1 chains are rich in hydroxylysine, glucosyl and galactosyl residues. These residues allow the binding to the PGs present in the ECM (Brewton, Wright, and Mayne 1991). A wide spectrum of chondrodysplasias has been associated with mutations in the gene encoding Col2a1. A heterozygous mutation in Col2a1 in the α chains is responsible for type II achondrogenesis-hypochondrogenesis, characterized by perinatal lethality and significant dwarfism (Körkkö et al. 2000). Other studies have shown that mutations in the Col2a1 gene cause Kniest-dysplasia characterized by a trunk and short limbs, kyphoscoliosis, frontonasal hypoplasia, severe myopia, and hearing loss. Stickler syndrome is also described in individuals with a truncated form of Col2a1 (Twine et al. 2014). Dominant mutations in the Col2a1 gene induce Strudwick-type spondylo-epimetaphysal-dysplasia characterized by short stature, cranial malformation,

and scoliosis (Shapiro, 2001). All these studies suggest significant role of Col2a1 in skeletal development.

Collagen type X

Collagen type X is a secreted protein which formed by a homotrimer of triple helix α1 (Col10a1) with a long C-terminal and a small N-terminal region. It is encoded by the COL10A1 gene and is expressed specifically in hypertrophic chondrocytes (Gelse, Pöschl, and Aigner 2003; Mundlos 1999). As a major component of the hypertrophic zone, type X collagen influences the deposition of other ECM molecules in this region and provides an environment conducive to hematopoiesis and mineralization, which are essential events for endochondral ossification (Grskovic et al. 2012). Collagen X is important for the development of the skeleton and is involved in the pathologies linked to this system. The mutations or an abnormal expression of COL10A1 lead to an abnormal enlargement of the chondrocytes observed in several cases of skeletal dysplasia and in osteoarthritis pathology (Zheng et al. 2005). A dominant mutation in the human COL10A1 gene induces Schmid metaphyseal chondrodysplasia (MCDS) characterized by short stature, Coxa vara associated with a disorganized growth plate and defects in the formation of endochondral bones (Grskovic et al. 2012; Shen 2005). In addition to Sox9 which regulates the expression of Col10a1 (Long and Ornitz, 2013), other studies have reported that Runx2 binds to the promoter of Col10a1 during chondrogenesis and regulates its expression (Lamas et al. 2010; Zheng et al. 2005). Thus, mice with a haplo-insufficiency of *RUNX2* exhibit defective endochondral ossification with a decrease in the expression of Col10a1 and a reduced hypertrophic zone (Gelse, Pöschl, and Aigner 2003). Human osteoarthritis cartilage has also been reported to have increased Col10a1 expression and increased chondrocyte enlargement, while mesenchymal stem cells from patients with osteoarthritis constitutively express type X collagen (Girkontaite et al. 1996).

1.2 Proteoglycans

PGs are important bio-macromolecules and major constituents of ECM. They are composed of core protein with one or several long unbranched polysaccharides chains named glycosaminoglycan (GAGs). In addition to expression on surface of cells, PGs are abundantly expressed in ECM of connective tissues **(Figure 1.5)** (Yanagishita 1993). These macromolecules perform several biological functions including ECM deposition, cell differentiation, cell adhesion, cell migration and proliferation through their interaction with various cytokines, growth factors, enzymes, and cell adhesion proteins (Iozzo and Schaefer, 2015; Li et al., 2012; Prydz and Dalen, 2000). Since PGs have diverse cellular functions, they are involved in many pathological conditions such as atherosclerosis, osteoarthritis, rheumatoid arthritis, skeletal muscle dystrophies, neurological disorders, nervous system injury, liver and lung fibrosis, tumours development and progression, and most significantly in heritable skeletal disorders named as chondroplasias (Schwartz and Domowicz, 2002).

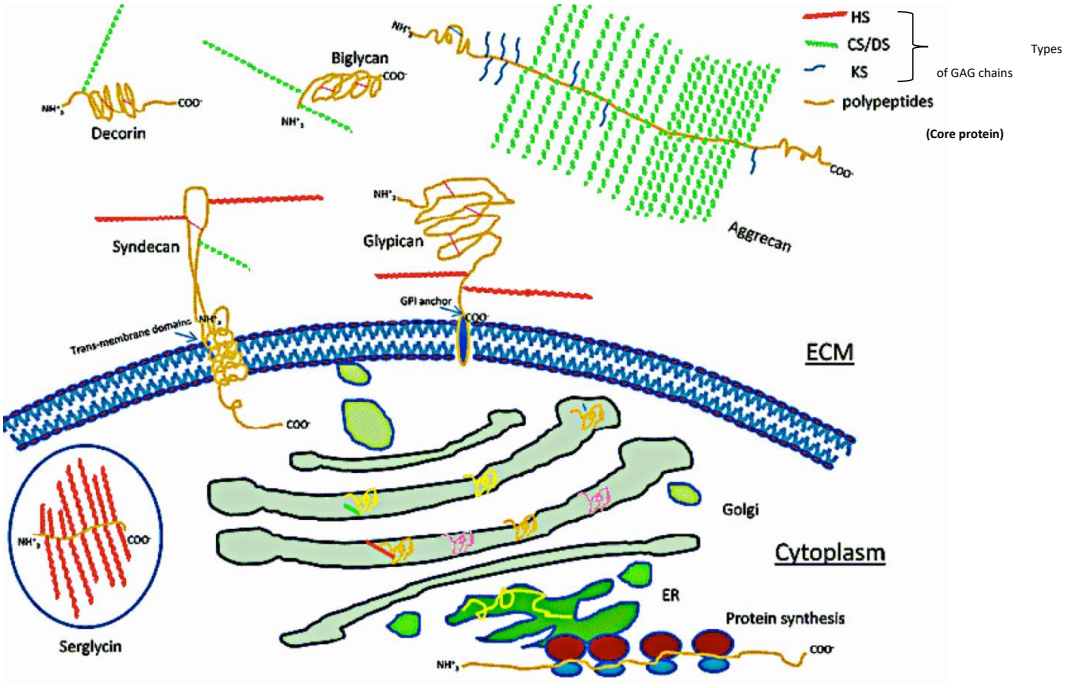

Figure 1. 5 : *Different proteoglycans present in cell and extracellular matrix* (Li, Ly, and Linhardt 2012)

PGs are known to modulate the bioactivity of growth factors and cytokines through interaction with their GAG chains by acting as co-receptors and reservoir for different ligands (Mythreye and Blobe 2009). Studies conducted on mesenchymal stem cells derived from the bone marrow of double-deficient mice in biglycan and decorin showed an increase in TGF-β signaling resulting from the inability of biglycan and decorin to sequester TGF-β in the ECM. This increase induces a decrease in the number of osteoblasts due to increased apoptosis. PGs regulate the bioavailability and activity of BMPs, which are essential factors in the cellular differentiation of mesenchymal stem cells into osteoblasts and chondroblasts (Beederman et al. 2013). They also regulate important genes including signaling factors (SHH, IHH) (Seki and Hata 2004), antagonists (Noggin) (Pang et al. 2015), ECM proteins (fibromodulin), (Balemans and Van Hul 2002; Zhang, Zhang, and Linhardt 2010) and transcription factors (Sox9, Cbfa1/Runx2, Osx) that are essential in bone formation (Ouyang et al. 2010; Wu, Chen, and Li 2016a).

Among PGs, small leucine-rich PGs (SLRPs) are involved in skeletal development, craniofacial structure (Ameye and Young 2002; Corsi et al. 2002), tooth formation and collagen fibrillogenesis (Ameye and Young, 2002). Models of PG-deficient knockout mice were generated to study their role in bone formation. Thus, mice deficient in biglycan show an alteration in postnatal bone formation leading to the early onset of osteoporosis. Decorin-deficient mice did not show histological or macroscopic bone changes but had collagen fibres of abnormal size, distribution, density, and morphology. Defects in the shape and size of bone collagen fibres in double biglycan- and decorin-deficient mice were detected by transmission electron microscopy, supporting the hypothesis that these PGs play an important role in collagen assembly and function. In addition, these mice show a decrease in bone mineralization (Corsi et al. 2002; Nikitovic et al. 2012). Lumican also plays an essential role in bone mineralization. It is highly expressed by mature osteoblasts and is considered as the major PG of the bone matrix (Raouf et al. 2002).

1.2.1 Glycosaminoglycans (GAGs) chains

Glycosaminoglycan chains (GAGs) are long unbranched polysaccharides with repeating disaccharide units composed of N-acetyl-galactosamine (GalNAc) or N-acetyl-glucosamine (GlcNAc) and an uronic acid (GlcA) or iduronate (IdoA). GAGs are covalently linked on the specific serine residues of core protein. Theses chains contribute to 50% or more of the total molecular mass of PGs and mediate the biological functions of most of them. These chains can be sulfated or non-sulfated. Sulfated GAGs includes chondroitin sulfates (CS), dermatan sulfates (DS), heparan sulfates (HS), heparins (Hep) and keratans sulfates (KS) while unsulfated group of GAGs include hyaluronic acid (HA) **(Table 1.1).** Hyaluronic acid is the simplest GAG and is devoid of core protein characterised by simple linear structure. Synthesis of hyaluronic acid takes place at the plasma membrane, then the growing chain is exported directly to the extracellular environment where it surrounds chondrocytes (Hiscock, Caterson, and Flannery 2000).

1.2.2 Biosynthesis of GAGs

Synthesis of GAG chains requires monosaccharides and sulfates moieties that are activated to form UDP-sugars and 3'-phosphoadenosine 5'-phosphosulfate (PAPS), respectively. Specific transporters then transfer the UDP-sugars and PAPS into ER and the lumen of Golgi apparatus (Prydz and Dalen 2000). GAG chain synthesis is shown in **Figure 1.6**. Correct GAG synthesis is essential as any mutations in genes encoding the enzymes involved in this synthetic pathway lead to severe disorders in human (Malfait et al. 2013). Disorders due to deficiency of genes encoding enzymes involved in GAG synthesis are shown in black boxes in **Figure 1.6**.

Table 1. 1 : *Repeating disaccharide units of glycosaminoglycans and their important features*

(Gandhi and Mancera 2008)

Glycosaminoglycans	Disaccharide units	Key Features
Hyaluronic acid	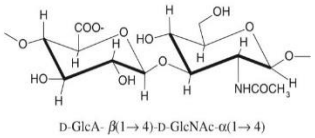 D-GlcA- β(1→ 4)-D-GlcNAc-α(1→ 4)	▪ Molecular mass 4000 to 8000 kDa ▪ Non-sulfated non-covalently attached to proteins in the ECM ▪ Usually found in synovial fluid, vitreous humour, and ECM of loose connective tissue ▪ Lubricant and shock absorber
Chondroitin sulfate	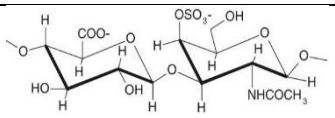 D-GlcA-β(1→ 3)-D-GalNAc4S-β(1→ 4)	▪ Molecular mass 5–50 kDa ▪ Most abundant GAG in the body ▪ Found in cartilage, tendon, ligament, and aorta ▪ Bind to proteins (like collagen) to form proteoglycan aggregates.
Heparan sulfate	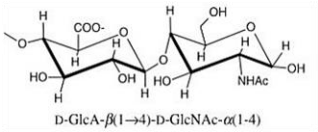 D-GlcA-β(1→4)-D-GlcNAc-α(1-4)	▪ Molecular mass 10–70 kDa ▪ Extracellular component found in the basement membrane and as a ubiquitous component of cell surfaces
Keratan sulfate I and II	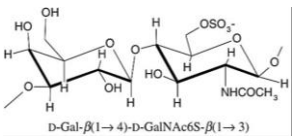 D-Gal-β(1→ 4)-D-GalNAc6S-β(1→ 3)	▪ Molecular mass 4–19 kDa ▪ Most heterogeneous GAG ▪ KS I is found in the cornea ▪ KS II is found in cartilage aggregated with CS
Dermatan sulfate	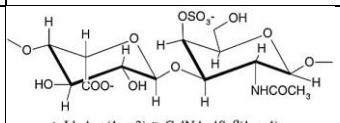 L-IdoA-α(1→ 3)-D-GalNAc4S-β(1→ 4)	▪ Molecular mass 15–40 kDa ▪ Found in skin, blood vessels and heart valves
Heparin	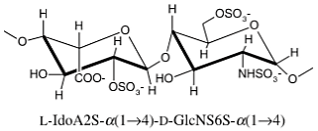 L-IdoA2S-α(1→4)-D-GlcNS6S-α(1→4)	▪ Molecular mass 10–12 kDa ▪ Intracellular component of mast cells, especially in the liver, intestine, lungs and skin

1.2.2.1 Formation of the tetrasaccharide primer

The initial step in the GAG synthesis (except for Keratan sulfate KS) is the formation of the tetrasaccharide primer by the sequential addition of four monosaccharide residues ie. xylose, galactose, galactose, and glucuronic acid. This process is initiated by Xylosyltransferase I and II (XylT1/2) which catalyse the transfer of a xylose residue from UDP-xylose to specific serine residues on the "core" protein, followed by the addition of a galactose residue by β1,4-galactosyltransferase-I (GalT-I/β4GalT7) and a second galactose by β1,3-galactosyltransferase-II (GalT-II/β3GALT6) (Okajima et al., 1999) and finally the addition of glucuronic acid by β1,3-glucuronyltransferase-I (GlcAT-I/β3GAT3). GAG chains are then extended by addition of an amino sugar GalNAc/GlcNAc and a glucuronic acid (GlcA). These chains are modified by transfer of sulfate groups to the specific positions by sulfotransferases. **Figure 1.6** illustrates different steps involved in GAG synthesis (Prydz and Dalen, 2000).

1.2.2.2 Elongation of CS chains

Chondroitin sulfate contains repeating disaccharide units $[–4GlcAβ1–3GalNAcβ1–]_n$ linked to PG core protein *via* the tetrasaccharide linker region. Glycosyltransferases (GTs) involved in synthesis of CS chains are chondroitin synthase-1 and 3 (CHSY1, CHSY3), chondroitin polymerizing factor (ChPF), and chondroitin N-acetyl-galactosaminyl transferases 1 and 2 (ChGn-1 and ChGn-2) (Izumikawa, 2019; Mikami and Kitagawa, 2013). CS polymerization requires co-expression of any two of the three enzymes CHSY1, CHSY3 and ChPF. ChGn-1 and ChGn-2 are involved in chain initiation and elongation (Izumikawa et al. 2015). CS chains are modified by sulfation at 2^{nd}, 4^{th}, and 6^{th} position of residues by sulfotransferases CHST11, CHST3 and CHST7 (Mikami and Kitagawa 2013).

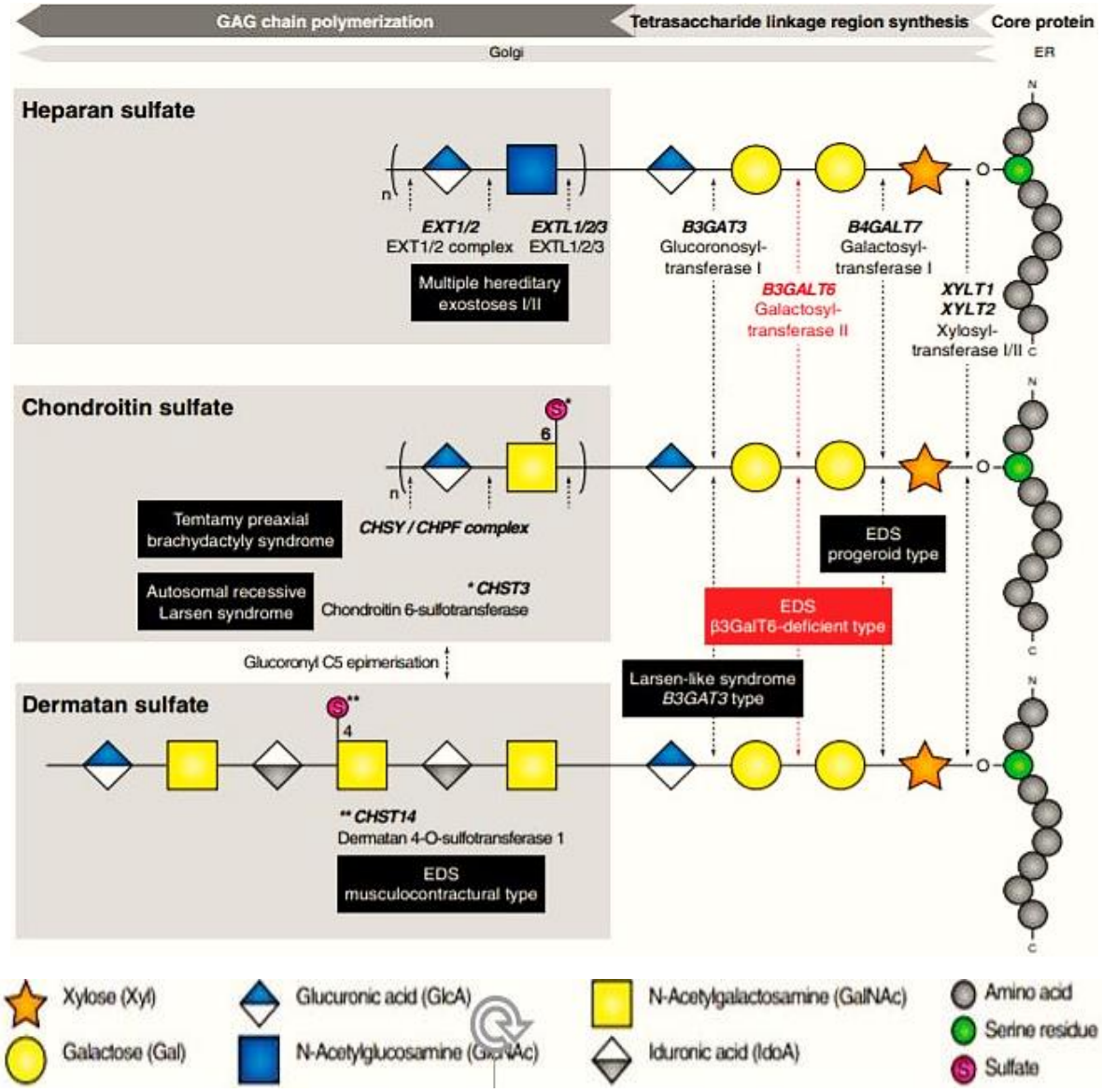

Figure 1. 6 : *Synthesis pathway of glycosaminoglycan and syndromes associated with mutations of genes involved: Core protein is synthesised in ER and transported to the Golgi apparatus. First step of GAG synthesis is the formation of the tetrasaccharide linker region formed by addition of Xylose (Xyl) to the serine residue of core protein, followed by addition of two galactose (Gal) and one glucuronic acid (GlcA) residues. Polymerisation of GAG chains is performed by addition of any of the repeating disaccharide units consisting of (GlcA-GalNAc)$_n$ or (GlcA-GlcNA)$_n$ to form CS/DS PGs or HSPGs respectively. The GAG chain is then modified by epimerisation and sulfation. Genes and enzymes and disorders caused by their deficiency are also shown (Malfait et al., 2013).*

1.2.2.3 Elongation of the HS Chains

The attachment of the N-acetylglucosamine (GlcNAc) residue to the non-reducing end of the tetrasaccharide linkage region by EXTL enzymes initiate the synthesis of HS chains **(Figure 1.7)**. The HS chain synthesis is initiated by the EXTL1-3, and all can transfer the α-GlcNAc for the HS synthesis. However, EXTL3 is the major enzyme that initiates HS synthesis. The EXTL2 enzyme can transfer GlcNAc or GalNAc to linker region and addition of α-GalNAc blocks GAG synthesis (Nadanaka and Kitagawa 2014). After initiation of the HS synthesis by the EXTL1-3, chain polymerization is catalysed by the EXT1 and EXT2 by sequential addition of GlcNAc and GlcA residues. Like CS, several modifications occur on the HS chain. The GlcNAc is deacetylated and sulfated by deacetylase-N-sulfotransferases (Ndst). The D-glucuronic acids are epimerized to L-iduronic acid (IdoA) by C5 epimerase. The HS chains are formed by domains that are N-sulfated (NS domains) and N-acetylated (NA domains). The region between these domains are called NA/NS domains. Sulfotransferases transfer sulfate at various position of the disaccharide unites. The 2-O-sulfotransferase (Hs2st) adds sulfate at C2 of the iduronic acids, 6-O-sulfotransferases (Hs6st1-3) transfers sulfate at C6 to the N-sulfoglucosamine units and 3-O sulfotransferases (Hs3st1, 2, 3a,3b, 4, 5, 6) adds sulfate at C3 of glucosamine units (Mikami and Kitagawa, 2013).

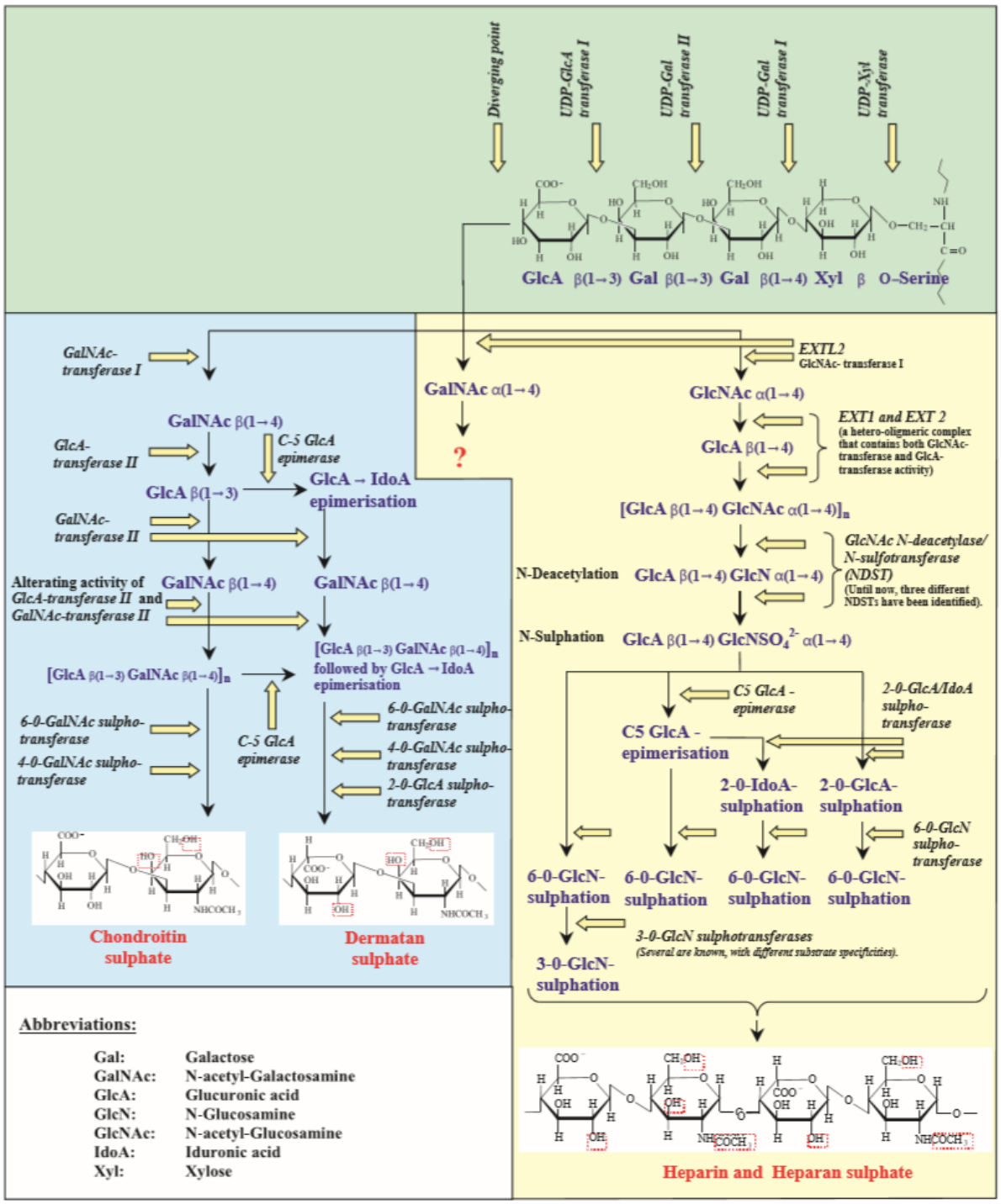

Figure 1. 7 : *Different steps of GAGs synthesis: The process begins with the addition of the tetrasaccharide primer consisting of a xylose, 2 galactoses and 1 glucuronic acid: GlcA1,3Gal1,3Gal1,4Xyl common to the chains of CS and HS, on serine residues of the core protein. This formation is initiated by Xylosyltransferase I and II catalyzing the transfer of xylose to the serine residues of the core protein. Then, the first GalNAc residue is transferred to the GlcA residue by GalNAcT 1, 2, which initiates the assembly of the CSs. On the other hand, the addition of the GlcNAc residue is catalysed by the EXTL enzymes, thus promoting the polymerization of the HS chains (Prydz and Dalen, 2000).*

1.2.3 Classification of PGs

1.2.3.1 Classification of PGs based on their cellular and sub-cellular localization

Iozzo and Schaefer (2015) have simplified the classification of PGs by classifying them based on their subcellular localization into four major groups. First group corresponds to intracellular PGs and contains only one member called serglycin which is packed inside the granules of mast cells (Kolset and Pejler 2011). Cell surface PGs is the second group of PGs that includes syndecan family (SYND-1, SYND-2, SYND-3 and SYND-4), chondroitin sulfate proteoglycan 4 (CSPG4 also called neuralglia-2 (NG2)), betaglycan and phosphacan (having transmembrane domain attached to the plasma membrane) and glypicans (1 to 6) that are attached to the plasma membrane *via* glycosyl-phosphatidyl-inositol (GPI) anchor. Third group of PGs is attached to the cell surface by integrin and are also present on basement membrane called pericellular and basement membrane PGs, including perlecan, agrin, collagens XVIII and XV. Fourth group includes extracellular PGs which are subdivided into three subgroups; first groups consist of hyalectans that includes aggrecan, versican, neurocan and brevican; second group consist of non-hyalectans that includes small leucine rich PGs (SLRPs) such as decorin, biglycan, fibromodulin and SPOCK containing testicans (1 to 3) (Iozzo and Schaefer 2015)**(Figure 1.8)**.

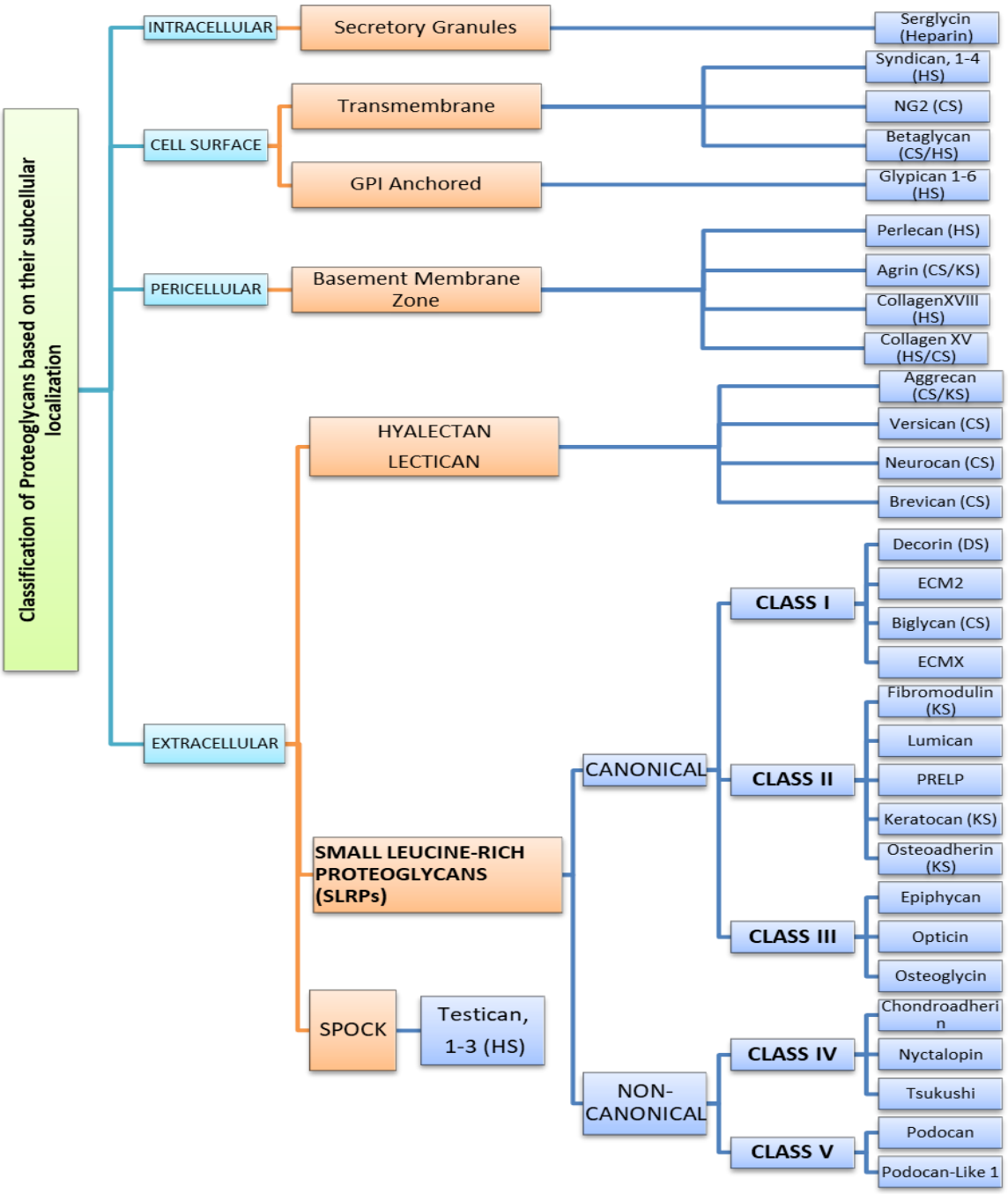

Figure 1. 8: *Classification of PGs based on their localisation (Adapted and modified from Iozzo and Schaefer, 2015).*

1.2.3.2 Classification of PGs based on GAG chains attached to the core protein

1.2.3.2.1 Chondroitin Sulfate Proteoglycans (CSPGs)

Aggrecan

Aggrecan is the most abundant PG secreted in ECM with a molecular mass of 250 kDa. There are almost 100 chondroitin sulfate chains and 30 keratan Sulfate chains attached to the core protein (Gibson and Briggs, 2016; Knudson and Knudson, 2001)**.** Aggrecan is not isolated within the ECM but occurs in the form of PG aggregates. Each aggregate is composed of a central filament of HA with multiple non-covalently attached aggrecan molecules (Roughley and Mort, 2014)**.** Aggrecan contains three domains (G1, G2, and G3). G1 is a N-terminal domain that interacts with hyaluronic acid (HA) and forms stable complex with the central filament. Next to G1 domain is G2 containing conserved sites for attachment of keratan sulfate (KS) chains. The C-terminal domain (G3) contains complementary regulatory protein, C-type lectin and two EGF like repeats. The central region between G2 and G3 contains several GAG attachments sites. This region is encoded by a large single exon with 120 ser-gly repeats for the attachment of the GAG chains. It has CS1 and CS2 region that provide attachment site to chondroitin sulfate GAG chains (Roughley and Mort, 2014)**.** Aggrecan form dense aggregates and is mainly present in cartilage where it attracts water and maintain the assembly of collagen fibres, it also acts as a lubricant and provides properties of load bearing to the cartilage **(Figure 1.9)**. Aggrecan is highly anionic due to the presence of large number of GAG chains that are responsible for its water holding capacity creating osmotic pressure, thus conferring to cartilage strength and resistance to compressive forces (Knudson and Knudson, 2001).

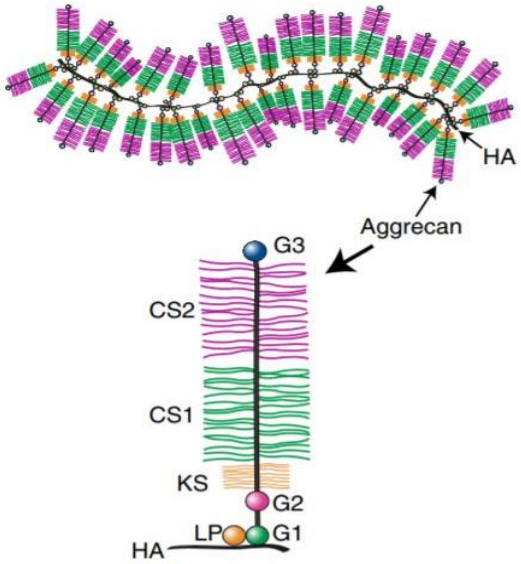

Figure 1. 9: *Aggrecan aggregates: Hyaluronic acid (HA) filament in the centre is attached to link proteins (LP) and aggrecan. G1, G2 and G3 are the three domains of aggrecan, chondroitin sulfate rich domains are CS1 and CS2, KS is keratan sulfate-rich domain* (Roughley and Mort 2014).

Aggrecan is also present in nervous tissue (Schwartz and Domowicz, 2002)**.** Mutations in the human ACAN gene are found in patients with Kimberley type spondylophysal dysplasia, characterized by severe dwarfism, facial dysmorphia, and early osteoarthritis (Tompson et al. 2009). Animal model studies have shown that mutations in the aggrecan gene induce chondrodysplasia in mice (Watanabe et al. 1997)**.** In addition, aggrecan has been found to bind to IHH (Driscoll 2006; Maeda et al. 2007) *via* its CS chains (Schwartz and Domowicz, 2002). This suggests that aggrecan establishes an IHH gradient in the epiphyseal growth plate. This gradient is necessary to control the process of cell differentiation (Domowicz et al. 2009). The catabolism of the aggrecan is increased in osteoarthritis (OA) following the action of cytokines such as interleukin-1 (IL-1) and tumor necrosis factor α (TNFα) that decrease synthesis and increase the expression of the enzymes that are responsible for its degradation (Roughley and Mort, 2014; Troeberg and Nagase, 2012).

Decorin

The name decorin is derived from earliest finding that decorin can bind to “decorate fibres” of collagen type I. Molecular mass of core protein of decorin is about 40 kDa and contains only one GAG chain that can either be CS or DS type. The core protein contains four domains. The N-terminal domain consists of a signal peptide containing 16 amino acids which is cleaved

before secretion of the protein into the ECM (Sainio and Järveläinen, 2019). The second domain contains several cysteine residues and a ^{31}DEASGIG^{37} motif containing a Ser34 residue for the attachment of GAG chain. The third domain contains leucine-rich repeats consisting of 12 repeats of 24 amino acids rich in leucine and three sites for the *N*-linked glycosylation (Asn211, Asn262 and Asn303) giving an arch shape to the structure. The fourth domain or C-terminal domain contains two cysteine and a disulfide loop (Sainio and Järveläinen, 2019) **(Figure 1.10).** The core protein interacts with type I and type II collagens and various growth factors.

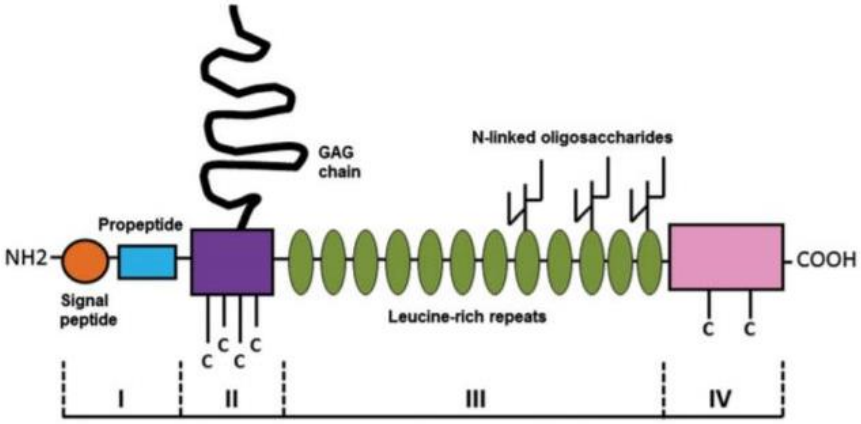

Figure 1. 10: *Graphic representation of decorin structure: The decorin core protein has four domains (I–IV). (I) the signal peptide that is cleaved before secretion of decorin into ECM. (II) a cysteine (C) rich domain where CS/DS GAG chain is attached to Ser34. The characteristic domain of decorin is domain (III) that consists of 12 leucine rich repeats (LRRs) and up to three N-linked oligosaccharides. Domain (IV) is like domain II as it contains two cysteine residues also called carboxy terminal domain (Sainio and Järveläinen, 2019).*

The LRR domain and GAG side chain are the main decorin interacting partners as they enable decorin to bind and sequester many molecules including macromolecules present in ECM, growth factors mainly TGFβ, receptors, cytokines, enzymes, hormones and lipoproteins (Ruoslahti and Yamaguchi, 1991; Sainio and Järveläinen, 2019). Fibroblasts and myofibroblasts produce a large amount of decorin which is secreted into the ECM as soluble form. It is produced by human skin fibroblasts and is major PGs expressed in dermal ECM. It has been reported that decorin from skin of young contains longer CS-GAG chains compared to decorin from aged skin (Lee et al., 2016).

Decorin stabilizes collagen fibres, its absence makes collagen fibres thin, while lack of GAG chain on decorin led to thicker collagen fibres (Seidler, 2012). Soluble form of decorin acts as endogenous pan-receptor tyrosine kinase (RTK) inhibitor. It down-regulates tumor development, migration, and angiogenesis (Neill et al., 2013). It induces accumulation of cells at G1 phase and counteracts the TGF-β1 effects and phosphorylation of EGFR. Soluble form of decorin interacts with various growth factors and cytokines receptors. This includes transforming growth factor (TGF-β1) receptor, epidermal growth factor receptor (EGFR), the insulin-like growth factor receptor I (IGF-IR), and the hepatocyte growth factor receptor (Met) (Sainio and Järveläinen, 2019; Bolton et al., 2008), thus influencing their intracellular signaling pathways.

Decorin GAG chain interacts with collagen fibrils and play a crucial role in matrix assembly and in the pathophysiology of angiogenesis. Decorin interacts with a wide set of different signaling molecules crucial for cancer growth. The active sites for binding with decorin for TGF-β, CCN2, c-Met, and EGFR reside in different parts of the protein **(Figure 1.11)**. Therefore, a single molecule of decorin can sequester multiple mediators and can antagonise multiple signaling pathways (Järvinen and Prince, 2015).

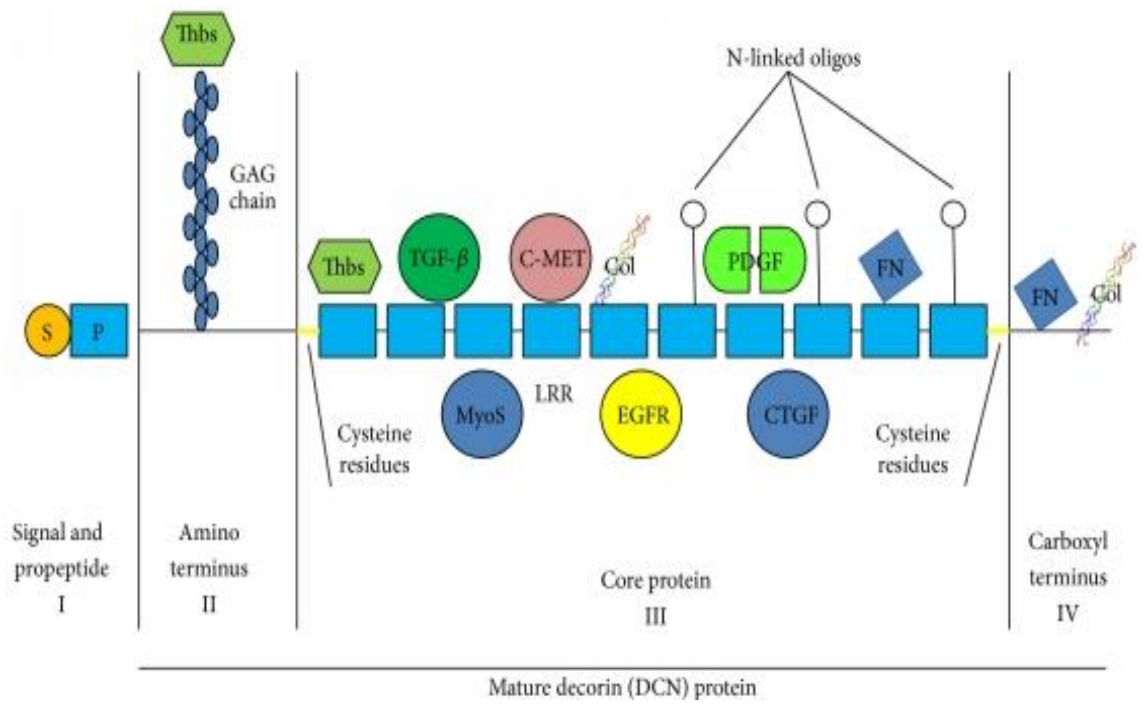

Figure 1. 11 : *Schematic illustration of molecular structure of decorin (showing all four domains I, II, III and IV). Decorin interacts with a wide set of different signaling molecules (Järvinen and Prince, 2015).*

Biglycan

Biglycan is a SLRP with a core protein of about 42 kDa and contains two GAG chains attached to the N-terminal part of the protein (Edwards, 2012). It is synthesized as a precursor with a signal peptide cleaved by BMP-I to release the active form. Biglycan interacts with many ECM components such as decorin, it also interacts with various growth factors and cytokines like TGF, BMP and TNF-α. It has an important role in signaling pathways because it acts as ligand for Toll-like receptors (TLRs)-2 and -4 (Schaefer et al., 2005), P2X7/P2X4 receptors, low-density lipoprotein receptor-related protein 6 (LRP6) and receptor tyrosine kinase (MuSK) (Amenta et al., 2012; Nastase et al., 2012). Biglycan also has an important role in the innate immunity and inflammation. Its expression is upregulated in the pulmonary inflammation and asthma. It stimulates the canonical Wnt/β-catenin signaling (Berendsen et al., 2011). Biglycan mediates the BMP, TGFβ and Wnt canonical signaling pathways to stimulate the osteoblast differentiation to form bone (Nastase et al., 2012). **Figure 1.12** shows structure of biglycan.

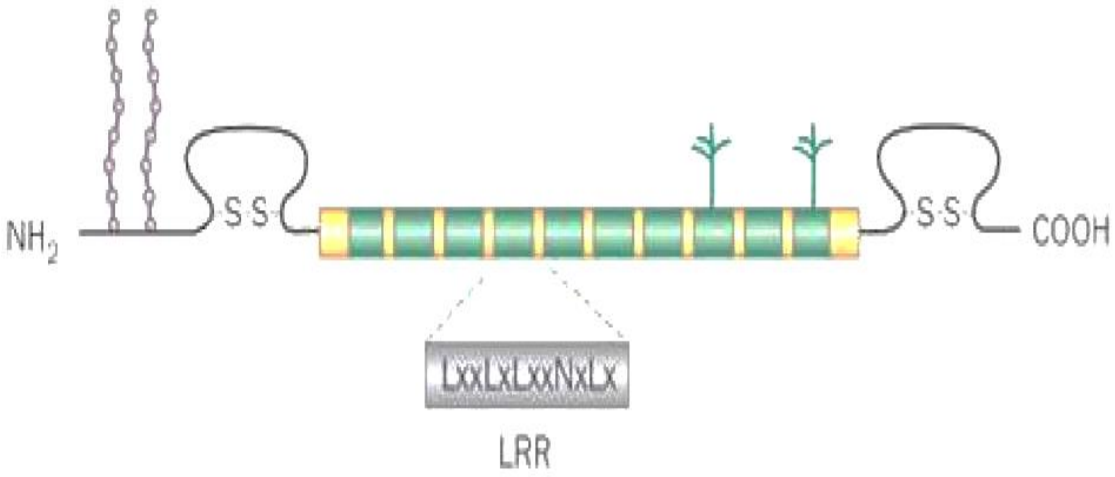

Figure 1. 12 :Structure of Biglycan: *Two GAG chains at N-terminal and several leucine rich repeats (Edwards, 2012).*

1.2.3.2.2 Heparan-Sulfate Proteoglycans (HSPGs)

Unbranched chains of repeating disaccharide units sulfated at multiple positions of their sugar residue are heparan sulfate GAGs. These chains are present either as unconjugated or as conjugated to amino acids forming heparan sulfate proteoglycans. Based on their localization, HSPGs can be classified as transmembrane proteoglycans (HSPGs that are connected to

plasma membrane of cells directly through an inserted core protein such as syndecans), glycosyl-phosphatidyl-inositol (GPI) anchored proteoglycans (glypicans) basement membrane or pericellular HSPGs including agrin that is the most abundant basement membrane HSPG functions in neurotransmission (Iozzo and San Antonio, 2001), perlecan and type XVIII collagen. HSPGs are considered as major biological modifiers of growth factors like fibroblast growth factors (FGF), vascular endothelial growth factor (VEGF) and Platelet-derived growth factor (PDGF) and transfer these growth factors to their respective receptors is the major function of HSPGs (Nagarajan et al., 2018; R. V. Iozzo and Schaefer, 2015; Sarrazin et al., 2011).

HSPGs are important for tissue homeostasis, they regulate diverse cell-autonomous functions and play an important role in cell survival, apoptosis, differentiation of cells and oncogenic signaling (Nagarajan et al., 2018). Deficiency of HSPGs during embryonic development leads to neural tube defects (Matsuo and Kimura-Yoshida, 2013). HSPGs play an essential role in several physiological processes, particularly in chondrogenesis. Indeed, invalidation of EXT1, the enzyme responsible for the synthesis of HS chains, has shown abnormalities in the growth plate due to a reduction in the rate of expression of HS which facilitates the transport of Ihh and the overexpression of PTHrP which in turn delays differentiation into hypertrophy, leading to dwarfism. (Gao et al., 2020; Koziel et al., 2004). These proteoglycans interact with different receptors through mediation by their GAG chains (Sarrazin et al., 2011). Transmembrane HSPGs shed on cell surface by specific matrix metalloproteinases (MMPs) and generate soluble proteins that are secreted in ECM. This shedding influence cellular proliferation by accumulation of these soluble proteins in intercellular spaces and sequestering growth factors thus influencing several signaling pathways (Manon-Jensen et al., 2013). **Figure 1.13** highlights various activities of HSPGs inside and outside cells. Basement membrane HSPGs collaborate with the component of extracellular matrix to facilitate cell migration and to define structure of basement membrane (Sarrazin et al., 2011).

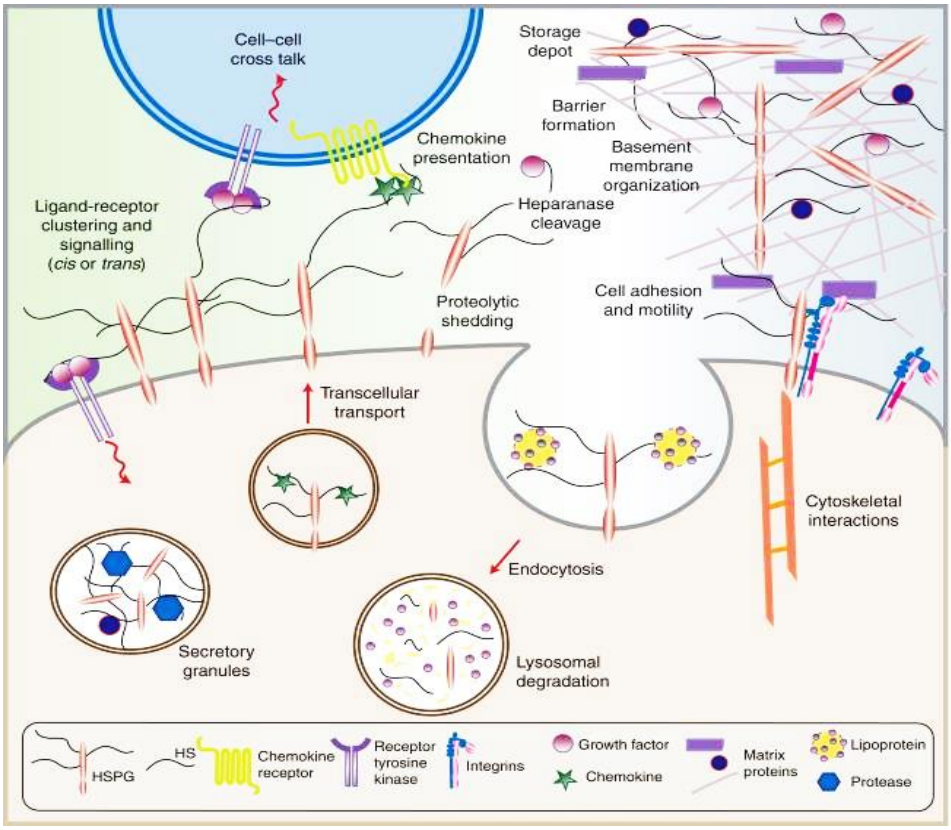

Figure 1. 13: *Distinct activities of HSPGs inside and outside the cell: Basement membrane HSPGs along with other components of matrix define structure to provide a matrix for migration of cells. Secretory vesicles HSPGs activate proteases to regulate several biological activities. HSPGs also binds to cytokines, chemokines, growth factors, and morphogens, protecting them against proteolysis. HSPGs of the cell membrane interact with integrins and other cell adhesion receptors to influence cell adhesion and motility. Membrane HSPGs act as coreceptors for various tyrosine kinase-type growth factor receptors via their HS chains to promote interactions with cognate receptors (Sarrazin et al., 2011).*

Syndecans

Syndecans (SYND) are cells surface HSPG family comprising four members containing a cytoplasmic domain at C- terminal, transmembrane domain, and a unique extracellular domain (ectodomain) (Choi et al. 2011a) **(Figure 1.14)**. SYND-1 is expressed by epithelial cells and some leucocytes. Cartilage significantly expresses SYND-1 and SYND-2 is expressed by cells in the perichondrium, periosteum, and connective tissue. SYND-3 (fibroglycan) is abundant in limb buds, brain, the neural tube (Pap and Bertrand, 2013) and in the chondrocytes of the proliferation zone during the development of the growth plate (Knudson and Knudson, 2001).

SYND-4 also called amphiglycan is expressed by cartilage tissue in mice during embryonic development. During endochondral ossification SYND-4 is highly expressed by proliferative chondrocytes and hypertrophic chondrocytes. In humans and mice, SYND-4 is expressed by articular cartilage during osteoarthritis (OA) (Pap and Bertrand, 2013).

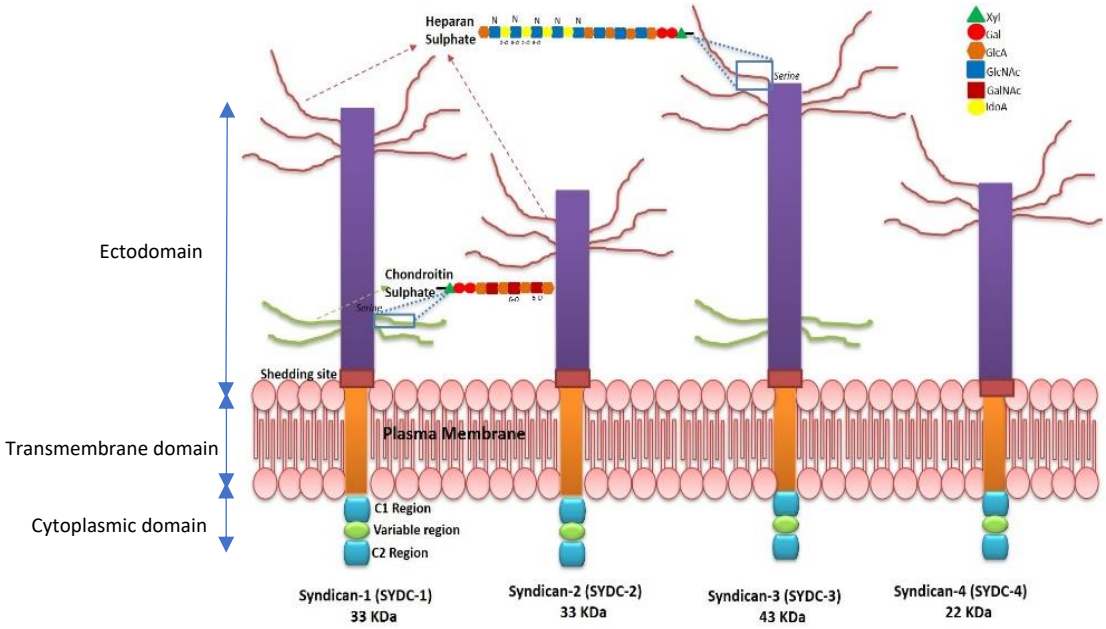

Figure 1. 14 : *Members and structure of syndecan family in vertebrates: Core protein of SYND-1 and 3 can attach both HS (brown) and -CS (green) GAG. The juxta-membranous shedding region is indicated by a brown box. Cytoplasmic domains exhibit highly conserved regions C1 and C2 separated by variable region (V) (adapted and modified from* Manon-Jensen et al., 2010).

Syndecans serve as adhesion molecules, bind chemokines, cytokines, growth factors, morphogens, pathogens, and metalloproteinases (MMPs) (Choi et al., 2011; Pap and Bertrand, 2013). This binding is mediated both by the core protein and by the GAG chains. SYND-4 interacts with protein kinase C (PKC) *via* its variable region and regulates the expression of adhesion molecules including fibronectin and its integrin receptor. Thus, SYND-4 and fibronectin interaction promote the formation of focal adhesions and the reorganization of the actin cytoskeleton. SYND-4 expression is associated with overexpression of MMPs and integrins and inhibition of Col2a1 expression. It is thus involved in the degradation of the

cartilage matrix, as shown by the significant reduction in the loss of cartilaginous PGs and the severity of osteoarthritis in mice deficient in SYND-4 (Pap and Bertrand, 2013). In contrast, syndecans are capable of binding pathogens such as the human immunodeficiency virus1 (HIV1), HIV2, herpes papilloma virus, simian immunodeficiency virus and the hepatitis C virus through their HS chains. These pathogens use syndecans as receptors that facilitate their entry into host cells (Choi et al., 2011). In addition to these activities, syndecans can bind to morphogens and limit their availability to their receptors on the cell as well as their loss in the extracellular space, thus creating a morphogen gradient. SYND-3 binds to IHH which promotes the proliferation of chondrocytes (Pap and Bertrand, 2013). Syndecans undergo a regulated proteolytic cleavage, in the variable domain, according to a process called "shedding" (Manon-Jensen et al., 2010) which is mediated by external factors such as plasmin, thrombin and MMPs. This cleavage generates a soluble HSPG which can compete with membrane-attached syndecans for the binding of ligands *via* the GAG chains. SYND-1 and SYND-4 are both cleaved by MMPs after injury, a process which promotes cell migration and facilitates wound healing (Pap and Bertrand, 2013; Manon-Jensen et al., 2010). Consequently, MMPs play an essential role in normal renewal of the matrix and in pathological remodelling during inflammation, invasion, and metastasis. On the other hand, syndecans are protected from MMPs by binding tissue inhibitor of metalloproteinases (TIMPs) via their GAG chains (Manon-Jensen et al., 2010).

Glypicans

Glypicans are HSPG attached to the cell membrane via a GPI-anchor and consist of a family of six members. The core protein of glypicans exhibits an extracellular globular region with three to four attachment sites for HS GAG chains. The consensus sequence DSGSGSG, to which the GAG chains attach, is located between the central domain and the C-terminus. The C-terminal portion has the signal sequence necessary for the insertion of glypicans at the plasma membrane via the GPI anchor. Glypicans are able, thanks to their HS chains, to stabilize the interaction of the ligand such as Wnt with its receptor or to act as a low affinity co-receptor. Glypicans can be released into the extracellular medium under the action of phosphatidylinositol phospholipase C, D and/or proteases. Glypicans can control, by trapping extracellular ligands, their diffusion. They are involved in the signaling and transport of growth

factors (Fico et al., 2011). Glypicans regulates Wnt signaling patway and promote growth. Glypican-3 deficient mice exhibit several of the clinical features observed in patients with Simpson-Golabi-Behmel syndrome, including developmental overgrowth, perinatal death, cystic and dysplastic kidneys, and abnormal lung development (Filmus et al.,2009).

Betaglycan

Betaglycan belongs to the group of HSPGs and contains two GAG chain binding sites; it has a molecular weight of approximately 93 kDa. Betaglycan belongs to the superfamily of TGFβ co-receptors, also called TGFβ type III receptors (TGFβR3). It has a single transmembrane segment. The extracellular domain contains a site for the attachment of GAGs at positions 534 and 545 and protease-sensitive sequences in the vicinity of the transmembrane domain. The GAG chains are important for the function and for the downstream signaling of TGFβ. Betaglycan GAG chains regulate cell migration by interaction with co-receptors in the ECM (Mythreye et al., 2009a). However, the mechanism by which changes in betaglycan GAG chains regulate cell migration is still unknown. The soluble form of betaglycan inhibits TGFβ signaling and migration of breast cancer cells (Elderbroom et al., 2014). The short intracellular domain of betaglycan contains numerous serine and threonine residues that are phosphorylated by the PKC kinase and a PDZ binding domain (López-Casillas et al., 1991). Betaglycan regulates cell migration by interaction with β-arrestin 2 via the PDZ domain and mediates the activation of Cdc42**.** The knockout of betaglycan in mice (TGFβR3$^{-/-}$) is embryo lethal (Mythreye et al., 2009b).

1.2.4 Regulation of PG synthesis

PG synthesis is regulated by various cytokines and growth factors. The proinflammatory cytokine interleukin 1β (IL-1β) suppresses GAG synthesis (Gouze et al., 2001), whereas growth factors such as TGF-β and PGDF promote the synthesis of GAG chains. TGF-β induces the synthesis of CS-GAGs in the rat dental pulp cells (Nishikawa et al., 2000) and enhances the GAG synthesis in mesenchymal cells derived from the murine embryonic palate (D'Angelo and Greene, 1991). The synthesis of CSPGs in the nervous tissue is regulated by TGF-β and accumulation of CSPGs after nervous tissue injury plays an inhibitory effect on the repair process. TGF-β also induces the expression of CSPG core protein like neurocan, phosphacan,

brevican and of glycosyltransferase XT I (Susarla et al., 2011). PG-GAGs are important component of the articular cartilage and their synthesis is regulated by TGF-β and IL-1β (Pujol et al., 2008). TGF-β upregulates the expression of XT I, a rate limiting enzyme in GAG synthetic pathway, and enhance GAG synthesis, whereas IL-1β suppresses GAG synthesis and downregulation the expression of XT I (Khair et al., 2013; Venkatesan et al., 2009). It has been recently shown that the accumulation of GAGs in pulmonary fibrosis is mediated by TGF-β1 through upregulation of XT I (Venkatesan et al., 2014). It is recently shown that phosphorylated xylose by Fam20B kinase is an important regulator of both CS and HS biosynthesis (Izumikawa et al., 2015; van Kooyk et al., 2013).

1.2.5 Glycosylation

Glycans, or carbohydrate sugar chains, are covalent assemblies of sugars (oligosaccharides and polysaccharides) that exist in either free form or in covalent complexes with proteins or lipids (Yamanishi, Bach, and Vert 2007). There are evidences which support crucial roles of glycans in many cellular processes, including cell–cell communication, immune system, protein interaction or tumor progression (Fuster and Esko, 2005). Secreted and membrane proteins of eukaryotic cells are modified with complex glycans. Membrane proteins are formed by different types of modifications including: *N-linked glycosylation,* the attachment of N-linked saccharides to asparagines; *O-Glycosylation,* the attachment of O-linked mannose glycans to serine or threonine residues (Herscovics and Orlean, 1993; Stanley, 2011).

Glycosylation is a complex process that involves a large number of molecules and organelles (van Kooyk, Kalay, and Garcia-Vallejo 2013), it begins in the rough endoplasmic reticulum (ER) as a co- or posttranslational event, and proceeds as the glycoproteins migrate through the Golgi to their final destination **(Figure 1.15)**. According to Ouyang et al. (2010), the elaboration of the carbohydrate groups depends on the expression and sub cellular localization of the specific enzymes required for their biosynthesis and on the final destination and rate of transport of individual glycoprotein through the various sub cellular compartments. In addition, the extent of maturation of each carbohydrate chain is influenced by its location within the peptide as a function of protein conformation (Kukuruzinska and Robbins, 1987)**.**

1.2.6 Golgi Glycosylation

The Golgi apparatus is a polar organelle comprised of a stack of membrane-bound sacs termed cisternae. The *cis* face accepts vesicular traffic from the ER, and the trans face acts as the exit site for vesicular traffic. In the Golgi apparatus, a complex array of protein modifications may occur including glycosylation, deglycosylation, *O*- and *N*-sulfation, and *O*-acetylation, resulting in the formation of O-linked glycans (e.g. mucin-type *O*-linked glycans and PGs).

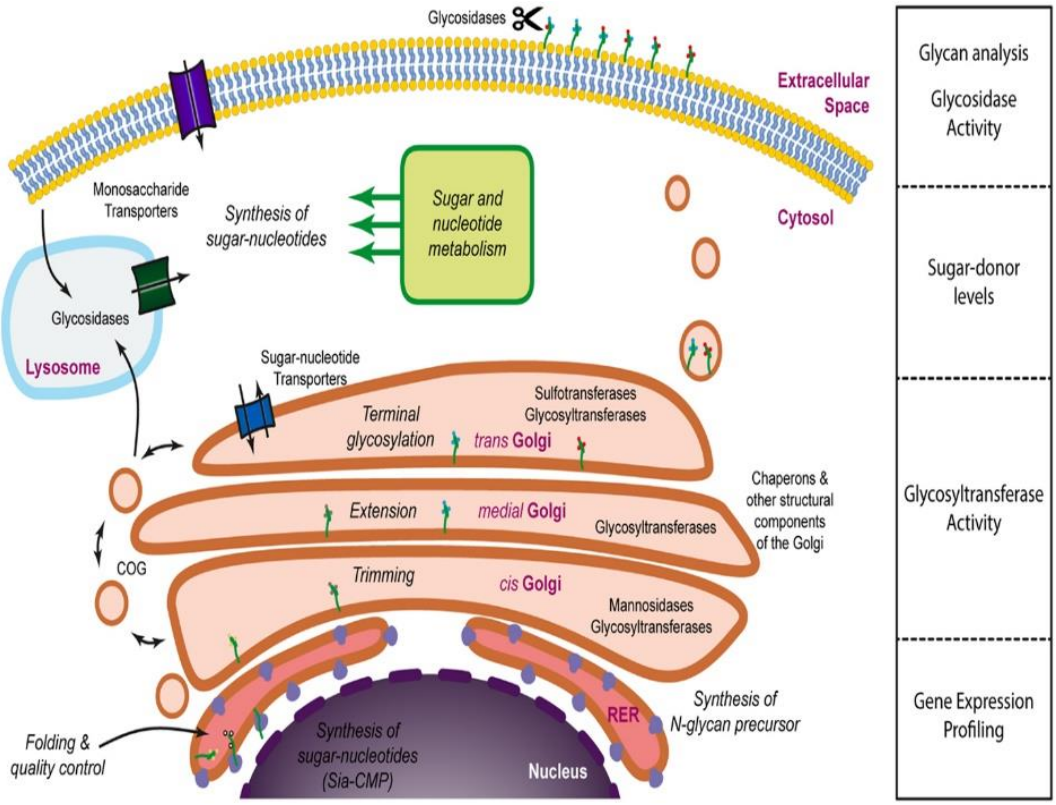

Figure 1. 15 : *Glycosylation machinery includes different enzymes, chaperones (proteins), transporters, sugar donors, and molecules necessary for the modification of proteins or lipids with carbohydrates (van Kooyk et al., 2013).*

Golgi glycosylation of proteins is a complex process depending on different activities of enzymes, transporters, but also a balance between vesicular Golgi trafficking, compartmental pH, and ion homeostasis. Protein glycosylation is certainly one of the major biosynthetic functions of the ER and Golgi compartments (**Figure 1.15)**. Any modification in the Golgi

stability/homeostasis can lead to abnormal glycosylation, this abnormal glycosylation may affect single or multiple organ system as shown in **Figure 1.16.**

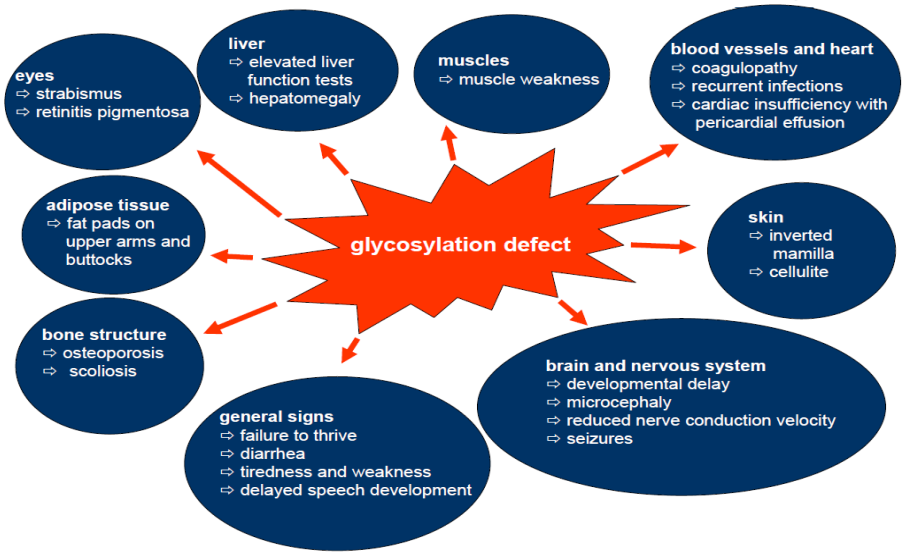

Figure 1. 16: *Glycosylation Defects in CDG patients. Individual present an extremely variable and complex phenotype, that ranges from single organ involvement to multisystem diseases.*

1.2.6.1 Factors Effecting Golgi Glycosylation

Golgi glycosylation is an extremely regulated process and relies on many different actors, including enzymes (directly related to glycosylation) and proteins (involved in the maintenance of the Golgi apparatus homeostasis). Each step depends on the existence of specific nucleotide sugar transporters and specific glycosyltransferases. **Figure 1.17** illustrates different factors regulating Golgi glycosylation.

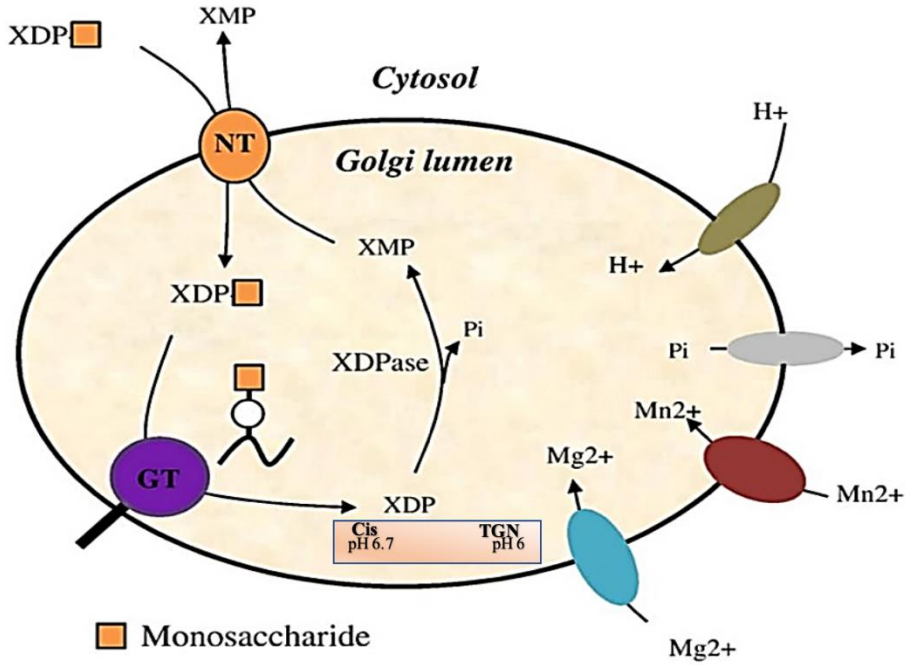

Figure 1. 17 : *Factors involved in Golgi Glycosylation regulation: The enzyme dependant process of glycosylation requires suitable environment and optimal pH, concentration of ions including H^+, Mn^{2+}, Mg^{2+} and inorganic phosphates (Pi). Example is the conversion of xylosyl diphosphate to xylosyl monophosphate and Pi by nucleotide diphosphatase activity. Synthesized dinucleotide sugars are transported from cytosol into Golgi Lumen via specific nucleotide sugar transporters (NT), these antiporters facilitate exchange with the respective mononucleotides to be used by Golgi GTs. (Adapted from Foulquier,2009).*

1.2.6.1.1 Divalent cations Mn^{2+} and Ca^{2+}

Divalent ions play a crucial role in Golgi homeostasis for a proper glycosylation process. Almost all Golgi GTs requires divalent cat ions such as Mn^{2+}, Mg^{2+}, Co^{2+} and Ca^{2+} for their activity (Powell and Brew, 1976).

Manganese (Mn2+)

Manganese is an essential transition element required by organisms of almost all the kingdoms. The primary source of Mn^{2+} is dietary intake that can provide the required amount

of Mn^{2+} for physiological processes including glycosylation, energy metabolism, immune functions, and antioxidant defence (Khoder-Agha et al., 2019). Mn^{2+} is important for several cellular processes including its non-enzymatic antioxidant property for neutralizing reactive oxygen species (ROS) and to constitute a co-factor for many enzymes such as mitochondrial enzymes, RNA and DNA polymerases, hydrolases, lyases, glutamine synthetase, integrins and Golgi GTs (Thines et al., 2019; Wedler et al., 1984). There are no strictly specific transporters for Mn^{2+} but a few actors of Golgi Mn^{2+} transport have been identified **(Table 1.2)** (Thines et al., 2019).

Table 1. 2: Manganese transporter in Human.

Human Transporter	Functions in Human Cells
DMT1 (Divalent metal transporter 1) *Smf1p and Smf2p* (yeast Mn^{2+}Transporting Ortholog)	Transport Mn^{2+} from endosomes to the cytosol Plasma membrane metal importer Involved in dietary manganese intake
NRAMP1 (Natural resistance-associated macrophage protein 2). *Smf1p and Smf2p* **(yeast Mn^{2+} Transporting Ortholog)**	Plasma membrane metal importer Mostly expressed in the phagosome of macrophages where it limits the bioavailability of metals to invading microbes
SPCA1 and SPCA2 (Secretory Pathway Calcium ATPase 1 and 2) *Pmr1p*	Golgi-localized Ca^{2+} and Mn^{2+} P-type ATPases Involved in manganese detoxification and Golgi Mn^{2+}supply
TMEM165 Gdt1p (yeast Mn^{2+} Transporting Ortholog)	Golgi-localized Ca^{2+} and Mn^{2+} secondary transporter Putatively involved in manganese detoxification and Golgi Mn^{2+}supply
ATP13A2 *Ypk9p* (yeast Mn^{2+} Transporting Ortholog)	Involved in Mn^{2+} transport from cytosol to the lysosome

ATP13A1 Cod1p (yeast Mn^{2+}Transporting Ortholog	Putative P-type ATPase transporter of Mn2+ into the ER
Transferrin receptor	Binds with $Fe^{3+}$and Mn^{3+}, transported to endosomes. Transferrin is then recycled and Mn^{3+} is reduced to Mn^{2+} and enters cytosol through DMT1
SLC39 family of transporters (SLC39A8 and SLC39A14)	Transports Mn^{2+} in addition to Zn^{2+}

Manganese trafficking across cells is regulated via several transporters localised in different organelles of the cells. Different transporters of Mn^{2+} across the cells are presented in **Figure 1.18**. Several studies have shown mechanisms of Mn^{2+} transport and homeostasis, however, mode of Mn^{2+} trafficking across the cells is still not clear. Influx, uptake, and efflux of Mn^{2+} is shared by Fe and/or Calcium and involves several shared transporters. Divalent metal transporter 1 (DMT1) facilitates absorption of Mn^{2+}/Fe and Ca^{2+} within enterocytes of the proximal part or small intestine. Since, DMT1 is also a H^+ symporter and transports one H^+ and one divalent cation in the same direction (Tuschl et al., 2013). Intake of Mn^{2+} rich diet can lead to increased transferrin (Tf) levels in plasma. DMT1 is encoded by gene SLC11A2 and mutation in this gene affects transport of Mn^{2+} and Fe across intestine and results in severe anemia in microcystic mice and Belgrade rats. (Burdo et al., 2001 and Chua and Morgan, 1997). Majority of the efflux of Mn^{2+} from enterocytes is via receptor Ferroportin (fpn). Mn^{2+} exposure significantly increases fpn expression with subsequent reduction of total cell Mn^{2+} and Mn^{2+} toxicity (Madejczyk and Ballatori, 2012).

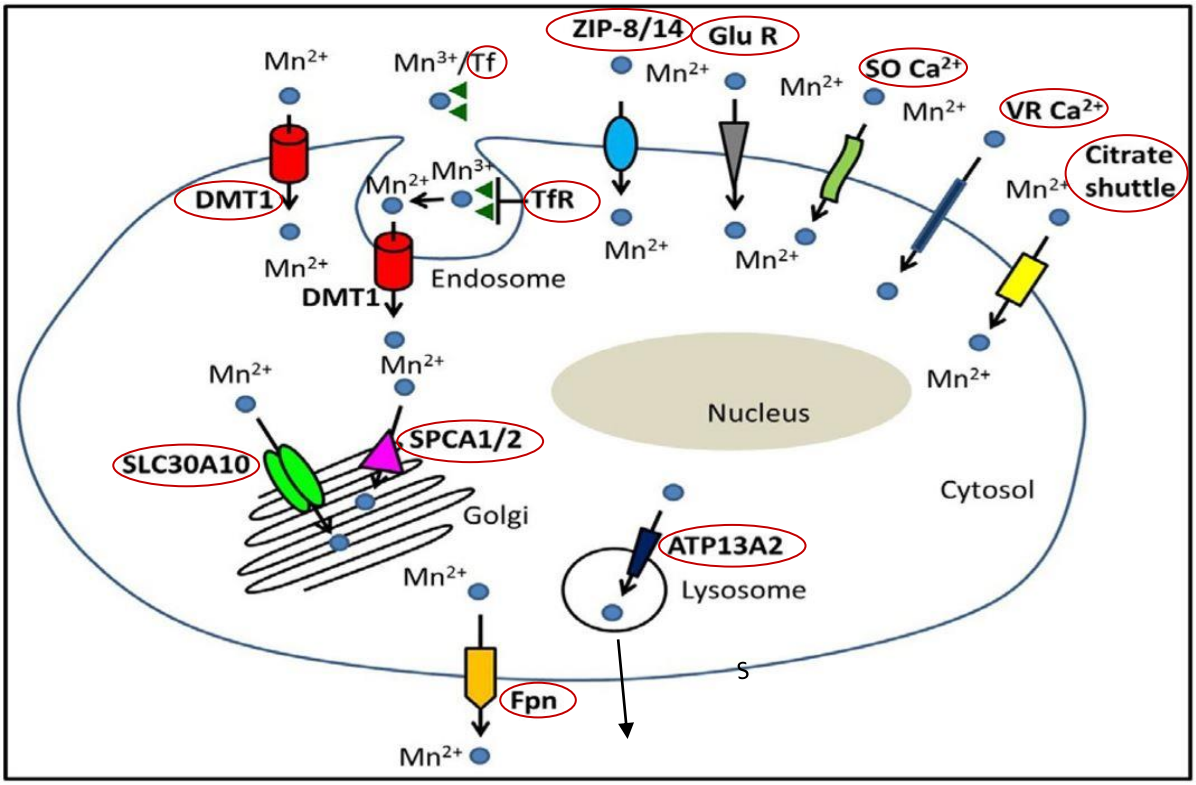

Figure 1. 18: *Mn^{2+} transporters across the cell (encircled): Manganese enters the cell mainly via Divalent metal transporter 1 (DMT1), Transferrin (Tf) and transferrin receptor (tfr); others receptors are glutamate receptor (Glu R); store-operated Ca^{2+} channel ($SOCa^{2+}$); voltage-regulated Ca^{2+} channel (VR Ca^{2+}) and it exits the cell mainly through fpn (ferroportin) and secretary pathways (Adapted and modified from Tuschl et al., 2013).*

Another key player in the regulation of Mn^{2+} homeostasis has recently been identified as a gene responsible for diseases in inherited Mn^{2+} overload syndrome. High concentrations of Mn^{2+} lead to increased SLC30A10 gene and protein expression in hepatocellular carcinoma cells suggesting role of SLC30A10 in detoxification of Mn^{2+} from cytoplasm. However, its role in efflux of Mn^{2+} outside the cell is needed to be studied. Another alternative for cytosolic Mn^{2+} detoxification is Golgi localised secretory pathway Ca^{2+}/Mn^{2+} ATPases 1 and 2 (SPCA1 and SPCA2). SPCA1 and SOPCA2 have high affinity for Ca^{2+}/Mn^{2+} therefore and regulate them within Golgi. Mn^{2+} accumulation in the Golgi and increased cell viability are caused by overexpression of SPCA1 (Mukhopadhyay and Linstedt, 2011). Golgi-localized Ca^{2+} and Mn^{2+} P-type ATPases 1 and2 (SPCA1 and SPCA2) are Involved in manganese detoxification and Golgi

Mn^{2+} supply. SPCA1 is encoded by ATP2C1 gene and is highly expressed, whereas SPCA2 expression if limited. Both the pumps control trafficking of Ca^{2+} and Mn^{2+} into the Golgi (Tuschl et al., 2013). Increased cell viability and accumulation of Mn^{2+} into the Golgi is associated with overexpression of SPCA1 (Mukhopadhyay and Linstedt, 2011). Mice exposed to higher concentrations of Mn^{2+} developed accumulation of Mn^{2+} in brain and showed high expression of SPCA1 that supports the role of SPCA1 in detoxification of Mn^{2+}. Loss of one copy of ATP2C (monoallelic mutations) in humans cause blistering skin disorder (Hailey–Hailey disease) (Vanoevelen et al., 2005; Roy et al. 2020). Mice exposed to high levels of Mn^{2+} develop Mn^{2+} accumulation in areas of the brain that show high expression of SPCA1 further supporting a role of SPCA1 in Mn^{2+} detoxification (Sepulveda et al., 2007). Recently, it has been published that SPCA1 governs the stability of TMEM165 in Hailey-Hailey disease (Roy et al., 2020). Mn^{2+} also compete for sarco-endoplasmic reticulum Ca^{2+} ATPase (SERCA) that transport both calcium and manganese across the cell (Tuschl et al., 2013). ATP13A2 (PARK9) encodes a P5type cation transporting ATPase located at the lysosome and is found to protect cells from Mn^{2+} induced toxicity. Overexpression of ATP13A2 leads to decreased levels of intracellular Mn^{2+}. Exposure to excess Mn^{2+} further induces ATP13A2 gene expression followed by sequestration of Mn^{2+} into the lysosomes (Tan et al., 2011).

The link between Mn^{2+} and glycosylation in human was revealed by studies on milk galactosyltransferases (Khatra et al., 1974). The enzyme β-1,4-Galactosyltransferase-I requires Mn^{2+} to be fully active. It has been shown that the synthesis of both N-acetyl-lactosamine and lactose requires the binding of Mn^{2+} to the co-substrate UDP-Gal before transfer to the acceptor monosaccharide substrate. In the case of the GTs involved in GAG chains synthesis such as the chondroitin synthases CHSY1 and CHSY2 that are responsible for CS chain elongation and possess both β-1,3-glucuronic acid and β-1,4-N-acetylgalactosamine transferase activities (Yada et al., 2003a). Divalent cations were essential for the function of the enzymes since the presence of EDTA completely abolished glycosyltransferase activities. In addition, β1,3-glucuronyltransferase 3 (β3GAT3) which is an important enzyme required for the synthesis of tetrasaccharide primer by the addition of the GlcUA residue to complete the tetrasaccharide linker of GAG chain contains a DXD motif (^{194}DDD^{196}) that has been shown to be in direct interaction with both UDP and Mn^{2+}. The β1,4-galactosyltransferase 7 (β4GALT7) enzyme that catalyses the transfer of the first galactose residue in the common

tetrasaccharide linker of GAG chain possesses a ^{163}DXD^{165} motif at the N-terminal hinge region of the long loop involved in Mn^{2+} binding. Isothermal calorimetric study revealed the conformational changes (closed conformation) in β4GALT7 upon binding to Mn^{2+} and UDP. In the absence of Mn^{2+} there was no closed conformation. It has been shown that the presence of Co^{2+} led to the highest level of β- 1,3-glucuronic acid activity, whereas Cd^{2+} and Mn^{2+} were 85% and 70% as effective as Co^{2+}, respectively. For β1,4-N-acetylgalactosamine transferase activity, Mn^{2+} exhibited the highest activity whereas Co^{2+} and Cd^{2+} were 70 and 53% as effective as Mn^{2+}. Chondroitin Polymerizing Factor (CHSY2, CHP) has been shown to require Mn^{2+} but can also be slightly activated by Co^{2+} (Müller et al., 2005). Potelle and contributors recently showed that Mn^{2+} supplementation is able to overcome the defects in N-glycosylation induced by deficiency of TMEM-165, therefore suggesting that TMEM165 is involved in Mn^{2+} homeostasis (Potelle et al., 2016; Potelle et al., 2017). Deficiency of Mn^{2+} can result in birth defects including abnormal or poor bone formation and susceptibility to seizures (Aschner et al., 2002; Wolff et al., 2018). Mn^{2+} overexposure has been reported to cause toxicity to the brain (Tuschl, Mills, and Clayton 2013).

Genetic Transportopathies of Manganese

Recently Anagianni and Tuschl (2019) have identified a new group of genetic defects caused by mutations in the carrier proteins of Mn^{2+}. These carrier proteins are SLC30A10 (Mn^{2+} efflux transporter) SLC39A14 (Mn^{2+} uptake transporter), and SLC39A8 (uptake of manganese).

SLC30A10 deficiency

SLC30A10 belongs to a family of metal transporters SLC30 family. Previously described as a Zn^{2+} transporter, however studies in yeast have shown that SLC30A10 is very important for Mn^{2+} transport (Tuschl et al., 2012). Deficiency of SLC30A10 lead to Hypermagnesemia with dystonia type 1 (HMNDYT1) (Anagianni and Tuschl, 2019). To date more than 30 patients have been reported with this disorder. Elevated levels of Mn^{2+} in blood (10 times more than normal) leads to hypermagnesemia, polycythaemia, chronic liver diseases (steatosis and cirrhosis) and iron depletion (as Mn^{2+} and Fe^{3+} compete for binding with several transporters) (Tavasoli et al. 2019). Mn^{2+} also induces erythropoietin gene expression as levels of erythropoietin were raised in some individuals with SLC30A10 mutations (Tuschl et al., 2008). The possible

effective treatment is iron supplementation in combination with EDTA-$CaNa_2$ (chelation therapy) to reduce Mn^{2+} accumulation, neurological symptoms, disease progression and stabilisation of blood Mn^{2+} levels.

SLC39A14 deficiency

Hypermagnesemia with dystonia 2 (HMNDYT2) syndrome is caused by bi-allelic mutations in SLC39A14 transporter. This syndrome is characterised by manganese neurotoxicity but not hepatotoxicity and polycythaemia (Anagianni and Tuschl, 2019). Dystonia caused by mutations in SLC39A14 progress rapidly with parkinsonism and several other neurological symptoms. Onset of symptoms is in early childhood and infancy. In *vitro* studies have shown that chelation may present a neuroprotective effect and some success has been obtained by chelation therapy with EDTA-$CaNa_2$ for individuals with mutations in SCL39A14 (Tuschl et al., 2016).

SLC39A8 Deficiency

Mutations in SLC29A8 transporter are characterised by low blood levels of Mn^{2+} associated with reduced activity of the β-1,4galactosyltransferase and Mn^{2+} superoxide dismutase (MnSOD) leading to congenital disorders of glycosylation type 2 N (CDG2N) and impaired mitochondrial function (Boycott et al., 2015; Park et al., 2015). Low blood levels of Mn^{2+} are associated with multiple signs including delayed development, dwarfism, seizures, dystonia short stature, deafness, and abnormal patterns of glycosylation. Initially one individual showed normalisation of glycosylation patterns when treated with oral galactose (Park et al., 2015), and two individuals treated with oral supplementation of MnSO4 showed significant improvement in motor and hearing abilities and normalization of β1,4galactosyltransferase function (Park et al., 2018).

1.3 Congenital Disorders of Glycosylation (CDG)

Congenital Disorders of Glycosylation (CDG) is a rare inherited metabolic disease characterised by defects in genes involved in the glycosylation process (biosynthesis of glycolipids and glycoproteins) (Jaeken 2003; Péanne et al. 2018; Potelle et al. 2016). The first identified cases of CDG were twin sisters in 1980. These twin sisters presented psychomotor retardation with multiple abnormalities in serum glycoproteins associated to deficiency in phosho-manno-mutase (PMM2) involved in the conversion of Man-6P to Man-1P during the biosynthesis of GDP-mannose, an essential nucleotide sugar for the synthesis of the oligosaccharide precursor of *N*-glycosylation in the ER (Jaeken & Péanne, 2017).

CDG can be associated with a broad variety of symptoms and can vary in severity from mild cases to severe disabilities or life-threatening cases. CDG are usually apparent from infancy. Individual CDG are caused by a mutation to a specific gene (Paesold-Burda et al., 2009). Over 100 human genetic disorders have been identified which results from mutations in glycosylation related genes and in vesicular trafficking and/or sorting of glycoprotein (Foulquier et al., 2006; Reynders et al., 2009; Kornak et al., 2008).

The first test classically used in CDG laboratory is the iso-electrofocalisation (IEF) of the serum transferrin that contains two N-glycosylation sites, which are occupied most of the time by bi-antennary complex N-glycans. The terminal sialic acid residues carried by complex N-glycans confer positive charges to transferrin. Therefore, serotransferrin can be analysed by IEF and the migration profile reflects the N- glycosylation pattern **(Figure 1.19)** (Jaeken et al., 2007; Jaeken et al.,2014; Jaeken et al.,2017).

Type I CDG causes abnormalities in the synthesis of precursors of glycosylation (ER) that result in type I pattern of serum transferrin **(Figure1.19)**. This results in complete loss of glycans at the glycosylation sites of serotransferrin (Jaeken et al., 2007). However, individuals with Type II CDG is associated with abnormal or incomplete glycans within the Golgi (Potelle et al., 2015).

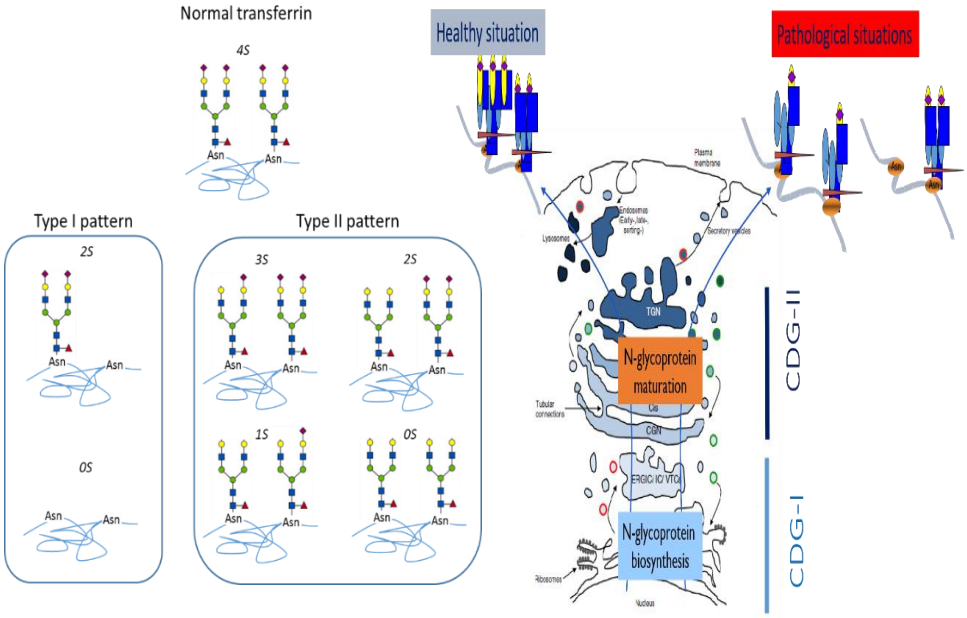

Figure 1. 19 : *Type I and type II CDG:* ***(A)*** *Structure of N-Glycans, Serum Transferrin represented as glycan structure in healthy conditions contains 4 sialic acids (4S). Isoforms are shown* ***(B)*** *Hyposialation and hypogalactosylation of serum N-glycoproteins result in type I and type II pattern of CDG.*

In 2012, Foulquier and collaborators using SiRNA technique in HEK cells discovered a new Golgi protein, TMEM165 (also named TPARL (OMIM entry #614727) as a gene involved in CDG causing Golgi glycosylation defects and is extremely conserved in eukaryotes. TMEM165 encodes a putative transmembrane 324 amino acid protein whose cellular functions are unknown (Foulquier et al., 2012). In addition to an unusual skeletal phenotype with growth defects, TMEM-165 CDG Individuals also present hyposialation and hypogalactosylation of their glycoproteins (Houdou et al., 2019). Almost a dozen patients have been reported as TMEM165-CDG to date (Lebredonchel et al., 2019). All of them present a type-II serotransferrin isoelectrofocalisation pattern. Most serious phenotypes present psychomotor disability, human growth hormone resistance, facial hypoplasia, microcephaly, elevated serum transaminases, seizures, hypotonia and hepatosplenomegaly, cardiac defects are also seen in some patients (Marques-da-Silva et al., 2017), however bone and cartilage dysplasia and severe osteoporosis remain the most significant signs. Strong defect in the Golgi

glycosylation characterised by Hypogalactosylation of N-Glycoprotein is common in all patients with TMEM165-CDG (Foulquier et al., 2012; Lebredonchel et al., 2019).

1.4 TMEM 165

TMEM165 is a Golgi transmembrane protein belonging to an uncharacterized family of transmembrane proteins named UPF0016 (uncharacterized protein family 0016) and is a 34.9 kDa protein predicted to encode 324 amino acids that is ubiquitously expressed. This protein is localized in Golgi. TMEM is characterized by two motifs E-LGD-K+ and E-WGD-R+ and is extremely well conserved. Even if it is highly conserved during evolution from yeast to human, its biological function is still debated. TMEM165 was first described as a Golgi cation antiporter by sequence analogy with other members of the family (Foulquier et al. 2012). Later it was demonstrated that the Golgi glycosylation defect due to TMEM165 deficiency in patients and in TMEM165 knockout (KO) cells resulted from a defect in Golgi Mn^{2+} homeostasis thus linking TMEM165 with Mn^{2+} homeostasis and suggesting that it may import Mn^{2+} into the Golgi stacks. This is reinforced by the thylakoid Mn^{2+} import *via* photosynthesis-affected mutant 71 (PAM71) transporter, the Arabidopsis thaliana ortholog of TMEM165 (Lebredonchel et al., 2019). TMEM165 deficiency resulted from Golgi manganese homeostasis defect and that 1 mM Mn^{2+} supplementation was sufficient to rescue N-glycosylation (Potelle et al., 2016, Vicogne et al., 2020). TMEM165-CDG patients present a broad range of clinical features. Some of them are found in most of the CDG, for example growth retardation, dysmorphy and failure to thrive **(Figure 1.20).**

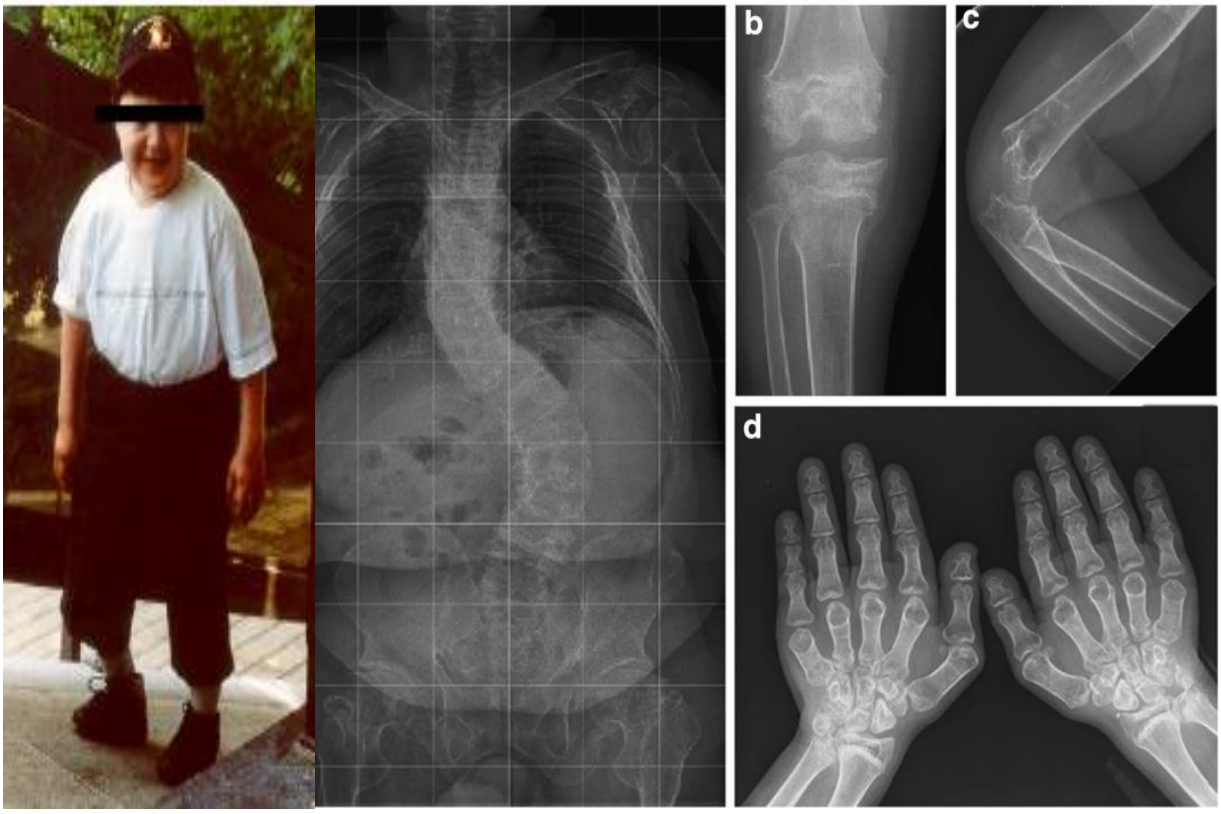

Figure 1. 20 : *Radiological presentation of the skeleton of patient (in the photo). (a) full spine at 20 years; (b) knee at 14 years 4 months; (c) elbow at 15 years 6 months; (d) hands at 15 years 6 months (adapted from Zeevaert et al., 2013).*

Among the first five TMEM165-CDG patients described, four of them present a major skeletal dysplasia (spondyloepimetaphyseal dysplasia) with spine curvature, joint flexibility, and short stature. This skeletal phenotype is a key feature of TMEM165-CDG, as it is not found in other CDG described to date (Zeevaert et al., 2013). The sixth reported patient did not show any clear skeletal abnormalities. However, this patient died at the age of 5 months due to complications and one is presumably too young to develop a strong skeletal dysplasia (Althoff et al., 2015).

Almost a dozen TMEM165-CDG patients have been reported but its cellular and molecular functions are still unknown. It may function as a calcium/proton transporter involved in calcium and in lysosomal pH homeostasis. Therefore, it may play an indirect role in protein glycosylation. TMEM165 deficiency is associated with Golgi glycosylation abnormalities that could result from a lack of Golgi Mn^{2+} as Mn^{2+} is proved to be an important co-factor of enzymes involved in Golgi glycosylation. By using UDP-sugars as a donor substrate, Golgi GTs require Mn^{2+} to be attached to their catalytic site to activate them completely and to induce an open conformation allowing binding of the substrates **(Figure 1.21)**.

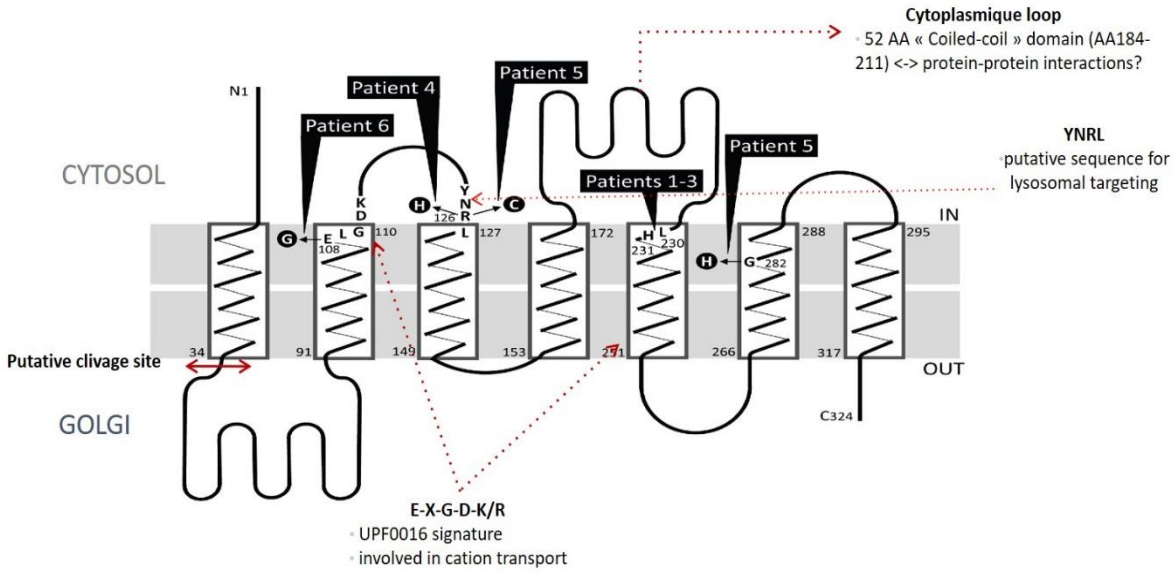

Figure 1. 21: *Predicted topography of TMEM-165 numbers indicate the positions of amino acid residues on the predicted topology model (Potelle et al., 2016).*

It has been shown that gdt1, the yeast ortholog of TMEM165 was involved in Ca^{2+} uptake, therefore suggesting the possible involvement of TMEM165 in Ca^{2+} homeostasis (Demaegd et al., 2013; Thines et al., 2018). Interestingly, Thapsigargin-induced Ca^{2+} release was reduced in cells overexpressing TMEM165 suggesting that TMEM165 may regulates cytosolic calcium homeostasis (Demaegd et al., 2013). However, it has also been studied that yeast lacking TMEM ortholog showed deficiencies in N-glycosylation caused by high concentration of Ca^{2+} and decreased Mn^{2+} as the deficiencies were restored by addition of 1µM $MnCl_2$ (Thines et al., 2018). Gdt1p is found to be an antiporter or cotransporter of Mn^{2+}/Ca^{2+} Since, Ca^{2+} and Mn^{2+} compete for Gdt1p inside Golgi lumen. Gdt1p is shown to extrude Ca^{2+} to reduce competition between the two ions (Colinet et al., 2016; Stribny et al., 2020). Higher Mn^{2+} concentration causes instability of TMEM165 and its ortholog in yeast. Higher Mn^{2+} led to degradation of

TMEM165 in lysosomes (TMEM165) or vacuoles (Gdt1p) (Dulary et al., 2017; Potelle et al., 2016).

On the other hand, studies have shown that TMEM165 may play a role in H^+ homeostasis in the Golgi. Indeed, deficiency of TMEM165 is found to a decrease in pH in of lysosomal and endosomal compartments (Jinn et al., 2017). Recently, TMEM165 expression has been found increased during lactation suggesting the role of TMEM 165 in Ca^{2+} homeostasis during first two weeks following parturition (Snyder et al., 2019). It has been demonstrated that TMEM 165 expression depends on SPCA1 (Secretory pathway Ca2+-ATPase pump type 1). SPCA1 is a Golgi localised protein that regulate Ca^{2+}/Mn^{2+} trafficking across the Golgi apparatus and its loss resulted in complete loss of TMEM165. Another study showed that TMEM expression is dependent on the ion (specifically Mn^{2+}) pumped by SPCA1 and the deficiency of TMEM165 expression if rescued by exogenous supplementation with Manganese (Lebredonchel et al., 2019). The molecular mechanisms how the SPC1 mutants maintain their glycosylation is unknow the deficiency of SPCA1 was not responsible for defects in glycosylation, but it is established that TMEM165 deficiency led to serious defect in glycosylation (Lebredonchel et al., 2019). It has been established that higher cytosolic concentration of Mn^{2+} causes TMEM165 degradation. And SPCA1 detoxify the cell by preventing Mn^{2+} influx in the cytosol (Potelle et al., 2016). All these research evidence confirm that TMEM165 is very important Golgi protein responsible for maintaining Golgi ion homeostasis and its deficiency leads to severe glycosylation defects.

Bone defects and skeletal abnormalities have been studied in human and animal models. The relationship between skeletal development and abnormalities in ECM are found associated with chondrogenesis and maturation of growth plate. In addition, several compounds of ECM mainly PGs have a significant role in chondrogenesis and osteogenesis. These PGs and their GAG chains play an important role as co-factors and regulators of signaling responsible for chondrocytes maturation and growth plate development. These distinct ECM compounds are the product of glycosylation that requires several glycosyl transferases for the synthesis of PGs and their GAG chains. Active binding sites of most of the GTs (XTI, XTII, β3Galt6 and many others) require Mn^{2+} for their enzymatic activity. Thus, any alteration or abnormalities in Manganese homeostasis due to TMEM165 deficiency can cause abnormalities in PGs and GAG

chain synthesis and consequently result in skeletal abnormalities observed in TMEM165 CDG patients. Indeed, GAG are key glycan structures of proteoglycans from the ECM.

Although it is now clear that the glycosylation defect in TMEM165 deficient cells is linked with disturbance of Golgi Mn^{2+} homeostasis. One of the main objectives of my thesis was to explore the molecular mechanisms leading to skeletal abnormalities in TMEM165-CDG patients.

2 Research objectives

The discovery of TMEM165 as a deficient protein in patient with congenital disorders of glycosylation has given a new direction to the glycosylation and CDG research. TMEM165-deficient CDG patients present bone abnormalities suggesting a potential involvement of TMEM165 in chondrogenesis and bone homeostasis. It is important to note that proteoglycan synthesis disturbances are associated with many conditions including cancer, osteoarthritis, fibrosis, diabetes, and Alzheimer's, as well as abnormalities in skeletal development such as chondrodysplasias.

Therefore, on basis of recent developments on TMEM165 and CDG, we hypothesize that there may be a relationship between TMEM165, proteoglycan synthesis and skeletal development. For this, we set specific objectives as:

1) Development and validation of TMEM165-knockout prechondrogenic cell line ATDC5 and human embryonic kidney cells, HEK293.

2) Determine the link, if any, between TMEM165 and proteoglycan synthesis and investigate the mechanisms involved using TMEM165-knock-out cells and human fibroblasts from TMEM165-deficient CDG patient.

3) Explore key signaling pathways that regulate chondrocytes maturation in TMEM165-deficient ATDC5 cells.

4) Investigate chondrocyte maturation and explore markers of chondrogenesis and osteogenesis to decipher the mechanisms and factors that may cause chondrocyte defects in skeletal development in TMEM165-deficinet CDG patients.

3 MATERIALS AND METHODS

3.1 Materials and Methods

3.1.1 Cell culture

In this thesis we have worked with four types of commercially available cell lines ATDC5 and HEK293, whereas human fibroblasts from CDG patients deficient in TMEM165 were given by a teamin Lille, France. **(Table 3.1)**. Cells were cultured in appropriate medium. The medium was supplemented with 2 mM glutamine, 100 IU/mL penicillin, 100 µg/mL streptomycin and heat inactivated foetal bovine serum (FBS). When cells are confluent, they are trypsinized with 0.05% trypsin in PBS. Briefly, the cells were washed with PBS and trypsinized at 37°C for 3 min. The detached cells were suspended in 10 mL complete medium and centrifuged at 1000 rpm (300xg) for 5 min. The cell pellet was suspended in 10 mL of complete medium and a fraction was stained with 0.1% (w/v) Trypan Blue then counted with TC20 automated cell counter (Bio-Rad). The cells were cultured in 6 and 12 well plates at 200,000 cells/ well and 100,000 cells/ well, respectively for subsequent experiments.

Table 3. 1: Different types of Cell lines and their respective medium

Cell line	Medium
Pre-Chondrogenic cell line ATDC5 *(mus musculus)*	DMEM-F12 supplemented with 2mM glutamine, 100 IU/ml penicillin, 100 µg/ml streptomycin and 5% heat inactivated feotal bovine serum (FBS)
Human skin fibroblasts from CDG patients deficient in TMEM165	DMEM supplemented with 2mM glutamine, 100 IU/ml penicillin, 100 µg/ml streptomycin and 10% heat inactivated foetal bovine serum (FBS)
Human embryonic Kidney cell line HEK293 *(Homo sapiens)*	DMEM supplemented with 2mM glutamine, 100 IU/ml penicillin, 100 µg/ml streptomycin and 10% heat inactivated foetal bovine serum (FBS)

3.1.2 Knocking down TMEM 165 using CRISPR CAS9

CRISPR (clustered regularly interspaced short palindromic repeats) is one of the current generations of genome editing technologies; the most rapidly developing is the class of RNA-guided endonucleases known as Cas9 from the microbial adaptive immune system, which can be easily targeted to virtually any genomic location of choice by a short RNA guide. This system enables targeted gene cleavage and gene editing in a variety of eukaryotic cell. By this system mutations are introduced into the DNA (Hsu, Lander, and Zhang 2014). CRISPR/Cas9 consist of two components **(Figure 3.1)**; an enzyme called Cas9 acts as a pair of 'molecular scissors', can cut the two strands of DNA at a specific location in the genome so that bits of DNA can then be added or removed. The other component is a piece of RNA called guide RNA (gRNA) consisting of a small piece of pre-designed RNA sequence (about 20 bases long) located within a longer RNA scaffold. The scaffold part binds to DNA and the pre-designed sequence 'guides' Cas9 to the right part of the genome. This makes sure that the Cas9 enzyme cuts at the right point in the genome.

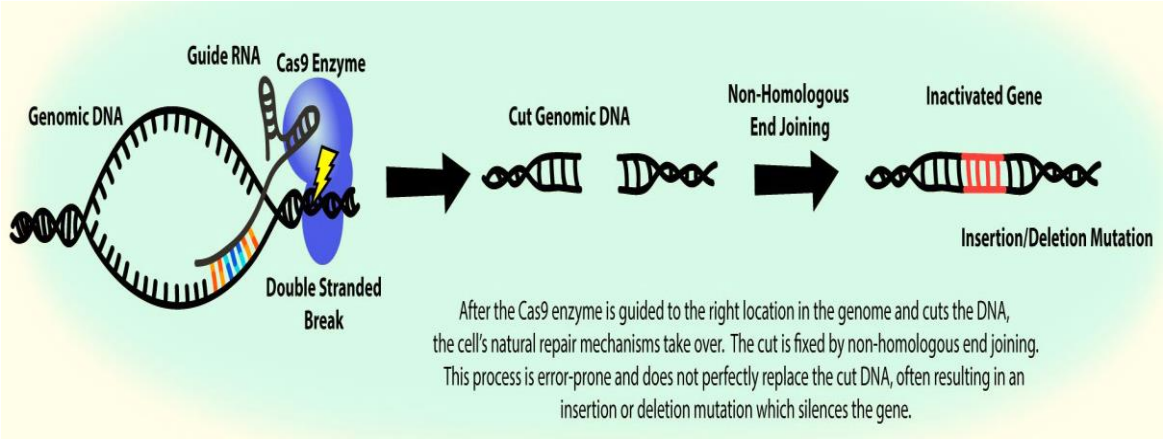

Figure 3. 1 : *Schematic representation of Gene Silencing using CRISPR/CAS9 (Adapted from:* https://i2.wp.com/sitn.hms.harvard.edu/wp-content/uploads/2017/01/CRISPR-Editing-Overview-02.jpg.

3.1.2.1 RNA guide vector construction

1µg of sense and antisense sequences for RNA guides are first annealed in annealing buffer (60mM Tris-HCl, pH7.5; 500mM NaCl; 60mM $MgCl_2$; 10mM DTT). Then annealed RNA

guide is diluted and ligated in pUC56 vector, previously digested by BbsI restriction enzyme. Insertion of the guide in the vector is verified by sequencing (Eurofins, Ebersberg, Germany). Sequence used are:

Forward CAC CGC TAT AAC CGG CTG ACT GTG C

Reverse AAA CGC ACA GTC AGC CGG TTA TAG C

3.1.2.2 Transfection

ATDC5 cells were seeded as $2x10^5$ cells per well in six well plates and allowed to grow for 24h until they reach 80% confluency, then transfected with 100ng SVneo vector (that confer resistance to geneticin), 1 µg DNA Guide for TMEM 165 and 1 µg Cas-9 vector in presence of 5 µL of transfection reagent Lipofectamine 2000© (Invitrogen) according to the purchaser's instruction. Briefly, vectors are mixed in 250 µL OptiMem© medium (Invitrogen) as well as 5 µL of transfection reagent Lipofectamine 2000© in 250 µL OptiMem medium. After 5 min incubation, the DNA mixture was added to transfection mix and incubated for 20 minutes at room temperature before being added drop wise to each well containing 1.5mL fresh complete medium. After overnight culture, the medium was replaced and when cells grown confluent, they were trypsinized and cultured in 2 round plates with a ratio of ½ and ¼, and the medium was replaced with medium containing 0.2 mg/mL geneticin after every 2 days until visible clones grow. Visible clones were picked using 5µl 10X trypsin and amplified. Genomic DNA was prepared for validation.

Briefly, the genomic DNA was extracted using QIAamp DNA Kit (Qiagen) according to manufacturer's instructions. The region containing the guide sequence was amplified by PCR using appropriate oligonucleotides. The PCR product was analysed by Agarose gel (2% w/volume) and sequenced (Eurofins Genomics). Clones that harbour mutations in the guide region were selected as positive clones, the other that do not show any mutation were used as negative control.

Sequences of primer used for amplification were:

Forward GACACCAGTCGCCCCAG TTCATACC

Reverse CCCCAATCACTGTGCTCC CGGTCA

3.1.3 Plasmids

3.1.3.1 Cloning of HA-SYND4 plasmid, promotors of TGFβ and BMP, Decorin-CMV

HA-SYND4 and Decorin were generated by polymerase chain reaction and were cloned into EcoRI and BamHI sites of empty vector pCMV purchased from Stratagene, Valencia, CA. TGFβ and BMP human gene promoters was generated by PCR and cloned into BamHI and HindIII sites of pGL3-Basic purchased from Promega, Madison, WI to generate TGFβ and BMP firefly reporter vector. These vectors were verified by sequencing.

3.1.3.2 Transformation

Chemically Competent One Shot® TOP10 E. coli obtained from Invitrogen was incubated with 2µg of plasmid by pipetting the required volume of plasmid containing 2µg plasmid into 30-50 µl of thawed One Shot® on ice for 30 min followed by incubating exactly for 30 seconds at 42 °C in a water bath. Vials were immediately placed on ice for several seconds. 250 µl of pre-warmed SOC medium (a rich medium) was added to each vial and cultured at 225 rpm in a shaking incubator at 37°C for exactly 1 hour. Cells were spread on Luria-Bertani (LB)-agar (Difco, France) plates containing 100 µg/ml ampicillin and incubated inverted at 37°C overnight. On the second day, colonies were isolated and analysed.

3.1.3.3 Purification and extraction of plasmid

Each plasmid was purified using QIAGEN Kits purchased from Qiagen, Hilden, Germany according to manufacturer's instructions. Bacterial cells were obtained by centrifugation (of transformed bacteria cultured in Luria-Bertani (LB) Medium purchased from *Difco, France* supplemented with 100 µg/ml ampicillin for 15 min, at 4 °C, at 6000 × g, the pallet was then resuspended in pre-cold Buffer P1. The Buffer P2 was added and sealed tube was vigorously inverted 4-6 times and incubated at room temperature for 5 minutes. Buffer P3 was added and mixed immediately, then incubated on ice for 5 min followed by centrifugation at 13000 x g, at 4°C for 10 min. The supernatant was applied carefully to the pre-equilibrated QIAGEN-tip 20. The DNA in the tip was washed twice with the QC Buffer QC which was then eluted by QF Buffer. 0.7 volumes of Isopropanol were added to precipitate the DNA by centrifugation for 30min, at 4°C, at 13000 rpm, supernatant was carefully decanted and DNA pallet was

washed with 70% ethanol and then air-dried for 5-10 min. Pallets were dissolved in DNase-free water and DNA concentration was measured using NanoDrop spectrophotometer (Thermo Scientific).

3.1.4 Proteoglycan anabolism

ATDC5 control and TMEM KO cells were cultured in plate 6 wells up to 90% confluence then they are labelled 6 h (for global anabolism analysis) or overnight (for SDS-PAGE analysis) in complete medium containing 10 µCi/mL Na_2 [^{35}S] SO_4. The medium was collected and then centrifuged for 10 minutes at 14,000 x g. The supernatant containing the radiolabelled PGs is digested with papain (0.1 µg/µL) overnight at 60°C to release the GAG chains. After digestion, the papain activity is inhibited by heating at 100°C for 10 min then the medium is centrifuged for 15 minutes at 14,000 x g to remove cellular debris. Then the chains of GAGs are precipitated with 5% CPC (Cetylpyridinium chloride) (w/v) and incubated at 37° C for 4h. After centrifugation for 15 min at 14,000 x g, the pellet is taken up in a volume of 1% CPC (w/v) and the mixture is incubated for 2 h and then centrifuged at 14,000 x g for 15 min. The same step is repeated with 0.5% CPC (w/v) and finally the pellet of GAGs radiolabelled is recovered and the samples are analysed either by counting in the scintillation liquid either by migration on a 10% polyacrylamide gel (SDS-PAGE).

3.1.5 Transfection of cells for proteoglycan synthesis analysis

Prechondrogenic ATDC5 cells were cultured in 6 well plates at $2.5x10^5$ cells /well. When cells reached about 80% confluency, they were transfected with 1 µg of Decorin CMV vector (expressing human decorin core protein) or Syndecan 4-HA CMV vector (expressing Syndecan 4 core protein tagged with HA motif) as previously described. After overnight culture, the medium was replaced with fresh complete medium (for Syndecan 4-HA transfected cells) or without FBS (for decorin transfected cells); after 24 h the medium of decorin transfected cells was collected and centrifuged at full speed for 20 min at 4°C the supernatant transferred to new tube. 5 µL of 2X Laemmli blue was added to 5 µl medium and proteins were analysed by western blotting. 48 h after adding fresh medium, proteins were extracted from cells transfected with syndecan 4-HA as described further to be analysed by western blotting.

3.1.6 Treatment of cells

In order to study the endogenous response of cells to $MnCl_2$ and to different growth factors that are responsible for induction of their respective signalling pathways, $2x5.10^6$ cells per well were seeded in a 6 well plate and they were grown until they reach 80% confluency in 6-well plate in the presence of complete medium. Cells were then starved in medium without of FBS for two hours and were treated with 1 µM concentration of $MnCl_2$ for 48 h and/or 1 ng/mL of TGFβ1 and 1ng/mL BMP2 in complete media for 1 h and or overnight, as mentioned in the figure legend.

3.1.7 Western blotting

3.1.7.1 Protein Extraction

Protein extraction was performed for intracellular analysis of proteins using western blot. After cells being cultured, they were transfected and/or treated, then, they were washed twice with ice cold phosphate buffer saline (PBS). The cells were then lysed by ice-cold radioimmunoprecipitation assay buffer (RIPA), this is an efficient and rapid buffer for solubilization and/or cell lysis for both adherent and suspension cultured mammalian cells. RIPA buffer is supplemented with protease inhibitor cocktail (Roche Molecular Biochemicals). After lysis, the cell lysate was transferred to tubes where the cell lysate was then sonicated (Vibra Cell, Bioblock Scientific) two times for five second and centrifuged at 12,000 x g for 20 min at 4°C. The supernatant was transferred to a new tube and the protein concentration was determined by the Bradford method (Bradford 1976).

3.1.7.2 SDS-Page Electrophoresis

30 µg of proteins with Laemmli buffer were heated at 95°C for 5 min and loaded onto 10% SDS-page gels with running buffer. Proteins were electrophoretically separated and transferred to a polyvinylidene difluoride (PVDF) membrane (Bio-Rad) using Trans-Blot turbo transfer system (Bio-Rad) with transfer buffer for 15 min at 12 V. The membranes were blocked in 5% (w/v) non-fat milk powder in TBST for 1 h at room temperature with mild agitation and washed 3 times for 5 min in TBST. The membranes were probed with appropriate primary antibodies and incubated overnight at 4°C. Next day, the membranes

were washed 3 times for 5 minutes in TBST and probed with appropriate secondary antibody (diluted in 5% milk) conjugated with horseradish peroxidase and incubated for 1 h at room temperature. After washing 3 times for 5 min in TBST, membranes were incubated in Clarity ECL reagent (Bio-Rad) for 5 min and wrapped in a plastic film and exposed to X-ray film (GE Healthcare). The film was then developed and fixed using Kodak developer and fixation solution (Sigma-Aldrich). Antibodies used for western blot are mentioned along with dilution in **Table 3.2**.

Table 3. 2: Antibodies used for the western blot

Antibodies	Dilution	BSA or Milk	Supplier
Anti-TMEM 165	1:1000	5% Milk in TBST	Sigma Aldrich
Anti-HA	1:10000	5% BSA in TBST	Biolegend
Anti -pERK1/2	1:1000	5% BSA in TBST	Cell Signalling
Anti -ERK1/2	1:1000	5% BSA in TBST	Cell Signalling
Anti -pSmad 1/5/9	1:1000	5% BSA in TBST	Cell Signalling
Anti -pSmad 2	1:1000	5% BSA in TBST	Cell Signalling
Anti -Smad total	1:1000	5% BSA in TBST	Cell Signalling
Anti- BMPRII	1:1000	5% BSA in TBST	Cell Signalling
Ant-TGFβR2	1:1000	5% BSA in TBST	Cell Signalling
Anti p-CamKII	1:1000	5% BSA in TBST	Cell Signalling
Anti CamKII	1:1000	5% BSA in TBST	Cell Signalling
Anti β-actin	1:6000	5% BSA in TBST	Sigma Aldrich
Anti-Asporin	1:1000	5% Milk in TBST	Abcam
Anti-rabbit IgG, HRP	1:2000	5% Milk in TBST	Cell Signalling
Anti-mouse IgG, HRP	1:2000	5% Milk in TBST	Cell Signalling
Anti-Human Decorin	1:1000	5% BSA in TBST	R&D Systems

3.1.8 Immunofluorescence

Cells were seeded (3000 cells/well) on to the coverslips in 24-well plate and allowed to grow for 24 h. Cells were washed with PBS and fixed with 4% (w/v) paraformaldehyde solution; after quenching with 150mM NH_4Cl, cells were permeabilized with 0.1% Triton-X100. The cells were

blocked in PBS containing 0.2% fish skin gelatine. Next, cells were incubated with anti TMEM165 antibody (1:200, sigma Aldrich) for 20 min and washed with PBS three times and incubated with Alexa-conjugated secondary antibodies. The nuclei were stained with DAPI. Digital images were captured with an inverted microscope, Leica DM13000 (Leica microsystem, Germany).

3.1.9 Cell proliferation assay

Cell proliferation was measured using CyQUANT NF Cell Proliferation Assay Kit (Invitrogen) according to manufacturer's instructions. Briefly, cells were seeded in 96 well plates at $2x10^4$ cells/well. After 24 h, cells were labelled with DNA binding dye for 1 h at 37°C and fluorescence of each sample was measured using a microplate reader Varioskan Flash Multimode reader (Fisher Scientific) with excitation at 485 nm and emission detection at 530 nm.

3.1.10 Gene expression analysis

3.1.10.1 Isolation of total RNA from cells

RNA was extracted from the cellular monolayer by RNA extraction kit (Qiagen). Briefly, cells were lysed in 600 µL of RLT buffer (containing 2-mercaptoethanol). The cell lysate was collected into the RNase free tube containing an equal amount of 70% ethanol. Afterwards, cell lysate was applied to the RNAeasy spin column and centrifuged 15 s at 8,000 rpm. Flow-through was discarded, 700 µL Buffer RW1 buffer was added and column was centrifuged for 15 s at 8,000 rpm. Flow-through was discarded and column was washed with 500µLRPE buffer, centrifuged for 15 sec at 8000 rpm followed by second centrifugation at 12,000 rpm for 2 min. RNeasy spin column was placed in a new 1.5 mL RNase free collection tube and total RNA were eluted in 30 µL of RNase free water.

Concentration of RNA was measured by a NanoDrop spectrophotometer (Thermo Scientific), and quality was assessed by A260/A280 ratio (1.8~2.1 was considered optimum**).**

3.1.10.2 Reverse Transcription (RT)

The cDNA was synthesized from total RNA using iScript reverse transcription supermax (Bio-Rad) according to manufacturer's instructions. Briefly, total RNA (500 ng) was mixed with 4 µL

of 5x iScript reaction mix (containing dNTPs, oligo(dT), random hexamer primers, buffer and MgCl2 iScript reverse transcriptase). Reaction volume was adjusted to 20 µL by nuclease-free water and RT was performed using Eppendorf thermal cycler. Reaction parameters were 5 min at 25°C, 30 min at 42°C and 5 min at 85°C. cDNAs were used for quantitative PCR or stored at -20°C for further experiments.

3.1.10.3 Real-time qPCR

The quantitative PCR reaction was carried out with the iTaq ™ Universal SYBER Green supermix kit (BIO-RAD, Hercules, CA) using the StepOnePlus ™ Real-Time PCR Systems (Applied Biosystems), in a final volume of 20 µL using the method of relative standard curve. Standard curves were made using matrices grouping together all the cDNAs used during the manipulation. 2 µL cDNAs diluted 1/10 dilution were amplified by Supermix iTaq Universal Syber Green, (10 µL per reaction) to which 10 pmol of specific primers of the cDNA to be detected were added. Of them amplifications are carried out in parallel, on the one hand with specific oligonucleotides of the gene studied **table 3.3**, on the other hand with oligonucleotides corresponding to a sequence of the gene ribosomal protein 29/ GADPH used as internal control. PCR conditions that have been used are as follows: one cycle at 94°C for 30 seconds, then 40 cycles at 95°C for 15 seconds and 60°C for 1 min. The melting curve was used to examine the specificity of PCR amplifications. Expression of the target gene is normalized relative to the expression of the S29 ribosomal protein/GADPH mRNAs for each sample. Gene expression analysis was performed using the comparative method of CT. The rates of variation were calculated from the values of ΔΔCT with the formula 2-ΔΔCT and the data relate to the control values (Schmittgen and Livak 2008).

Table 3. 3 : Primer sequences used in the relative quantitative real time PCR

Gene (Mouse)	Primer sequence (mouse)	Gene (Human)	Primer sequence (human)
mGADPH-fwd	5'-TCACCACCATGGAGAAGG-3'	**hRP29-fwd**	5'-TTCAAACCGGCACGGTCTGA-3'
mGADPH- rev	5'-GCTAAGCAGTTGGTGGTGC A-3'	**hRP29-rev**	5'-TGCCGTACTGACGGAAACAC-3'
mCol2a1-fwd	5'- GGGTCACAGAGGTTACCCAG-3'	**hEXT1-fwd**	5'- GCTCTTGTCTCGCCCTTTTGT -3'
m Col2a1- rev	5'- ACCAGGGGAACCACTCTCAC-3'	**hEXT1-rev**	5'- GTGGTGCAAGCCATTCCTAC -3'
mSerpine-fwd	5'-ACCGCAACGTGGTTTTCTCA-3'	**hEXT2-fwd**	5'- ATGTGTGCGTCGGTCAAGTAT -3'
mSerpine- rev	5'-TTGAATCCCATAGCTGCTTGAAT-3'	**hEXT2-rev**	5'- AGAATGGGGCCAAAACTGAAA -3'

mAsporin-fwd	5'- CCATTTGGGTGCCAATGTTACT-3'	**hChsy1-fwd**	5'- CTGGGCACCACGGAAGAAAT-3'
mAsporin- rev	5'- TGGGTGAATCTTTGTTAGCTTGT-3'	**hChsy1-rev**	5'- GGCACCATTCTCCGAAGCA-3'
mSox9-fwd	5'-AGTACCCGCATCTGCACAAC-3'	**hChsy2-fwd**	5'- TGGATGAGCGTGGCATTAGG-3'
mSox9- rev	5'-ACGAAGGGTCTCTTCTCGCT-3'	**hChsy2-rev**	5'- AGCGACCGTAGTAGGAGCAG-3'
mIHH-fwd	5'- CTCTTGCCTACAAGCAGTTCA -3'	**hXT1-fwd**	5'- CTTCCAGCGAGTTCCAAATCA-3'
mIHH- rev	5'- CCGTGTTCTCCTCGTCCTT -3'	**hXT1-rev**	5'- CAGATGACAACAAGGACCGTG-3'
mOCN-fwd	5'- CTCTGACCTCACAGATGCCAA -3'	**hXT2-fwd**	5'-GGACAAGGCCACCTTAATATGG-3'
mOCN- rev	5'- CTGGTCTGATAGCTCGTCACA -3'	**hXT2-rev**	5'-TGGAACTCACTAGAAGGCAATGT-3'
mEXT1-fwd	5'- AAAACGAGGATTCCAGCGTG-3'	**hB3galt6-fwd**	5'- GACGCCTACGAAAACCTCAC-3'
mEXT1-rev	5'- AAGGGTGAAATCGAAGCAGGA-3'	**hB3galt6-Rev**	5'- CCTTGAGCACGAACTCGAAG-3'
mEXT2-fwd	5'- GATGCTCTGAAGCCCGAGTTT-3'	**hB4galt7-fwd**	5'- ATCCGGCACCACATCTACG-3'
mEXT2-rev	5'- TGTGATAGGGTAGAGTCTGTGC-3'	**hB4galt7-Rev**	5'- CAACGTCGTGCATGGCAAT-3'
mEXTL3-fwd	5'- AACGGTGGTCAGACCTGTATG-3'	**hBMPR1A-fwd**	5'- TGAAATCAGACTCCGACCAGA-3'
mEXTL3-rev	5'- GATCGAGGACGTGCTTTACCT-3'	**hBMPR1A-rev**	5'- TGGCAAAGCAATGTCCATTAGTT-3'
mChsy1-fwd	5'- GTGGCCGCCTACAGAACAT-3'	**hBMPR1B-fwd**	5'- CTTTTGCGAAGTGCAGGAAAAT-3'
mChsy1-rev	5'- TCTGCCCTCATAAACCACTCG-3'	**hBMPR1B-rev**	5'- TGTTGACTGAGTCTTCTGGACAA-3'
mChsy2-fwd	5'- AGGTCCCAGTTTTCGGAGC-3'	**hBMPR2-fwd**	5'- CGGCTGCTTCGCAGAATCA-3'
mChsy2-rev	5'- CACACCCACGTACAGGAAGTC-3'	**hBMPR2-rev**	5'- TCTTGGGGATCTCCAATGTGAG-3'
mXT1-fwd	5'- CGACTATGGATAAGCGGCGTC-3'	**hAsporin-fwd**	5'- CTCTGCCAAACCCTTCTTTAGC-3'
mXT1-rev	5'- CCACGCTGATTTGGAACTCAC-3'	**hAsporin- rev**	5'- CGTGAATAGCACTGACATCCAA-3'
mXT2-fwd	5'- GATGCTCTGAAGCCCGAGTTT-3'	**hSerpine-fwd**	5'- CCTGGGCACTTACAGGAAGG -3'
mXT2-rev	5'- TGTGATAGGGTAGAGTCTGTGC-3'	**hSerpine- rev**	5'- GGTCCGATTCGTCGTCAAATAAC -3'
mB3galt6-fwd	5'- GCGTGGACTTCGAGTTCGT-3'	**hTGFβR1-fwd**	5'- TCCTTCAAACGTGCTGCTG ACATC -3'
mB3galt6-Rev	5'- AGGTAGTAGTCGCAGAGTTGC-3'	**hTGFβR1-rev**	5'- TGGAACATCGTCGAGCAAT TT -3'
mB4galt7-fwd	5'- CCACATGCACCGCTTCCTAA-3'	**hTGFβR2-fwd**	5'- CAACCACCAGGGCATCCA -3'
mB4galt7-Rev	5'- CGATTGAACCTGAAATGGTCCA-3'	**hTGFβR2-rev**	5'- TCGTGGTCCCAGCACTCA -3'
mBMPR1A-fwd	5'-TGGCACTGGTATGAAATCAGAC-3'		
mBMPR1A-rev	5'-CAAGGTATCCTCTGGTGCTAAAG-3'		
mBMPR1B-fwd	5'-CCTCGGCCCAAGATCCTAC-3'		

mBMPR1B-rev	5'-CCTAGACATCCAGAGGTGACA-3'		
mBMPR2-fwd **mBMPR2-rev**	5'-GTGTTATGGTCTGTGGGAGAAAT-3' 5'-AAAGCGGTACGTTCCATTCTG-3'		
mAggrecan-fwd **mAggrecan-rev**	5'- GTGGAGCCGTGTTTCCAAG -3' 5'- AGATGCTGTTGACTCGAACCT -3'		
mTGFβR1-fwd **mTGFβR1-rev**	5'-AGAGCGTTCATGGTTCCGA G -3' 5'-CTGCGTCCATGTCCCATTG T -3'		
mTGFβR2-fwd **mTGFβR2-rev**	5'-CCGCTGCATATCGTCCTGT G-3' 5'-AGTGGATGGATGGTCCTAT TACA-3'		

3.1.10.4 Statistical Analysis

Results are presented as mean ± SD of three independent experiments. Statistical differences between control and treated groups were evaluated using Student's test. A two-sided P-value <0.05 was considered statistically significant for all analysis.

3.1.10.5 Firefly and Renilla luciferase reporter gene assay

TMEM control and KO cells were seeded in a 24 wells plate with $6x10^4$ cells per well and cultured in complete medium until the cells reach 80% confluency. Then cells were transfected with 500 ng of firefly reporter vector (pGL3-Basic, TOP-FLASH, TGFβ-firefly reporter or BMP-firefly reporter vector) and vector pRL-TK (endogenous control) at a ratio of 10:1. Medium was replaced after 24 h for each well. Cells transfected with TGFβ-firefly reporter/ or BMP-firefly reporter vector. Next morning the Firefly and Renilla activities were measured using the Dual-Luciferase kit Assay System (Promega, Madison, WI), using the Berthold Luminometer (BadWildbad, Germany). Cells of each well were lysed using 100 µL of passive lysis buffer with mild agitation at room temperature for 20 min. 20 µL of cell lysate were mixed with 50 µL of LAR II then the Luciferase Firefly activity was measured. Then 50 µl of Stop & Glo® reagent was added and the Luciferase Renilla activity was measured. Luciferase Firefly activities were normalized with the activity of vector pRL-TK with respect to the basal activity of the empty vector pGL3-Basic.

3.1.11. Chondrocyte Differentiation

TMEM165 control and KO ATDC5 cell were seeded in 12 wells plates with 2400 cells per well in DMEM-F12 supplemented with 2 mM glutamine, 100 IU/ml penicillin, 100 µg/ml streptomycin and 5% heat inactivated feotal bovine serum (FBS), transferrin and selenium (medium was labelled as TS) until they were 70-75% confluent; this was termed as day 0 (zero), then the medium was switched with DMEM-F12 supplemented with 2 mM glutamine, 100 IU/ml penicillin, 100 µg/ml streptomycin and 5% heat inactivated feotal bovine serum (FBS), transferrin and selenium with 10 µg/ml human insulin (DMEM/F12, ITS); medium was changed three times a week. The cells were stopped at day 0 and 7 after washing 2 times with phosphate buffer saline (PBS). mRNA was extracted and the qPCR was performed on the cDNA obtained from RT for the expression analysis of genes responsible for chondrogenesis and osteogenesis.

4 RESULTS

4.1 Knocking down TMEM165 in a mouse chondrogenic cell line ATDC5 using CRISPR/Cas9 technique

Congenital disorders of Glycosylation (CDG) is a group of human genetic disorders in which biosynthesis of glycoproteins and/or glycolipids is affected. Over 100 human genetic disorders have been identified which results from mutation in glycosylation related genes. Recently studies have discovered TMEM 165 as a novel deficient protein involved in CDG. Although the functions of this Golgi resident protein are unknown so far, it is established that the TMEM165-deficient CDG patients present skeletal and bone abnormalities (Foulquier et al. 2012) suggesting a potential involvement of TMEM165 in chondrogenesis and bone homeostasis. PGs play, via their GAG chains, a key role in several biological processes including chondrocytes differentiation and maturation, growth plate development, bone development and intracellular signaling. Synthesis of PG-GAG chains take place in the Golgi apparatus and genetic mutations or knockout of GTs involved in the GAG synthesis pathway such as XylT1, EXTL3, GaTI, CHSY1 and CHSY3 causes chondrodysplasia. We therefore hypothesized that potential defects in GAG chains may occur following TMEM165 deficiency which may lead to skeletal defects observed in TMEM 165-deficient CDG patients. To determine the link, if any, between TMEM165 deficiency and the synthesis of PGs, we generated TMEM 165 knockout prechondrogenic ATDC5 cell line using CRISPR-Cas9 technique by targeting three different regions of *TMEM165* gene. Several TMEM165-knockout clones were isolated and the genomic DNA fragments spanning the targeted regions were amplified by PCR and analysed by sequencing. Four TMEM165-knockout clones harbouring deletion mutations leading to premature stop codon were selected for further studies **(Figure 4.1)**.

Figure 4. 1: *Alignment of TMEM165 targeted sequence from wild-type (W)T* ***(A)*** *and a representative mutant clone (KO)* ***(B)****. Guide sequence is red boxed.*

To confirm that deletion mutations abolished the synthesis of TMEM165 protein, expression of the protein was analysed in wild-type and mutant ATDC5 cells by immunoblot using anti-TMEM165 antibodies. As expected, expression of a polypeptide of about 39 kDa corresponding to TMEM165 was detected in wild-type ATDC5 cells, whereas no polypeptide was revealed by the anti-TMEM165 antibodies in TMEM165-knockout cells **(Figure 4.2)**, indicating that the expression of TMEM165 protein is efficiently knocked down in mutant cells.

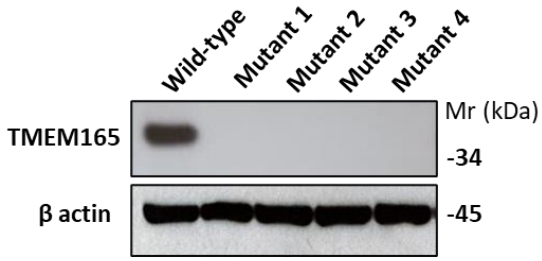

Figure 4. 2: *Expression analysis of TMEM165 in wild-type and mutant cells. Western blot analysis of cell lysates from ATDC5 control cells and TMEM165-deficient cells (G1B2, G1B3, G1B4 and G1B5). β actin was used as loading control. One representative blot of three independent experiments is shown*.

To further confirm these results, immunofluorescence analysis of the expression of TMEM165 was carried out in wild-type and in TMEM165-knockout ATDC5 cells. As shown in **figure 4.3** TMEM165 is clearly detected in wild-type ATDC5 cells displaying a perinuclear Golgi distribution and colocalize with the Golgi (GM130) marker**.** However, no staining with anti-TMEM165 was observed in TMEM165-knockout ATDC5 cells, whereas the Golgi marker

GM130 was clearly detected, indicating that the expression of TMEM165 is knocked down in mutant cells. Altogether, these data showed that TMEM165 is efficiently knocked down in ATDC5 mutant cells.

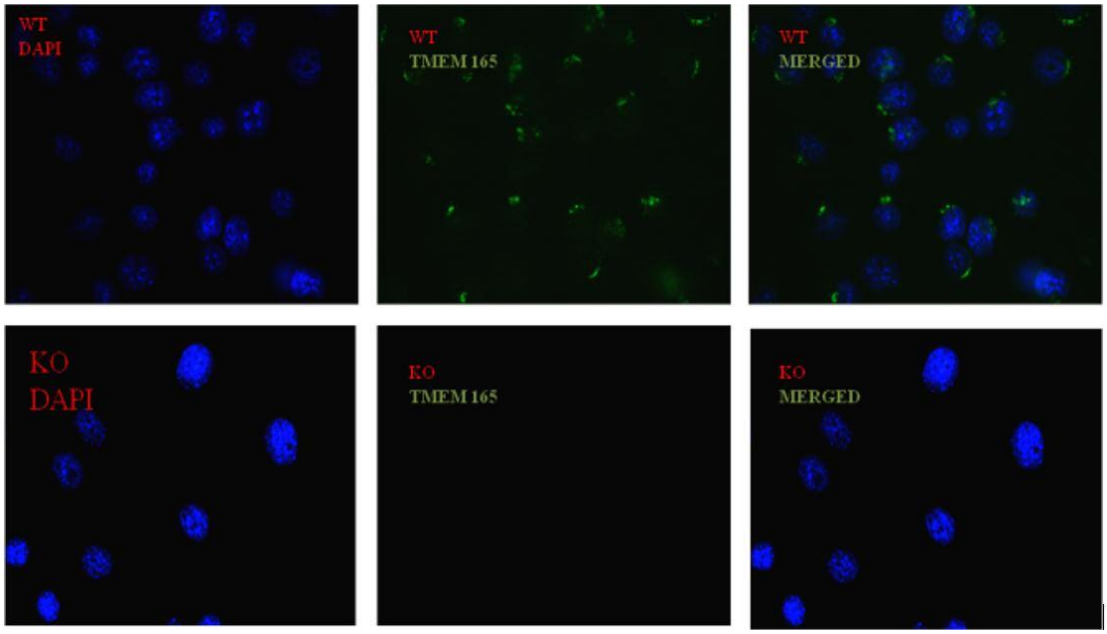

Figure 4.3: *Immunofluorescence analysis of the expression of TMEM165: ATDC5 control and TMEM165-Knock-out cells were fixed and labelled with antibodies against TMEM165 (green). Nucleus were stained with DAPI (Blue). Digital images were captured with an inverted microscope, Leica DM13000 (Leica microsystem).*

4.2 TMEM165 deficiency induces defects in the synthesis of HS- and CS-GAG chains of PGs

Owing to their role in the regulation of key signaling pathways and cell-matrix interactions, PGs play an important role in different events of skeletal development including chondrocytes differentiation and maturation, and bone formation. This led us to hypothesize that alterations in PG synthesis may contribute to skeletal defects observed in TMEM165-deficient CDG patients. To uncover the link, if any, between TMEM165 and PGs, we evaluated the level of PG synthesis in wild-type and TMEM165-deficient prechondrogenic ATDC5 cells by using metabolic incorporation of radiolabelled ^{35}S-sulfate into GAG chains. Interestingly, the results showed a decrease of about 75 % in PG synthesis in TMEM165-deficient cells compared to control cells **(Figure 4.4A)**. This was confirmed by SDS-PAGE analysis of radiolabelled PG-GAG

chains which showed a significant decrease in overall PG-GAG chains produced in TMEM165 knock-out cells, compared to control **(Figure 4.4B).**

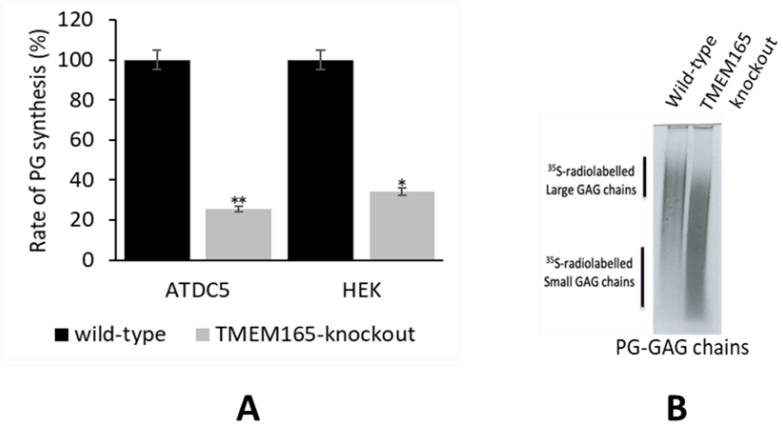

Figure 4.4: *Analysis of PG synthesis in wild-type and TMEM165-knock-out cells: Analysis of the synthesis of PGs in ATDC5 and HEK293 control and TMEM165-knock-out cells by evaluating the incorporation rate of ^{35}S-sulfate in the GAG chains of PGs* ***(A).*** *Analysis of the neosynthesized radiolabelled GAG chains in ATDC5 control and TMEM165-knock-out cells by SDS-PAGE and autoradiography* ***(B)****. One representative blot of three independent experiments is shown. Data are expressed as mean ±S.D. Statistical analysis was performed with an unpaired Student's t test (*p<0.05; **p<0.01)*

To determine whether the reduction in GAG synthesis affects both CS- and HS-GAG chains, we used decorin and syndecan 4 as reporter for the synthesis of CS-PG and HS-PG, respectively. For these purposes wild-type and mutant ATDC5 cells were transfected with expression vector for decorin and HA-tagged syndecan 4, respectively. Of note, CS- and HS-attached PGs migrate as an elongated smear during gel electrophoresis due to heterogeneity of attached GAG chains. As expected, transfection of wild-type and mutant ATDC5 cells with decorin expression vector resulted in the secretion of GAG-attached decorin in the culture medium as shown by Western blot using anti-decorin specific antibodies **(Figure 4.5A).** However, the amount found in the culture medium of TMEM-165-deficient ATDC5 cells was strongly reduced compared to that present in the culture medium of wild-type ATDC5. Importantly, there is a loss of high sized GAG-attached decorin in TMEM-165-deficient ATDC5 cells as evidenced by predominance of GAG-attached decorin with significantly reduced size compared to wild-type.

To confirm whether this is also the case in other cell lines, we generated TMEM165-knockout HEK293 cells and analysed decorin produced in culture medium of wild-type and mutant HEK293 cells after transfection with decorin expression vector. As shown in **Figure 4.5B**, GAG-attached decorin from TMEM165-deficient HEK293 cells exhibited strong reduction in size with predominance of low sized GAG-attached decorin compared to wild-type. This indicate that defects in PG synthesis produced by TMEM165 deficiency is not cell type specific. To rule out an effect of TMEM165 on decorin core protein expression or secretion, we generated and expressed a decorin mutant lacking GAG chain attached site by mutation of serine residue at position 35, which is used for the attachment of the CS-GAG chain on the core protein, to alanine residue (S35A). Expression of the mutant decorin S35A in wild-type ATDC5 cells led, as expected, to the secretion of a polypeptide of about 74 kDa corresponding to decorin core protein without attached GAG chain. Similarly, TMEM165-deficient ATDC5 cells secreted decorin lacking GAG chain in the medium at similar amount compared to wild-type cells (**Figure 4.5C)**. These data indicate that TMEM165-deficiency did not affect neither synthesis nor secretion of decorin core protein. Altogether, these results suggest that TMEM165 rather affects the synthesis of decorin with attached GAGs.

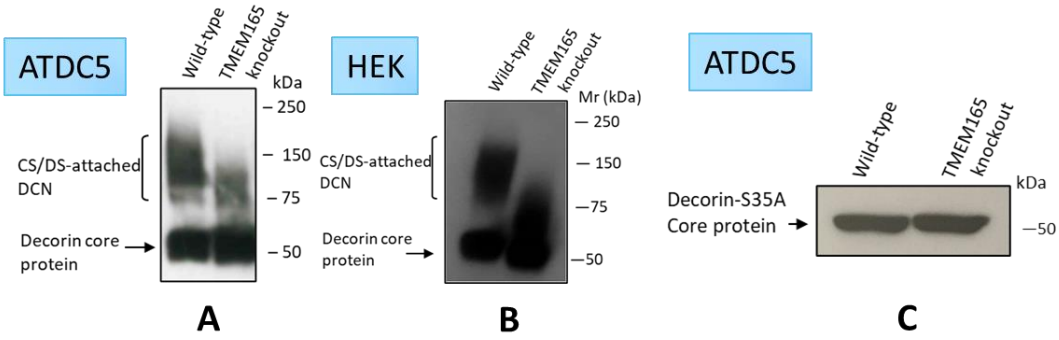

Figure 4.5: *Western bot analysis of expression of decorin and decorin mutant S35A: wild-type and TMEM165-mutant* ***(A)*** *ATDC5 and* ***(B)*** *HEK293 were transfected with expression vector for decorin and decorin produced in culture medium was analysed by immunoblot using anti-decorin aspecific antibodies.* ***(C)*** *decorine mutant S35A was expressed in wild-type and TMEM165-mutant ATDC5 cells and revealed in cell lysate by western blot. One representative blot of three independent experiments is shown*

Given that TMEM165 did not affect the synthesis of decorin core protein, we sought to determine whether it affects the synthesis of the attached GAG chain. For these purposes, we

used 4-Methylumbelliferyl-β-D-xylopyranoside (4MU-Xyl) as acceptor substrate for the synthesis of GAG chains. Indeed, it is well known that the biosynthesis of GAG chains can also be initiated in the absence of a core protein by xyloside analogues carrying a hydrophobic aglycon, such as 4MU-Xyloside (4MU-Xyl). The xyloside can, when exogenously supplied to cells, acts as acceptor substrate for β4GalT7, then elongated by other glycosyltransferases leading to the production in the medium of xyloside-primed GAG chains. Therefore, we cultured TMEM165-knockout and wild-type ATDC5 cells in the presence of 4MU-Xyl and of ^{35}S Sulfate to metabolically radiolabel the newly synthesized GAG chains. 4MU-Xyl-primed GAG chains produced were isolated by Cetylpyridinium chloride method from culture medium and analysed by SDS-PAGE. The results showed that wild-type ATDC5 cells produced significant amount of radiolabelled GAG chains, whereas TMEM165-knockout ATDC5 cells produced only few amounts **(Figure 4.5D)**, indicating that the synthesis of GAG chains is affected in TMEM165-deficient cells.

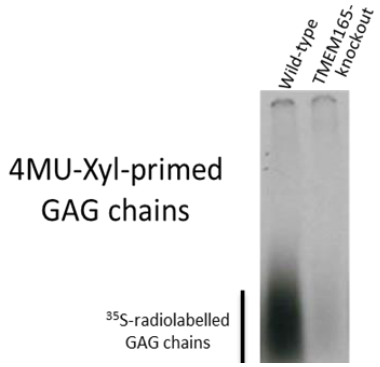

Figure 4.5D *Analysis of the neosynthesized radiolabelled GAG chains primed by 4MU-Xyl in ATDC5 control and TMEM165-knock-out cells. Radiolabelled GAG chains produced in the culture medium of wild-type and TMEM165-knockout cells were analyzed by SDS-PAGE and autoradiography.*

To determine whether reduction in the size of decorin produced in TMEM165-deficient ATDC5 cells results from defects in polymerization of CS GAG chains, decorin from wild-type and TMEM165-mutant ATDC5 cells were subjected to treatment with chondroitinase ABC that degrades CS-GAG chains but not the tetrasaccharide linkage primer. Interestingly, treatment of decorin from wild-type and ATDC5-knock-out cells with chondroitinase ABC led to change in the migration pattern in SDS-PAGE from a smear to a single band corresponding to decorin core protein without GAG chains in both case **(Figure 4.6)**. These data indicate that decorin

produced in ATDC5 mutant cells is sensitive to chondroitinase ABC and therefore contains elongated CS-GAG chains but shorter in size compared to those present on decorin produced by wild-type cells. This indicated that CS-GAG chains elongation take place in TMEM165-knockout cells but with reduced efficiency leading the formation of short GAG chains compared to wild-type cells. Together, these data suggest that that TMEM165-deficiency lead to defects in CS chain elongation and therefore in the polymerization process. However, we cannot rule out defects also in GAG chain initiation process.

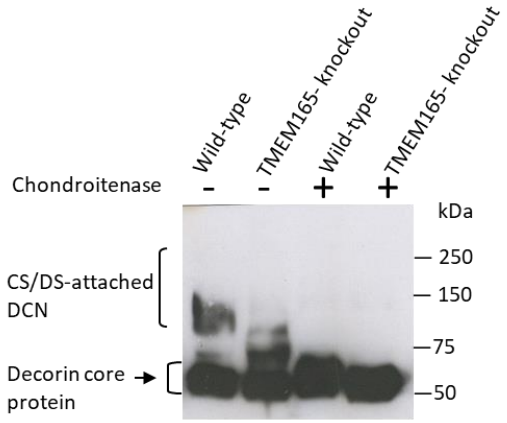

Figure 4.6: *Analysis of the sensitivity of decorin to chondroitinase ABC. ATDC5 control and TMEM165 Knock-out cells were transfected with decorin expression vector and decorin produced in culture medium was treated with or without chondroitinase ABC and the patterns were analysed by SDS-PAGE.*

We next investigated whether the synthesis of HS-GAG chains is altered in TMEM165-deficient cells. For this purpose, we expressed syndecan 4, an HSPG with four HS-attached GAG chains, in TMEM165-knockout and wild-type ATDC5 cells by transfection with an expression vector encoding HA-tagged syndecan 4. As shown in **Figure 4.7**, syndecan 4 was expressed as a smear in both TMEM165-knockout and wild-type ATDC5 cells, however the amount of HS-attached syndecan 4 was significantly reduced in mutant cells compared to wild-type ATDC5 cells **(Figure 4.7)**.

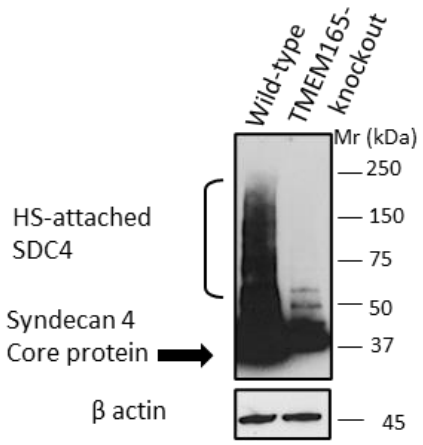

Figure 4.7: *SDS-PAGE analysis of HS-GAG Chains. ATDC5 control and TMEM165-Knockout cells were transfected with HA-syndecan-4 expression vector and cell lysate was analysed by immunoblot using anti-HA antibodies. β actin was used as loading control.*

These results indicate that extension of HS chains is reduced, suggesting defects in polymerization of HS-GAG chains in TMEM165-knockout cells. Altogether, these results revealed a key role of TMEM165 in the synthesis of HS- and CS-GAG chains, mainly in the polymerization process.

Given that CS and HS synthetic pathway involves several enzymes each of which is involved in a specific step of the synthesis process, we sought to determine whether defects in the polymerization of CS and HS in TMEM165-deficient cells may result from defects in the gene expression of CS and HS polymerizing enzymes. To this end, RT-qPCR analysis were performed using mRNA from TMEM165-deficient and wild-type ATDC5 cells to evaluate gene expression of CS polymerizing enzymes, CHSY1 and CHSY3 and of HS polymerizing enzymes, EXT1 and EXT2. The results showed that the level of expression of CS polymerizing enzymes CHSY1 and CHSY3 is higher in TMEM165-deficient ATDC5 cells compared to wild-type cells, suggesting that reduced CS GAG chains extension is not due to inhibition in gene expression of polymerizing enzymes. Likewise, the level of expression of HS polymerizing enzymes, EXT1 and EXT2 is increased in TMEM165-deficient ATDC5 cells compared to wild-type cells, indicating that defect in the extension of HS chains in TMEM165-deficient cells is not due to reduced gene expression of HS elongation enzymes **(Figure 4.8)**.

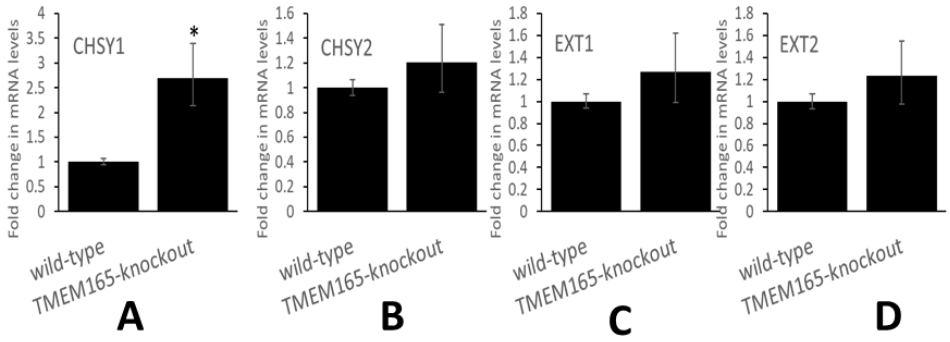

Figure 4.8: *Gene expression analysis of CS and HS polymerizing enzymes in ATDC5 control and TMEM165-knockout cells. Relative mRNA levels of CS polymerising enzymes* ***(A)*** *CHSY1 and* ***(B)*** *CHSY2, and HS polymerising enzymes* ***(C)*** *EXT1 and* ***(D)*** *EXT2. qPCR values were normalized for the housekeeping gene ribosomal protein S29 and are expressed as the relative expression compared with control. Data are expressed as mean ±S.D. Statistical analysis was performed with an unpaired Student's t test (*p<0.05; **p<0.01).*

We also analysed the expression of the enzymes XylT1/XylT2, GalT1, GalT2 and GlcAT-I involved in the synthesis of the tetrasaccharide linker used as a primer for elongation of both CS and HS chains. As shown for CS and HS polymerizing enzymes, the level of gene expression of these enzymes is higher or similar in TMEM165-knockout compared to wild-type ATDC5 cells **(Figure 4.9)**.

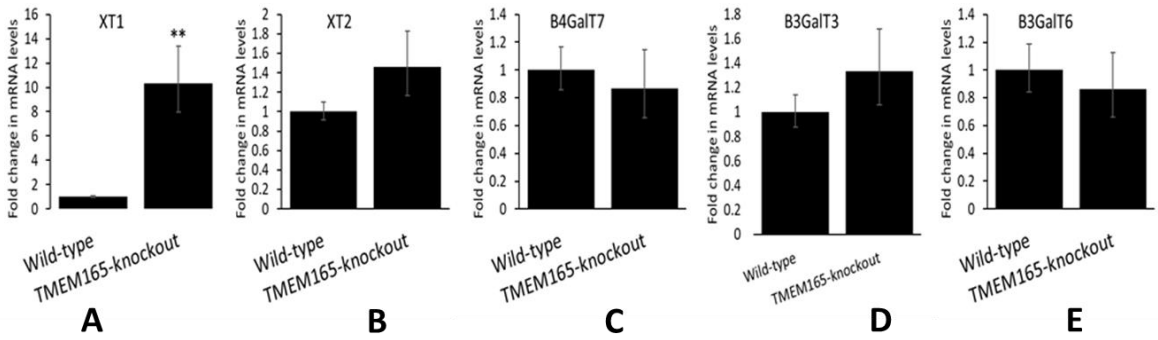

Figure 4.9: *Gene expression analysis of enzymes involved in tetrasaccharide linker synthesis. Relative mRNA levels of* ***(A)*** *XT1,* ***(B)*** *XT2,* ***(C)*** *β4GalT7I,* ***(D)*** *β3gaT3I and* ***(E)*** *β3GalT6 in ATDC5 control and TMEM165-konckout cells. qPCR values were normalized for the housekeeping gene ribosomal protein S29 and are expressed as the relative expression compared with control. Data are expressed as mean ±S.D. Statistical analysis was performed with an unpaired Student's t test (*p<0.05; **p<0.01).*

Similar analysis was carried out in human fibroblast cells from control and TMEM165-deficient patient. Likewise, gene expression of CS and HS polymerizing enzymes were similar or higher in patient's fibroblasts **(Figure 4.10)**.

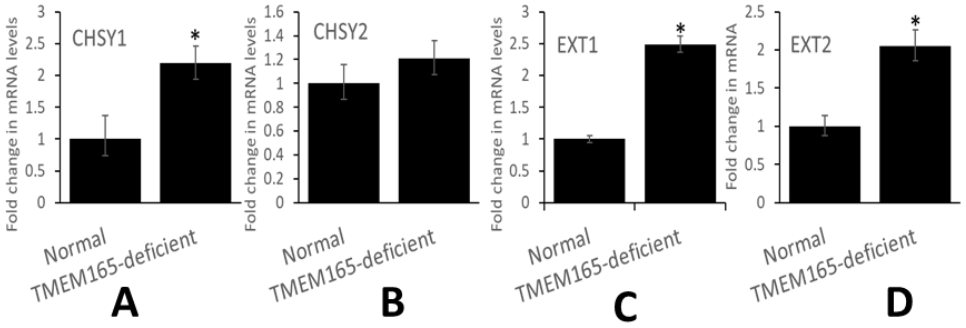

Figure 4.10: *Analysis of gene expression of CS and HS polymerizing enzymes in human fibroblast control and patient cells. qPCR analysis of CS polymerising enzymes CHSY1* ***(A)*** *and CHSY2* ***(B)****, and HS polymerising enzymes EXT1* ***(C)*** *and EXT2* ***(D)****. qPCR values were normalized for the housekeeping gene ribosomal protein S29 and are expressed as the relative expression compared with control. Data are expressed as mean ±S.D. Statistical analysis was performed with an unpaired Student's t test (*p<0.05; **p<0.01).*

Analysis of the mRNA levels of the enzymes involved in the synthesis of the tetrasaccharide primer in human fibroblast cells from control and TMEM165-deficent patient showed that the expression levels are similar or higher in TMEM165-deficient patient for XT1/XT2, β4GalT7, β 3GaT3 and β 3GalT6 **(Figure 4.11)**.

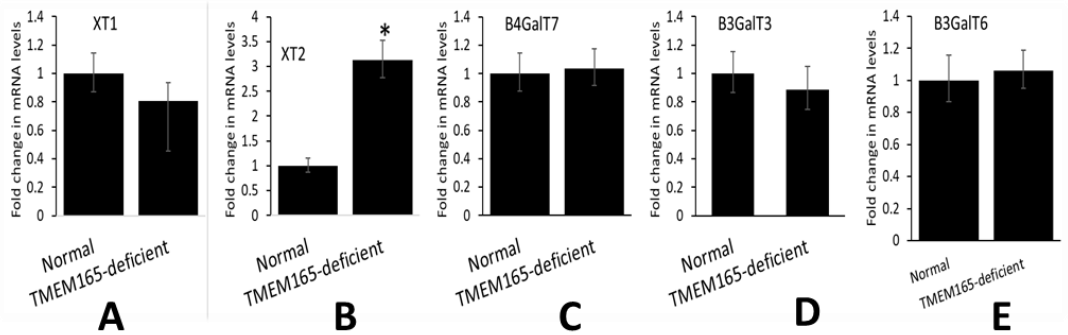

Figure 4.11: *Gene expression analysis of enzymes involved in tetrasaccharide linker synthesis. Relative mRNA levels of* ***(A)*** *XT1,* ***(B)*** *XT2,* ***(C)*** *β4GalT7l,* ***(D)*** *β 3gaT3 and* ***(E)*** *β 3GalT6 in fibroblast control and TMEM165-deficient patient cells. qPCR values were normalized for the housekeeping gene ribosomal protein S29 and are expressed as the relative expression*

*compared with control. Data are expressed as mean ±S.D. Statistical analysis was performed with an unpaired Student's t test (*p<0.05; **p<0.01).*

Altogether, these data indicate that TMEM165-deficiency did not affect the expression level of the enzymes involved in CS and HS synthesis, therefore indicating that defects in polymerization of CS and HS chains is not related to the expression level of the enzymes involved.

4.3 Expression of CS synthase, CHSY1 and CHSY2 did not rescue the polymerization defects induced by loss of TMEM165.

We showed above that gene expression of CS and HS polymerizing enzymes is not inhibited but rather increased in TMEM165-defiicient ATDC5 cells and patient fibroblasts, compared to control cells. However, we cannot rule out a decrease in the protein level that may result from increased protein instability and/or degradation. Given that the level of protein expression of glycosyltransferases involved in GAG synthetic pathway is very low and their detection by antibodies (commercially available) is very challenging, it is therefore difficult to evaluate and compare the protein level of CS and HS polymerizing enzymes in normal and mutant cells. We can however hypothesize that overexpression of these enzymes may overcome the instability or degradation induced by TMEM165-deficiency, if any. To support the expression of CS polymerizing enzymes, we designed expression vectors for Myc-tagged CHSY1 and HA-tagged CHSY2 and used them to overexpress each of the two enzymes individually or together in TMEM165-deficient ATDC5 cells. As shown by Western blot, transfection of TMEM165-deficient HEK293 cells with CHSY1 expression vector resulted in high level of expression of CHSY1 protein **(Figure 4.12)**. Similarly, high level of expression of CHSY2 protein was observed by Western blot when cells were transfected with CHSY2 expression vector **(Figure 4.12)**. In addition, co-transfection of mutant HEK293 cells with both CHSY1 and CHSY2 expression vectors resulted in strong expression of both CHSY1 and CHSY3 proteins **(Figure 4.12)**. Next, we investigated whether overexpression of CHSY1 and CHSY2 individually or in combination rescue the polymerization of CS GAG chains in TMEM165-deficient HEK293 cells. For this purpose, we transfected TMEM165-deficient cells with CHSY1, CHSY2 or CHSY1 and CHSY2 expression vectors along with the decorin expression vector. Cells transfected with empty

vector along with decorin expression vector were used as control. Next, decorin produced in the culture medium of transfected cells was analysed by Western blot and compared to decorin produced in wild-type cells. As shown in **Figure 4.12,** TMEM165-deficient cells transfected with CHSY1, CHSY2 or CHSY1 and CHSY2 produced decorin with reduced size compared to that produced in wild-type cells but like that expressed in cells transfected with empty vector (TMEM165 KO). Similar result was observed for cell transfected with both CHSY1 and CHSY2. The expression of CHSY1 and CHSY2 was confirmed by Western blot in all the cells transfected. These data indicated that overexpression of CHSY1 and CHSY2 individually or together did not restore CS elongation in TMEM165-deficient cells, suggesting that defects in CS polymerisation process did not result from reduced protein expression of the polymerizing enzymes, CHSY1 and CHSY2.

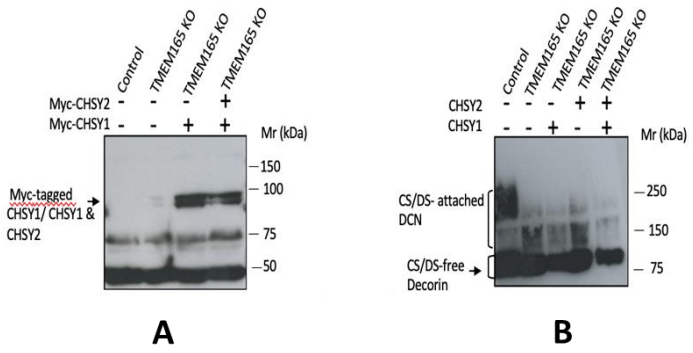

Figure 4.12: *CHSY1 and CHSY3 did not rescue the polymerization defects induced by loss of TMEM165.* ***(A)*** *HEK293 control and TMEM165-Knockout cells were transfected with Myc-tagged CHSY1 and/or HA-tagged CHSY2 and their e*xpression *was analysed by Western blot.* ***(B)*** *Analysis of effects of e*xpression of CS synthase *on CS-GAG chain synthesis in HEK293 control and TMEM165-Knockout cells.*

As overexpression of CS polymerizing enzyme did not rescue the elongation of CS GAG chains, we sought to determine whether supplying the cell culture medium with sugar monosaccharides used for the synthesis of CS-GAG chains such as xylose and galactose may restore CS elongation in TMEM165-deficient cells. To this end, TMEM165-mutant cells were transfected with decorin expression vector and incubated in the presence or absence of 1 mM of xylose and galactose, respectively. As shown in **figure 4.13**, the size of decorin produced in TMEM165-mutant cells is significantly reduced compared to that of wild-type cells and has not change with treatment with either xylose or galactose. These data indicate that supplying

cells with monosaccharides which constitute CS-GAG chains did not overcome the blockage in the polymerization process. Altogether, these data suggest that impaired elongation of CS-GAG chains induced by deficiency in TMEM165 is probably not due to defects in supply of monosaccharide substrates.

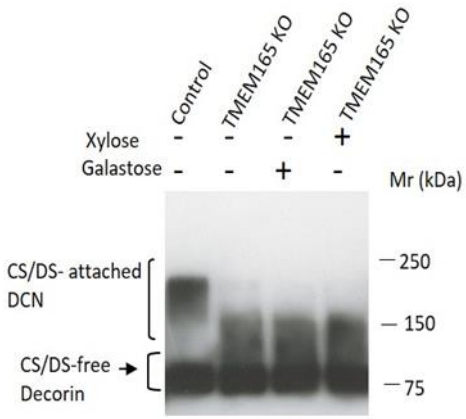

Figure 4.13: *Analysis of effects of monosaccharides supply on CS-GAG chain synthesis: HEK293 control and TMEM165-Knockout cells were transfected with decorin expression vector followed by treatment with either xylose (1 mM) or galactose (1 mM). Expression patterns of decorin was analysed by SDS-PAGE.*

4.4 Manganese rescues the synthesis of both CS and HS GAG chains impaired by TMEM165 deficiency

It has been established that Mn^{2+} participates in the catalytic activity of various Golgi glycosyltransferases including CS and HS polymerizing enzymes. CHSY1 and CHSY2 involved in CS chain elongation exhibit both β-1,3-glucuronic acid and β-1,4-N-acetylgalactosamine transferase activities. Evaluation of CHSY1 and CHSY2 enzyme activities *in vitro* by incorporation of UDP-[^{14}C]GlcUA and UDP-[^{3}H]-GalNAc on acceptor substrates showed that divalent ions were essential for the enzymatic activities. Mn^{2+} achieved the highest β-1,4-N-acetylgalactosamine transferase activity and was 70% as effective as Co^{2+} in achieving the highest level of β1,3-glucuronic acid activity (Yada et al., 2003b)**.** CHSY2 has been shown to require Mn^{2+} but can also be slightly activated by Co^{2+}. Similarly, requirement on Mn^{2+} for HS polymerizing enzymes was also reported (Yada et al., 2003a)**.** Therefore, we sought to determine whether defects in the elongation of CS and HS in TMEM165-deficient cells is due to lack of Mn^{2+}, the divalent ion activator of GAG polymerizing enzymes. For this purpose,

wild-type and TMEM165-deficient cells were transfected with decorin expression vector then cultured in the absence or presence of 1μM of Mn^{2+}. Western blot analysis of decorin produced in wild-type ATDC5 cells showed similar pattern either in the absence or presence of Mn^{2+}, indicating that Mn^{2+} did not affect the synthesis of decorin. Importantly, decorin expressed in TMEM165-deficient cells that were cultured in the presence of Mn^{2+} was larger in size compared to that produced in the absence of Mn^{2+} and exhibited a pattern similar to that of decorin produced in wild-type cells **(Figure 4.14A)**. These data showed that supplementation of the culture medium with Mn^{2+} increases the size of decorin and therefore support the notion that Mn^{2+} restores polymerization of decorin CS-GAG chains in TMEM165-deficient cells.

We next analyzed whether treatment with Mn^{2+} affects the synthesis and secretion of decorin core protein. To this end, we expressed decorin S35A mutant lacking the CS attachment site in wild-type and TMEM165-knockout cells and analyzed decorin produced in the culture medium by immunoblot. As shown in **figure 4.14B** both wild-type and TMEM165-deficent cells efficiently expressed decorin core protein. The pattern of decorin core protein produced is similar in the absence or presence of 1 μM of Mn^{2+} in the culture medium, indicating that treatment of wild-type and TMEM165-knockout cells with Mn^{2+} did not affect the synthesis and secretion of decorin core protein. Therefore, changes in the size of decorin following treatment with Mn^{2+} only affects the attached GAG chain.

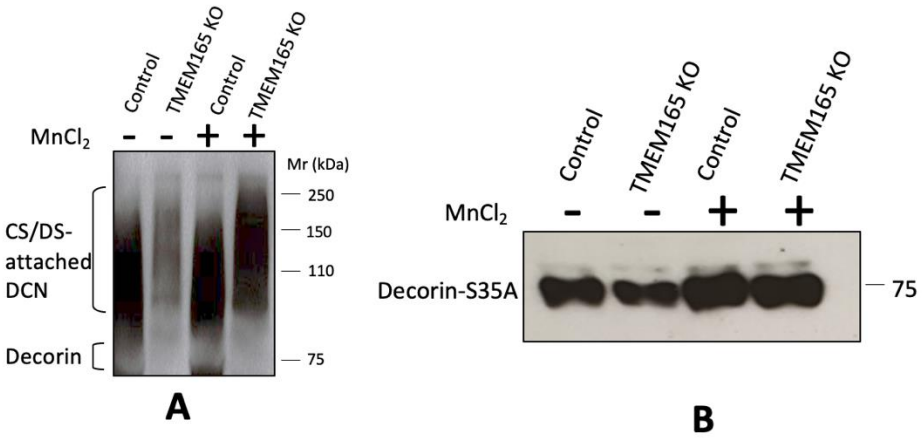

Figure 4.14: *Manganese rescues the synthesis of CS-GAG chains. ATDC5 control and TMEM165-Knockout cells were transfected with decorin expression vector* ***(A)*** *and decorinS35A mutant expression vector (B) and cells were grown in the absence and presence of MnCl2 (1 µM). Decorin in the medium was analysed by immunoblot. One representative blot of three independent experiments is shown.*

As polymerization HS GAG chains are also impaired in TMEM165-deficient cells, we investigated whether Mn^{2+} is able to restore the polymerization of HS-GAG chains as observed above for CS-GAG chains. Wild-type and TMEM165-deficient ATDC5 cells were transfected with HA-syndecan 4 expression vector and cultured in the absence or presence of 1µM of Mn^{2+}. Western blot analysis of HA-syndecan 4 indicated the presence of a high molecular weight smear corresponding to HA-syndecan 4 PG attached with large HS-GAG chains. This pattern is similar in cells cultured in the presence or absence of Mn^{2+}, suggesting that the divalent ion Mn^{2+} did not affect the synthesis of HS-GAG chains in wild-type cells at the concentration used. Remarkably, supplementation of Mn^{2+} in the culture medium of TMEM165-deficient cells resulted in the synthesis of HA-syndecan 4 with higher molecular weight compared to that produced in the absence of Mn^{2+} **(Figure 4.16)**, indicating that HS-GAG chains attached to HA-syndecan 4 are of larger size when Mn^{2+} is supplied in the culture medium. These data strongly suggest that Mn^{2+} rescues the polymerization of HS-GAG chains.

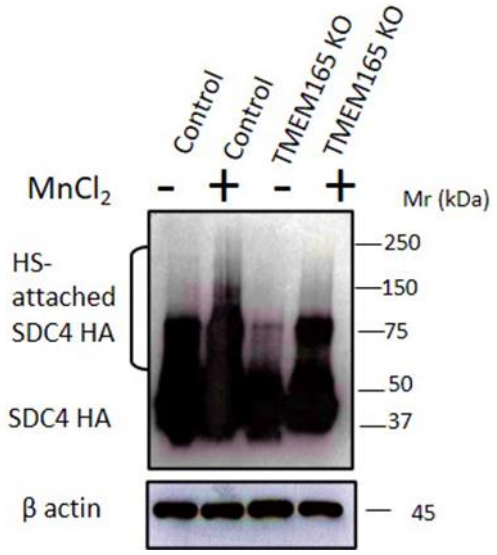

Figure 4.15: *Manganese rescues polymerisation of HS-GAG chains. ATDC5 control and TMEM165-Knockout cells were transfected with HA-syndecan 4 expression vector and cultured in the absence or presence of MnCl2 (1 µM). Cell lysate was analysed by immunoblot for the expression and pattern of HA-syndecan 4. One representative blot of three independent experiments is shown.*

To further confirm that Mn^{2+} rescues GAG polymerization in TMEM165-deficient cells, 4MU-Xyl was used as exogenous substrate to monitor the synthesis of GAG chains. Wild-type and mutant ADTC5 cells were cultured in the presence or absence of Mn^{2+} along with 4MU-Xyl and [^{35}S]-sulfate to radiolabel newly synthesized GAG chains. SDS-PAGE analysis of radiolabelled 4MU-Xyl-primed GAG chains showed that in the absence of Mn^{2+}, high amount of GAG chains was produced in wild-type cells, whereas very week signal was observed in TMEM165-deficient cells, indicating that the polymerization process is impaired in these cells. Interestingly, supplementation of Mn^{2+} in the culture medium restores the synthesis of GAG chains in TMEM165-deficient cells leading to production of significant amount of radiolabelled GAG chains. Noteworthy, Mn^{2+} did not affect the synthesis process in wild-type cells **(Figure 4.16).**

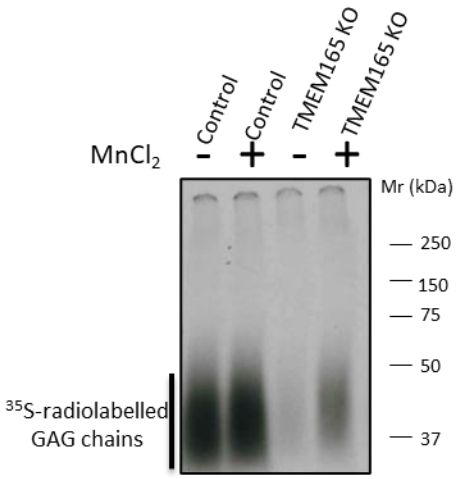

Figure 4. 16: *Manganese rescues GAG chains polymerization in TMEM165-Knockout cells: Wild-type and TMEM165-mutant ATDC5 cells were cultured in the absence or presence of Mn^{2+} along with 4MU-Xyl and [^{35}S]-sulfate and neosynthesized radiolabelled 4MU-Xyl-primed GAG chains were analysed by SDS-PAGE and revealed by autoradiography.*

Altogether, these results demonstrate that TMEM165-deficiency induces defects in the synthesis of PGs and mainly in the polymerization of their GAG chains, both HS and CS types, which is likely due to unviability in the Golgi of the divalent ion Mn^{2+} at the concentration required to fully activates the GAG polymerizing enzymes.

4.5 TMEM165-deficiency impairs TGF-β and BMP signaling Pathways

We showed above that TMEM165-deficiency led to defects in synthesis of PG-GAG chains. As a number of human genetic mutations causing a wide range of inheritable diseases of skeletal development are related to TGF-β and BMP signaling (Wu, Chen, and Li 2016b) and owing to the key role of GAG chains in the regulation of several signaling pathways, we sought to investigate whether TMEM165-deficiency affects TGF-β and BMP signaling pathways. We first explored the TGF-β signaling by analysis of the phosphorylation status of Smad2, a downstream mediator of TGF-β receptor activation, in wild-type and TMEM165-knockout cells. Interestingly, Western blot analysis showed that phospho-Smad2 level (but not total Smad2 level) was reduced in TMEM165-deficient cells compared to wild-type **(Figure 4.17A)**, indicating that the TGF-β/Smad2 axis was functionally impaired in mutant cells. This data suggests that the expression of TGF-β-induced genes in TMEM165-deficient cells would also

be downregulated. To test this, the mRNA levels of the serpine 1 (PAI-1) gene, which is positively correlated with TGF-β signaling activation were examined. As expected, serpine1 mRNA levels were significantly lower in TMEM165-deficient cells compared to wild-type **(Figure 4.17B),** therefore indicating that TMEM165-deficiency perturbs TGF-β signaling in mutant cells. These data were further confirmed by transfecting the p(CAGA)12-luc reporter plasmid into TMEM165-deficient and wild-type cells. This plasmid contains a firefly luciferase gene, located downstream of a TGF-β-responsive promoter derived from serpine1 gene. Therefore, the luciferase activity is a measure of TGF-β signaling. The luciferase activity was markedly (7.5 folds) lower in mutant cells compared to wild-type cells, confirming that the TGF-β/Smad axis is functionally impaired in TMEM165-mutant cells **(Figure 4.17C)**.

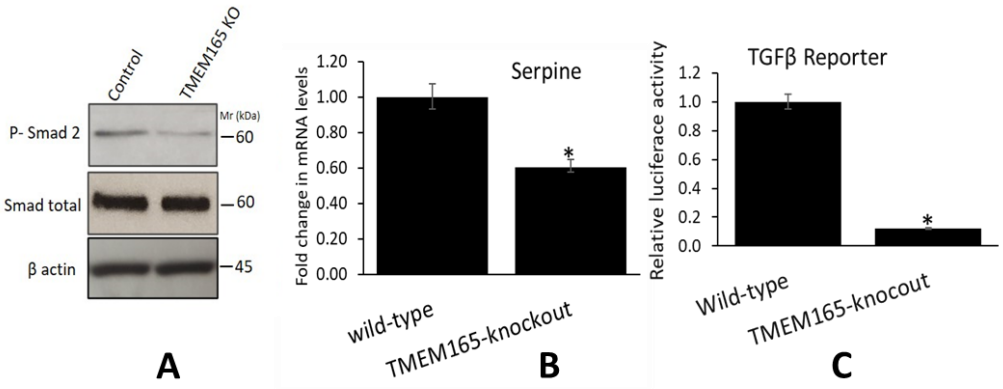

Figure 4. 17: *Analysis of TGF-β signaling pathway in wild-type and TMEM165-Knockout ATDC5 cells.* ***(A)*** *Cell lysate from ATDC5 control and TMEM165-Knockout cells were analysed by western blot for the phosphorylation status of smad 2, β actin was used as loading control.* ***(B)*** *qPCR analysis of mRNA levels of Serpine in ATDC5 control and TMEM165-Knockout cells. qPCR values were normalized for the housekeeping gene ribosomal protein S29 and are expressed as the relative expression compared with control.* ***(C)*** *ATDC5 control and TMEM165 Knockout cells were co-transfected with plasmid expressing TGF-β1 reporter (firefly) and Renilla, then luciferase reporter activity was measured. Data are expressed as the fold change relative to control as mean ±S.D. Statistical analysis was performed with an unpaired Student's t test (NS, statistically not significant; *p<0.05; **p<0.01).*

To determine whether this is also the case in patient fibroblast cells, we evaluated the phosphorylation status of Smad2 in normal and TMEM165-deficient human fibroblasts. As

shown in **Figure 4.18**, phospho-Smad2 level was reduced in TMEM165-deficient fibroblasts compared to normal fibroblasts, whereas total Smad2 level was not affected, indicating that the TGF-β/Smad2 axis was functionally impaired in fibroblast mutant cells. Analysis of the expression of serpine1 gene used as a marker for TGF-β signaling activation, showed significant (two-fold) downregulation, indicating that TMEM165-deficiency impairs the expression of the TGF-β/Smad downstream responsive genes in patient fibroblasts.

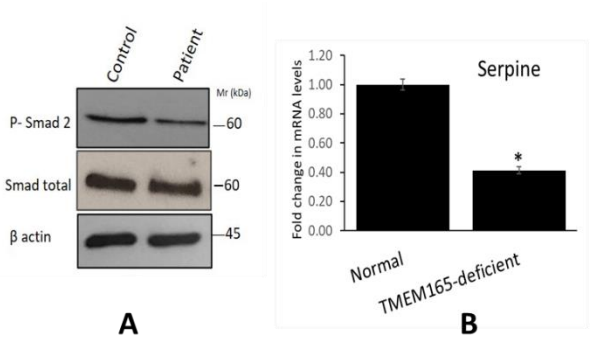

Figure 4.18: *Analysis of TGF-β signaling pathway in human fibroblasts (control and patient).* ***(A)*** *Cell lysate from fibroblast control and TMEM165-deficient patient were subjected to western blot analysis for phosphorylation status of smad 2 using anti-phosphoSmad2 specific antibodies. β actin was used as loading control.* ***(B)*** *qPCR analysis of mRNA levels of serpine in fibroblast cells from normal and TMEM165-deficient patient. qPCR values were normalized for the housekeeping gene ribosomal protein S29 and are expressed as the relative expression compared with control. Data are expressed as the fold change relative to control as mean ±S.D. Statistical analysis was performed with an unpaired Student's t test (NS, statistically not significant; *p<0.05; **p<0.01).*

To determine whether response to TGF-β stimulation is affected in mutant cells, phosphorylation level of Smad2 in response to TGF-β was examined. As shown in **Figure 4.19**, treatment of TMEM165-deficient ATDC5 cells with TGF-β induced the phosphorylation of Smad2, however the level of phospho-Smad2 is lower compared to that observed in wild-type cells, indicating that mutant cells were less responsive to TGF-β than wild-type cells.

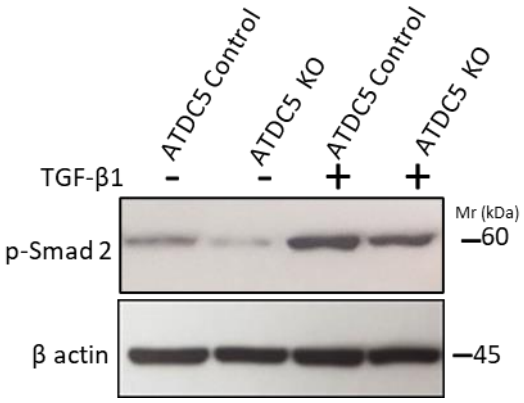

Figure 4.19: *Analysis of the response of wild-type and TMEM165-mutant cells to TGF-β1 stimulation: Western blot analysis of p-Smad2 in cell lysates from wild-type and TMEM165-deficient ATDC5 cells treated or not with the growth factor TGF-β1 (1ng/ml) for 1 hour using anti-phosphoSmad2 specific antibodies. β actin was used as loading control (n=3).*

To find out if this is also the case in patient fibroblasts, both normal and TMEM165-deficient fibroblast cells were stimulated with TGF-β and the phosphorylation status of Smad2 was analysed by Western-blot. The results showed that the level of phospho-Smad2 in mutant fibroblasts was reduced compared to normal fibroblasts **(Figure 4.20)**

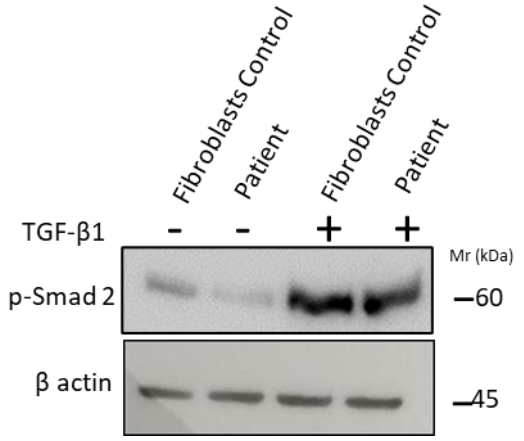

Figure 4.20: *Analysis of the response of normal and TMEM165-mutant fibroblast cells to TGF-β1 stimulation: Western blot analysis of p-Smad2 in cell lysates from normal and TMEM165-mutant fibroblast cells treated or not with the growth factor TGF-β1 (1ng/ml) for 1 hour using anti-phosphoSmad2 specific antibodies. β actin was used as loading control (n=3).*

Altogether, these results showed that both the baseline and TGF-β-induced levels of phospho-Smad2 were significantly reduced in mutant cells, therefore revealing for the first time that TMEM165-deficiency functionally impaired the TGF-β/Smad2 signaling axis.

To identify the mechanism involved in the alteration of the TGF-β/Smad signaling pathway, we investigated the mRNA expression levels of TGF-β receptors, TGFβR1 and TGFβR2 in TMEM165-deficient and wild-type cells. As shown in **figure 4.21A and 4.21C**, a slight decrease in the expression of mRNA encoding TGFβR1 was observed by Realtime RT-PCR in mutant ATDC5 cells, compared to wild-type **(figure 4.21A)**. Interestingly, a significant decrease (about two-fold) in the mRNA expression level of TGFβR2 was observed in mutant ATDC5 **(figure 4.21B)**. To determine whether changes in TGFβR2 mRNA expression reflect changes in the protein expression, TGFβR2 protein expression was assessed by immunoblotting. Consistent with RT-PCR data, strong reduction in the protein level of TGFβR2 was observed in TMEM165-deficient ATDC5 **(Figure 4.21C).**

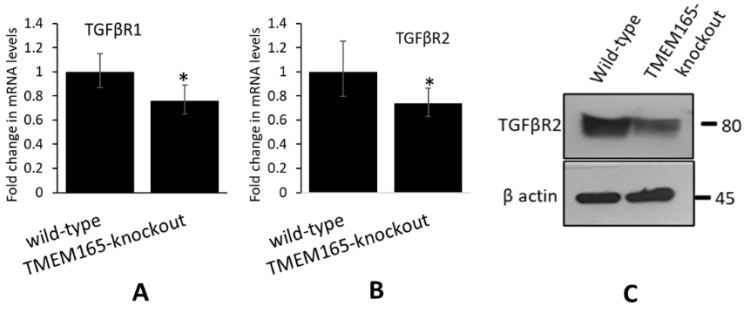

Figure 4.21: *Expression analysis of TGF-βR1 and TGF-βR2 in wild-type and TMEM165-mutant ATDC5 cells: mRNA expression levels of* ***(A)****TGF-βR1 and* ***(B)*** *TGF-βR2 were assessed by qPCR analysis. qPCR values were normalized for the housekeeping gene ribosomal protein S29 and are expressed as the relative expression compared with control. Data are expressed as the fold change relative to control as mean ±S.D. Statistical analysis was performed with an unpaired Student's t test (NS, statistically not significant; *p<0.05; **p<0.01).* ***(C)*** *Cell lysate of wild-type and TMEM165-Knockout ATDC5 cells was analyzed by western blot using anti-TGFβR2 specific antibodies. β-actin was used as loading control.*

Likewise, significant decrease in the mRNA levels of TGFβR2 was observed in TMEM165-deficients fibroblasts from CDG patient compared to normal fibroblasts, whereas no significant changes were observed in the mRNA levels of TGFβR1 (**Figure 4.22A and 4.22B**).

Western blot analysis of the expression of TGFβR2 protein confirmed the mRNA data and showed strong decrease in the expression of receptor (**Figure 4.22C**)

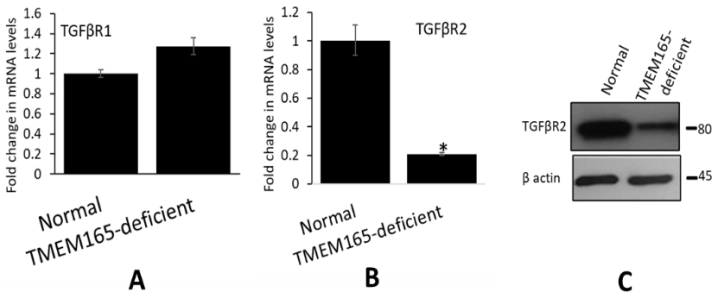

Figure 4.22: *Expression analysis of TGF-βR1 and TGF-βR2 in human normal and TMEM165-deficient fibroblast cells: mRNA expression levels of* ***(A)****TGF-βR1 and* ***(B)*** *TGF-βR2 were assessed by qPCR analysis. qPCR values were normalized for the housekeeping gene ribosomal protein S29 and are expressed as the relative expression compared with control. Data are expressed as the fold change relative to control as mean ±S.D. Statistical analysis was performed with an unpaired Student's t test (NS, statistically not significant; *p<0.05; **p<0.01).* ***(C)*** *Cell lysate from human normal and TMEM165-deficient fibroblast cells was analyzed by western blot using anti-TGFβR2 specific antibodies. β-actin was used as loading control.*

These data revealed that TMEM165-deficiency led to decreased expression of the TGF-β receptor, TGFβR2 which may account for downregulation of TGF-β signaling in TMEM165-deficient cells. Downregulation of TGF-β signaling may also result from up-regulation of negative regulators such as asporin, an extracellular protein belonging to a leucine-rich PG family, that suppresses TGF-β signaling by direct interaction with TGF-β thus preventing its binding to TGFβR2. Therefore, we sought to determine whether TMEM165-deficiency affects the expression of asporin. Investigation of the level of mRNA expression of asporin in TMEM165-deficient ATDC5 cells and patient fibroblasts showed a remarkable increase (4-fold) in the expression of asporin in mutant cells compared to normal cells **(Figure 4.23A and 4.23B).** Assessment of asporin protein expression by immunoblot showed higher levels of expression in TMEM-deficient ATDC5 and patient fibroblast cells, compared to normal cells **(Figure 4.23C).** Therefore, these results showed that expression of asporin was significantly upregulated in TMEM165-deficient cells. Altogether, these data indicated that TMEM165 deficiency impairs TGF-β signalling through downregulation of the expression of TGFβR2 receptor and upregulation TGF-β signaling antagonist, asporin.

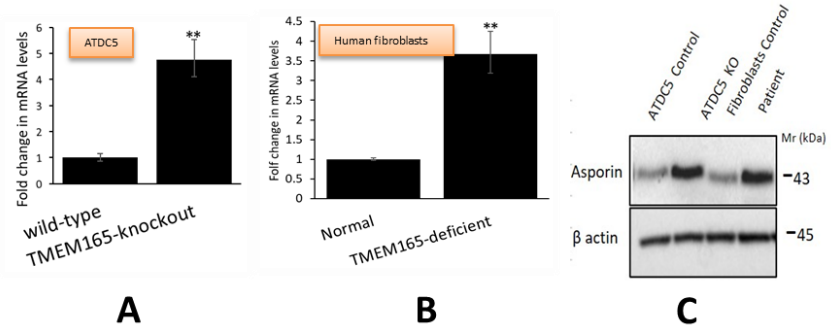

Figure* 4.23:** *Analysis of expression of TGF-β signaling antagonist asporin. Relative mRNA levels of asporin was evaluated by RT-qPCR in* ***(A) *wild-type and TMEM165-mutant ATDC5 cells and in* ***(B)*** *normal and TMEM165 deficient patient fibroblast cells. qPCR values were normalized for the housekeeping gene ribosomal protein S29 and are expressed as the relative expression compared with control. Data are expressed as the fold change relative to control as mean ±S.D. Statistical analysis was performed with an unpaired Student's t test (NS, statistically not significant; *p<0.05; **p<0.01).* ***(C)*** *Cell lysate of wild-type and TMEM165-Knockout ATDC5 cells and of normal and TMEM165 deficient patient fibroblast cells were analyzed by western blot using anti-asporin specific antibodies. β-actin was used as loading control.*

BMP signaling plays a key role in skeletal development and alterations in BMP signaling pathway are major underlying cause of human skeletal disorders (Salazar, Gamer, and Rosen 2016a). BMP signaling relies on secreted ligands and on a type I and type II BMP receptors that activate downstream mediators, notably the canonical SMAD pathway. To determine whether TMEM165 deficiency affects BMP signaling, we examined the phosphorylation status of Smad 1,5,9 downstream mediators of BMP receptor activation. Interestingly, immunoblot analysis showed that the level of phospho-Smad 1,5,9 was higher in TMEM165-deficient ATDC5, compared to wild-type cells **(Figure 4.24A)**. This result was confirmed in patient fibroblast cells which showed increased level of phospho-Smad 1,5,9 compared to normal fibroblasts **(Figure 4.24B)**.

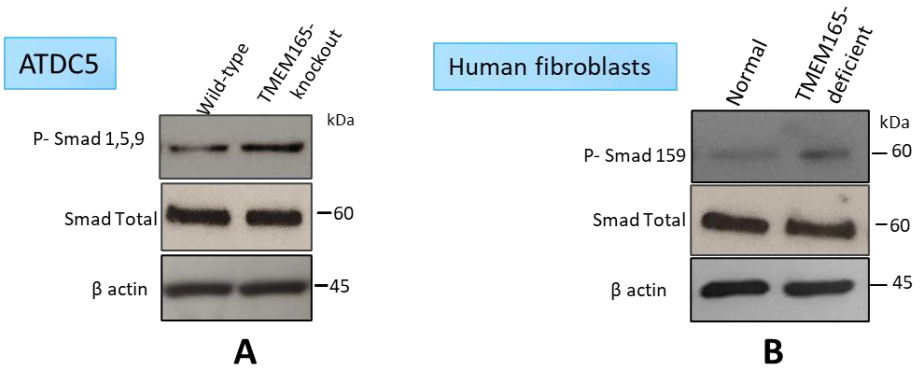

Figure 4. 24: *Analysis of BMP signalling pathway in normal and TMEM165-deficient cells. Cell lysate of wild-type and TMEM165-Knockout ATDC5 cells and of normal and TMEM165 deficient patient fibroblast cells were analyzed by western blot for the evaluation of phosphorylation status of Smad 1,5,9 using anti-phospho-Smad1,5,9 and anti-Smad1,5,9 specific antibodies. β-actin was used as loading control.*

Therefore, these data revealed that deficiency in TMEM165 functionally impairs BMP/Smad signaling leading to activation of the signaling pathway. Indeed, analysis of the mRNA expression level of Id1 gene, a BMP downstream target gene, showed a significant increase in TMEM165-deficient cells compared to normal cells **(Figure 4.25A).** To further confirm the increase of BMP signaling in TMEM165-deficient cells, a BMP signaling reporter vector pGL3-BRE-Luc containing a BMP responsive promoter element (BRE) was used to transfect wild-type and mutant ATDC5 cells. As shown in **Figure 4.25B**, analysis of luciferase activity, which is a measure of BMP signaling, showed a significant increase in mutant cells compared to wild-type cells (**Figure 4.25B),** thus bringing evidence that BMP signaling is activated in TMEM165-deficient cells.

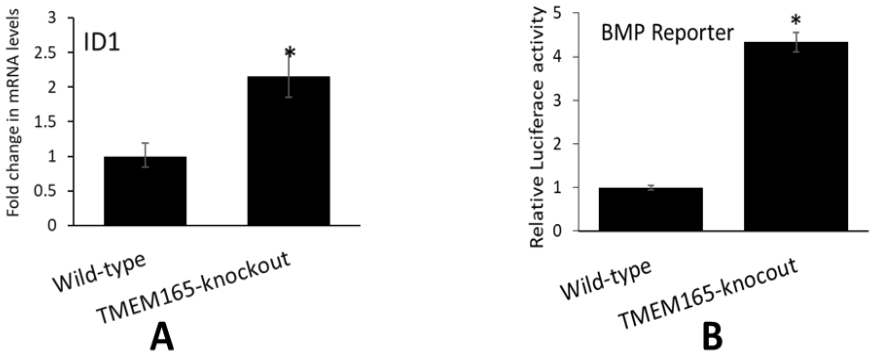

***Figure 4. 25**: Analysis of expression of ID1 gene and luciferase activity of BMP reporter in normal and TMEM165-Knockout ATDC5 cells. **(A)** Relative mRNA levels of ID1 gene were evaluated by RT-qPCR. qPCR values were normalized for the housekeeping gene ribosomal protein S29 and are expressed as the relative expression compared with control. **(B)** ATDC5 control and TMEM165-Knockout cells were co-transfected with plasmid expressing BMP reporter (firefly) and Renilla and luciferase reporter activity of BMP was measured. Data are expressed as the fold change relative to control as mean ±S.D. Statistical analysis was performed with an unpaired Student's t test (NS, statistically not significant; *p<0.05; **p<0.01).*

The observation that BMP/Smad signaling axis is functionally impaired in TMEM165-deficient cells prompted us to investigate whether the response of mutant cells to BMP stimulation was affected. To this end, wild-type and mutant ATDC5 were stimulated with BMP2, a potent activator of BMP/Smad signaling pathway in chondrocytes, and the phosphorylation level of Smad 1,5,9 was analyzed by immunoblotting. The result showed that the level of phospho-Smad 1,5,9 increased significantly in both wild-type and mutant cells following stimulation with BMP2, but the increase was more pronounced in mutant cells, compared to wild-type cells **(Figure 4.26)**.

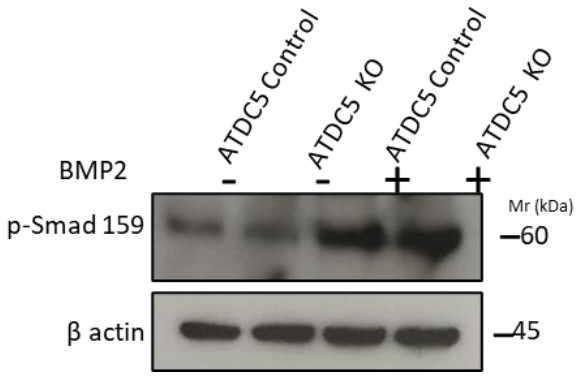

Figure 4. 26: *Analysis of the response of mutant cells to BMP stimulation: Western blot analysis of cell lysates from wild-type and TMEM165-KnockouO cells treated or not with BMP2 (1ng/ml) for 1 hour. β actin was use as loading control (n=3).*

In an attempt to identify the mechanism involved in the alteration of the BMP/Smad signaling pathway, we investigated the mRNA expression levels of type I and type II BMP receptors, BMPR1A (ALK3), BMR1B (ALK6) and BMPR2 by RT-qPCR in TMEM165-deficient and wild-type cells. As shown in **Figure 4.27**, mRNA expression levels of BMP receptors were increased with BMPR1B showing the highest increase (2-fold) in TMEM165-deficent ATDC5, compared to wild-type cells **(Fig 4.27B)**.

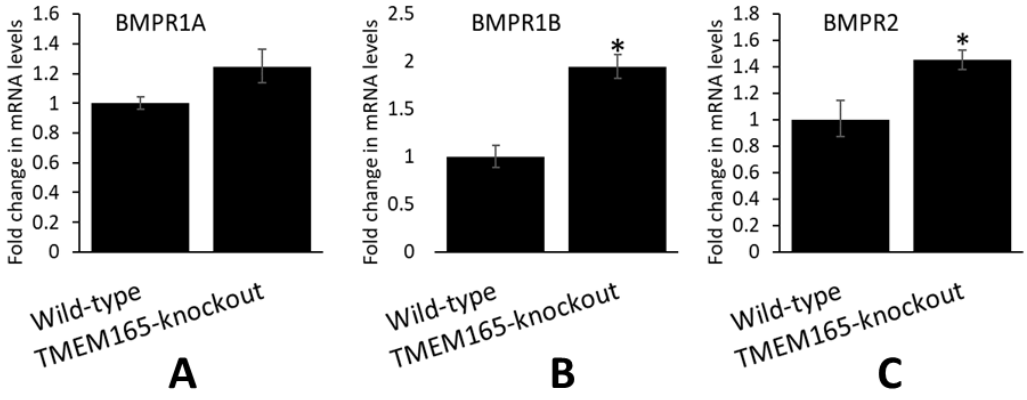

Figure 4.27: *Expression analysis of BMP receptors in wildtype and TMEM165-mutant cells: Relative mRNA levels of* ***(A)*** *BMPR1A,* ***(B)*** *BMPR1B and* ***(C)*** *BMPR2were evaluated by RT-qPCR in wild-type and TMEM165-mutant cells. qPCR values were normalized for the housekeeping gene ribosomal protein S29 and are expressed as the relative expression compared with control. Data are expressed as the fold change relative to control as mean ±S.D. Statistical analysis was performed with an unpaired Student's t test (NS, statistically not significant; *p<0.05; **p<0.01).*

To confirm the increase in the expression of BMP receptor BMPR2 at the protein level, Western blot analysis of the expression of BMPR2 receptor was carried out using cell lysates of wild-type and TMEM165-deficient ATDC5 cells. The results showed an increase in the protein expression level of the receptor in mutant cells compared to normal cells **(figure 4.28)**.

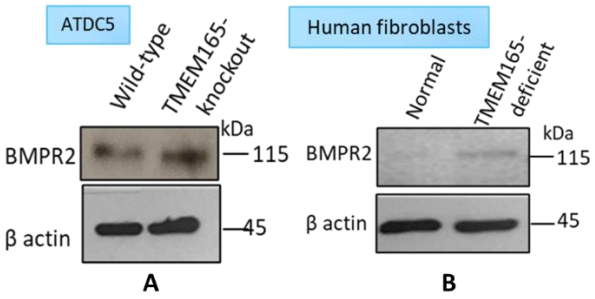

Figure 4.28: *Analysis of the protein expression of the BMP receptor, BMPR2: Immunoblot analysis of the expression of BMPR2 in* ***(A)*** *wildtype and TMEM165-mutant ATDC5 cells****,*** *and in* ***(B)*** *fibroblast cells from normal and TMEM165-deficient patient. β actin was used as loading control (n=3).*

Similar results were observed, either for mRNA expression levels of BMPR1A, BMR1B and BMPR2 **(Figure 4.29A, B and C)** or for BMPR2 protein expression **(Figure 4.28B)** in *fibroblast cells from TMEM165-deficient patient compared to normal fibroblast cells*.

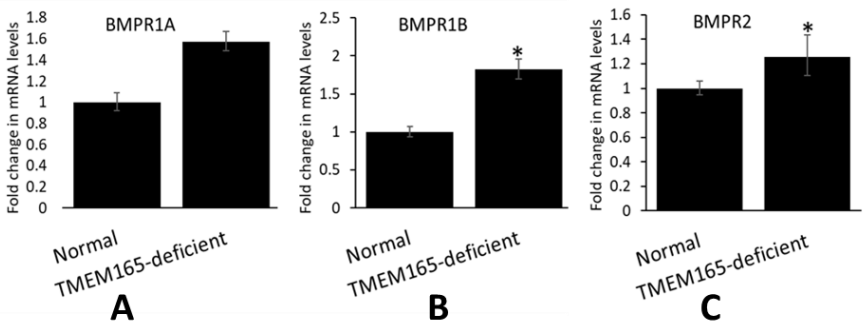

Figure 4. 29: *Expression analysis of BMP receptors in normal and TMEM165-deficient fibroblast cells: Relative mRNA levels of* ***(A)*** *BMPR1A,* ***(B)*** *BMPR1B and* ***(C)*** *BMPR2 were evaluated by RT-qPCR in normal and TMEM165-deficient fibroblast cells. qPCR values were normalized for the housekeeping gene ribosomal protein S29 and are expressed as the relative expression compared with control. Data are expressed as the fold change relative to control as mean ±S.D. Statistical analysis was performed with an unpaired Student's t test (NS, statistically not significant; *p<0.05; **p<0.01).*

Upregulation of the expression of BMP receptors may therefore account for increased BMP signaling in mutant cells. It is also well known that BMP signaling is regulated by ligand antagonists such as noggin that antagonizes the signaling by directly binding BMP proteins thereby preventing receptor activation. Therefore, to determine if the expression of noggin is altered in TMEM165-deficient cells, mRNA level of NOG gene was assessed by RT-qPCR in TMEM165-deficient and normal cells. As shown in **Figure 4.30A** mRNA expression level of noggin was significantly reduced in mutant ATDC5, compared to wild-type cells. Similar results were observed in human patient fibroblasts, compared to normal cells **(Figure 4.30B)**.

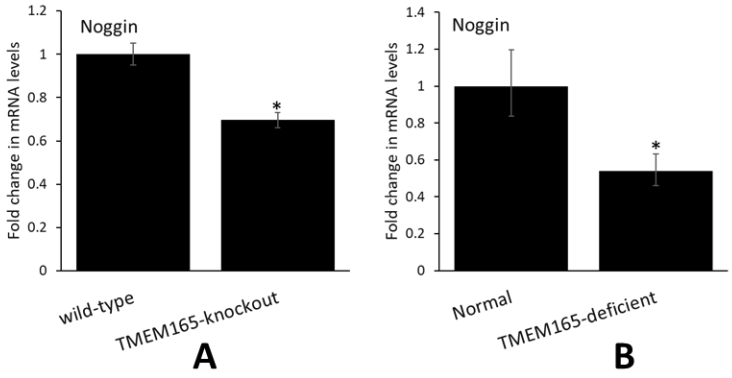

Figure 4. 30: *Analysis of expression of the BMP antagonist, NOG gene. Relative mRNA levels of NOGGIN were analysed by qPCR in* ***(A)*** *wild-type and TMEM165-Knockout ATDC5 cells and in* ***(B)*** *normal and TMEM165-deficient fibroblast cells. qPCR values were normalized for the housekeeping gene ribosomal protein S29 and are expressed as the relative expression compared with control. Data are expressed as the fold change relative to control as mean ±S.D. Statistical analysis was performed with an unpaired Student's t test (NS, statistically not significant; *p<0.05; **p<0.01).*

These data raise the possibility that downregulation of expression of the BMP antagonist noggin may participate to the increased BMP signaling observed in mutant cells. Altogether, these data revealed the upregulation of BMP signaling in TMEM165-deficient cells which may result from increased expression of BMP receptors and decreased expression of BMP antagonist. Overall, this study showed that TMEM165-deficiency led to downregulation of TGF-β/Smad2 and upregulation of BMP/Smad 1,5,9 axis and thus functionally impairs these signalling pathways in mutant cells.

4.6 TMEM165-deficiency accelerates cell proliferation

Chondrogenesis is a well-coordinated multi-step differentiation process in which chondrocytes proliferate to produce terminally differentiated hypertrophic chondrocytes. Owing to the role of GAG chains and of TGF-β in the regulation of cell proliferation, reduced GAG chain polymerization and TGF-β signaling in TMEM165-deficient cell prompted us to investigate whether proliferation was affected in mutant cells. To this end, proliferation of TMEM 165-deficient ATDC5 and patient fibroblasts cells was measured using CyQUANT Cell Proliferation Assay Kit.

As shown in **Figure 4.31A and 4.31B**, the proliferation rate in TMEM165-deficient ATDC5 and fibroblast cells was significantly increased (1.5-fold), compared to normal cells, therefore indicating that TMEM165-deficiency promotes cell proliferation. Accordingly, analysis of the activation status of extracellular signal-regulated kinase (ERK) 1/2 mitogen-activated protein (MAP) kinase pathway, that plays a central role in cell proliferation control, showed higher level of activation in TMEM165-deficient ATDC5 and patient fibroblast cells compared to normal cells.

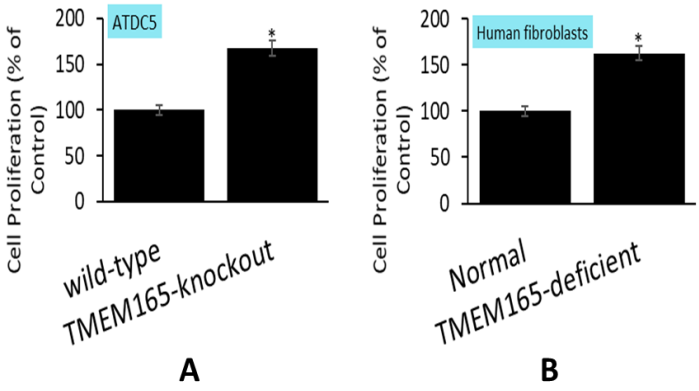

Figure 4.31: *Analysis of cell proliferation in* ***(A)*** *wild-type and TMEM165-deicient ATDC5 cells and in* ***(B)*** *Human fibroblasts from control and CDG patients deficient in TMEM165 using Cyquant® proliferation assay kit.*

Indeed, phospho-ERK1/2 level but not total ERK1/2 level was strongly increased in TMEM165-deficient cells, compared to normal cells **(Figure 4.32A and 4.32B)**, indicating a sustained activation of ERK1/2 signaling that may promote proliferation in mutant cells.

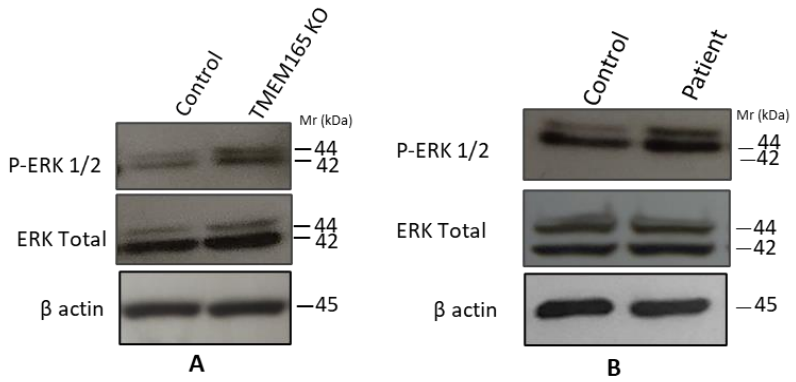

Figure 4.32: *Immunoblot analysis of ERK 1/2 signaling pathway in normal and TMEM165-mutant cells. Cell lysate from* ***(A)*** *wild-type and TMEM165-deficient cells ATDC5 control and from* ***(B)*** *fibroblasts control and fibroblasts from CDG patients deficient in TMEM-165 were analysed for the phosphorylation of ERK1/2 using antiphospho-ERK1/2 and anti-ERK1/2 antibodies. β actin was used as loading control (n=3).*

4.7 Ca^{2+}/calmodulin-dependent protein kinase II pathway is activated in TMEM165-deficient cells

It has been proposed that TMEM165 may exchange Golgi luminal H^+ for cytoplasmic Ca^{2+}, whereas other studies suggested that it may be involved in the transport of cytoplasmic Mn^{2+} to the Golgi lumen. Direct implication of TMEM165 in the transport of either Ca^{2+} or Mn^{2+} is not yet been reported. However, it is well known that Ca^{2+}/calmodulin-dependent protein kinase II (CaMkII) is activated when intracellular concentration in Ca^{2+} is elevated and Ca^{2+}/calmodulin complex binds to CaMkII regulatory domain. We hypothesized that if TMEM165 is involved in Ca^{2+} homeostasis then deficiency in TMEM165 may lead to impaired transport of cytoplasmic Ca^{2+} to the Golgi and therefore to elevated [Ca^{2+}] in the cytoplasm. To verify this hypothesis, we analysed the phosphorylation status of CaMkIIα by immunoblotting in TMEM165-deficient and wild-type ATDC5 cells. Interestingly, as shown in **Figure 4.33A,** the level of phospho-CaMkIIα (pCaMkIIα) was strongly increased in TMEM165-deficient cells compared to wild-type cells, indicating that CaMkIIα was strongly activated in TMEM165-deficient cells.

Likewise, as observed in ATDC5 cells, the phosphorylation level of CaMkIIα is remarkably increased in TMEM165-deficient patient fibroblast cells, compared to normal fibroblasts **(Figure 4.33B).** These results indicate that CaMkIIα is activated in mutant cells and therefore that intracellular Ca^{2+} is probably elevated in these cells. Altogether, these data strongly support the notions that TMEM165 is implicated in the regulation of Ca^{2+} homeostasis.

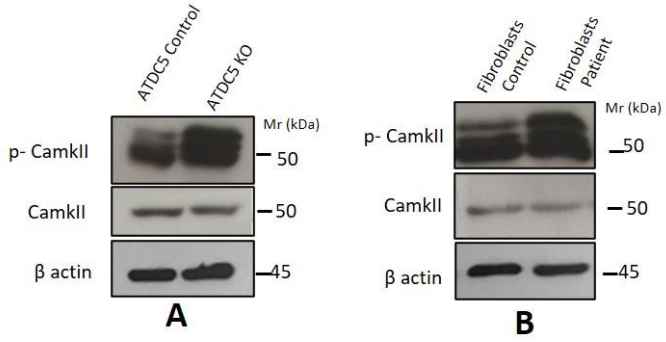

Figure 4. 33: *Immunoblot analysis of* CaMkIIα *signaling pathway in normal and TMEM165-mutant cells. Cell lysate from* ***(A)*** *wild-type and TMEM165-deficient cells ATDC5 control and from* ***(B)*** *fibroblasts control and fibroblasts from CDG patients deficient in TMEM-165 were analysed for the phosphorylation of* CaMkIIα *using antiphospho-*CaMkIIα *and anti-*CaMkIIα *antibodies. β actin was used as loading control (n=3).*

4.8 TMEM165-deficiency promotes chondrocyte differentiation towards hypertrophic phenotype

The long bones of mammals are formed by endochondral ossification process that involves the formation of a cartilaginous draft in which the chondrocytes undergo a maturation process before being replaced by a mature bone. Chondrogenesis process is tightly regulated during skeletal development and alteration of the chondrocyte maturation result in defects in endochondral bone development. To investigate whether chondrogenic differentiation of ATDC5 cells is affected in the absence of TMEM165, wild-type and TMEM165-deficient ATDC5 cells were induced by insulin into chondrogenic differentiation and the levels of expression of chondrogenic markers including Sox9, Col2a1, AGN, Ihh and OCN were measured by RT-qPCR before induction and at seven days post-induction. The results showed that at steady state (day 0), ATDC5 mutants cells express high levels of the chondrogenic markers Sox9, Col2a1 and AGN **(Figure 4.34A, B, and C** respectively), and decreased levels of pre-hypertrophic and hypertrophic markers Ihh and OCN, compared to wild-type cells (**Figure 4.34D and**

4.34E).These results indicate that loss of TMEM165 expression induces chondrogenic differentiation of ATDC5 cells. Importantly, analysis of the expression of the markers at seven days post-induction revealed that ATDC5 mutant cells undergo rapid maturation as evidenced by downregulation of chondrogenic markers Sox9, Col2a1, AGN and upregulation of chondrocyte pre-hypertrophic and hypertrophic markers Ihh and OCN **(Figure 4.34D and 4.34E**). In contrast, in wild-type cells, the chondrogenic markers were up-regulated and pre-hypertrophic and hypertrophic markers were down regulated **(Fig 4.34A and B respectively).** Altogether, these data bring evidence that TMEM165-deficiency promote premature chondrocyte maturation, a process which affects endochondral ossification and may lead to dwarfism.

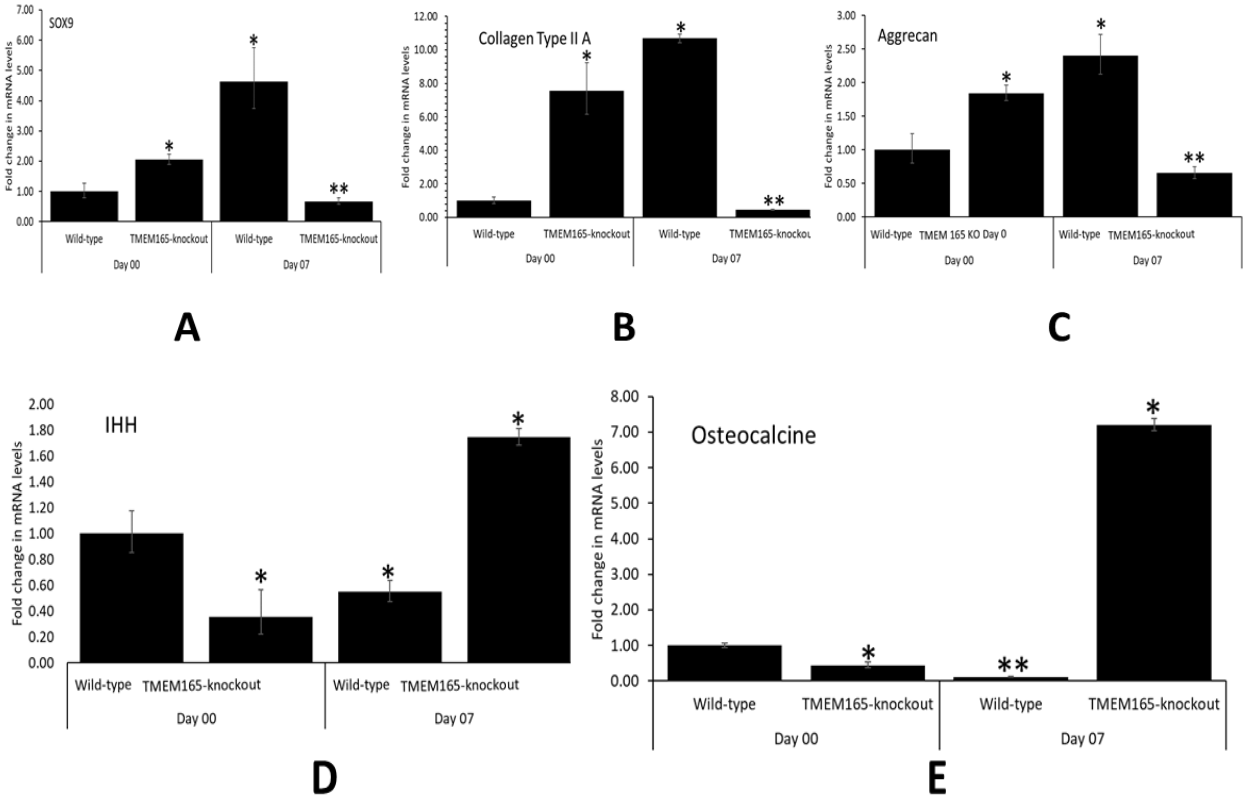

Figure 4. 34: *RT-qPCR analysis of the expression of chondrogenic markers in ATDC5 control and TMEM165-knockout cells. mRNA levels of* ***(A)*** *SOX9,* ***(B)*** *Col2A and* ***(C)*** *Aggrecan* ***(D)*** *IHH-Indian hedgehog and* ***(E)*** *OCN-osteocalcin were evaluated by RT-qPCR. qPCR values were normalized for the housekeeping gene ribosomal protein S29 and are expressed as the relative expression compared with control. Data are expressed as mean ± S.D. Statistical analysis was performed with an unpaired Student's t test (*p<0.05; **p<0.01).*

5 DISCUSSION

Human skeleton is a highly complex and dynamic organ that serves as a body frame. Bones and cartilage with other types of tissues provide the framework of the skeletal system during development (Kobayashi and Kronenberg 2014). Development of skeleton begins at the early days of the vertebrate embryo with evolution of multipotent mesenchymal cells from ectoderm and mesoderm that migrate to specific locations in the body and undergoes skeletal fate. Most of these multipotent mesenchymal cells develop into chondrocytes (that form cartilage), articular or synovial cells (joint cells) and osteoblasts (bone cells), whereas some remain as mesenchymal stem cells throughout life. Cartilage is considered as an embryonic tissue because of its extensive distribution during foetal development providing the templates for skeletal elements developing through endochondral ossification. The chondrocytes are responsible for longitudinal growth within the epiphyseal growth plate hence are major contributor to growth of the body. Bones are formed by endochondral ossification that forms a cartilage template where chondrocytes undergo a maturation before being replaced by bone. This process begins with the condensation and aggregation of mesenchymal cells, which then differentiate into chondrocytes (Shimizu, Yokoyama, and Asahara 2007).

PGs are formed by the covalent attachment of GAG chains onto the core protein. Unlike DNA/RNA and proteins, the synthesis of GAG chains is not template derived, they are synthesized by stepwise addition of sugar units by various glycosyltransferases. These sugar units are modified by sulfation at different positions and by epimerization. PGs are complex biomacromolecules present on the cell surface and in ECM. They regulate various biological processes including chondrocyte differentiation and maturation. It has been established that GAG chains of PGs are responsible for most functions of PGs (Couchman 2010; Gesslbauer et al. 2013; Manon-Jensen, Itoh, and Couchman 2010b). Owing to their position in ECM, pericellular region and cell surface PGs play a key role in ECM structure and organization, cell signaling, adhesion and proliferation. They also act as co-receptors for several ligands and regulate the bioavailability of growth factors. TMEM165 protein is involved in CDG although the functions are unknown so far, but it is established that the TMEM165-deficient CDG patients present bone abnormalities suggesting potential involvement of TMEM165 in chondrogenesis and bone homeostasis (Foulquier et al. 2012). In this study, we hypothesized that alterations in the synthesis of PGs may contribute to skeletal defects observed in TMEM

165-deficient CDG patients. Indeed, it is established that impaired activities of GTs involved in the synthesis of GAG chains of PGs led to skeletal defects. Mutation in EXT1 and EXT2 genes encoding HS polymerising enzymes are known to cause hereditary multiple exostoses due to defects in HS chains (McCormick et al. 1998). Mutations in gene β4GALT7 that encodes β4-galactosyltransferase-7 cause defects in DS chains resulting in Ehlers-Danlos syndrome (EDS) progeroid form characterised by delayed development, premature aging, short stature and generalised osteopenia (Okajima et al. 1999). Similarly, mutations in β3GAT3 causes Larsen-like syndrome with congenital heart defects and joint dislocations (Baasanjav et al. 2011). HS and CS/DS biosynthetic enzymes are crucial to bone development and skin integrity in humans.

Here, we generated TMEM165-deficient pre-chondrocyte ATDC5 and HEK293 cells. We clearly showed that loss of TMEM165 in either mouse cells ATDC5 or human cells HEK293 led strong reduction in the elongation of PG-GAG chains of both types HS (syndecan 4) and CS (decorin), suggesting a link between PGs, GAGs and TMEM165. Supporting these findings, we also found defect in decorin synthesis in TMEM165-CDG patients' fibroblasts. Noteworthy, Syndican-4 is excessively expressed by proliferative chondrocytes, hypertrophic chondrocytes, and epiphyseal cartilage. In humans and mice, it is expressed by joint/articular cartilage during osteoarthritis (Pap and Bertrand 2013). Syndicans serve as adhesion molecules, binding to chemokines, cytokines, growth factors, morphogens, pathogens, and metalloproteinases (MMP) (Choi et al. 2011b; Pap and Bertrand 2013). On the other hand, decorin interacts with type I and type II collagens and various growth factors. The LRR (leucine rich repeat) domain and GAG side chain are the main decorin interacting partners as they enable decorin to bind and sequester many molecules including marcomolecules present in ECM, growth factors, receptors, cytokines, enzymes, hormones and lipoproteins (Bi et al. 2012; Gubbiotti et al. 2016; Ruoslahti and Yamaguchi 1991; Sainio and Järveläinen 2019; Torres, Gubbiotti, and Iozzo 2017). These raises many questions including why and how TMEM165 deficiency is disturbing PG-GAG synthesis, what are the consequences and how can this be reversed.

Evaluation of mRNA levels of genes encoding enzymes involved in formation of tetrasaccharide linker region including β4Galt7, β3GalT3, β3Galt6, XT1 and XT2, and those involved in polymerisation of GAG chains *ie.* EXTL3, EXT1, EXT2, CHSY1 and CHSY2 showed that the mRNA levels were not significantly disturbed, suggesting that defects in the synthesis of

GAG chains in TMEM165 deficient cells is not due to alterations in the expression of these enzymes. We also showed that overexpression of CS elongating enzymes CHSY1 and CHSY2 did not rescue the elongation of CS-GAG chains using either decorin or 4MU-xyloside as substrates, thus confirming that defect in GAG synthesis was not due to lack of sufficient expression of the polymerizing enzymes.

As overexpression of CS polymerizing enzyme did not rescue the elongation of CS GAG chains, we sought to determine whether supplying the cell culture medium with sugar monosaccharides used for the synthesis of CS-GAG chains such as xylose and galactose may restore CS elongation in TMEM165-deficient cells. Our data indicated that supplying cells with monosaccharides which constitute CS-GAG chains did not overcome the blockage in the polymerization process. Altogether, these data suggest that impaired elongation of CS-GAG chains induced by deficiency in TMEM165 is probably not due to defects in the expression of the enzymes involved or the monosaccharide substrates.

Golgi GTs use UDP-sugars as a donor substrate and require Mn^{2+} at their catalytic site to be fully active. Decreased cellular Mn^{2+} has recently been shown to cause Congenital Disorders of Glycosylation (CDG) (Park et al. 2015; Potelle et al. 2017). Therefore, we analysed the expression patterns of GAG chains after treatment of cells with MnCl2 (1 µM). Mn^{2+} supplementation increases the size of CS-attached decorin and HS-attached syndecan 4 in TMEM165-knockout cells and therefore support the notion that Mn^{2+} restores polymerization of decorin CS-GAG and syndecan 4 HS-GAG chains in TMEM165-deficient cells and strongly suggest that Mn^{2+} rescue GAG polymerization in TMEM165-deficient cells. These findings reaveled that TMEM165 plays an essential role in the synthesis of PGs by supplying the Golgi with the co-factor Mn^{2+} required for optimal GT enzyme activities.

Analysis of BMP and TGF-β signaling pathways revealed that BMP and TGF-β signaling are impaired in TMEM165-deficient cells. TGF-βs and BMPs, play an important role in several stages of chondrogenesis. TGF-β1 promotes cell chondrogenesis and inhibits the terminal differentiation of chondrocytes in high-density chondrocyte pellets or long bone cultures *in vitro* (Tracy Ballock et al. 1993). We found that TMEM165-deficiency led to down regulation of TGF-β signaling by down regulation of TGF-β receptors. The signaling was activated when the cells were exogenously treated with growth factor TGF-β1 but at lower extent compared

to wild-type cells indicating that both basal and inducible TGF-β signaling activation is impaired in TMEM-165-deficient cells. This also suggest that impaired activity of TGF-β signaling is not due to lower levels, if any, of endogenous cytokines. Asporin has been shown to suppresses TGF-β signaling by direct binding of the cytokine in the ECM thus preventing its interaction with the receptor. Interestingly, our study clearly showed that deletion of TMEM165 resulted in significant upregulation of asporin protein expression, suggesting a role in downregulation of both basal and inducible activation of TGF-β/smad signaling pathway in TMEM165-deficient cells. TGFβ activates Smad2 and Smad3 through binding to TGFβRII receptor and recruitment of ALK5 receptor (TGFβRI) (Derynck and Zhang 2003). Noteworthy, mice lacking TGFβRII or ALK5 in chondrocytes exhibit developmental anomalies at the base of the skull and in the vertebrae, such as those observed in mice disabled for the TGFβ2 (Sanford et al. 1997). TGFβ signaling maintain metabolic homeostasis of cartilage and is involved in pathogenesis of arthritis. Inhibition of TGFβ signaling induce chondrocyte hypertrophy and results in degeneration of cartilage (Wu, Chen, and Li 2016b).

We have evaluated BMP signaling pathway in TMEM 165-deficient cells and observed that phospho-Smad 1/5/9 is upregulated in TMEM165 KO cells, suggesting that BMP signaling is upregulated in these cells. BMP signaling activation is regulated by the BMP antagonist noggin. We found that, in addition to upregulation of BMP receptors, expression of *NOG* gene is downregulated in TMEM165-deficient cells which may account for upregulation of BMP/Smad1,5,9 signaling. Noteworthy, BMP regulates longitudinal growth and excessive BMP signaling has been shown to accelerated chondrogenesis and chondrocyte differentiation (Dathe et al. 2009; Freire-Maia, Maia, and Pacheco 1980; Salazar, Gamer, and Rosen 2016b). Brachydactylies type 2 (BDB2) is a *NOG* mutation characterised by absence of terminal structures of the toes and digits due to excessive BMP signaling (Lehmann et al. 2007). Mutations in *NOG* causes inability of the antagonist to bind BMP or heparin and to sequester BMPs in ECM which results in excessive BMP signaling (Masuda et al. 2014; Pang et al. 2015). Similarly, excessive activation of BMP signaling due to mutation in GDF6 and GDF3 cause Klippel Feil disorder characterised by malformation of larynx, and vertebral dysostoses (Ye et al. 2009).

Studies of the regulation of growth factor function has shown that binding to GAGs is necessary in the activation of many soluble growth factors and cytokines. BMP and TGFβ are

important for embryonic skeletal development and growth. They regulate cell proliferation, differentiation, apoptosis, and migration. Both BMP and TGFβ are regulated by different factors and receptors (Tian H. et al 2007; Kei sako et al 2009). We have found that TGF-β and BMP signaling are functionally impaired in TMEM165-deficient cells. Taking into account the key role of these signaling pathways in chondrocyte differentiation and maturation, it is tempting to speculate that this may account for defects in skeletal development observed in TMEM165-deficient patients.

The primary skeleton is entirely cartilaginous. It grows quickly and most of it is progressively replaced by bone throughout foetal and postnatal growth. The process is called endochondral ossification. Concomitantly, joints and additional bones form. The latter develop upon a mesenchymal template, without cartilage intermediate, through a process called intramembranous ossification. Bone, cartilage, and joints differ in composition and regulation, but their associated developments are tightly coordinated. The impaired levels of hypertrophic marker Ihh and osteocalcin in TMEM165-deficient prechondrocyte cells during differentiation process may lead to early hypertrophy of chondrocytes. It has been suggested that TGFβ inhibits hypertrophy induced by Ihh (Chen et al. 2019). Overexpression of Ihh induces early chondrocyte hypertrophy and ossification during chondrogenesis resulting in hypertrophic cartilage formation. Our study has shown that TGFβ signaling is downregulated and Ihh is upregulated in TMEM165-deficient ATDC5 cells, suggesting accelerated chondrocyte hypertrophy. We argue that, because of deficient chondrocyte PG production, mutant chondrocytes accelerate the timing of Ihh expression upregulate BMP and downregulate TGFβ signaling, which causes early chondrocyte differentiation.

GDT1 is a yeast ortholog of TMEM165. This ortholog is involved in Ca^{2+} homeostasis (Colinet et al. 2016; Thines et al. 2018). Overexpression of phosphorylated calcium calmodulin kinase II (p-CamkII) in TMEM165 KO cells suggests that intracellular calcium level is increased in these cells. It has been established that Ca^{2+}/Calmodulin-dependent kinase II (CamKII) signaling causes skeletal overgrowth and early chondrocyte maturation (Taschner et al. 2008). Therefore, TMEM165-knockout chondrocytes showed early maturation and accelerated terminal differentiation resulting in impaired chondrogenesis. Our findings suggest that TMEM165 deficiency causes abnormalities in PG synthesis and aberrant signaling that resulted

in disturbances in chondrocyte maturation. All these findings have given new directions to explore the functions of TMEM165 in skeletal development and bone homeostasis.

6 CONCLUSIONS AND PERSPECTIVES

This thesis work has allowed us to elucidate the crucial role of TMEM165 in PG synthesis and chondrocyte maturation. TMEM165 plays an essential role in the synthesis of PGs. There are alterations in the synthesis of PGs mainly impaired polymerization of heparin-sulfate as well as chondroitin-sulfate GAG chains in TMEM165-deficient cells. PGs play an important role in the structure and organisation of ECM, availability of growth factors, chondrocytes maturation, growth plate development and intracellular signaling.

Moreover, we have demonstrated that by supplying the cells with Mn^{2+} the defects in polymerisation were overcome as Mn^{2+} is used as a co-factor of Golgi glycosyltransferases and required for full enzyme activity. These findings suggested that TMEM165 regulate Golgi Mn^{2+} homeostasis.

Given that TGFβ and BMP signaling regulate chondrogenesis and they are the key signaling pathways that regulate chondrocytes maturation. We have revealed for the first time that TMEM165-deficiency resulted in an impaired TGF-β/Smad2 signaling axis led to downregulation of TGF-β/Smad2 signaling. In addition, deficiency of TMEM165 caused an activation of the BMP/Smad 1,5,9 axis and therefore functionally impairing the signalling pathway in both ATDC5 mutant cells and in fibroblasts from TMEM165-deficient patient. Disruption of these different pathways leads to increased proliferation and early hypertrophy of chondrocytes.

It will be interesting to determine the factors and mechanisms responsible for the disruption of the expression of TGF-β and BMP signaling components. *In vitro* study of ATDC5 cell differentiation revealed that TMEM165 deficiency promotes differentiation of ATDC5 cells towards hypertrophy and this may cause premature chondrocyte maturation and can result in skeletal abnormalities observed in TMEM165-deficient CDG patients. These chondrogenesis abnormalities result in an early and accelerated ossification which leads to dwarfism and various abnormalities. Moreover, Increased levels of phosphorylated calcium calmodulin kinase II (p-CamKII) in TMEM165 KO cells suggest that TMEM 165 is involved in Ca^{2+} homeostasis causing skeletal overgrowth and early chondrocyte. It will be interesting to

determine whether this stands through *in vivo* using animal models such as mice knockout for TMEM165 in cartilage available in our laboratory.

On the other hand, it would be important to study the role of TMEM-165 in osteoblasts both *in vivo* and *in vitro* to determine the role of this protein in bone formation and homeostasis.

RÉSUMÉ EN FRANÇAIS

Situation du sujet

Les PG sont des biomacromolécules importantes et des constituants majeurs de l'ECM. Elles sont composées d'une protéine centrale avec une ou plusieurs longues chaînes de polysaccharides non ramifiées appelées glycosaminoglycanes (GAG). Outre l'expression à la surface des cellules, les GAGs sont abondamment exprimés dans les ECM des tissus conjonctifs . Ces macromolécules remplissent plusieurs fonctions biologiques, notamment le dépôt d'ECM, la différenciation cellulaire, l'adhésion cellulaire, la migration et la prolifération des cellules par leur interaction avec diverses cytokines, facteurs de croissance, enzymes et protéines d'adhésion cellulaire. Comme les PG ont des fonctions cellulaires diverses, elles sont impliquées dans de nombreux états pathologiques tels que l'athérosclérose, l'arthrose, la polyarthrite rhumatoïde, les dystrophies des muscles squelettiques, les troubles neurologiques, les lésions du système nerveux, la fibrose du foie et des poumons, le développement et la progression des tumeurs, et plus particulièrement dans les troubles squelettiques héréditaires appelés chondroplasies.

La glycosylation est l'une des modifications post-traductionnelles les plus courantes et les plus importantes des protéines. Les défauts génétiques de la glycosylation des protéines peuvent conduire à des troubles congénitaux de la glycosylation (CDG), un groupe de maladies héréditaires associées à une grande variété de symptômes pathologiques. Parmi ceux-ci, le sous-type CDG récemment identifié est lié à des mutations dans la TMEM165 (protéine transmembranaire 165). Le gène TMEM165 est situé sur le chromosome 4q12 et se compose de six exons codant pour une protéine de 324 acides aminés. La protéine TMEM165 appartient à la famille de protéines non caractérisées appelée UPF0016 (Uncharacterized Protein Family 0016; Pfam PF01169), qui comprend des protéines membranaires intégrales à la fonction mal caractérisée et contenant une ou deux copies du motif EXGDK/R hautement conservé. Le déficit en gène du TMEM165 a été associé à un léger défaut de sialylation et de galactosylation des N-glycanes chez les patients déficients en TMEM165. De nombreuses glycosyltransférases utilisent des ions métalliques tels que Mg2+ ou Mn2+ comme cofacteur. L'ajout de Mn2+ au milieu de culture des cellules Hela permet de remédier aux défauts de N-glycosylation sur les LAMP2 et TGN46 recombinantes après l'épuisement de la TMEM165, ce qui suggère que les défauts de glycosylation résultent de défauts de Mn2+. Par conséquent, TMEM165 est

impliqué dans l'homéostasie du Mn2+ et il peut importer le Mn2+ dans les piles de Golgi. Bien que l'activité de transport de TMEM165 dans les cellules humaines n'ait pas encore été démontrée, plusieurs observations indirectes suggèrent que TMEM165 pourrait être impliqué dans le maintien de l'homéostasie de Golgi Ca2+, H+, Mn2+.

Différentes mutations ont été détectées dans TMEM165 chez les patients souffrant de GDC, Il est intéressant de noter qu'un phénotype similaire a été observé chez des patients présentant des mutations génétiques dans les gènes codant les enzymes impliquées dans la synthèse des protéoglycanes (PG), suggérant un lien potentiel entre le TMEM165 et la synthèse des PG. Ici, nous avons généré des cellules pré-chondrocytaires ATDC5 de la souris TMEM165 et des cellules HEK293 humaines en utilisant la technique CRISPR/Cas9 et nous avons montré que le knockout de TMEM165 entraînait une déficience profonde dans la polymérisation des chaînes GAG d'héparane-sulfate (HS) et de chondroïtine-sulfate (CS) des PG.

Objectifs du travail

1) Développement et validation de la lignée cellulaire préchondrogène ATDC5 de TMEM165-knockout et des cellules rénales embryonnaires humaines, HEK293.

2) Déterminer le lien, le cas échéant, entre TMEM165 et la synthèse de protéoglycanes et étudier les mécanismes impliqués en utilisant des cellules TMEM165-knock-out et des fibroblastes humains provenant d'un patient atteint d'un déficit en CDG avec TMEM165.

3) Explorer les principales voies de signalisation qui régulent la maturation des chondrocytes dans les cellules ATDC5 déficientes en TMEM165.

4) Étudier la maturation des chondrocytes et explorer les marqueurs de la chondrogenèse et de l'ostéogenèse afin de déchiffrer les mécanismes et les facteurs qui peuvent provoquer des défauts des chondrocytes dans le développement du squelette chez les patients atteints d'un déficit en CDG de la cellule TMEM165.

Des cellules ATDC5 (cellule de Riken, Tsukubai, Japon) et des cellules HEK293 (ATCC, LGC Standards, France) ont été cultivées dans un milieu complet DMEM-F12 (2 mM de glutamine, 100 µg/ml de streptomycine, 100 UI/ml de pénicilline et 5% (v/v) de sérum foetal bovin pour les cellules ATDC5 et 10% (v/v) pour HEK293) à 37°C en atmosphère humidifiée complétée par 5% de CO2.

Les oligonucléotides sens 5 "CACCGCTATAACCGGCTGACTGTGC3" et antisens 5 "AAACGCACAGTCAG CCGGTTATAGC3" (1 g) contenant une séquence de 20 pb (souligné) ciblant l'exon 2 de TMEM165 et les extrémités cohésives (en gras) avec le vecteur ont été recuits dans un tampon d'annelage (60 mM Tris-HCl, pH7. 5 ; 500 mM NaCl ; 60 mM MgCl2 ; 10 mM DTT) et ligaturées dans les sites BbsI du vecteur sgARN pUC57-attbU6. Ce vecteur est un vecteur basique avec des promoteurs U6 et des sites de liaison Cas9 améliorés. 1 g

Résultats obtenus et discussion

Nous avons donc émis l'hypothèse que des défauts dans les chaînes GAG peuvent se produire à la suite d'un déficit en TMEM165, entraînant des défauts squelettiques observés chez les patients atteints d'un déficit en TMEM 165. Pour déterminer le lien éventuel entre la déficience de TMEM165 et la synthèse des GAG, nous avons généré la lignée cellulaire ATDC5 préchondrogène de TMEM165-knockout en utilisant la technique CRISPR-Cas9 en ciblant trois régions différentes du gène TMEM165. Plusieurs clones de TMEM165-knockout ciblant l'exon2 du gène TMEM165 ont été isolés et des fragments d'ADN génomique couvrant les régions ciblées ont été amplifiés par PCR et analysés par séquençage. Quatre clones de TMEM165-knockout portant des mutations de délétion conduisant à un codon stop prématuré ont été sélectionnés pour des études complémentaires. Pour confirmer que les mutations de délétion ont aboli la synthèse de la protéine TMEM165, l'expression de la protéine a été analysée dans des cellules ATDC5 de type sauvage et mutantes par immunoblot en utilisant des anticorps anti-TMEM165. Comme prévu, l'expression d'un polypeptide d'environ 35 kDa correspondant à TMEM165 a été détectée dans les cellules ATDC5 de type sauvage, alors qu'aucun polypeptide n'a été révélé par les anticorps anti-TMEM165 dans les cellules knockout TMEM165, ce qui indique que l'expression de la protéine TMEM165 est efficacement knockée dans les cellules mutantes. Pour confirmer ces résultats, une analyse d'immunofluorescence de l'expression de TMEM165 a été effectuée dans des cellules ATDC5 de type sauvage et dans des cellules TMEM165-knockout. Dans l'ensemble, ces données ont montré que TMEM165 est inhibé dans les cellules mutantes ATDC5.

Pour découvrir le lien éventuel entre TMEM165 et les PG, nous avons évalué le niveau de synthèse des PG dans les cellules ATDC5 de type sauvage et de type TMEM165 en utilisant l'incorporation métabolique de sulfate [35S] radiomarqué dans les chaînes GAG. Il est intéressant de noter que les résultats ont montré une diminution d'environ 70 % du taux de

synthèse de PG dans les cellules TMEM165-knockout par rapport aux cellules de type sauvage. Il est intéressant de noter que l'analyse SDS-PAGE des chaînes PG-GAG radiomarquées a montré une prédominance des chaînes GAG plus courtes dans les cellules TMEM165-knockout, par rapport aux cellules de type sauvage. Pour déterminer si les défauts de synthèse des GAG affectent les chaînes CS- et HS-GAG, nous avons utilisé la décorine et le syndecan 4 comme rapporteur pour la synthèse des CS-PG et HS-PG, respectivement. À cette fin, des cellules ATDC5 de type sauvage et mutantes ont été transfectées avec un vecteur d'expression pour la décorine et pour le syndecan 4 marqué HA. Il est à noter que les PG liées aux CS et aux HS migrent sous la forme d'un frottis allongé lors de l'électrophorèse sur gel en raison de l'hétérogénéité des chaînes GAG liées. Comme prévu, la transfection de cellules ATDC5 de type sauvage et TMEM165-knockout avec un vecteur d'expression de la décorine a entraîné la sécrétion de la décorine fixée au CS/DS et de la protéine de noyau de la décorine dans le milieu de culture, comme le montre le Western blot avec des anticorps spécifiques de la décorine, mais il y a une perte d'espèces de décorine fixée au CS/DS de taille plus importante dans les cellules ATDC5 TMEM165-knockout par rapport aux cellules de type sauvage, comme le montre la prédominance de la décorine avec des chaînes GAG de taille significativement réduite. Pour confirmer si c'est également le cas dans d'autres lignées cellulaires, nous avons généré des cellules HEK293 TMEM165-knockout et analysé la décorine produite dans un milieu de culture de cellules HEK293 de type sauvage et mutantes après transfection avec un vecteur d'expression de la décorine, la décorine fixée par GAG et exprimée par les cellules HEK293 TMEM165-knockout a montré une prédominance de la décorine fixée par GAG de taille inférieure, par rapport aux cellules de type sauvage. Cela indique que les défauts de synthèse de PG produits par la perte de TMEM165 ne sont pas spécifiques au type de cellule. Pour exclure un effet de TMEM165 sur l'expression ou la sécrétion de la protéine de noyau de la décorine, nous avons généré et exprimé un mutant de la décorine manquant du site d'attachement GAG par mutation du résidu sérine en position 34, qui est utilisé pour l'attachement de la chaîne CS-GAG sur la protéine de noyau, au résidu alanine (S34A). L'expression de la décorine mutante S34A dans les cellules ATDC5 de type sauvage a conduit, comme prévu, à la sécrétion d'un polypeptide d'environ 50 kDa correspondant à la protéine centrale de la décorine sans chaîne GAG attachée. Il convient de noter que l'ETM Il est à noter que les cellules ATDC5 de TMEM165-knockout sécrétaient de la décorine mutante en quantité similaire à celle produite par les cellules de type sauvage. Ces données indiquent que la

déficience de TMEM165 n'a pas affecté la synthèse ni la sécrétion de la protéine de noyau de la décorine. Dans l'ensemble, ces résultats suggèrent que la perte de TMEM165 affecte plutôt la synthèse de la chaîne GAG attachée à la protéine de noyau de la décorine.

Étant donné que le knockdown de TMEM165 n'a pas affecté la synthèse de la protéine de noyau de la décorine, nous avons émis l'hypothèse qu'il pourrait affecter la synthèse de la chaîne GAG. Pour vérifier cette hypothèse, nous avons utilisé le 4-Méthylumbelliféryl-β-D-xylopyranoside (4MU-Xyl) comme substrat accepteur pour la synthèse des chaînes GAG. En effet, il est bien connu que la biosynthèse des chaînes GAG peut également être initiée en l'absence d'une protéine centrale par des analogues de xyloside portant un aglycone hydrophobe, comme le 4MU-Xyloside (4MU-Xyl). Le xyloside peut, lorsqu'il est fourni de manière exogène aux cellules, agir comme substrat accepteur pour β4GalT7, puis s'allonger et conduire à la production dans le milieu de chaînes GAG amorcées par le xyloside. Nous avons donc cultivé des cellules TMEM165-knockout et ATDC5 de type sauvage en présence de 4MU-Xyl et de sulfate [35S] pour radiomarquer métaboliquement les chaînes GAG nouvellement synthétisées. Les chaînes GAG amorcées au 4MU-Xyl produites ont été isolées par la méthode au chlorure de Cetylpyridinium à partir du milieu de culture et analysées par SDS-PAGE et autoradiographie. Les résultats ont montré que les cellules ATDC5 de type sauvage produisent une quantité significative de chaînes GAG radiomarquées, alors que les cellules ATDC5 de type TMEM165 ne produisent que peu de chaînes, ce qui indique que la synthèse des chaînes GAG est affectée dans les cellules TMEM165 de type knockout. Pour déterminer si la réduction de la taille de la décorine produite dans les cellules ATDC5 mutantes TMEM165 résulte de défauts de polymérisation des chaînes CS-GAG, la décorine provenant de cellules ATDC5 de type sauvage et mutantes TMEM165 a été soumise à un traitement à la chondroïtinase ABC qui dégrade les chaînes CS-GAG des PG. Il est intéressant de noter que le traitement de la décorine produite dans les cellules TMEM165-knockout avec la chondroïtinase ABC a conduit à un changement du schéma de migration en SDS-PAGE, passant d'un frottis à une seule bande correspondant à la protéine de noyau de la décorine, ce qui indique que, bien qu'elle soit plus courte, la décorine des cellules mutantes est sensible à la chondroïtinase ABC et contient donc des chaînes CS-GAG allongées. Ces résultats indiquent que les cellules TMEM165-knockout allongent les chaînes CS-GAG sur la protéine de noyau de la décorine mais avec une efficacité réduite, ce qui entraîne la formation de chaînes GAG plus

courtes. Ensemble, ces données suggèrent que la déficience de TMEM165 a conduit à des défauts d'allongement des chaînes CS-GAG et donc à une altération du processus de polymérisation des GAG.

Nous avons ensuite cherché à savoir si la synthèse des chaînes HS-GAG est également altérée dans les cellules TMEM165-knockout. À cette fin, nous avons exprimé le syndecan 4, une HSPG avec trois chaînes GAG attachées au HS, dans des cellules TMEM165-knockout et ATDC5 de type sauvage par transfection avec un vecteur d'expression codant pour le syndecan 4 marqué HA. le syndecan 4 exprimé dans les cellules ATDC5 de type sauvage a présenté un frottis en SDS-PAGE correspondant au syndecan 4 lié au SH en plus d'un polypeptide correspondant à la protéine centrale du syndecan 4, alors que dans les cellules TMEM165-knockout, le frottis était de taille fortement réduite, ce qui indique une perte d'espèces de syndecan 4 de taille plus importante dans les cellules ATDC5 TMEM165-knockout, par rapport aux cellules de type sauvage. Ces résultats indiquent que le syndécan 4 contient des chaînes HS-GAG plus courtes, ce qui suggère que l'élongation des chaînes HS est altérée dans les cellules mutantes. Pour confirmer davantage ce résultat, nous avons effectué une analyse par immunofluorescence indirecte des HSPG de surface des cellules de type sauvage et des cellules TMEM165-knockout, en utilisant l'anticorps monoclonal anti-HS 10E4, qui est couramment utilisé pour détecter les chaînes HS des PG. Une coloration importante de la membrane cellulaire a été observée dans les cellules de type sauvage (en vert), alors qu'un signal très faible a pu être observé dans les cellules TMEM165-knockout. Lorsque les cellules ont été sondées avec des anticorps anti-TMEM165, une expression efficace de la protéine a été révélé alors qu'aucune coloration n'a été observée dans les cellules TMEM165-knockout. Dans l'ensemble, ces résultats ont révélé un rôle clé de TMEM165 dans la synthèse des chaînes HS- et CS-GAG des PGs.

Étant donné que les voies de synthèse des CS et des HS impliquent plusieurs enzymes dont chacune est impliquée dans une étape spécifique du processus de synthèse, nous avons cherché à déterminer si l'allongement altéré des chaînes CS- et HS-GAG dans les cellules knockout de TMEM165 résultait de défauts dans l'expression génique des enzymes de polymérisation CS et HS. À cette fin, des analyses RT-qPCR ont été effectuées en utilisant l'ARNm des cellules TMEM165-knockout et ATDC5 de type sauvage pour évaluer l'expression génique des enzymes polymérisantes CS, CHSY1 et CHSY2 et des enzymes polymérisantes HS,

EXT1 et EXT2. Les résultats ont montré que les niveaux d'ARNm des enzymes polymérisantes CS CHSY1 et CHSY2 sont similaires dans les cellules ATDC5 de type sauvage et de type TMEM165-knockout, ce qui suggère que la réduction de l'allongement de la chaîne CS-GAG n'est pas due à un défaut d'expression génique des enzymes polymérisantes. De même, les niveaux d'ARNm des enzymes polymérisantes HS, EXT1 et EXT2 ne sont pas significativement différents dans les cellules ATDC5 de type sauvage et de type TMEM165-knockout, ce qui indique que le défaut d'allongement des chaînes HS-GAG dans les cellules mutantes n'est pas dû à une régulation à la baisse de l'expression génique des enzymes polymérisantes HS. Nous avons également analysé l'expression des enzymes XylT1/XylT2, GalT1, GalT2 et GlcAT-I impliquées dans la synthèse du lieur tétrasaccharidique utilisé comme amorce pour l'allongement des chaînes CS et HS et avons constaté que les niveaux d'expression génique de ces enzymes ne sont pas modifiés dans les cellules TMEM165-knockout par rapport aux cellules ATDC5 de type sauvage.

Des analyses similaires ont été effectuées sur des fibroblastes humains normaux et des fibroblastes déficients en TMEM165 de patients atteints de GDC et ont montré que l'expression génique des enzymes polymérisantes CS- et HS-GAG était similaire ou supérieure dans les fibroblastes des patients, par rapport au contrôle. Dans l'ensemble, ces données suggèrent que les défauts de polymérisation des chaînes CS- et HS-GAG ne sont pas dus à des altérations de l'expression génique des enzymes impliquées. Nous avons montré ci-dessus que l'expression de l'ARNm des enzymes de polymérisation CS et HS n'est pas modifiée dans les cellules ATDC5 déficientes en TMEM165 et dans les fibroblastes de patients CDG, par rapport aux cellules témoins. Cependant, nous ne pouvons pas exclure une diminution du niveau de protéines qui pourrait résulter d'une instabilité et/ou d'une dégradation accrue des protéines. Étant donné que le niveau d'expression protéique des glycosyltransférases impliquées dans la voie de synthèse des GAG est très faible et que leur détection par des anticorps (disponibles dans le commerce) est très difficile, il est donc difficile d'évaluer et de comparer les niveaux protéiques des enzymes polymérisantes CS et HS dans les cellules normales et mutantes. Nous pouvons cependant émettre l'hypothèse que la surexpression de ces enzymes peut surmonter l'instabilité ou la dégradation de ces protéines, le cas échéant. Pour soutenir l'expression des enzymes de polymérisation CS, nous avons conçu des vecteurs d'expression pour CHSY1 à marqueur Myc et CHSY2 à marqueur HA et les avons utilisés pour surexprimer chacune des

deux enzymes individuellement ou ensemble dans les cellules ATDC5 de TMEM165-knockout. Ensuite, nous avons cherché à savoir si la surexpression de ces enzymes favorisait la polymérisation des chaînes CS-GAG. À cette fin, nous avons transfecté des cellules TMEM165-knockout avec des vecteurs d'expression CHSY1, CHSY2 ou CHSY1 et CHSY2 ainsi qu'un vecteur d'expression de la décorine. Les cellules transfectées avec le vecteur vide ainsi que le vecteur d'expression de la décorine ont été utilisées comme témoin. les cellules TMEM165-knockout transfectées avec CHSY1, CHSY2 ou CHSY1 et CHSY2 ont produit une décorine de taille réduite par rapport à celle produite dans les cellules de type sauvage. L'expression de CHSY1 et CHSY2 a été confirmée par Western blot dans toutes les cellules transfectées. Ces données ont indiqué que la surexpression de CHSY1 et CHSY2, individuellement ou ensemble, ne sauvait pas l'élongation du CS dans les cellules déficientes en TMEM165, ce qui suggère que les défauts dans le processus de polymérisation du CS ne résultent pas d'une expression protéique réduite des enzymes de polymérisation, CHSY1 et CHSY2. Ensuite, nous avons cherché à déterminer si l'apport au milieu de culture cellulaire de monosaccharides de sucre utilisés dans la synthèse des chaînes CS-GAG telles que le xylose et le galactose pouvait restaurer l'allongement CS dans les cellules ATDC5 de TMEM165-knockout. À cette fin, les cellules mutantes TMEM165 ont été transfectées avec un vecteur d'expression de la décorine et incubées en présence ou en l'absence de 1 mM de xylose et de galactose, respectivement. La taille de la décorine produite dans les cellules TMEM165-knockout est considérablement réduite par rapport à celle des cellules de type sauvage et n'a pas changé avec le traitement au xylose ou au galactose, ce qui indique que l'apport de monosaccharides aux cellules n'a pas permis de surmonter le blocage du processus de polymérisation. Il a été établi que le Mn2+ participe à l'activité catalytique de diverses glycosyltransférases de Golgi, notamment les enzymes polymérisantes CS et HS 11,12. Nous avons donc cherché à déterminer si les défauts d'allongement des chaînes CS- et HS-GAG dans les cellules à nœuds TMEM165 sont dus à un manque de Mn2+. À cette fin, des cellules de type sauvage et des cellules mutantes TMEM165 ont été transfectées avec un vecteur d'expression de la décorine puis cultivées en l'absence ou en présence de 1M de Mn2+. L'analyse par Western blot de la décorine produite dans les cellules ATDC5 de type sauvage a montré un schéma similaire en l'absence ou en présence de Mn2+, tandis que la décorine exprimée dans les cellules TMEM165-knockout cultivées en présence de Mn2+ était de taille plus importante, similaire à celle produite en l'absence de Mn2+, et montrait un schéma similaire à la décorine produite dans les cellules de type

sauvage. Ces données ont montré que la supplémentation du milieu de culture en Mn2+ a induit une augmentation de la taille de la décorine et indiquent que le Mn2+ restaure la polymérisation des chaînes CS-GAG de la décorine dans les cellules TMEM165-knockout. Pour exclure un effet de Mn2+ sur la synthèse ou la sécrétion de la protéine de base de la décorine, nous avons exprimé le mutant S34A de la décorine, dépourvu du site de fixation CS, dans des cellules de type sauvage et des cellules TMEM165-knockout et analysé la décorine produite par immunoblot les cellules de type sauvage et TMEM165-knockout ont exprimé efficacement la protéine de noyau de la décorine mutante avec un schéma similaire soit en l'absence soit en présence de Mn2+, indiquant que le traitement des cellules avec Mn2+ n'a pas affecté la synthèse et la sécrétion de la protéine de noyau de la décorine. Par conséquent, les modifications de la taille de la décorine après le traitement par Mn2+ résultaient de changements dans la longueur de la chaîne CS-GAG attachée. Comme la polymérisation des chaînes HS-GAG est également altérée dans les cellules TMEM165-knockout, nous avons cherché à savoir si le Mn2+ est capable de restaurer la polymérisation des chaînes HS-GAG, comme observé ci-dessus pour les chaînes CS-GAG. Des cellules ATDC5 de type sauvage et mutantes TMEM165 ont été transfectées avec le vecteur d'expression HA-syndecan 4 et cultivées en l'absence ou en présence de 1µM de Mn2+. L'analyse par Western blot de HA-syndécan 4 a indiqué l'expression d'un frottis de haut poids moléculaire correspondant à HA-syndécan 4 avec des chaînes HS-GAG présentant un schéma similaire en présence ou en absence de Mn2+, ce qui suggère que l'ion divalent Mn2+ n'a pas affecté la synthèse des chaînes HS-GAG dans les cellules de type sauvage à la concentration utilisée. Il est remarquable que la supplémentation en Mn2+ dans le milieu de culture des cellules TMEM165-knockout ait entraîné la synthèse de HA-syndécan 4 de poids moléculaire plus élevé que celui produit en l'absence de Mn2+, ce qui indique que les chaînes HS-GAG attachées à HA-syndécan 4 sont de plus grande taille lorsque le Mn2+ est fourni dans le milieu de culture. Ces données suggèrent fortement que le Mn2+ sauve la polymérisation des chaînes HS-GAG dans les cellules TMEM165-knockout.

Pour confirmer davantage que le Mn2+ sauve l'élongation des chaînes GAG dans les cellules TMEM165-knockout, le 4MU-Xyl a été utilisé comme substrat exogène pour surveiller la synthèse des chaînes GAG. Des cellules ADTC5 de type sauvage et de type TMEM165 mutant ont été cultivées en présence ou en absence de Mn2+ avec une amorce 4MU-Xyl et du sulfate

[35S] pour radiomarquer les chaînes GAG nouvellement synthétisées. L'analyse par SDS-PAGE des chaînes GAG radiomarquées à amorce 4MU-Xyl a montré qu'en l'absence de Mn2+, une grande quantité de chaînes GAG était produite dans les cellules de type sauvage, alors qu'un signal très hebdomadaire était observé dans les cellules TMEM165-knockout, indiquant que le processus de polymérisation est altéré dans ces cellules. Il est intéressant de noter que la supplémentation de Mn2+ dans le milieu de culture rétablit la synthèse des chaînes GAG dans les cellules TMEM165-knockout, ce qui entraîne la production d'une quantité importante de chaînes GAG radiomarquées. Dans l'ensemble, ces résultats démontrent que la déficience de TMEM165 induit des défauts dans la synthèse des GAG en altérant l'élongation des chaînes GAG, ce qui conduit à la synthèse de GAG avec des chaînes GAG plus courtes. Ils apportent également la preuve que le défaut d'élongation des CS- et HS-GAG est sauvé par la supplémentation des cellules en Mn2+, ce qui suggère fortement que la fonction des enzymes de polymérisation des GAG, dont on sait qu'elles requièrent que le Mn2+ soit pleinement actif, est altérée dans les cellules du knockout TMEM165 et que l'homéostasie du Mn2+ de Golgi est perturbée dans les cellules mutantes. Il a été proposé que le TMEM165 puisse échanger la lumière de Golgi H+ contre le Ca2+ cytoplasmique, alors que d'autres études ont suggéré qu'il pourrait être impliqué dans le transport du Mn2+ cytoplasmique vers la lumière de Golgi. L'implication directe du TMEM165 dans le transport du Ca2+ ou du Mn2+ n'a pas encore été signalée. Cependant, il est bien connu que la protéine kinase II dépendante du Ca2+/calmoduline (CaMkII) est activée lorsque la concentration intracellulaire en Ca2+ est élevée et que le complexe Ca2+/calmoduline se lie au domaine de régulation du CaMkII. Nous avons émis l'hypothèse que si la TMEM165 est impliquée dans l'homéostasie du Ca2+, alors une déficience de la TMEM165 peut entraîner une altération du transport du Ca2+ cytoplasmique vers le Golgi et donc un taux élevé de [Ca2+] dans le cytoplasme. Pour vérifier cette hypothèse, nous avons analysé le statut de phosphorylation de CaMkIIα dans les cellules TMEM165-knockout et ATDC5 de type sauvage. Il est intéressant de noter que, comme le montre le Western blot, le niveau de phospho-CaMkIIα (pCaMkIIα) était fortement augmenté dans les cellules TMEM165-knockout par rapport aux cellules de type sauvage, ce qui indique que CaMkIIα était fortement activé dans les cellules TMEM165-knockout. De même, comme observé dans les cellules ATDC5, le niveau de phosphorylation de CaMkIIα a été remarquablement augmenté dans les cellules de fibroblastes de patients CDG déficients en TMEM165, par rapport aux fibroblastes normaux. Ces résultats indiquent que CaMkIIα est

activé dans les cellules mutantes, ce qui suggère fortement que le taux intracellulaire [Ca2+] est élevé dans ces cellules. Dans l'ensemble, ces données indiquent que la perte de TMEM165 induit des défauts dans l'homéostasie du Ca2+ et du Mn2+ et soutiennent l'idée que TMEM165 est probablement impliquée dans la régulation de l'homéostasie du Ca2+ et du Mn2+. La déficience du TMEM165 entrave les voies de signalisation du TGF-β et de la BMP

Nous avons montré ci-dessus que la déficience du TMEM165 entraînait des défauts dans la synthèse des chaînes PG-GAG. Comme uncertain nombre de mutations génétiques humaines à l'origine d'un large éventail de maladies héréditaires du développement du squelette sont liées aux voies de signalisation TGF-β et BMP 13 et en raison du rôle clé des chaînes GAG dans la régulation de plusieurs voies de signalisation, nous avons cherché à savoir si la perte de TMEM165 affecte les voies de signalisation TGF-β et BMP. Nous avons d'abord exploré la signalisation du TGF-β dans les cellules ATDC5 de type sauvage et de désactivation de TMEM165 en analysant l'état de phosphorylation de Smad2, un médiateur en aval de l'activation du récepteur TGF-β. Il est intéressant de noter que l'analyse par Western blot a montré que le niveau de phospho-Smad2 (mais pas le niveau total de Smad2) était réduit dans les cellules TMEM165-knockout par rapport aux cellules de type sauvage, ce qui indique que l'axe TGF-β/Smad2 est fonctionnellement altéré dans les cellules mutantes. Ces données suggèrent que l'expression des gènes induits par le TGF-β dans les cellules TMEM165-knockout serait également régulée à la baisse. Pour le vérifier, on a examiné les niveaux d'ARNm du gène de la serpine 1 (PAI-1), qui est positivement corrélé avec l'activation de la signalisation du TGF-β. Comme prévu, les niveaux d'ARNm de la serpine 1 étaient significativement plus bas dans les cellules assommées pour TMEM165 que dans les cellules de type sauvage ce qui indique que la perte de TMEM165 perturbe la signalisation du TGF-β dans les cellules mutantes. Ces données ont été confirmées par la transfection du plasmide rapporteur p(CAGA)12-luc dans des cellules déficientes en TMEM165 et des cellules de type sauvage. Ce plasmide contient un gène de luciférase de luciole, situé en aval d'un promoteur réagissant au TGF-β dérivé du gène de la serpine1. Par conséquent, l'activité de la luciférase est une mesure de la signalisation du TGF-β. Les données ont montré que l'activité de la luciférase était nettement (7 fois) plus faible dans les cellules mutantes, par rapport aux cellules de type sauvage, ce qui confirme que l'axe TGF-β-Smad est fonctionnellement altéré dans les cellules TMEM165-knockout.

Pour déterminer si c'est également le cas dans les fibroblastes de patients atteints de GDC, nous avons évalué l'état de phosphorylation de Smad2 dans des fibroblastes normaux et des fibroblastes déficients en TMEM165 de patients atteints de GDC. Le niveau de phospho-Smad2 était réduit dans les fibroblastes déficients en TMEM165 par rapport aux fibroblastes normaux, alors que le niveau total de Smad2 n'était pas affecté, ce qui indique que l'axe TGF-β/Smad2 était fonctionnellement altéré dans les cellules mutantes des fibroblastes. L'analyse de l'expression du gène serpine1 utilisé comme marqueur de l'activation de la signalisation du TGF-β a montré une baisse significative (2 fois) de la régulation, indiquant que le déficit en TMEM165 entrave l'expression des gènes réagissant en aval du TGF-β/Smad dans les fibroblastes de patients atteints de GDC.

Pour déterminer si la réponse à la stimulation du TGF-β est affectée dans les cellules mutantes, le niveau de phosphorylation de Smad2 en réponse au TGF-β a été examiné. Le traitement des cellules ATDC5 de TMEM165-knockout par le TGF-β a induit la phosphorylation de Smad2, mais le niveau de phospho-Smad2 est inférieur à celui observé dans les cellules de type sauvage, ce qui indique que les cellules mutantes ont moins bien répondu au TGF-β que les cellules de type sauvage. Pour savoir si c'est également le cas dans les fibroblastes de patients CDG, les cellules de fibroblastes normales et celles déficientes en TMEM165 ont été stimulées par le TGF-β et le statut de phosphorylation de Smad2 a été analysé par Western-blot. Les résultats ont montré que le niveau de phospho-Smad2 dans les fibroblastes mutants TMEM165 était réduit par rapport aux fibroblastes normaux. Dans l'ensemble, ces résultats ont montré que les niveaux de phospho-Smad2 de base et ceux induits par le TGF-β étaient significativement réduits dans les cellules mutantes, révélant ainsi pour la première fois que le déficit de TMEM165 altérait fonctionnellement l'axe de signalisation du TGF-β/Smad2. Afin d'identifier le mécanisme impliqué dans l'altération de la voie de signalisation TGF-β-Smad, nous avons étudié les niveaux d'expression de l'ARNm des récepteurs TGF-β, TGFβR1 et TGFβR2 dans les cellules TMEM165-knockout et ATDC5 de type sauvage. Une légère diminution des niveaux d'ARNm de TGFβR1 associée à une diminution significative des niveaux d'ARNm de TGFβR2 a été observée par RT-qPCR dans les cellules ATDC5 mutantes de TMEM165, par rapport au type sauvage. Pour déterminer si les changements dans l'expression de l'ARNm de TGFβR2 reflètent des changements dans l'expression de la protéine, l'expression de la protéine TGFβR2 a été évaluée par immunoblotting. Conformément aux données de RT-

qPCR, une réduction significative du niveau de protéine de TGFβR2 a été observée dans les cellules ATDC5 mutantes de TMEM165, par rapport aux cellules de type sauvage. Il est intéressant de noter qu'une forte diminution des niveaux d'ARNm de TGFβR2 a été observée dans les fibroblastes de patients CDG déficients en TMEM165 par rapport aux fibroblastes normaux, alors qu'aucun changement significatif n'a été observé dans les niveaux d'ARNm de TGFβR1. L'analyse Western blot de l'expression de la protéine TGFβR2 a confirmé les données de l'ARNm et a montré une diminution dramatique de l'expression du récepteur. Ces données ont révélé que la déficience de TMEM165 entraînait une diminution de l'expression du récepteur TGF-β, TGFβR2, ce qui pourrait expliquer la régulation à la baisse de la signalisation du TGF-β dans les cellules déficientes en TMEM165. La régulation à la baisse de la signalisation du TGF-β peut également résulter de la régulation à la hausse des régulateurs négatifs tels que l'asporine, une protéine extracellulaire qui supprime la signalisation du TGF-β par interaction directe avec le TGF-β, empêchant ainsi sa liaison à TGFβR2. Nous avons donc cherché à déterminer si la déficience en TMEM165 affecte l'expression de l'asporine. L'analyse des niveaux d'ARNm de l'asporine dans les cellules ATDC5 du TMEM165-knockout et dans les fibroblastes d'un patient CDG a montré une augmentation remarquable (4 fois) de l'expression de l'asporine dans les cellules mutantes par rapport aux cellules normales. L'évaluation de l'expression de la protéine asporine par immunoblot a montré des niveaux d'expression plus élevés dans les cellules de fibroblastes de patients atteints d'un déficit en ATDC5 et en CDG, par rapport aux cellules normales. Par conséquent, ces résultats ont montré que l'expression de l'asporine était significativement régulée à la hausse dans les cellules déficientes en TMEM165. Dans l'ensemble, ces données confirment l'idée que l'altération de la signalisation du TGF-β dans les cellules déficientes en TMEM165 est associée à une régulation à la baisse de l'expression du récepteur TGFβR2 et à une régulation à la hausse de l'antagoniste de la signalisation du TGF-β, l'asporine.

La signalisation de la BMP joue un rôle clé dans le développement du squelette et les altérations de la voie de signalisation de la BMP sont la principale cause sous-jacente des troubles du squelette humain 14. La signalisation des BMP repose sur des ligands sécrétés et sur des récepteurs de BMP de type I et de type II qui activent des médiateurs en aval, notamment la voie canonique de la SMAD. Pour déterminer si la déficience en TMEM165 affecte la signalisation des BMP, nous avons examiné le statut de phosphorylation des

médiateurs en aval de l'activation des récepteurs BMP, Smad 1,5,9. Il est intéressant de noter que l'analyse par immunoblot a montré que le niveau de phospho-Smad 1,5,9 (pSmad1,5,9) était plus élevé dans les cellules ATDC5 de TMEM165, par rapport aux cellules de type sauvage. Ce résultat a été confirmé dans les fibroblastes de patients CDG qui ont montré un niveau plus élevé de phospho-Smad 1,5,9 par rapport aux fibroblastes normaux. Par conséquent, ces données ont révélé qu'une déficience du TMEM165 entrave fonctionnellement la signalisation de la BMP/Smad, ce qui entraîne l'activation de la voie de signalisation. En effet, l'analyse des niveaux d'ARNm du gène Id1, un gène cible en aval de la BMP, a montré une multiplication par deux du nombre de cellules de désactivation de TMEM165, par rapport aux cellules de type sauvage. Pour confirmer l'augmentation de la signalisation de la BMP dans les cellules TMEM165, un vecteur rapporteur de signalisation de la BMP pGL3-BRE-Luc contenant un élément promoteur sensible à la BMP (BRE) a été utilisé pour transfecter des cellules ATDC5 de type sauvage et de type TMEM165 mutant. L'analyse de l'activité de la luciférase, qui est une mesure de la signalisation de la BMP, a montré une augmentation significative (4 fois) des cellules ATDC5 knockout TMEM165 par rapport aux cellules de type sauvage, ce qui prouve que la signalisation de la BMP est activée dans les cellules mutantes TMEM165. Afin de tenter d'identifier le mécanisme impliqué dans l'altération de la voie de signalisation BMP/Smad, nous avons étudié les niveaux d'ARNm des récepteurs BMP de type I et de type II, c'est-à-dire BMPR1A (ALK3), BMR1B (ALK6) et BMPR2 par RT-qPCR dans les cellules déficientes de TMEM165 et de type sauvage. Les niveaux d'ARNm des récepteurs BMP ont augmenté dans les cellules ATDC5 déficientes en TMEM165, par rapport aux cellules de type sauvage, BMPR1B présentant la plus forte augmentation (2 fois). L'expression accrue de BMPR2 au niveau de la protéine a été confirmée par une analyse Western blot dans des cellules mutantes utilisant des lysats de cellules ATDC5 de type sauvage et de cellules TMEM165-knockout. Des résultats similaires ont été observés, soit pour les niveaux d'expression de l'ARNm de BMPR1A, BMR1B et BMPR2 soit pour l'expression de la protéine BMPR2 dans les cellules de fibroblastes de patients CDG déficients en TMEM165, par rapport aux cellules de fibroblastes normales. La régulation à la hausse de l'expression des récepteurs de la BMP peut donc expliquer l'augmentation de la signalisation de la BMP dans les cellules mutantes de TMEM165. Il est également bien connu que la signalisation de la BMP est régulée par des antagonistes de ligands tels que le noggin qui antagonise la signalisation en se liant directement aux protéines de la BMP, empêchant ainsi l'activation des récepteurs.

Par conséquent, pour déterminer si l'expression de noggin est altérée dans les cellules déficientes en TMEM165, les niveaux d'ARNm du gène NOG ont été évalués par RT-qPCR dans les cellules TMEM165-knockout et ATDC5 de type sauvage. le niveau d'expression de l'ARNm de noggin a été réduit de manière significative dans les cellules ATDC5 mutantes de TMEM165, par rapport aux cellules de type sauvage. Des résultats similaires ont été observés dans les fibroblastes déficients en TMEM165 de patients atteints de GDC, par rapport aux fibroblastes normaux. Ces données soulèvent la possibilité que la régulation à la baisse de l'expression de l'antagoniste de la BMP noggin puisse participer à l'augmentation de la signalisation de la BMP observée dans les cellules mutantes. Au total, ces données ont révélé que la signalisation de la BMP est régulée à la hausse dans les cellules déficientes en TMEM165 et pourrait être le résultat d'une expression accrue des récepteurs de la BMP et d'une expression réduite de l'antagoniste de la BMP. Dans l'ensemble, cette étude a montré que la déficience de TMEM165 entraînait une régulation à la baisse du TGF-β-Smad2 et une régulation à la hausse des axes BMP/Smad 1,5,9, et donc une altération fonctionnelle de ces voies de signalisation dans les cellules déficientes en TMEM165.

La chondrogenèse est un processus de différenciation bien coordonné en plusieurs étapes dans lequel les chondrocytes prolifèrent pour produire des chondrocytes hypertrophiques différenciés en phase terminale. En raison du rôle des chaînes GAG et du TGF-β dans la régulation de la prolifération cellulaire, nous avons cherché à savoir si la prolifération était affectée dans les cellules mutantes. À cette fin, la prolifération des cellules ATDC5 du TMEM 165-knockout et des fibroblastes d'un patient CDG a été mesurée à l'aide du kit de test de prolifération cellulaire CyQUANT. le taux de prolifération des cellules de fibroblastes ATDC5 et déficientes en TMEM165 a été considérablement augmenté (1,5 fois) par rapport aux cellules normales, ce qui indique que la déficience en TMEM165 favorise la prolifération cellulaire. En conséquence, l'analyse du statut d'activation de la voie de la kinase extracellulaire régulée par le signal (ERK) 1/2 protéine activée par le mitogène (MAP) kinase, qui joue un rôle central dans le contrôle de la prolifération cellulaire, a montré un niveau d'activation plus élevé dans les cellules ATDC5 et les fibroblastes de patients CDG mutants de TMEM165 par rapport aux cellules normales. En effet, les niveaux de phospho-ERK1/2 (pERK1/2) mais pas les niveaux totaux d'ERK1/2 ont été fortement augmentés dans les cellules de fibroblastes mutantes ATDC5 et TMEM165 déficientes par rapport aux cellules normales,

indiquant une activation soutenue de la voie de signalisation ERK1/2 qui peut favoriser la prolifération dans les cellules mutantes.

Les os longs des mammifères sont formés par un processus d'ossification endochondrale qui implique la formation d'un dessin cartilagineux dans lequel les chondrocytes subissent un processus de maturation avant d'être remplacés par un os mature. Le processus de chondrogenèse est étroitement régulé pendant le développement du squelette et les altérations de la maturation des chondrocytes entraînent des défauts dans le développement de l'os endochondral. Pour déterminer si la différenciation chondrogénique des cellules ATDC5 est affectée en l'absence de TMEM165, des cellules ATDC5 de type sauvage et de type TMEM165-knockout ont été induites par l'insuline en différenciation chondrogénique et les niveaux d'ARNm des marqueurs chondrogéniques, dont Sox9, Col2a1, AGN, Ihh et OCN, ont été mesurés par RT-qPCR avant l'induction et sept jours après l'induction. Les résultats ont montré qu'avant l'induction (jour 0), par rapport au type sauvage, les cellules ATDC5-knockout expriment des niveaux d'ARNm plus élevés des marqueurs chondrogènes Sox9, Col2a1 et AGN et des niveaux d'ARNm plus faibles des marqueurs préhypertrophiques et hypertrophiques Ihh et OCN (jour 0). Ces résultats indiquent que la perte d'expression de TMEM165 induit une différenciation chondrogénique des cellules ATDC5 préchondrogéniques. Il est important de noter que l'analyse de l'expression des marqueurs sept jours après l'induction a révélé que les cellules ATDC5 déficientes en TMEM165 subissent une maturation rapide, comme le montrent la régulation à la baisse des marqueurs chondrogènes Sox9, Col2a1, AGN et la régulation à la hausse des marqueurs préhypertrophiques et hypertrophiques Ihh et OCN. En revanche, dans les cellules de type sauvage, les marqueurs chondrogéniques ont été régulés à la hausse et les marqueurs préhypertrophiques et hypertrophiques à la baisse sept jours après l'induction (jour7). Au total, ces données apportent la preuve que la déficience en TMEM165 favorise la maturation prématurée des chondrocytes, un processus qui affecte l'ossification endochondrale et peut conduire au nanisme.

Conclusions et perspectives

Ce travail de thèse nous a permis d'élucider le rôle crucial de TMEM165 dans la synthèse de PG et la maturation des chondrocytes. TMEM165 joue un rôle essentiel dans la synthèse des PG. Il y a des altérations dans la synthèse des PGs, principalement une altération

de la polymérisation des chaînes GAG du sulfate d'héparine ainsi que du sulfate de chondroïtine dans les cellules déficientes en TMEM165. Les PG jouent un rôle important dans la structure et l'organisation de l'ECM, la disponibilité des facteurs de croissance, la maturation des chondrocytes, le développement des plaques de croissance et la signalisation intracellulaire. De plus, nous avons démontré qu'en fournissant aux cellules du Mn2+, les défauts de polymérisation étaient surmontés car le Mn2+ est utilisé comme cofacteur des glycosyltransférases de Golgi et nécessaire à la pleine activité enzymatique. Ces résultats suggèrent que la TMEM165 régule l'homéostasie du Mn2+ de Golgi. Étant donné que TGFβ et la signalisation BMP régulent la chondrogenèse et qu'elles sont les principales voies de signalisation qui régulent la maturation des chondrocytes. Nous avons révélé pour la première fois que la déficience de TMEM165 entraînait une altération de l'axe de signalisation TGF-β/Smad2, ce qui a conduit à une régulation à la baisse de la signalisation TGF-β/Smad2. De plus, la déficience de TMEM165 a provoqué une activation de l'axe BMP/Smad 1,5,9 et donc une altération fonctionnelle de la voie de signalisation dans les cellules mutantes ATDC5 et dans les fibroblastes du patient déficient en TMEM165. La perturbation de ces différentes voies entraîne une prolifération accrue et une hypertrophie précoce des chondrocytes. Il sera intéressant de déterminer les facteurs et les mécanismes responsables de la perturbation de l'expression des composants de signalisation TGF-β et BMP. L'étude in vitro de la différenciation des cellules ATDC5 a révélé que le déficit en TMEM165 favorise la différenciation des cellules ATDC5 vers l'hypertrophie, ce qui peut provoquer une maturation prématurée des chondrocytes et peut entraîner des anomalies squelettiques observées chez les patients atteints de GDC déficiente en TMEM165. Ces anomalies de la chondrogenèse entraînent une ossification précoce et accélérée qui conduit au nanisme et à diverses anomalies. De plus, l'augmentation des niveaux de calcium caloduline kinase II phosphorylée (p-CamKII) dans les cellules KO de la TMEM165 suggère que la TMEM 165 est impliquée dans l'homéostasie du Ca2+, provoquant une surcroissance du squelette et un chondrocyte précoce. Il sera intéressant de déterminer si cela se vérifie in vivo en utilisant des modèles animaux tels que le knockout de souris pour TMEM165 dans le cartilage disponible dans notre laboratoire.

D'autre part, il serait important d'étudier le rôle de TMEM-165 dans les ostéoblastes à la fois in vivo et in vitro pour déterminer le rôle de cette protéine dans la formation osseuse et l'homéostasie.

REFERENCES

Abad, V., Meyers, J. L., Weise, M., Gafni, R. I., Barnes, K. M., Nilsson, O., Bacher, J. D., and Baron, J. (2002). The role of the resting zone in growth plate chondrogenesis. *Endocrinology*. https://doi.org/10.1210/endo.143.5.8776

Akiyama, H., Chaboissier, M. C., Martin, J. F., Schedl, A., and De Crombrugghe, B. (2002). The transcription factor Sox9 has essential roles in successive steps of the chondrocyte differentiation pathway and is required for expression of Sox5 and Sox6. *Genes and Development*. https://doi.org/10.1101/gad.1017802

Althoff, K. N., McGinnis, K. A., Wyatt, C. M., Freiberg, M. S., Gilbert, C., Oursler, K. K., Rimland, D., Rodriguez-Barradas, M. C., Dubrow, R., Park, L. S., Skanderson, M., Shiels, M. S., Gange, S. J., Gebo, K. A., & Justice, A. C. (2015). Comparison of risk and age at diagnosis of myocardial infarction, end-stage renal disease, and non-AIDS-defining cancer in HIV-infected versus uninfected adults. *Clinical Infectious Diseases*, *60*(4), 627–638. https://doi.org/10.1093/cid/ciu869

Amenta, A. R., Creely, H. E., Mercado, M. L. T., Hagiwara, H., McKechnie, B. A., Lechner, B. E., Rossi, S. G., Wang, Q., Owens, R. T., Marrero, E., Mei, L., Hoch, W., Young, M. F., McQuillan, D. J., Rotundo, R. L., & Fallon, J. R. (2012). Biglycan is an extracellular MuSK binding protein important for synapse stability. *Journal of Neuroscience*. https://doi.org/10.1523/JNEUROSCI.4610-11.2012

Ameye, L., & Young, M. F. (2002). Mice deficient in small leucine-rich proteoglycans: Novel in vivo models for osteoporosis, osteoarthritis, Ehlers-Danlos syndrome, muscular dystrophy, and corneal diseases. In *Glycobiology*. https://doi.org/10.1093/glycob/cwf065

Anagianni, S., & Tuschl, K. (2019). Genetic Disorders of Manganese Metabolism. *Current Neurology and Neuroscience Reports*, *19*(6). https://doi.org/10.1007/s11910-019-0942-y

Aschner, M., Shanker, G., Erikson, K., Yang, J., & Mutkus, L. A. (2002). The uptake of manganese in brain endothelial cultures. *NeuroToxicology*. https://doi.org/10.1016/S0161-813X(02)00056-6

Balemans, W., & Van Hul, W. (2002). Extracellular regulation of BMP signaling in vertebrates: A cocktail of modulators. In *Developmental Biology*. https://doi.org/10.1016/S0012-1606(02)90779-7

Barna, M., and Niswander, L. (2007). Visualization of Cartilage Formation: Insight into Cellular Properties of Skeletal Progenitors and Chondrodysplasia Syndromes. *Developmental Cell*.

https://doi.org/10.1016/j.devcel.2007.04.016

Baasanjav, S., Al-Gazali, L., Hashiguchi, T., Mizumoto, S., Fischer, B., Horn, D., Seelow, D., Ali, B. R., Aziz, S. A. A., Langer, R., Saleh, A. A. H., Becker, C., Nürnberg, G., Cantagrel, V., Gleeson, J. G., Gomez, D., Michel, J. B., Stricker, S., Lindner, T. H., … Hoffmann, K. (2011). Faulty initiation of proteoglycan synthesis causes cardiac and joint defects. *American Journal of Human Genetics*. https://doi.org/10.1016/j.ajhg.2011.05.021

Becker, F. G., Kilic, I., Aydin, G., Puarungroj, W., Boonsirisumpun, N., Gerrikagoitia, J. K., Castander, I., Rebón, F., Alzua-sorzabal, A., George, F. H., Gupta, P., Bhushan, B., Jabar, K.

Beederman, M., Lamplot, J. D., Nan, G., Wang, J., Liu, X., Yin, L., Li, R., Shui, W., Zhang, H., Kim, S. H., Zhang, W., Zhang, J., Kong, Y., Denduluri, S., Rogers, M. R., Pratt, A., Haydon, R. C., Luu, H. H., Angeles, J., … He, T.-C. (2013). BMP signaling in mesenchymal stem cell differentiation and bone formation. *Journal of Biomedical Science and Engineering*. https://doi.org/10.4236/jbise.2013.68a1004

Benyi, E., and Sävendahl, L. (2017). The physiology of childhood growth: Hormonal regulation. In *Hormone Research in Paediatrics*. https://doi.org/10.1159/000471876

Berendsen, A. D., Fisher, L. W., Kilts, T. M., Owens, R. T., Robey, P. G., Gutkind, J. S., & Younga, M. F. (2011). Modulation of canonical Wnt signaling by the extracellular matrix component biglycan. *Proceedings of the National Academy of Sciences of the United States of America*. https://doi.org/10.1073/pnas.1110629108

Berendsen, A. D., and Olsen, B. R. (2015). Bone development. *Bone*, *80*, 14–18. https://doi.org/10.1016/j.bone.2015.04.035

Bhosale, A. M., and Richardson, J. B. (2008). Articular cartilage: Structure, injuries and review of management. In *British Medical Bulletin*. https://doi.org/10.1093/bmb/ldn025

Bi, W., Deng, J. M., Zhang, Z., Behringer, R. R., and De Crombrugghe, B. (1999). Sox9 is required for cartilage formation. *Nature Genetics*. https://doi.org/10.1038/8792

Bi, X., Pohl, N. M., Qian, Z., Yang, G. R., Gou, Y., Guzman, G., Kajdacsy-Balla, A., Iozzo, R. V., & Yang, W. (2012). Decorin-mediated inhibition of colorectal cancer growth and migration is associated with E-cadherin in vitro and in mice. *Carcinogenesis*, *33*(2), 326–330. https://doi.org/10.1093/carcin/bgr293

Bolton, K., Segal, D., McMillan, J., Jowett, J., Heilbronn, L., Abberton, K., Zimmet, P., Chisholm, D., Collier, G., & Walder, K. (2008). Decorin is a secreted protein associated with obesity and type 2 diabetes. *International Journal of Obesity*. https://doi.org/10.1038/ijo.2008.41

Boycott, K. M., Beaulieu, C. L., Kernohan, K. D., Gebril, O. H., Mhanni, A., Chudley, A. E., Redl, D., Qin, W., Hampson, S., Küry, S., Tetreault, M., Puffenberger, E. G., Scott, J. N., Bezieau,

S., Reis, A., Uebe, S., Schumacher, J., Hegele, R. A., McLeod, D. R., … Abou Jamra, R. (2015). Autosomal-Recessive Intellectual Disability with Cerebellar Atrophy Syndrome Caused by Mutation of the Manganese and Zinc Transporter Gene SLC39A8. *American Journal of Human Genetics*, *97*(6), 886–893. https://doi.org/10.1016/j.ajhg.2015.11.002

Brewton, R. G., Wright, D. W., and Mayne, R. (1991). Structural and functional comparison of type IX collagen-proteoglycan from chicken cartilage and vitreous humor. *Journal of Biological Chemistry*.

Buckwalter, J. A. (1997). Maintaining and restoring mobility in middle and old age: the importance of the soft tissues. In *Instructional course lectures*.

Buckwalter, J. A., and Mankin, H. J. (1998). Articular cartilage: degeneration and osteoarthritis, repair, regeneration, and transplantation. In *Instructional course lectures*.

Burdo, J. R., Menzies, S. L., Simpson, I. A., Garrick, L. M., Garrick, M. D., Dolan, K. G., Haile, D. J., Beard, J. L., & Connor, J. R. (2001). Distribution of Divalent Metal Transporter 1 and Metal Transport Protein 1 in the normal and Belgrade rat. *Journal of Neuroscience Research*. https://doi.org/10.1002/jnr.1256

Cancedda, R., Castagnola, P., Descalzi Cancedda, F., Dozin, B., and Quarto, R. (2000). Developmental control of chondrogenesis and osteogenesis. *International Journal of Developmental Biology*. https://doi.org/10.1387/ijdb.11061435

Catistagnola, P., Dozin, B., Moro, G., and Cancedda, R. (1988). Changes in the expression of collagen genes show two stages in chondrocyte differentiation in vitro. *Journal of Cell Biology*, *106*(2), 461–467. https://doi.org/10.1083/jcb.106.2.461

Chen, X. D., Allen, M. R., Bloomfield, S., Xu, T., & Young, M. (2003). Biglycan-deficient mice have delayed osteogenesis after marrow ablation. *Calcified Tissue International*. https://doi.org/10.1007/s00223-002-1101-y

Chen, L., Liu, G., Li, W., & Wu, X. (2019). Chondrogenic differentiation of bone marrow-derived mesenchymal stem cells following transfection with Indian hedgehog and sonic hedgehog using a rotary cell culture system. *Cellular and Molecular Biology Letters*, *24*(1), 1–16. https://doi.org/10.1186/s11658-019-0144-2

Choi, Y., Chung, H., Jung, H., Couchman, J. R., and Oh, E. S. (2011). Syndecans as cell surface receptors: Unique structure equates with functional diversity. *Matrix Biology*, *30*(2), 93–99. https://doi.org/10.1016/j.matbio.2010.10.006

Chua, A. C. G., & Morgan, E. H. (1997). Manganese metabolism is impaired in the Belgrade laboratory rat. *Journal of Comparative Physiology - B Biochemical, Systemic, and Environmental Physiology*. https://doi.org/10.1007/s00360005008Chuang, Y., Lill, C. M., Lee, P., Hansen, J., Lassen, C. F., Bertram, L., Greene, N., and Janet, S. (2017). *HHS Public*

Access. *47*(310), 192–200. https://doi.org/10.1159/000450855.Gene-environment

Chung, U. I. (2004). Essential Role of Hypertrophic Chondrocytes in Endochondral Bone Development. In *Endocrine Journal*. https://doi.org/10.1507/endocrj.51.19

Clarke, B. (2008). Normal bone anatomy and physiology. In *Clinical journal of the American Society of Nephrology : CJASN*. https://doi.org/10.2215/CJN.04151206

Colinet, A. S., Sengottaiyan, P., Deschamps, A., Colsoul, M. L., Thines, L., Demaegd, D., Duchêne, M. C., Foulquier, F., Hols, P., & Morsomme, P. (2016). Yeast Gdt1 is a Golgi-localized calcium transporter required for stress-induced calcium signaling and protein glycosylation. *Scientific Reports*, *6*(April), 1–11. https://doi.org/10.1Cserjesi, P., Brown, D., Ligon, K. L., Lyons, G. E., Copeland, N. G., Gilbert, D. J., Jenkins, N. A., and Olson, E. N. (1995). Scleraxis: A basic helix-loop-helix protein that prefigures skeletal formation during mouse embryogenesis. *Development*, *121*(4), 1099–1110.

Colinet, A. S., Sengottaiyan, P., Deschamps, A., Colsoul, M. L., Thines, L., Demaegd, D., Duchêne, M. C., Foulquier, F., Hols, P., & Morsomme, P. (2016). Yeast Gdt1 is a Golgi-localized calcium transporter required for stress-induced calcium signaling and protein glycosylation. *Scientific Reports*, *6*. https://doi.org/10.1038/srep24282

Corsi, A., Xu, T., Chen, X. D., Boyde, A., Liang, J., Mankani, M., Sommer, B., Iozzo, R. V., Eichstetter, I., Robey, P. G., Bianco, P., & Young, M. F. (2002). Phenotypic effects of biglycan deficiency are linked to collagen fibril abnormalities, are synergized by decorin deficiency, and mimic Ehlers-Danlos-like changes in bone and other connective tissues. *Journal of Bone and Mineral Research*. https://doi.org/10.1359/jbmr.2002.17.7.1180

Couchman, J. R. (2010). Transmembrane Signaling Proteoglycans. *Annual Review of Cell and Developmental Biology*, *26*(1), 89–114. https://doi.org/10.1146/annurev-cellbio-100109-104126

Cserjesi, P., Brown, D., Ligon, K. L., Lyons, G. E., Copeland, N. G., Gilbert, D. J., Jenkins, N. A., & Olson, E. N. (1995). Scleraxis: A basic helix-loop-helix protein that prefigures skeletal formation during mouse embryogenesis. *Development*, *121*(4), 1099–1110.

D'Angelo M. and Greene, R.M. (1991). Transforming growth factor β modulation of glycosaminoglycan production by mesenchymal cells of the developing murine secondary palate..pdf. *Developmental Biology*, *145*, 374–378.

Dao, D. Y., Jonason, J. H., Zhang, Y., Hsu, W., Chen, D., Hilton, M. J., and O'Keefe, R. J. (2012). Cartilage-specific β-catenin signaling regulates chondrocyte maturation, generation of ossification centers, and perichondrial bone formation during skeletal development. *Journal of Bone and Mineral Research*. https://doi.org/10.1002/jbmr.1639

Dathe, K., Kjaer, K. W., Brehm, A., Meinecke, P., Nürnberg, P., Neto, J. C., Brunoni, D.,

Tommerup, N., Ott, C. E., Klopocki, E., Seemann, P., & Mundlos, S. (2009). Duplications Involving a Conserved Regulatory Element Downstream of BMP2 Are Associated with Brachydactyly Type A2. *American Journal of Human Genetics*. https://doi.org/10.1016/j.ajhg.2009.03.001

Demaegd, D., Foulquier, F., Colinet, A. S., Gremillon, L., Legrand, D., Mariot, P., Peiter, E., Van Schaftingen, E., Matthijs, G., & Morsomme, P. (2013). Newly characterized Golgi-localized family of proteins is involved in calcium and pH homeostasis in yeast and human cells. *Proceedings of the National Academy of Sciences of the United States of America*, *110*(17), 6859–6864. https://doi.org/10.1073/pnas.1219871110

Derynck, R., & Zhang, Y. E. (2003). Smad-dependent and Smad-independent pathways in TGF-β family signalling. In *Nature*. https://doi.org/10.1038/nature02006

Domowicz, M. S., Cortes, M., Henry, J. G., & Schwartz, N. B. (2009). Aggrecan modulation of growth plate morphogenesis. *Developmental Biology*. https://doi.org/10.1016/j.ydbio.2009.02.024

Driscoll, P. (2006). Gray's Anatomy, 39th Edition. *Emergency Medicine Journal*, *23*(6), 492–492. https://doi.org/10.1136/emj.2005.027847

Dulary, E., Potelle, S., Legrand, D., & Foulquier, F. (2017). TMEM165 deficiencies in Congenital Disorders of Glycosylation type II (CDG-II): Clues and evidences for roles of the protein in

Golgi functions and ion homeostasis. *Tissue and Cell*, *49*(2), 150–156. https://doi.org/10.1016/j.tice.2016.06.006

Edwards, I. J. (2012). Proteoglycans in prostate cancer. In *Nature Reviews Urology*. https://doi.org/10.1038/nrurol.2012.19

Elderbroom, J. L., Huang, J. J., Gatza, C. E., Chen, J., How, T., Starr, M., Nixon, A. B., & Blobe, G. C. (2014). Ectodomain shedding of TβRIII is required for TβRIII-mediated suppression of TGF-β signaling and breast cancer migration and invasion. *Molecular Biology of the Cell*. https://doi.org/10.1091/mbc.E13-09-0524

Freire-Maia, N., Maia, N. A., & Pacheco, C. N. A. (1980). Mohr-Wriedt (A2) brachydactyly: Analysis of a large brazilian kindred. *Human Heredity*. https://doi.org/10.1159/000153133

Fico, A., Maina, F., & Dono, R. (2011). Fine-tuning of cell signaling by glypicans. *Cellular and Molecular Life Sciences*. https://doi.org/10.1007/s00018-007-7471-6

Filmus, J., Capurro, M., & Rast, J. (2009). Glypicans. In *Genome Biology*. https://doi.org/10.1186/gb-2008-9-5-224

Foster, J. W., Dominguez-Steglich, M. A., Guioli, S., Kwok, C., Weller, P. A., Stevanović, M.,

Weissenbach, J., Mansour, S., Young, I. D., Goodfellow, P. N., Brook, J. D., and Schafer, A.

J. (1994). Campomelic dysplasia and autosomal sex reversal caused by mutations in an SRY-related gene. *Nature*. https://doi.org/10.1038/372525a0

Foulquier, F., Vasile, E., Schollen, E., Callewaert, N., Raemaekers, T., Quelhas, D., Jaeken, J., Mills, P., Winchester, B., Krieger, M., Annaert, W., & Matthijs, G. (2006). *Conserved oligomeric Golgi complex subunit 1 deficiency reveals a previously uncharacterized congenital disorder of glycosylation type II*. www.pnas.orgcgidoi10.1073pnas.0507685103

Foulquier, F. (2009). COG defects, birth and rise! *Biochimica et Biophysica Acta - Molecular Basis of Disease*, *1792*(9), 896–902. https://doi.org/10.1016/j.bbadis.2008.10.020

Foulquier, F., Amyere, M., Jaeken, J., Zeevaert, R., Schollen, E., Race, V., Bammens, R., Morelle, W., Rosnoblet, C., Legrand, D., Demaegd, D., Buist, N., Cheillan, D., Guffon, N., Morsomme, P., Annaert, W., Freeze, H. H., Van Schaftingen, E., Vikkula, M., and Matthijs, G. (2012). TMEM165 deficiency causes a congenital disorder of glycosylation. *American Journal of Human Genetics*, *91*(1), 15–26. https://doi.org/10.1016/j.ajhg.2012.05.002

Fuster, M. M., and Esko, J. D. (2005). The sweet and sour of cancer: Glycans as novel therapeutic targets. *Nature Reviews Cancer*, *5*(7), 526–542. https://doi.org/10.1038/nrc1649

Gandhi, N. S., & Mancera, R. L. (2008). The structure of glycosaminoglycans and their interactions with proteins. *Chemical Biology and Drug Design*, *72*(6), 455–482. https://doi.org/10.1111/j.1747-0285.2008.00741.x

Gao, Ying, Gui, F., Li, D., Zhang, R., Sun, Q., & Guo, X. (2020). Fluoride regulates the expression of extracellular matrix HSPG and related signaling pathways FGFR3 and Ihh/PTHrP feedback loop during endochondral ossification. *Environmental Toxicology and Pharmacology*. https://doi.org/10.1016/j.etap.2019.103275

Gao, Yue, Liu, S., Huang, J., Guo, W., Chen, J., Zhang, L., Zhao, B., Peng, J., Wang, A., Wang, Y., Xu, W., Lu, S., Yuan, M., & Guo, Q. (2014). The ECM-cell interaction of cartilage extracellular matrix on chondrocytes. In *BioMed Research International*. https://doi.org/10.1155/2014/648459

Gelse, K., Pöschl, E., and Aigner, T. (2003). Collagens - Structure, function, and biosynthesis. *Advanced Drug Delivery Reviews*. https://doi.org/10.1016/j.addr.2003.08.002

Gentili S., C., & Cancedda, R. (2009). Cartilage and Bone Extracellular Matrix. *Current Pharmaceutical Design*, *15*(12), 1334–1348. https://doi.org/10.2174/138161209787846739

Gesslbauer, B., Theuer, M., Schweiger, D., Adage, T., & Kungl, A. J. (2013). New targets for

glycosaminoglycans and glycosaminoglycans as novel targets. In *Expert Review of Proteomics* (Vol. 10, Issue 1, pp. 77–95). https://doi.org/10.1586/epr.12.75

Gibson, B. G., and Briggs, M. D. (2016). The aggrecanopathies; An evolving phenotypic spectrum of human genetic skeletal diseases. *Orphanet Journal of Rare Diseases*, *11*(1). https://doi.org/10.1186/s13023-016-0459-2

Gilbert, S. F. (2000). Osteogenesis: The Development of Bones (endochondral ossification). In *Development Biology: 6th edition*. https://doi.org/10: 0-87893-243-7

Girkontaite, I., Frischholz, S., Lammi, P., Wagner, K., Swoboda, B., Aigner, T., and Von Der Mark, K. (1996). Immunolocalization of type X collagen in normal fetal and adult osteoarthritic cartilage with monoclonal antibodies. *Matrix Biology*. https://doi.org/10.1016/S0945-053X(96)90114-6

Goldring, M. B., Tsuchimochi, K., and Ijiri, K. (2006). The control of chondrogenesis. In *Journal of Cellular Biochemistry*. https://doi.org/10.1002/jcb.20652

Gouze, J. N., Bordji, K., Gulberti, S., Terlain, B., Netter, P., Magdalou, J., Fournel-Gigleux, S., & Ouzzine, M. (2001). Interleukin-1β down-regulates the expression of glucuronosyltransferase I, a key enzyme priming glycosaminoglycan biosynthesis: Influence of glucosamine on interleukin-1β-mediated effects in rat chondrocytes. *Arthritis and Rheumatism*. https://doi.org/10.1002/1529-0131(200102)44:2<351: AID-ANR53>3.0.CO;2-M

Grskovic, I., Kutsch, A., Frie, C., Groma, G., Stermann, J., Schlötzer-Schrehardt, U., Niehoff, A., Moss, S. E., Rosenbaum, S., Pöschl, E., Chmielewski, M., Rappl, G., Abken, H., Bateman, J. F., Cheah, K. S. E., Paulsson, M., & Brachvogel, B. (2012). Depletion of annexin A5, annexin A6, and collagen X causes no gross changes in matrix vesicle-mediated mineralization, but lack of collagen X affects hematopoiesis and the Th1/Th2 response. *Journal of Bone and Mineral Research*, *27*(11), 2399–2412. https://doi.org/10.1002/jbmr.1682

Gubbiotti, M. A., Vallet, S. D., Ricard-Blum, S., & Iozzo, R. V. (2016). Decorin interacting network: A comprehensive analysis of decorin-binding partners and their versatile functions. In *Matrix Biology* (Vol. 55, pp. 7–21). Elsevier B.V. https://doi.org/10.1016/j.matbio.2016.09.009

Hall, B. K., and Miyake, T. (2000). All for one and one for all: Condensations and the initiation of skeletal development. In *BioEssays*. https://doi.org/10.1002/(SICI)1521-1878(200002)22:2<138::AID-BIES5>3.0.CO;2-4

Hay, E. D. (1991). *Cell Biology of Extracellular Matrix*. https://doi.org/10.1007/978-1-4615-3770-0

Heinegård, D., and Saxne, T. (2011). The role of the cartilage matrix in osteoarthritis. *Nature*

Reviews Rheumatology, *7*(1), 50–56. https://doi.org/10.1038/nrrheum.2010.198

Herscovics, A., & Orlean, P. (1993). Glycoprotein biosynthesis in yeast. *The FASEB Journal*. https://doi.org/10.1096/fasebj.7.6.8472892

Hiscock, D. R. R., Caterson, B., & Flannery, C. R. (2000). Expression of hyaluronan synthases in articular cartilage. *Osteoarthritis and Cartilage*, *8*(2), 120–126. https://doi.org/10.1053/joca.1999.0280

Houdou, M., Lebredonchel, E., Garat, A., Duvet, S., Legrand, D., Decool, V., Klein, A., Ouzzine, M., Gasnier, B., Potelle, S., & Foulquier, F. (2019). Involvement of thapsigargin- And cyclopiazonic acid-sensitive pumps in the rescue of TMEM165-associated glycosylation defects by Mn2+. *FASEB Journal*, *33*(2), 2669–2679. https://doi.org/10.1096/fj.201800387R

Hsu, P. D., Lander, E. S., and Zhang, F. (2014). Development and applications of CRISPR-Cas9 for genome engineering. *Cell*, *157*(6), 1262–1278. https://doi.org/10.1016/j.cell.2014.05.010

Hu, K., Xu, L., Cao, L., Flahiff, C. M., Brussiau, J., Ho, K., Setton, L. A., Youn, I., Guilak, F., Olsen, B. R., and Li, Y. (2006). Pathogenesis of osteoarthritis-like changes in the joints of mice deficient in type IX collagen. *Arthritis and Rheumatism*. https://doi.org/10.1002/art.22040

Iozzo, R. V., & San Antonio, J. D. (2001). Heparan sulfate proteoglycans: heavy hitters in the angiogenesis arena. *Journal of Clinical Investigation*, *108*(3), 349–355. https://doi.org/10.1172/jci13738

Iozzo, R. V., and Schaefer, L. (2015). Proteoglycan form and function: A comprehensive nomenclature of proteoglycans. *Matrix Biology*, *42*, 11–55. https://doi.org/10.1016/j.matbio.2015.02.003

Iyama, K.I. , Ninomiya, Y., Olsen, B. R., Linsenmayer, T. F., Trelstad, R. L., and Hayashi, M. (1991). Spatiotemporal pattern of type X collagen gene expression and collagen deposition in embryonic chick vertebrae undergoing endochondral ossification. *The Anatomical Record*. https://doi.org/10.1002/ar.1092290405

Izumikawa, T., Sato, B., Mikami, T., Tamura, J. I., Igarashi, M., & Kitagawa, H. (2015). GlcUAβ1-3Galβ1-3Galβ1-4xyl(2-o-phosphate) is the preferred substrate for chondroitin N-acetylgalactosaminyltransferase-1. *Journal of Biological Chemistry*. https://doi.org/10.1074/jbc.M114.603266

Izumikawa, T. (2019). Regulatory mechanism of 2-o-phosphorylation of xylose in the glycosaminoglycan-linkage region of the tetrasaccharide. *Trends in Glycoscience and Glycotechnology*. https://doi.org/10.4052/tigg.1955.2E

Jaeken, J. (2003). Congenital disorders of glycosylation (CDG): It's all in it! In *Journal of Inherited Metabolic Disease*. https://doi.org/10.1023/A:1024431131208

Jaeken, J., & Matthijs, G. (2007). Congenital Disorders of Glycosylation: A Rapidly Expanding Disease Family. *Annual Review of Genomics and Human Genetics*, *8*(1), 261–278. https://doi.org/10.1146/annurev.genom.8.080706.092327

Jaeken, J., Lefeber, D., & Matthijs, G. (2014). Clinical utility gene card for: Phosphomannomutase 2 deficiency. *European Journal of Human Genetics*, *22*(8), 1054. https://doi.org/10.1038/ejhg.2013.298

Jaeken, J., & Péanne, R. (2017). What is new in CDG? In *Journal of inherited metabolic disease*. https://doi.org/10.1007/s10545-017-0050-6

Järveläinen, H., Sainio, A., and Wight, T. N. (2015). Pivotal role for decorin in angiogenesis. In *Matrix Biology*. https://doi.org/10.1016/j.matbio.2015.01.023

Järvinen, T. A. H., & Prince, S. (2015). Decorin: A Growth Factor Antagonist for Tumor Growth Inhibition. *BioMed Research International*, *2015*. Knudson, C. B., and Knudson, W. (2001). Cartilage proteoglycans. *Seminars in Cell and Developmental Biology*, *12*(2), 69–78. https://doi.org/10.1006/scdb.2000.0243

Jinn, S., Drolet, R. E., Cramer, P. E., Wong, A. H. K., Toolan, D. M., Gretzula, C. A., Voleti, B., Vassileva, G., Disa, J., Tadin-Strapps, M., & Stone, D. J. (2017). TMEM175 deficiency impairs lysosomal and mitochondrial function and increases α-synuclein aggregation. *Proceedings of the National Academy of Sciences of the United States of America*. https://doi.org/10.1073/pnas.1616332114

Khair, M., Bourhim, M., Barré, L., Li, D., Netter, P., Magdalou, J., Fournel-Gigleux, S., & Ouzzine, M. (2013). Regulation of xylosyltransferase i gene expression by interleukin 1β in human primary chondrocyte cells: Mechanism and impact on proteoglycan synthesis. *Journal of Biological Chemistry*. https://doi.org/10.1074/jbc.M112.419887

Khatra, B. S., Herries, D. G., & Brew, K. (1974). Some Kinetic Properties of Human-Milk Galactosyl Transferase. *European Journal of Biochemistry*. https://doi.org/10.1111/j.1432-1033.1974.tb03513.x

Khoder-Agha, F., Sosicka, P., Escriva Conde, M., Hassinen, A., Glumoff, T., Olczak, M., & Kellokumpu, S. (2019). N-acetylglucosaminyltransferases and nucleotide sugar transporters form multi-enzyme–multi-transporter assemblies in golgi membranes in vivo. *Cellular and Molecular Life Sciences*. https://doi.org/10.1007/s00018-019-03032-5

Knudson, C. B., & Knudson, W. (2001). Cartilage proteoglycans. *Seminars in Cell and Developmental Biology*, *12*(2), 69–78. https://doi.org/10.1006/scdb.2000.0243

Kobayashi, T., and Kronenberg, H. M. (2014). Overview of skeletal development. *Methods in*

Molecular Biology. https://doi.org/10.1007/978-1-62703-989-5_1

Kolb, M., Margetts, P. J., Sime, P. J., and Gauldie, J. (2001). Proteoglycans decorin and biglycan differentially modulate TGF-β-mediated fibrotic responses in the lung. *American Journal of Physiology - Lung Cellular and Molecular Physiology*, *280*(6 24-6), 1327–1334. https://doi.org/10.1152/ajplung.2001.280.6.l1327

Kolset, S. O., & Pejler, G. (2011). Serglycin: A Structural and Functional Chameleon with Wide Impact on Immune Cells. In *the Journal of Immunology* (Vol. 187, Issue 10, pp. 4927–4933). https://doi.org/10.4049/jimmunol.1100806

Körkkö, J., Cohn, D. H., Ala-Kokko, L., Krakow, D., and Prockop, D. J. (2000). Widely distributed mutations in the COL2A1 gene produce achondrogenesis type II/hypochondrogenesis. *American Journal of Medical Genetics*, *92*(2), 95–100. https://doi.org/10.1002/(SICI)1096-8628(20000515)92:2<95::AID-AJMG3>3.0.CO;2-9

Kornak, U., Reynders, E., Dimopoulou, A., Van Reeuwijk, J., Fischer, B., Rajab, A., Budde, B.,

Koziel, L., Kunath, M., Kelly, O. G., & Vortkamp, A. (2004). Ext1-dependent heparan sulfate regulates the range of Ihh signaling during endochondral ossification. *Developmental Cell*. https://doi.org/10.1016/j.devcel.2004.05.009

Kukuruzinska, M. a, & Robbins, P. W. (1987). Protein glycosylation in yeast: transcript heterogeneity of the ALG7 gene. *Proceedings of the National Academy of Sciences of the United States of America*, *84*(8), 2145–2149. https://doi.org/10.1073/pnas.84.8.2145

Kuss, P., Kraft, K., Stumm, J., Ibrahim, D., Vallecillo-Garcia, P., Mundlos, S., and Stricker, S. (2014). Regulation of cell polarity in the cartilage growth plate and perichondrium of metacarpal elements by HOXD13 and WNT5A. *Developmental Biology*. https://doi.org/10.1016/j.ydbio.2013.10.013

Lamas, J. R., Rodríguez-Rodríguez, L., Vigo, A. G., Álvarez-Lafuente, R., López-Romero, P., Marco, F., Camafeita, E., Dopazo, A., Callejas, S., Villafuertes, E., Hoyas, J. A., Tornero-Esteban, M. P., Urcelay, E., and Fernández-Gutiérrez, B. (2010). Large-scale gene expression in bone marrow mesenchymal stem cells: A putative role for COL10A1 in osteoarthritis. *Annals of the Rheumatic Diseases*. https://doi.org/10.1136/ard.2009.122564

Lebredonchel, E., Houdou, M., Hoffmann, H. H., Kondratska, K., Krzewinski, M. A., Vicogne, D., Rice, C. M., Klein, A., & Foulquier, F. (2019). Investigating the functional link between TMEM165 and SPCA1. *Biochemical Journal*. https://doi.org/10.1042/BCJ20190488

Lee, D. H., Oh, J. H., & Chung, J. H. (2016). Glycosaminoglycan and proteoglycan in skin aging. In *Journal of Dermatological Science*. https://doi.org/10.1016/j.jdermsci.2016.05.016

Lefebvre, V., and Bhattaram, P. (2010a). Chapter Eight - Vertebrate Skeletogenesis. In *Current*

Topics in Developmental Biology: Evolution and Development. https://doi.org/10.1016/S0070-2153(10)90008-2

Lefebvre, V., and Bhattaram, P. (2010b). Vertebrate skeletogenesis. *Current Topics in Developmental Biology*, *90*(C), 291–317. https://doi.org/10.1016/S0070-2153(10)90008-2

Lehmann, K., Seemann, P., Silan, F., Goecke, T. O., Irgang, S., Kjaer, K. W., Kjaergaard, S., Mahoney, M. J., Morlot, S., Reissner, C., Kerr, B., Wilkie, A. O. M., & Mundlos, S. (2007). A new subtype of brachydactyly type B caused by point mutations in the bone morphogenetic protein antagonist NOGGIN. *American Journal of Human Genetics*. https://doi.org/10.1086/519697

Li, L., Ly, M., and Linhardt, R. J. (2012). Proteoglycan sequence. *Molecular BioSystems*, *8*(6), 1613. https://doi.org/10.1039/c2mb25021g

Long, F., and Ornitz, D. M. (2013). Development of the endochondral skeleton. *Cold Spring Harbor Perspectives in Biology*, *5*(1), 1–20. https://doi.org/10.1101/cshperspect.a008334

López-Casillas, F., Cheifetz, S., Doody, J., Andres, J. L., Lane, W. S., & Massague, J. (1991). Structure and expression of the membrane proteoglycan betaglycan, a component of the TGF-β receptor system. *Cell*. https://doi.org/10.1016/0092-8674(91)90073-8

Mackie, E. J., Ahmed, Y. A., Tatarczuch, L., Chen, K. S., and Mirams, M. (2008). Endochondral ossification: How cartilage is converted into bone in the developing skeleton. *International Journal of Biochemistry and Cell Biology*, *40*(1), 46–62. https://doi.org/10.1016/j.biocel.2007.06.009

Madejczyk, M. S., & Ballatori, N. (2012). The iron transporter ferroportin can also function as a manganese exporter. *Biochimica et Biophysica Acta - Biomembranes*. https://doi.org/10.1016/j.bbamem.2011.12.002

Maeda, Y., Nakamura, E., Nguyen, M. T., Suva, L. J., Swain, F. L., Razzaque, M. S., Mackem, S., and Lanske, B. (2007). Indian Hedgehog produced by postnatal chondrocytes is essential for maintaining a growth plate and trabecular bone. *Proceedings of the National Academy of Sciences of the United States of America*, *104*(15), 6382–6387. https://doi.org/10.1073/pnas.0608449104

Malfait, F., Kariminejad, A., Van Damme, T., Gauche, C., Syx, D., Merhi-Soussi, F., Gulberti, S., Symoens, S., Vanhauwaert, S., Willaert, A., Bozorgmehr, B., Kariminejad, M. H., Ebrahimiadib, N., Hausser, I., Huysseune, A., Fournel-Gigleux, S., & De Paepe, A. (2013). Defective initiation of glycosaminoglycan synthesis due to B3GALT6 mutations causes a pleiotropic Ehlers-Danlos-syndrome-like connective tissue disorder. *American Journal of Human Genetics*, *92*(6), 935–945. https://doi.org/10.1016/j.ajhg.2013.04.016

Manduca, P., Castagnola, P., and Cancedda, R. (1988). Dimethyl sulfoxide interferes with in vitro differentiation of chick embryo endochondral chondrocytes. *Developmental Biology*. https://doi.org/10.1016/0012-1606(88)90078-4

Manon-Jensen, T., Itoh, Y., and Couchman, J. R. (2010). Proteoglycans in health and disease: The multiple roles of syndecan shedding. *FEBS Journal*, *277*(19), 3876–3889.

Marques-da-Silva, D., Francisco, R., Webster, D., dos Reis Ferreira, V., Jaeken, J., & Pulinilkunnil, T. (2017). Cardiac complications of congenital disorders of glycosylation (CDG): a systematic review of the literature. *Journal of Inherited Metabolic Disease*, *40*(5), 657–672. https://doi.org/10.1007/s10545-017-0066-y

Matsuo, I., & Kimura-Yoshida, C. (2013). Extracellular modulation of Fibroblast Growth Factor signaling through heparan sulfate proteoglycans in mammalian development. In *Current Opinion in Genetics and Development*. https://doi.org/10.1016/j.gde.2013.02.004

Masuda, S., Namba, K., Mutai, H., Usui, S., Miyanaga, Y., Kaneko, H., & Matsunaga, T. (2014). A mutation in the heparin-binding site of noggin as a novel mechanism of proximal symphalangism and conductive hearing loss. *Biochemical and Biophysical Research Communications*, *447*(3), 496–502. https://doi.org/10.1016/j.bbrc.2014.04.015

McCormick, C., Leduc, Y., Martindale, D., Mattison, K., Esford, L. E., Dyer, A. P., & Tufaro, F. (1998). The putative tumour suppressor EXT1 alters the expression of cell- surface heparan sulfate. *Nature Genetics*. https://doi.org/10.1038/514

Mikami, T., & Kitagawa, H. (2013). Biosynthesis and function of chondroitin sulfate. In *Biochimica et Biophysica Acta - General Subjects*. https://doi.org/10.1016/j.bbagen.2013.06.006

Moss, S. E., Rosenbaum, S., Pöschl, E., Chmielewski, M., Rappl, G., Abken, H., Bateman, J. F., Cheah, K. S. E., Paulsson, M., and Brachvogel, B. (2012). Depletion of annexin A5, annexin A6, and collagen X causes no gross changes in matrix vesicle-mediated mineralization, but lack of collagen X affects hematopoiesis and the Th1/Th2 response. *Journal of Bone and Mineral Research*, *27*(11), 2399–2412. https://doi.org/10.1002/jbmr.1682

Mundlos, S. (1999). Cleidocranial dysplasia: Clinical and molecular genetics. In *Journal of Medical Genetics*. https://doi.org/10.1136/jmg.36.3.177

Mythreye, K., & Blobe, G. C. (2009a). Proteoglycan signaling co-receptors: Roles in cell adhesion, migration and invasion. In *Cellular Signalling*. https://doi.org/10.1016/j.cellsig.2009.05.001

Mythreye, K., & Blobe, G. C. (2009b). The type III TGF-β receptor regulates epithelial and cancer cell migration through β-arrestin2-mediated activation of Cdc42. *Proceedings of the National Academy of Sciences of the United States of America*. https://doi.org/10.1073/pnas.0812879106

Nadanaka, S., & Kitagawa, H. (2014). EXTL2 controls liver regeneration and aortic calcification through xylose kinase-dependent regulation of glycosaminoglycan biosynthesis. In *Matrix Biology*. https://doi.org/10.1016/j.matbio.2013.10.010

Nagarajan, A., Malvi, P., & Wajapeyee, N. (2018). Heparan sulfate and Heparan Sulfate Proteoglycans in cancer initiation and progression. *Frontiers in Endocrinology*, *9*(AUG), 1–11. https://doi.org/10.3389/fendo.2018.00483

Nastase, M. V., Young, M. F., & Schaefer, L. (2012). Biglycan: A Multivalent Proteoglycan Providing Structure and Signals. *Journal of Histochemistry and Cytochemistry*. https://doi.org/10.1369/0022155412456380

Neill, T., Torres, A., Buraschi, S., & Iozzo, R. V. (2013). Decorin has an appetite for endothelial cell autophagy. *Autophagy*. https://doi.org/10.4161/auto.25881

Nikitovic, D., Aggelidakis, J., Young, M. F., Iozzo, R. V., Karamanos, N. K., & Tzanakakis, G. N. (2012). The biology of small leucine-rich proteoglycans in bone pathophysiology. In *Journal of Biological Chemistry*. https://doi.org/10.1074/jbc.R112.379602

Nishikawa, T., Edelstein, D., Du, X. L., Yamagishi, S. I., Matsumura, T., Kaneda, Y., Yorek, M. A., Beebe, D., Oates, P. J., Hammes, H. P., Glardino, I., & Brownlee, M. (2000). Normalizing mitochondrial superoxide production blocks three pathways of hyperglycaemic damage. *Nature*, *404*(6779), 787–790. https://doi.org/10.1038/35008121

Nürnberg, P., Foulquier, F., Dobyns, W. B., Quelhas, D., Vilarinho, L., Leao-Teles, E., Greally, M., Seemanova, E., Simandlova, M., Salih, M., Nanda, A., Basel-Vanagaite, L., … Mundlos, S. (2008). Impaired glycosylation and cutis laxa caused by mutations in the Kukuruzinska, M. a, and Robbins, P. W. (1987). Protein glycosylation in yeast: transcript heterogeneity of the ALG7 gene. *Proceedings of the National Academy of Sciences of the United States of America*, *84*(8), 2145–2149. https://doi.org/10.1073/pnas.84.8.2145

Okajima, T., Fukumoto, S., Furukawat, K., Urano, T., & Furukawa, K. (1999). Molecular basis for the progeroid variant of Ehlers-Danlos syndrome. Identification and characterization of two mutations in galactosyltransferase I gene. *Journal of Biological Chemistry*. https://doi.org/10.1074/jbc.274.41.28841

Ornitz, D. M., and Marie, P. J. (2002). FGF signaling pathways in endochondral and intramembranous bone development and human genetic disease. *Genes and Development*, *16*(12), 1446–1465. https://doi.org/10.1101/gad.990702

Ouyang, H., Luo, Y., Zhang, L., Li, Y., and Jin, C. (2010). Proteome analysis of Aspergillus fumigatus total membrane proteins identifies proteins associated with the glycoconjugates and cell wall biosynthesis using 2D LC-MS/MS. *Molecular Biotechnology*, *44*(3), 177–189. https://doi.org/10.1007/s12033-009-9224-2

Paesold-Burda, P., Maag, C., Troxler, H., Foulquier, F., Kleinert, P., Schnabel, S., Baumgartner, M., & Hennet, T. (2009). Deficiency in COG5 causes a moderate form of congenital disorders of glycosylation. *Human Molecular Genetics*, *18*(22), 4350–4356. https://doi.org/10.1093/hmg/ddp389

Pang, X., Wang, Z., Chai, Y., Chen, H., Li, L., Sun, L., Jia, H., Wu, H., & Yang, T. (2015). A novel missense mutation of NOG interferes with the dimerization of NOG and causes proximal symphalangism syndrome in a Chinese family. *Annals of Otology, Rhinology and Laryngology*. https://doi.org/10.1177/0003489415582257

Pap, T., and Bertrand, J. (2013). Syndecans in cartilage breakdown and synovial inflammation. *Nature Reviews Rheumatology*, *9*(1), 43–55. https://doi.org/10.1038/nrrheum.2012.178

Park, J. H., Hogrebe, M., Fobker, M., Brackmann, R., Fiedler, B., Reunert, J., Rust, S., Tsiakas, K., Santer, R., Grüneberg, M., & Marquardt, T. (2018). SLC39A8 deficiency: Biochemical correction and major clinical improvement by manganese therapy. *Genetics in Medicine*. https://doi.org/10.1038/gim.2017.106

Park, J. H., Hogrebe, M., Grüneberg, M., Duchesne, I., Von Der Heiden, A. L., Reunert, J., Schlingmann, K. P., Boycott, K. M., Beaulieu, C. L., Mhanni, A. A., Innes, A. M., Hörtnagel, K., Biskup, S., Gleixner, E. M., Kurlemann, G., Fiedler, B., Omran, H., Rutsch, F., Wada, Y., … Marquardt, T. (2015). SLC39A8 Deficiency: A Disorder of Manganese Transport and Glycosylation. *American Journal of Human Genetics*. https://doi.org/10.1016/j.ajhg.2015.11.003

Péanne, R., de Lonlay, P., Foulquier, F., Kornak, U., Lefeber, D. J., Morava, E., Pérez, B., Seta, N., Thiel, C., Van Schaftingen, E., Matthijs, G., & Jaeken, J. (2018). Congenital disorders of glycosylation (CDG): Quo vadis? In *European Journal of Medical Genetics*. https://doi.org/10.1016/j.ejmg.2017.10.012

Potelle, S., Dulary, E., Duvet, S., Morelle, W., Vicogne, D., Spriet, C., Foulquier, F., & Krzewinski-, M.-A. (2017). *HHS Public Access*. *47*(310), 192–200. https://doi.org/10.1159/000450855.Gene-environment

Potelle, S., Klein, A., & Foulquier, F. (2015). Golgi post-translational modifications and associated diseases. In *Journal of Inherited Metabolic Disease* (Vol. 38, Issue 4, pp. 741–751). Kluwer Academic Publishers. https://doi.org/10.1007/s10545-015-9851-7

Potelle, S., Morelle, W., Dulary, E., Duvet, S., Vicogne, D., Spriet, C., Krzewinski-Recchi, M. A., Morsomme, P., Jaeken, J., Matthijs, G., De Bettignies, G., & Foulquier, F. (2016).

Glycosylation abnormalities in Gdt1p/TMEM165 deficient cells result from a defect in Golgi manganese homeostasis. *Human Molecular Genetics*, *25*(8), 1489–1500. https://doi.org/10.1093/hmg/ddw026

Potelle, S., Dulary, E., Climer, L., Duvet, S., Morelle, W., Vicogne, D., Lebredonchel, E., Houdou, M., Spriet, C., Krzewinski-Recchi, M. A., Peanne, R., Klein, A., De Bettignies, G., Morsomme, P., Matthijs, G., Marquardt, T., Lupashin, V., & Foulquier, F. (2017). Manganese-induced turnover of TMEM165. *Biochemical Journal*, *474*(9), 1481–1493. https://doi.org/10.1042/BCJ20160910

Powell, J. T., & Brew, K. (1976). Metal ion activation of galactosyltransferase. *Journal of Biological Chemistry*.

Prydz, K., and Dalen, K. T. (2000). Synthesis and sorting of proteoglycans. *Journal of Cell Science*, *113 Pt 2*, 193–205.

Pujol, J. P., Chadjichristos, C., Legendre, F., Bauge, C., Beauchef, G., Andriamanalijaona, R., Galera, P., & Boumediene, K. (2008). Interleukin-1 and transforming growth factor-β 1 as crucial factors in osteoarthritic cartilage metabolism. In *Connective Tissue Research*. https://doi.org/10.1080/03008200802148355

Raouf, A., Ganss, B., McMahon, C., Vary, C., Roughley, P. J., & Seth, A. (2002). Lumican is a major proteoglycan component of the bone matrix. *Matrix Biology*. https://doi.org/10.1016/S0945-053X(02)00027-6

Reynders, E., Foulquier, F., Teles, E. L., Quelhas, D., Morelle, W., Rabouille, C., Annaert, W., & Matthijs, G. (2009). Golgi function and dysfunction in the first COG4-deficient CDG type II patient. *Human Molecular Genetics*, *18*(17), 3244–3256. https://doi.org/10.1093/hmg/ddp262

Roughley, P. J., and Lee, E. R. (1994). Cartilage proteoglycans: Structure and potential functions. *Microscopy Research and Technique*, *28*(5), 385–397. https://doi.org/10.1002/jemt.1070280505

Roughley, P. J., and Mort, J. S. (2014). The role of aggrecan in normal and osteoarthritic cartilage. *Journal of Experimental Orthopaedics*, *1*(1), 1–11. https://doi.org/10.1186/s40634-014-0008-7

Roy, A. S., Miskinyte, S., Garat, A., Hovnanian, A., Krzewinski-recchi, M. A., & Foulquier, F. (2020). SPCA1 governs the stability of TMEM165 in Hailey-Hailey disease. *Biochimie*. https://doi.org/10.1016/j.biochi.2020.04.017

Ruoslahti, E., & Yamaguchi, Y. (1991). Proteoglycans as modulators of growth factor activities. In *Cell*. https://doi.org/10.1016/0092-8674(91)90308-L

Sainio, A. O., & Järveläinen, H. T. (2019). Decorin-mediated oncosuppression – a potential

future adjuvant therapy for human epithelial cancers. In *British Journal of Pharmacology*. https://doi.org/10.1111/bph.14180

Salazar, V. S., Gamer, L. W., and Rosen, V. (2016). BMP signalling in skeletal development, disease and repair. *Nature Reviews Endocrinology*, *12*(4), 203–221. https://doi.org/10.1038/nrendo.2016.12

Sanford, L. P., Ormsby, I., Gittenberger-de Groot, A. C., Sariola, H., Friedman, R., Boivin, G. P., Cardell, E. Lou, & Doetschman, T. (1997). TGFβ2 knockout mice have multiple developmental defects that are non-overlapping with other TGFβ knockout phenotypes. *Development*.

Sarrazin, S., Lamanna, W. C., & Esko, J. D. (2011). Heparan sulfate proteoglycans. *Cold Spring Harbor Perspectives in Biology*, *3*(7), 1–33. https://doi.org/10.1101/cshperspect.a004952

Schaefer, L., Babelova, A., Kiss, E., Hausser, H. J., Baliova, M., Krzyzankova, M., Marsche, G., Young, M. F., Mihalik, D., Götte, M., Malle, E., Schaefer, R. M., & Gröne, H. J. (2005). The matrix component biglycan is proinflammatory and signals through Toll-like receptors 4 and 2 in macrophages. *Journal of Clinical Investigation*. https://doi.org/10.1172/JCI23755

Schmittgen, T. D., and Livak, K. J. (2008). Analyzing real-time PCR data by the comparative C(T) methodSchmittgen, T.D., Livak, K.J., 2008. Analyzing real-time PCR data by the comparative C(T) method. Nat. Protoc. 3, 1101–1108.. *Nature Protocols*.

Schwartz, N. B., and Domowicz, M. (2002). Chondrodysplasias due to proteoglycan defects. *Glycobiology*, *12*(4), 57–68. https://doi.org/10.1093/glycob/12.4.57R

Seidler, D. G. (2012). The galactosaminoglycan-containing decorin and its impact on diseases. In *Current Opinion in Structural Biology*. https://doi.org/10.1016/j.sbi.2012.07.012

Seki, K., & Hata, A. (2004). Indian Hedgehog Gene Is a Target of the Bone Morphogenetic Protein Signaling Pathway. *Journal of Biological Chemistry*. https://doi.org/10.1074/jbc.M311592200

Sepulveda, W., Wong, A. E., & Dezerega, V. (2007). First-trimester ultrasonographic screening for trisomy 21 using fetal nuchal translucency and nasal bone. *Obstetrics and Gynecology*. https://doi.org/10.1097/01.AOG.0000259311.87056.5e

Shapiro, F. (2001). CHAPTER 9 – Skeletal Dysplasias. In *Pediatric Orthopedic Deformities*. https://doi.org/10.1016/B978-012638651-6/50010-1

Shen, G. (2005). The role of type X collagen in facilitating and regulating endochondral ossification of articular cartilage. *Orthodontics and Craniofacial Research*. https://doi.org/10.1111/j.1601-6343.2004.00308.x

Shim, K. S. (2015). Pubertal growth and epiphyseal fusion. *Annals of Pediatric Endocrinology*

and Metabolism. https://doi.org/10.6065/apem.2015.20.1.8

Shimizu, H., Yokoyama, S., & Asahara, H. (2007). Growth and differentiation of the developing limb bud from the perspective of chondrogenesis. In *Development Growth and Differentiation* (Vol. 49, Issue 6, pp. 449–454). https://doi.org/10.1111/j.1440-169X.2007.00945.x

Silva-Almeida, M., Carvalho, L. O., Abreu-Silva, A. L., Souza, C. S., Hardoim, D. J., and Calabrese, K. S. (2012). Extracellular matrix alterations in experimental Leishmania amazonensis infection in susceptible and resistant mice. *Veterinary Research*. https://doi.org/10.1186/1297-9716-43-10

Snyder, N. A., Palmer, M. V., Reinhardt, T. A., & Cunningham, K. W. (2019). Milk biosynthesis requires the Golgi cation exchanger TMEM165. *Journal of Biological Chemistry*, *294*(9), 3181–3191. https://doi.org/10.1074/jbc.RA118.006270

Šošić, D., Brand-Saberi, B., Schmidt, C., Christ, B., and Olson, E. N. (1997). Regulation of paraxis expression and somite formation by ectoderm- and neural tube-derived signals. *Developmental Biology*, *185*(2), 229–243. https://doi.org/10.1006/dbio.1997.8561

Stanley, P. (2011). Golgi glycosylation. *Cold Spring Harbor Perspectives in Biology*, *3*(4), 1–13. https://doi.org/10.1101/cshperspect.a005199

Stribny, J., Thines, L., Deschamps, A., Goffin, P., Morsomme, P., & Shipston, M. (2020). The human Golgi protein TMEM165 transports calcium and manganese in yeast and bacterial cells. *Journal of Biological Chemistry*, *295*(12), 3865–3874. https://doi.org/10.1074/jbc.RA119.012249

Susarla, B. T. S., Laing, E. D., Yu, P., Katagiri, Y., Geller, H. M., & Symes, A. J. (2011). Smad proteins differentially regulate transforming growth factor-β-mediated induction of chondroitin sulfate proteoglycans. *Journal of Neurochemistry*. https://doi.org/10.1111/j.1471-4159.2011.07470.x

Tan, Y., Yamada-Mabuchi, M., Arya, R., Pierre, S. S., Tang, W., Tosa, M., Brachmannspi-Sup, C., & White, K. (2011). Coordinated expression of cell death genes regulates neuroblast apoptosis. *Development*. https://doi.org/10.1242/dev.058826

Taschner, M. J., Rafigh, M., Lampert, F., Schnaiter, S., & Hartmann, C. (2008). Ca2+/Calmodulin-dependent kinase II signaling causes skeletal overgrowth and premature chondrocyte maturation. *Developmental Biology*, *317*(1), 132–146. https://doi.org/10.1016/j.ydbio.2008.02.007

Tavasoli, A., Arjmandi Rafsanjani, K., Hemmati, S., Mojbafan, M., Zarei, E., & Hosseini, S. (2019). A case of dystonia with polycythemia and hypermanganesemia caused by SLC30A10 mutation: A treatable inborn error of manganese metabolism. *BMC Pediatrics*.

https://doi.org/10.1186/s12887-019-1611-7

Theocharis, A. D., Skandalis, S. S., Gialeli, C., and Karamanos, N. K. (2016). Extracellular matrix structure. In *Advanced Drug Delivery Reviews*. https://doi.org/10.1016/j.addr.2015.11.001

Thines, L., Deschamps, A., Sengottaiyan, P., Savel, O., Stribny, J., & Morsomme, P. (2018). The yeast protein Gdt1p transports Mn2 ions and thereby regulates manganese homeostasis in the Golgi. *Journal of Biological Chemistry*, *293*(21), 8048–8055. https://doi.org/10.1074/jbc.RA118.002324

Thines, L., Deschamps, A., Stribny, J., & Morsomme, P. (2019). Yeast as a tool for deeper understanding of human manganese-related diseases. In *Genes*. https://doi.org/10.3390/genes10070545

Tompson, S. W., Merriman, B., Funari, V. A., Fresquet, M., Lachman, R. S., Rimoin, D. L., Nelson, S. F., Briggs, M. D., Cohn, D. H., and Krakow, D. (2009). A Recessive Skeletal Dysplasia, SEMD Aggrecan Type, Results from a Missense Mutation Affecting the C-Type Lectin Domain of Aggrecan. *American Journal of Human Genetics*, *84*(1), 72–79. https://doi.org/10.1016/j.ajhg.2008.12.001

Torres, A., Gubbiotti, M. A., & Iozzo, R. V. (2017). Decorin-inducible Peg3 evokes beclin 1-mediated autophagy and thrombospondin 1-mediated angiostasis. *Journal of Biological Chemistry*, *292*(12), 5055–5069. https://doi.org/10.1074/jbc.M116.753632

Tracy Ballock, R., Heydemann, A., Wakefield, L. M., Flanders, K. C., Roberts, A. B., & Sporn, M. B. (1993). TGF-β1 prevents hypertrophy of epiphyseal chondrocytes: Regulation of gene expression for cartilage matrix proteins and metalloproteases. *Developmental Biology*. https://doi.org/10.1006/dbio.1993.1200

Troeberg, L., & Nagase, H. (2012). Proteases involved in cartilage matrix degradation in osteoarthritis. In *Biochimica et Biophysica Acta - Proteins and Proteomics*. https://doi.org/10.1016/j.bbapap.2011.06.020

Tsang, K. Y., Chan, D., and Cheah, K. S. E. (2015). Fate of growth plate hypertrophic chondrocytes: Death or lineage extension? *Development Growth and Differentiation*, *57*(2), 179–192. https://doi.org/10.1111/dgd.12203

Tuschl, K., Mills, P. B., Parsons, H., Malone, M., Fowler, D., Bitner-Glindzicz, M., & Clayton, P. T. (2008). Hepatic cirrhosis, dystonia, polycythaemia and hypermanganesaemia - A new metabolic disorder. *Journal of Inherited Metabolic Disease*. https://doi.org/10.1007/s10545-008-0813-1

Tuschl, K., Clayton, P. T., Gospe, S. M., Gulab, S., Ibrahim, S., Singhi, P., Aulakh, R., Ribeiro, R. T., Barsottini, O. G., Zaki, M. S., Del Rosario, M. L., Dyack, S., Price, V., Rideout, A., Gordon,

K., Wevers, R. A., Kling Chong, W. K., & Mills, P. B. (2012). Syndrome of hepatic cirrhosis, dystonia, polycythemia, and hypermanganesemia caused by mutations in SLC30A10, a manganese transporter in man. *American Journal of Human Genetics*. https://doi.org/10.1016/j.ajhg.2012.01.018

Tuschl, K., Mills, P. B., & Clayton, P. T. (2013). Manganese and the Brain. In *International Review of Neurobiology*. https://doi.org/10.1016/B978-0-12-410502-7.00013-2

Tuschl, K., Meyer, E., Valdivia, L. E., Zhao, N., Dadswell, C., Abdul-Sada, A., Hung, C. Y., Simpson, M. A., Chong, W. K., Jacques, T. S., Woltjer, R. L., Eaton, S., Gregory, A., Sanford, L., Kara, E., Houlden, H., Cuno, S. M., Prokisch, H., Valletta, L., … Wilson, S. W. (2016). Mutations in SLC39A14 disrupt manganese homeostasis and cause childhood-onset parkinsonism-dystonia. *Nature Communications*. https://doi.org/10.1038/ncomms11601

Twine, N. A., Chen, L., Pang, C. N., Wilkins, M. R., and Kassem, M. (2014). Identification of differentiation-stage specific markers that define the ex vivo osteoblastic phenotype. *Bone*, *67*, 23–32. https://doi.org/10.1016/j.bone.2014.06.027

van Kooyk, Y., Kalay, H., and Garcia-Vallejo, J. J. (2013). Analytical tools for the study of cellular glycosylation in the immune system. In *Frontiers in Immunology* (Vol. 4, Issue DEC, pp. 1–6). https://doi.org/10.3389/fimmu.2013.00451

Vanoevelen, J., Dode, L., Van Baelen, K., Fairclough, R. J., Missiaen, L., Raeymaekers, L., & Wuytack, F. (2005). The secretory pathway Ca2+/Mn2+-ATPase 2 is a Golgi-localized pump with high affinity for Ca2+ ions. *Journal of Biological Chemistry*, *280*(24), 22800–22808. https://doi.org/10.1074/jbc.M501026200

Velleman, S. G. (2000). The role of the extracellular matrix in skeletal development. *Poultry Science*, *79*(7), 985–989. https://doi.org/10.1093/ps/79.7.985

Venkatesan, N., Barré, L., Magdalou, J., Mainard, D., Netter, P., Fournel-Gigleux, S., & Ouzzine, M. (2009). Modulation of xylosyltransferase I expression provides a mechanism regulating glycosaminoglycan chain synthesis during cartilage destruction and repair. *The FASEB Journal*. https://doi.org/10.1096/fj.08-118166

Venkatesan, N., Tsuchiya, K., Kolb, M., Farkas, L., Bourhim, M., Ouzzine, M., & Ludwig, M. S. (2014). Glycosyltransferases and glycosaminoglycans in bleomycin and transforming growth factor-β1-induced pulmonary fibrosis. *American Journal of Respiratory Cell and Molecular Biology*. https://doi.org/10.1165/rcmb.2012-0226OC

Vicogne, D., Houdou, M., Garat, A., Climer, L., Lupashin, V., Morelle, W., & Foulquier, F. (2020). Fetal bovine serum impacts the observed N-glycosylation defects in TMEM165 KO HEK cells. *Journal of Inherited Metabolic Disease*, *43*(2), 357–366. https://doi.org/10.1002/jimd.12161

Watanabe, H., Nakata, K., Kimata, K., Nakanishi, I., and Yamada, Y. (1997). Dwarfism and age-associated spinal degeneration of heterozygote cmd mice defective in aggrecan. *Proceedings of the National Academy of Sciences of the United States of America*, *94*(13), 6943–6947. https://doi.org/10.1073/pnas.94.13.6943

Wedler, F. C., & Denman, R. B. (1984). Glutamine synthetase: the major Mn(II) enzyme in mammalian brain. In *Current topics in cellular regulation*. https://doi.org/10.1016/b978-0-12-152824-9.50021-6

Wolff, N. A., Garrick, M. D., Zhao, L., Garrick, L. M., Ghio, A. J., & Thévenod, F. (2018). A role for divalent metal transporter (DMT1) in mitochondrial uptake of iron and manganese. *Scientific Reports*. https://doi.org/10.1038/s41598-017-18584-4

Wu, M., Chen, G., and Li, Y. P. (2016). TGF-b and BMP signaling in osteoblast, skeletal development, and bone formation, homeostasis and disease. *Bone Research*, *4*(December 2015). https://doi.org/10.1038/boneres.2016.9

Yada, T., Gotoh, M., Sato, T., Shionyu, M., Go, M., Kaseyama, H., Iwasaki, H., Kikuchi, N., Kwon, Y. D., Togayachi, A., Kudo, T., Watanabe, H., Narimatsu, H., and Kimata, K. (2003a). Chondroitin sulfate synthase-2: Molecular cloning and characterization of a novel human glycosyltransferase homologous to chondroitin sulfate glucuronyltransferase, which has dual enzymatic activities. *Journal of Biological Chemistry*. https://doi.org/10.1074/jbc.M303657200

Yada, T., Sato, T., Kaseyama, H., Gotoh, M., Iwasaki, H., Kikuchi, N., Kwon, Y. D., Togayachi, A., Kudo, T., Watanabe, H., Narimatsu, H., and Kimata, K. (2003b). Chondroitin sulfate synthase-3. Molecular cloning and characterization. *Journal of Biological Chemistry*. https://doi.org/10.1074/jbc.M304421200

Yamanishi, Y., Bach, F., and Vert, J. P. (2007). Glycan classification with tree kernels. *Bioinformatics*, *23*(10), 1211–1216. https://doi.org/10.1093/bioinformatics/btm090

Yanagishita, M. (1993). Function of proteoglycans in the extracellular matrix. *Pathology International*, *43*(6), 283–293. https://doi.org/10.1111/j.1440-1827.1993.tb02569.x

Ye, M., Berry-Wynne, K. M., Asai-Coakwell, M., Sundaresan, P., Footz, T., French, C. R., Abitbol, M., Fleisch, V. C., Corbett, N., Allison, W. T., Drummond, G., Walter, M. A., Underhill, T. M., Waskiewicz, A. J., & Lehmann, O. J. (2009). Mutation of the bone morphogenetic protein GDF3 causes ocular and skeletal anomalies. *Human Molecular Genetics*. https://doi.org/10.1093/hmg/ddp496

Young, M. F., & Ameye, L. (2002). Mice deficient in small leucine-rich proteoglycans: novel in vivo models for osteoporosis, osteoarthritis, Ehlers-Danlos syndrome, muscular dystrophy, and corneal diseases. *Glycobiology*.

Zeevaert, R., de Zegher, F., Sturiale, L., Garozzo, D., Smet, M., Moens, M., Matthijs, G., & Jaeken, J. (2013). Bone dysplasia as a key feature in three patients with a novel congenital disorder of glycosylation (CDG) type II due to a deep intronic splice mutation in TMEM165. In *JIMD Reports*. https://doi.org/10.1007/8904_2012_172

Zhang, F., Zhang, Z., & Linhardt, R. J. (2010). Glycosaminoglycans. *Handbook of Glycomics*, 59–80. https://doi.org/10.1016/B978-0-12-373600-0.00003-2

Zheng, Q., Sebald, E., Zhou, G., Chen, Y., Wilcox, W., Lee, B., and Krakow, D. (2005). Dysregulation of chondrogenesis in human cleidocranial dysplasia. *American Journal of Human Genetics*. https://doi.org/10.1086/432261

TEMM165 a new player in proteoglycan synthesis and chondrocyte differentiation

Sajida Khan, Lydia Barré-vancome, Mohamed Ouzzine*

UMR 7365 CNRS-University of Lorraine, Biopôle, Faculty of Medicine, CS 50184, 54505, Vandoeuvre-lès-Nancy, France.

*Corresponding author: mohamed.ouzzine@univ-lorraine.fr

Tel : (33) 372 746 563

Email : mohamed.ouzzine@univ-lorraine.fr

Running title: TMEM165 and chondrocyte differentiation

Conflict of Interest: The authors declare no competing financial interests

Abstract

TMEM165 is a novel protein deficient in CDG (Congenital disorders of Glycosylation) patients with new features including bone defects and pronounced dwarfism, suggesting a role of TMEM165 in chondrogenesis and skeletal development. Here, we showed for the first time that TMEM165 deficiency impairs the synthesis of proteoglycans in chondrocyte cells by producing a blockage in the elongation of their glycosaminoglycan chains which can be rescued by supplementation of cell with Mn^{2+}, suggesting a role of TMEM165 in Mn^{2+} Golgi homeostasis. Interestingly, we found that loss of TMEM165 activates CamKIIα and functionally impairs TGFβ/BMP signaling pathways and promotes differentiation of chondrocyte ATDC5 cells towards hypertrophy. Importantly, lack of TMEM165 accelerates the timing of Ihh expression during differentiation leading to early chondrocyte maturation. These data may account for skeletal defects observed in TMEM165-deficient CDG patients.

Keywords: TMEM165, proteoglycans, glycosaminoglycans, Congenital disorders of glycosylation, differentiation.

Introduction

Glycosylation is one of the most common and important posttranslational modifications of protein[1,2]. Genetic defects in protein glycosylation can lead to Congenital Disorders of Glycosylation (CDGs) which is a group of inherited diseases associated with a broad variety of pathological symptoms [3]. Among these, the recently identified CDG subtype linked to mutations in TMEM165 (transmembrane protein 165)[4]. The *TMEM165* gene is located on chromosome 4q12 and consists of six exons encoding a protein of 324 amino acids. TMEM165 protein belongs to the family of uncharacterized proteins named UPF0016 (Uncharacterized Protein Family 0016; Pfam PF01169), which comprises integral membrane proteins with poorly characterized function and containing one or two copies of highly conserved EXGDK/R motif. Mutation of the yeast ortholog of TMEM165, termed Gdt1 induced sensitivity to high external concentrations of Ca^{2+}, suggesting its participation to Ca^{2+} transport by reducing the concentration of Ca^{2+} in the cytosol. The sensitivity of Gdt1-mutant yeast to high Ca^{2+} concentrations was reversed by expression of TMEM165, suggesting that TMEM165 likely functions as a Golgi Ca^{2+} transporter. In the other hand, fibroblasts from TMEM165-deficient patients display acidification of the late endosomes and lysosomes, suggesting that TMEM165 is involved in pH homeostasis. Therefore, it has been suggested that TMEM165 may function as a Golgi Ca^{2+}/H^{+} antiporter regulating both Golgi Ca^{2+} and pH homeostasis [3]. In line with this, Gdt1 has been suggested to transport luminal H^{+} produced as a by-product of glycosylation reactions to the cytoplasm in exchange for cytoplasmic Ca^{2+} [5]. TMEM165 gene deficiency was associated with a slight defect in sialylation and galactosylation of *N*-glycans in TMEM165-deficient patients. Many glycosyltransferases use metal ions such as Mg^{2+} or Mn^{2+} as co-factor. Supplementation of the culture medium of Hela cells with Mn^{2+} rescue the *N*-glycosylation defects on recombinant LAMP2 and TGN46 following TMEM165 depletion, suggesting that

defects in glycosylation results from defects in Mn^{2+}. Therefore, TMEM165 is involved in Mn^{2+} homeostasis and it may import Mn^{2+} into the Golgi stacks [6]. Although, the transport activity of TMEM165 in human cells have not been demonstrated yet, several indirect observations suggest that TMEM165 may be involved in maintaining Golgi Ca^{2+}, H^{+}, Mn^{2+} homeostasis.

Different mutations were detected in TMEM165 in the patients suffering from CDGs, including missense mutations R126H and R126C located in the putative lysosomal targeting motif ^{124}YNRL^{127}, the mutation E108G lying in the highly conserved motif ^{108}ELGDKT^{113} , the double mutations R126C/G304R and intronic splice mutation leading to skipping of the exon four and generation of truncated protein. The major clinical findings in the individuals with a homozygous splice mutation leading to total loss of TMEM165 are severe psychomotor retardation, major skeletal dysplasia, pronounced dwarfism and severe osteopenia which are not observed in other mutant patients. Interestingly, similar phenotype was observed in patients harbouring genetic mutations in genes encoding enzymes involved in the synthesis of proteoglycans (PGs) [7–10], suggesting a potential link between TMEM165 and PG synthesis. Here, we generated TMEM165-knockout pre-chondrocyte mouse ATDC5 and human HEK293 cells using CRISPR/Cas9 technique and showed that knockdown of TMEM165 resulted in profound deficiency in polymerization of heparan-sulfate (HS) and chondroitin-sulfate (CS) GAG chains of PGs. We demonstrated that defects in GAG elongation was not due to impaired expression of GAG polymerizing enzymes, but rather to deficiency in their enzymes activities that can be overcome by supplementation of culture cell medium with the divalent cation Mn^{2+}, suggesting a role of TMEM165 in the homeostasis of Golgi Mn^{2+}. Importantly, we found that loss of TMEM165 functionally down-regulates TGFβ and upregulates BMP signaling pathways which may lead to accelerated chondrocyte maturation. Finally, differentiation of pre-chondrocyte ATDC5 cells showed that cells lacking TMEM165 accelerate timing of Ihh expression and undergo early hypertrophic differentiation.

Results

Knocking down TMEM165 in a mouse chondrogenic cell line ATDC5 using CRISPR/Cas9 technique

It has been reported that TMEM165-deficient CDG patients present skeletal and bone abnormalities [4]**,** suggesting a role of TMEM165 in chondrogenesis and bone homeostasis. PGs play, *via* their GAG chains, a key role in several biological processes including chondrocytes differentiation and maturation, growth plate development and signaling. Genetic mutations or knockout of glycosyltransferases involved in GAG synthetic pathway cause chondrodysplasia. We therefore hypothesized that defects in GAG chains may occur following TMEM165 deficiency leading to skeletal defects observed in TMEM 165-deficient CDG patients. To determine the link, if any, between TMEM165 deficiency and the synthesis of PGs, we generated TMEM165-knockout prechondrogenic ATDC5 cell line using CRISPR-Cas9 technique by targeting three different regions of *TMEM165* gene. Several TMEM165-knockout clones targeting the exon2 of *TMEM165* gene were isolated and genomic DNA fragments spanning the targeted regions were amplified by PCR and analyzed by sequencing. Four TMEM165-knockout clones harbouring deletion mutations leading to premature stop codon were selected for further studies **(Fig. 1a)**. To confirm that deletion mutations abolished the synthesis of TMEM165 protein, expression of the protein was analyzed in wild-type and mutant ATDC5 cells by immunoblot using anti-TMEM165 antibodies. As expected, expression of a polypeptide of about 35 kDa corresponding to TMEM165 was detected in wild-type ATDC5 cells, whereas no polypeptide was revealed by the anti-TMEM165 antibodies in TMEM165-knockout cells **(Fig. 1b)**, indicating that expression of TMEM165 protein is efficiently knocked down in mutant cells. To further confirm these results, immunofluorescence analysis of the expression of TMEM165 was carried out in wild-type and in TMEM165-knockout ATDC5 cells. As shown in **figure 1c** TMEM165 is clearly detected in wild-type ATDC5 cells displaying

a perinuclear Golgi distribution and colocalize with the Golgi (GM130) marker**.** However, no staining with anti-TMEM165 was observed in TMEM165-knockout ATDC5 cells, whereas the Golgi marker GM130 was clearly detected, indicating that the expression of TMEM165 is knocked down in mutant cells. Altogether, these data showed that TMEM165 is knocked down in ATDC5 mutant cells.

TMEM165 deficiency impairs elongation of heparan- and chondroitin-sulfate chains

To uncover the link, if any, between TMEM165 and PGs, we evaluated the level of PG synthesis in wild-type and TMEM165-knockout ATDC5 cells by using metabolic incorporation of radiolabelled [^{35}S]-sulfate into GAG chains. Interestingly, the results showed a decrease of about 70 % in the rate of PG synthesis in TMEM165-knockout cells compared to wild-type cells **(Fig. 2a)**. Interestingly, SDS-PAGE analysis of radiolabelled PG-GAG chains showed predominance of shorter GAG chains in TMEM165-knockout cells, compared to wild-type **(Fig. 2b).** To determine whether the defects in GAG synthesis affects both CS- and HS-GAG chains, we used decorin and syndecan 4 as reporter for the synthesis of CS-PGs and HS-PGs, respectively. For these purposes wild-type and mutant ATDC5 cells were transfected with expression vector for decorin and for HA-tagged syndecan 4. Of note, CS- and HS-attached PGs migrate as an elongated smear during gel electrophoresis due to heterogeneity of attached GAG chains. As expected, transfection of wild-type and TMEM165-knockout ATDC5 cells with decorin expression vector resulted in the secretion of CS/DS attached decorin and decorin core protein in the culture medium as shown by Western blot using anti-decorin specific antibodies **(Fig. 2c),** however there is a loss of higher sized CS/DS attached decorin species in TMEM165-knockout ATDC5 cells compared to wild-type cells as evidenced by predominance of decorin with significantly small sized GAG chains **(Fig. 2c**). To confirm whether this is also the case in other cell lines, we generated TMEM165-knockout HEK293 cells and analyzed

decorin produced in culture medium of wild-type and mutant HEK293 cells after transfection with decorin expression vector. As shown in **figure 2d**, GAG-attached decorin expressed by TMEM165-knockout HEK293 cells showed predominance of lower sized GAG-attached decorin, compared to wild-type cells. This indicate that defects in PG synthesis produced by the loss of TMEM165 is not cell type specific. To rule out an effect of TMEM165 on decorin core protein expression or secretion, we generated and expressed a decorin mutant lacking GAG-attachement site by mutation of serine residue at position 34, which is used for the attachment of the CS-GAG chain on the core protein, to alanine residue (S34A). Expression of the mutant decorin S34A in wild-type ATDC5 cells led, as expected, to the secretion of a polypeptide of about 50 kDa corresponding to decorin core protein without attached GAG chain (**Fig. 2e)**. Of note, TMEM165-knockout ATDC5 cells secreted mutant decorin at similar amount to that produced by wild-type cells. These data indicate that TMEM165 deficiency did not affect neither synthesis nor secretion of decorin core protein. Altogether, these results suggest that the loss of TMEM165 rather affects the synthesis of GAG chain attached to decorin core protein.

Given that the knockdown of TMEM165 did not affect the synthesis of decorin core protein, we hypothesized that it may affect the GAG chain synthesis. To verify this hypothesis, we used 4-Methylumbelliferyl-β-D-xylopyranoside (4MU-Xyl) as acceptor substrate for the synthesis of GAG chains. Indeed, it is well known that the biosynthesis of GAG chains can also be initiated in the absence of a core protein by xyloside analogues carrying a hydrophobic aglycon, such as 4MU-Xyloside (4MU-Xyl). The xyloside can, when exogenously supplied to cells, acts as acceptor substrate for β4GalT7, then elongated and leading to the production in the medium of xyloside-primed GAG chains. Therefore, we cultured TMEM165-knockout and wild-type ATDC5 cells in the presence of 4MU-Xyl and [^{35}S]-sulfate to metabolically radiolabel the newly synthesized GAG chains. 4MU-Xyl-primed GAG chains produced were isolated by

Cetylpyridinium chloride method from culture medium and analyzed by SDS-PAGE and autoradiography. The results showed that wild-type ATDC5 cells produced significant amount of radiolabelled GAG chains, whereas TMEM165-knockout ATDC5 cells produced only few amounts **(Fig. 2f)**, indicating that the synthesis of GAG chains is affected in TMEM165-knockout cells. To determine whether reduction in the size of decorin produced in TMEM165-mutant ATDC5 cells results from defects in polymerization of CS-GAG chains, decorin from wild-type and TMEM165-mutant ATDC5 cells were subjected to treatment with chondroitinase ABC that degrades CS-GAG chains of PGs. Interestingly, treatment of decorin produced in TMEM165-knockout cells with chondroitinase ABC led to change in the migration pattern in SDS-PAGE from a smear to a single band corresponding to decorin core protein **(Fig. 2g)**, indicating that, although it is shorter in size, decorin from mutant cells is sensitive to chondroitinase ABC and therefore contains elongated CS-GAG chains. These results indicated that TMEM165-knockout cells elongate CS-GAG chains on decorin core protein but with reduced efficiency leading to the formation of shorter GAG chains. Together, these data suggest that TMEM165 deficiency led to defects in elongation of CS-GAG chains and therefore to impairment in GAG polymerization process.

We next investigated whether the synthesis of HS-GAG chains is also altered in TMEM165-knockout cells. For this purpose, we expressed syndecan 4, an HSPG with three HS-attached GAG chains, in TMEM165-knockout and wild-type ATDC5 cells by transfection with an expression vector encoding HA-tagged syndecan 4. As shown by Western blot in **figure 2h**, syndecan 4 expressed in wild-type ATDC5 cells exhibited a smear pattern in SDS-PAGE corresponding to HS-attached syndecan 4 in addition to a polypeptide corresponding to syndecan 4 core protein, whereas in TMEM165-knockout the smear was strongly reduced in size indicating a loss of higher sized syndecan 4 species in TMEM165-knockout ATDC5 cells, compared to wild-type cells. These results indicate that syndecan 4 contains shorter HS-GAG

chains suggesting that elongation of HS chains is impaired in mutant cells. To further confirm this result, we carried out indirect immunofluorescence analysis of cell surface HSPGs in wild-type and TMEM165-knockout cells, using anti-HS monoclonal antibody 10E4, which is commonly used to detect HS chains of PGs. Prominent staining of the cell membrane was observed in wild-type cells (green), whereas very low signal could be observed in TMEM165-knockout cells (**Fig.2i**). When cells were probed with anti-TMEM165 antibodies, efficient expression of the protein was revealed (red), whereas no staining was observed in TMEM165-knockout cells (**Fig. 2i**). Altogether, these results revealed a key role of TMEM165 in the synthesis of both HS- and CS-GAG chains of PGs.

Given that CS and HS synthetic pathways involve several enzymes each of which is involved in a specific step of the synthesis process, we sought to determine whether impaired elongation of CS- and HS-GAG chains in TMEM165-knockout cells resulted from defects in the gene expression of CS and HS polymerizing enzymes. To this end, RT-qPCR analysis were performed using mRNA from TMEM165-knockout and wild-type ATDC5 cells to evaluate gene expression of CS polymerizing enzymes, CHSY1 and CHSY2 and of HS polymerizing enzymes, EXT1 and EXT2. The results showed that mRNA levels of CS polymerizing enzymes CHSY1 and CHSY2 is similar in wild-type and TMEM165-knockout ATDC5 cells **(Fig. 2j**), suggesting that reduced CS-GAG chain elongation is not due to defect in gene expression of polymerizing enzymes. Likewise, mRNA levels of HS polymerizing enzymes, EXT1 and EXT2 is not significantly different in wild-type and TMEM165-knockout ATDC5 cells, indicating that defect in elongation of HS-GAG chains in mutant cells is not due to downregulation of gene expression of HS polymerizing enzymes **(Fig. 2j)**. We also analyzed the expression of the enzymes XylT1/XylT2, GalT1, GalT2 and GlcAT-I involved in the synthesis of the tetrasaccharide linker used as a primer for elongation of both CS and HS chains and found that levels of gene expression of these enzymes are not altered in TMEM165-

knockout compared to wild-type ATDC5 cells **(data not shown)**. Similar analyses were carried out in human normal fibroblast cells and TMEM165-deficient fibroblasts from CDG patient and showed that gene expression of CS- and HS-GAG polymerizing enzymes were similar or higher in patient's fibroblasts, compared to control **(Fig. 2k)**. Altogether, these data suggest that defects in polymerization of CS- and HS-GAG chains are not due to alterations in gene expression of the enzymes involved.

Expression of chondroitin-polymerizing enzymes did not overcome GAG elongation defects induced by loss of TMEM165

We showed above that mRNA expression of CS and HS polymerizing enzymes is not altered in TMEM165-deficient ATDC5 cells and in CDG patient fibroblasts, compared to control cells. However, we cannot rule out a decrease in the protein level that may result from increased protein instability and/or degradation. Given that the level of protein expression of glycosyltransferases involved in GAG synthetic pathway is very low and their detection by antibodies (commercially available) is very challenging, it is therefore difficult to evaluate and compare the protein levels of CS and HS polymerizing enzymes in normal and mutant cells. We can however hypothesize that overexpression of these enzymes may overcome the instability or degradation of these proteins, if any. To support the expression of CS polymerizing enzymes, we designed expression vectors for Myc-tagged CHSY1 and HA-tagged CHSY2 and used them to overexpress each of the two enzymes individually or together in TMEM165-knockout ATDC5 cells. Next, we investigated whether overexpression of theses enzymes rescue the polymerization of CS-GAG chains. For this purpose, we transfected TMEM165-knockout cells with CHSY1, CHSY2 or CHSY1 and CHSY2 expression vectors along with decorin expression vector. Cells transfected with empty vector along with decorin expression vector were used as control. As shown in **figure 3a,** TMEM165-knockout cells

transfected with CHSY1, CHSY2 or CHSY1 and CHSY2 produced decorin with reduced size compared to that produced in wild-type cells. The expression of CHSY1 and CHSY2 was confirmed by Western blot in all the cells transfected **(Figure 3b and 3c)**. These data indicated that overexpression of CHSY1 and CHSY2 individually or together did not rescue CS elongation in TMEM165-deficient cells, suggesting that defects in CS polymerisation process did not result from reduced protein expression of the polymerizing enzymes, CHSY1 and CHSY2.

Next, we sought to determine whether supplying the cell culture medium with sugar monosaccharides used in the synthesis of CS-GAG chains such as xylose and galactose may restore CS elongation in TMEM165-knockout ATDC5 cells. To this end, TMEM165-mutant cells were transfected with decorin expression vector and incubated in the presence or absence of 1 mM of xylose and galactose, respectively. As shown in **figure 3d**, the size of decorin produced in TMEM165-knockout cells is significantly reduced compared to that of wild-type cells and has not change with treatment with either xylose or galactose, indicating that supplying cells with monosaccharides did not overcome the blockage in the polymerization process.

Manganese rescues the synthesis of chondroitin-sulfate and heparan-sulfate GAG chains in TMEM165-deficient cells

It has been established that Mn^{2+} participates in the catalytic activity of various Golgi glycosyltransferases including CS and HS polymerizing enzymes [11,12]**.** Therefore, we sought to determine whether defects in the elongation of CS- and HS-GAG chains in TMEM165-knockot cells is due to lack of Mn^{2+}. For this purpose, wild-type and TMEM165-mutant cells were transfected with decorin expression vector then cultured in the absence or presence of 1μM of Mn^{2+}. Western blot analysis of decorin produced in wild-type ATDC5 cells showed similar

pattern either in the absence or presence of Mn^{2+}, whereas decorin expressed in TMEM165-knockout cells that were cultured in the presence of Mn^{2+} was larger in size similar compared to that produced in the absence of Mn^{2+} and showed a pattern similar to decorin produced in wild-type cells **(Fig. 4a)**. These data showed that supplementation of the culture medium with Mn^{2+} induced an increase in the size of decorin and indicate that Mn^{2+} restores polymerization of decorin CS-GAG chains in TMEM165-knockout cells. To rule out an effect of Mn^{2+} on the synthesis or secretion of decorin core protein we expressed decorin S34A mutant, lacking the CS attachment site, in wild-type and TMEM165-knockout cells and analyzed decorin produced by immunoblot. As shown in **figure 4b**, both wild-type and TMEM165-knockout cells efficiently expressed the mutant decorin core protein with similar pattern either in the absence or presence of Mn^{2+}, indicating that treatment of cells with Mn^{2+} did not affect the synthesis and secretion of decorin core protein. Therefore, changes in the size of decorin following treatment with Mn^{2+} resulted from changes in the length of the attached CS-GAG chain. As polymerization of HS-GAG chains are also impaired in TMEM165-knockout cells, we investigated whether Mn^{2+} is able to restore the polymerization of HS-GAG chains, as observed above for CS-GAG chains. Wild-type and TMEM165-mutant ATDC5 cells were transfected with HA-syndecan 4 expression vector and cultured in the absence or presence of 1µM of Mn^{2+}. Western blot analysis of HA-syndecan 4 indicated the expression of a high molecular weight smear corresponding to HA-syndecan 4 with HS-GAG chains exhibiting a similar pattern either in the presence or absence of Mn^{2+} **(Fig. 4c)**, suggesting that the divalent ion Mn^{2+} did not affect the synthesis of HS-GAG chains in wild-type cells at the concentration used. Remarkably, supplementation of Mn^{2+} in the culture medium of TMEM165-knockout cells resulted in the synthesis of HA-syndecan 4 with higher molecular weight compared to that produced in the absence of Mn^{2+} **(Fig. 4c)**, indicating that HS-GAG chains attached to HA-syndecan 4 are of

larger size when Mn^{2+} is supplied in the culture medium. These data strongly suggest that Mn^{2+} rescues the polymerization of HS-GAG chains in TMEM165-knockout cells.

To further confirm that Mn^{2+} rescues GAG chains elongation in TMEM165-knockout cells, 4MU-Xyl was used as exogenous substrate to monitor the synthesis of GAG chains. Wild-type and TMEM165-mutant ADTC5 cells were cultured in the presence or absence of Mn^{2+} along with 4MU-Xyl primer and [^{35}S]-sulfate to radiolabel newly synthesized GAG chains. SDS-PAGE analysis of radiolabelled 4MU-Xyl-primed GAG chains showed that in the absence of Mn^{2+}, high amount of GAG chains was produced in wild-type cells, whereas very week signal was observed in TMEM165-knockout cells, indicating that the polymerization process is impaired in these cells. Interestingly, supplementation of Mn^{2+} in the culture medium restores the synthesis of GAG chains in TMEM165-knockout cells leading to production of significant amount of radiolabelled GAG chains **(Fig. 4d)**. Altogether, these results demonstrate that TMEM165 deficiency induces defects in the synthesis of PGs by impairing the elongation of GAG chains leading to synthesis of PGs with shorter GAG chains. They also bring evidence that defect in CS- and HS-GAG elongation is rescued by supplementation of cells with Mn^{2+}, suggesting strongly that the function of GAG polymerizing enzymes, known to require Mn^{2+} to be fully active, is impaired in TMEM165-knockout cells and that Golgi Mn^{2+} homeostasis is disturbed in mutant cells.

Ca^{2+}/calmodulin-dependent protein kinase IIα pathway is activated in TMEM165-deficient cells

It has been proposed that TMEM165 may exchange Golgi luminal H^+ for cytoplasmic Ca^{2+}, whereas other studies suggested that it may be involved in the transport of cytoplasmic Mn^{2+} to the Golgi lumen. Direct implication of TMEM165 in the transport of either Ca^{2+} or Mn^{2+} is not yet been reported. However, it is well known that Ca^{2+}/calmodulin-dependent protein kinase II

(CaMkII) is activated when intracellular concentration in Ca^{2+} is elevated and binding of Ca^{2+}/calmodulin complex to CaMkII regulatory domain. We hypothesized that if TMEM165 is involved in Ca^{2+} homeostasis then deficiency in TMEM165 may lead to impaired transport of cytoplasmic Ca^{2+} to the Golgi and therefore to elevated [Ca^{2+}] in the cytoplasm. To verify this hypothesis, we analysed the phosphorylation status of CaMkIIα in TMEM165-knockout and wild-type ATDC5 cells. Interestingly, as shown by Western blot, the level of phospho-CaMkIIα (pCaMkIIα) was strongly increased in TMEM165-knockout cells compared to wild-type cells **(Figure 5a**), indicating that CaMkIIα was strongly activated in TMEM165-knockout cells. Likewise, as observed in ATDC5 cells, the phosphorylation level of CaMkIIα was remarkably increased in TMEM165-deficient CDG patient fibroblast cells, compared to normal fibroblasts **(Figure 5b).** These results indicate that CaMkIIα is activated in mutant cells strongly suggesting that intracellular [Ca^{2+}] is elevated in these cells. Altogether, these data indicated that the loss of TMEM165 induces defects in both Ca^{2+} and Mn^{2+} homeostasis and support the notion of that TMEM165 is probably involved in the regulation of both Ca^{2+} and Mn^{2+} homeostasis.

TMEM165 deficiency impairs TGF-β and BMP signaling pathways

We showed above that TMEM165 deficiency led to defects in synthesis of PG-GAG chains. As a number of human genetic mutations causing a wide range of inheritable diseases of skeletal development are related to TGF-β and BMP signaling [13] and owing to the key role of GAG chains in the regulation of several signaling pathways, we sought to investigate whether loss of TMEM165 affects TGF-β and BMP signaling pathways. We first explored the TGF-β signaling in wild-type and TMEM165-knockout ATDC5 cells by analysis of the phosphorylation status of Smad2, a downstream mediator of TGF-β receptor activation. Interestingly, Western blot analysis showed that phospho-Smad2 level (but not total Smad2 level) was reduced in

TMEM165-knockout cells compared to wild-type **(Fig. 6a)**, indicating that the TGF-β/Smad2 axis was functionally impaired in mutant cells. This data suggests that the expression of TGF-β-induced genes in TMEM165-knockout cells would also be downregulated. To test this, the mRNA levels of the serpine 1 (PAI-1) gene, which is positively correlated with TGF-β signaling activation were examined. As expected, serpine1 mRNA levels were significantly lower in cells knocked down for TMEM165 compared to wild-type cells **(Fig. 6b),** therefore indicating that the loss of TMEM165 perturbs TGF-β signaling in mutant cells. These data were further confirmed by transfecting the p(CAGA)12-luc reporter plasmid into TMEM165-deficient and wild-type cells. This plasmid contains a firefly luciferase gene, located downstream of a TGF-β-responsive promoter derived from serpine1 gene. Therefore, the luciferase activity is a measure of TGF-β signaling. The data showed that the luciferase activity was markedly (7-fold) lower in mutant cells, compared to wild-type cells confirming that the TGF-β/Smad axis is functionally impaired in TMEM165-knockout cells **(Fig. 6c)**.

To determine whether this is also the case in fibroblast cells from CDG patient, we evaluated the phosphorylation status of Smad2 in normal fibroblasts and TMEM165-deficient fibroblasts from CDG patient. As shown in **figure 6d**, phospho-Smad2 level was reduced in TMEM165-deficient fibroblasts compared to normal fibroblasts, whereas total Smad2 level was not affected, indicating that the TGF-β/Smad2 axis was functionally impaired in fibroblast mutant cells. Analysis of the expression of serpine1 gene used as a marker for TGF-β signaling activation showed significant (2-fold) downregulation **(Fig. 6e)**, indicating that TMEM165 deficiency impairs the expression of the TGF-β/Smad downstream responsive genes in fibroblasts of CDG patient.

To determine whether response to TGF-β stimulation is affected in mutant cells, phosphorylation level of Smad2 in response to TGF-β was examined. As shown in **figure 6f**, treatment of TMEM165-knockout ATDC5 cells with TGF-β induced the phosphorylation of

Smad2, however the level of phospho-Smad2 is lower compared to that observed in wild-type cells, indicating that mutant cells were less responsive to TGF-β than wild-type cells. To find out if this is also the case in CDG patient fibroblasts, both normal and TMEM165-deficient fibroblast cells were stimulated with TGF-β and the phosphorylation status of Smad2 was analyzed by Western-blot. The results showed that the level of phospho-Smad2 in TMEM165-mutant fibroblasts was reduced compared to normal fibroblasts **(Fig. 6g).** Altogether, these results showed that both the baseline and TGF-β-induced levels of phospho-Smad2 were significantly reduced in mutant cells, therefore revealing for the first time that TMEM165 deficiency functionally impaired the TGF-β/Smad2 signaling axis. To identify the mechanism involved in the alteration of the TGF-β/Smad signaling pathway, we investigated the mRNA expression levels of TGF-β receptors, TGFβR1 and TGFβR2 in TMEM165-knockout and wild-type ATDC5 cells. As shown in **figure 6h** a slight decrease in the mRNA levels of TGFβR1 associated to a significant decrease in mRNA levels of TGFβR2 was observed by RT-qPCR in TMEM165-mutant ATDC5 cells, compared to wild-type. To determine whether changes in TGFβR2 mRNA expression reflect changes in the protein expression, TGFβR2 protein expression was assessed by immunoblotting. Consistent with RT-qPCR data, significant reduction in the protein level of TGFβR2 was observed in TMEM165-knockout ATDC5 cells, compared to wild-type cells **(Fig. 6i).** Interestingly, strong decrease in the mRNA levels of TGFβR2 was observed in TMEM165-deficient CDG-patient fibroblasts compared to normal fibroblasts, whereas no significant changes were observed in the mRNA levels of TGFβR1 (**Fig. 6j**). Western blot analysis of the expression of TGFβR2 protein confirmed the mRNA data and showed dramatical decrease in the expression of the receptor (**Fig. 6k**). These data revealed that TMEM165 deficiency led to decreased expression of the TGF-β receptor, TGFβR2 which may account for downregulation of TGF-β signaling in TMEM165-deficient cells. Downregulation of TGF-β signaling may also result from up-regulation of negative regulators

such as asporin, an extracellular protein that suppresses TGF-β signaling by direct interaction with TGF-β thus preventing its binding to TGFβR2. Therefore, we sought to determine whether TMEM165 deficiency affects the expression of asporin. Analysis of mRNA levels of asporin in TMEM165-knockout ATDC5 cells and in fibroblasts from CDG patient showed a remarkable increase (4-fold) in the expression of asporin in mutant cells compared to normal cells **(Fig. 6l).** Assessment of asporin protein expression by immunoblot showed higher levels of expression in TMEM-deficient ATDC5 and CDG patient fibroblast cells, compared to normal cells **(Fig. 6m).** Therefore, these results showed that expression of asporin was significantly upregulated in TMEM165-deficient cells. Altogether, these data support the notion that impaired TGF-β signaling in TMEM165-deficient cells is associated with downregulation of the expression of TGFβR2 receptor and upregulation TGF-β signaling antagonist, asporin.

BMP signaling plays a key role in skeletal development and alterations in BMP signaling pathway are major underlying cause of human skeletal disorders [14]. BMP signaling relies on secreted ligands and on a type I and type II BMP receptors that activate downstream mediators, notably the canonical SMAD pathway. To determine whether TMEM165 deficiency affects BMP signaling, we examined the phosphorylation status of Smad 1,5,9 downstream mediators of BMP receptor activation. Interestingly, immunoblot analysis showed that the level of phospho-Smad 1,5,9 (pSmad1,5,9) was higher in TMEM165-knockout ATDC5 cells, compared to wild-type cells **(Fig. 7a)**. This result was confirmed in fibroblast cells from CDG patient which showed increased level of phospho-Smad 1,5,9 compared to normal fibroblasts **(Fig. 7b)**. Therefore, these data revealed that deficiency in TMEM165 functionally impairs BMP/Smad signaling leading to activation of the signaling pathway. Indeed, analysis of the mRNA levels of *Id1* gene, a BMP downstream target gene, showed two-fold increase in TMEM165-knockout cells, compared to wild-type cells **(Fig. 7c).** To further confirm the

increase of BMP signaling in TMEM165-knockout cells, a BMP signaling reporter vector pGL3-BRE-Luc containing a BMP responsive promoter element (BRE) was used to transfect wild-type and TMEM165-mutant ATDC5 cells. As shown in **figure 7d**, analysis of luciferase activity, which is a measure of BMP signaling, showed a significant increase (4-fold) in TMEM165-knockout ATDC5 cells compared to wild-type cells**,** thus bringing evidence that BMP signaling is activated in TMEM165-mutant cells. In an attempt to identify the mechanism involved in the alteration of the BMP/Smad signaling pathway, we investigated the mRNA levels of type I and type II BMP receptors *ie.* BMPR1A (ALK3), BMR1B (ALK6) and BMPR2 by RT-qPCR in TMEM165-deficient and wild-type cells. As shown in **figure 7e**, mRNA levels of BMP receptors were increased in TMEM165-knockout ATDC5 cells, compared to wild-type cells with BMPR1B showing the highest increase (2-fold). The increased expression of BMPR2 at the protein level was confirmed by Western blot analysis in mutant cells using cell lysates of wild-type and TMEM165-knockout ATDC5 cells **(Fig. 7f)**. Similar results were observed, either for mRNA expression levels of BMPR1A, BMR1B and BMPR2 **(Fig. 7g)** or for BMPR2 protein expression **(Fig. 7h)** in TMEM165-deficient CDG patient fibroblast cells, compared to normal fibroblast cells. Upregulation of the expression of BMP receptors may therefore account for increased BMP signaling in TMEM165-mutant cells. It is also well known that BMP signaling is regulated by ligand antagonists such as noggin that antagonizes the signaling by directly binding BMP proteins thereby preventing receptor activation. Therefore, to determine if the expression of noggin is altered in TMEM165-deficient cells, mRNA levels of *NOG* gene was assessed by RT-qPCR in TMEM165-knockout and wild-type ATDC5 cells. As shown in **figure 7i** mRNA expression level of noggin was significantly reduced in TMEM165-mutant ATDC5 cells, compared to wild-type cells. Similar results were observed in TMEM165-deficient fibroblasts from CDG patient, compared to normal fibroblast cells **(Fig. 7j)**. These data raise the possibility that downregulation of expression of the BMP antagonist noggin may

participate to the increased BMP signaling observed in mutant cells. Altogether, these data revealed that BMP signaling is upregulated in TMEM165-deficient cells and may be a result of increased expression of BMP receptors and decreased expression of BMP antagonist. Overall, this study showed that TMEM165 deficiency led to downregulation of TGF-β/Smad2 and upregulation of BMP/Smad 1,5,9 axes and thus functionally impairs these signaling pathways in TMEM165-deficient cells.

TMEM165 deficiency accelerates cell proliferation

Chondrogenesis is a well-coordinated multi-step differentiation process in which chondrocytes proliferate to produce terminally differentiated hypertrophic chondrocytes. Owing to the role of GAG chains and of TGF-β in the regulation of cell proliferation prompted us to investigate whether proliferation was affected in mutant cells. To this end, proliferation of TMEM 165-knockout ATDC5 and of fibroblasts cells from CDG patient was measured using CyQUANT Cell Proliferation Assay Kit. As shown in **figure 8a**, the proliferation rate in TMEM165-knockout ATDC5 and TMEM165-deficient fibroblast cells was significantly increased (1.5-fold) compared to normal cells, therefore indicating that TMEM165 deficiency promotes cell proliferation. Accordingly, analysis of the activation status of extracellular signal-regulated kinase (ERK) 1/2 mitogen-activated protein (MAP) kinase pathway, that plays a central role in cell proliferation control, showed higher level of activation in TMEM165-mutant ATDC5 and fibroblast cells from CDG patient compared to normal cells (**Fig. 8b).** Indeed, phospho-ERK1/2 (pERK1/2) levels but not total ERK1/2 levels were strongly increased in TMEM165-deficient ATDC5 and TMEM165-mutant fibroblast cells compared to normal cells **(Fig. 8b)**, indicating a sustained activation of ERK1/2 signaling pathway that may promote proliferation in mutant cells.

TMEM165 deficiency promotes chondrocyte differentiation towards hypertrophic phenotype

The long bones of mammals are formed by endochondral ossification process that involves the formation of a cartilaginous draft in which the chondrocytes undergo a maturation process before being replaced by a mature bone. Chondrogenesis process is tightly regulated during skeletal development and alterations in the chondrocyte maturation result in defects in endochondral bone development. To investigate whether chondrogenic differentiation of ATDC5 cells is affected in the absence of TMEM165, wild-type and TMEM165-knockout ATDC5 cells were induced by insulin into chondrogenic differentiation and the mRNA levels of chondrogenic markers including Sox9, Col2a1, AGN, Ihh and OCN were measured by RT-qPCR before induction and at seven days post-induction. The results showed that before induction (day 0), compared to wild-type, ATDC5-knockout cells express higher mRNA levels of the chondrogenic markers Sox9, Col2a1 and AGN and lower mRNA levels of pre-hypertrophic and hypertrophic markers Ihh and OCN (**Fig. 9a and 9b (day 0))**. These results indicate that loss of TMEM165 expression induces chondrogenic differentiation of prechondrogenic ATDC5 cells. Importantly, analysis of the expression of the markers at seven days post-induction revealed that TMEM165-deficient ATDC5 cells undergo rapid maturation as evidenced by downregulation of chondrogenic markers Sox9, Col2a1, AGN and upregulation of pre-hypertrophic and hypertrophic markers Ihh and OCN. In contrast, in wild-type cells the chondrogenic markers were up-regulated and pre-hypertrophic and hypertrophic markers were down regulated at seven days post-induction **(Fig. 9a and 9b (day7)).** Altogether, these data bring evidence that TMEM165 deficiency promotes premature chondrocyte maturation, a process which affects endochondral ossification and may lead to dwarfism.

Discussion

PGs are formed by the covalent attachment of GAG chains onto the core protein. Unlike DNA/RNA and proteins, the synthesis of GAG chains is not template derived, they are synthesized by stepwise addition of sugar units by various glycosyltransferases. It has been established that GAG chains of PGs are responsible for most functions of PGs [15–17]. Owing to their position in ECM, pericellular region and cell surface PGs play a key role in ECM structure and organization, cell signaling, adhesion and proliferation. They also act as co-receptors for several ligands and regulate the bioavailability of growth factors. TMEM165 protein is involved in CDG although the functions are unknown so far, but it is established that the TMEM165-deficient CDG patients present bone abnormalities, suggesting potential involvement of TMEM165 in chondrogenesis and bone homeostasis [4]**.** On the other hand, it is established that defects in the synthesis of GAG chain of PGs due to genetic mutations of glycosyltransferases led to skeletal defects. Indeed, mutations in glycosyltransferase genes involved in elongation of GAG chains including *EXT1*/*EXT2* genes encoding HS are known to cause hereditary multiple exostoses [18] and mutations in *CHSY1/CHSY2* genes encoding CS polymerising enzymes cause skeletal defects, growth retardation and dwarfism [19]. Similarly, mutations in glycosyltransferase genes involved in the synthesis of the tetrasaccharide primer including *β4GALT7* gene that encodes β4-galactosyltransferase 7 cause defects in CS chains resulting in Ehlers-Danlos syndrome (EDS) progeroid form characterized by delayed development, premature aging, short stature and generalised osteopenia [20] and mutations in *β3GAT3* gene encoding for β1,3-glucuronosyltransferase I cause Larsen-like syndrome with congenital heart defects and joint dislocations [21]. Therefore, HS and CS biosynthetic enzymes are crucial to bone development and skin integrity in humans. Here, we generated TMEM165-knockout pre-chondrocyte ATDC5 and HEK293 cells and showed that loss of TMEM165 led to strong decrease in the synthesis of PGs. Decrease content of PGs in cartilage was also reported in TMEM165-deficient

zebrafish [22]. Importantly, we showed a dramatical reduction in the length of HS- and CS-GAG chains, revealing for the first time that elongation of PG-GAG chains is impaired in TMEM165-deficient cells. Evaluation of mRNA levels of genes encoding enzymes involved in formation of tetrasaccharide linker region including β4Galt7, β3GalT3, β3Galt6, XT1 and XT2, and enzymes involved in polymerisation of GAG chains *ie.* EXTL3, EXT1, EXT2, CHSY1 and CHSY2 showed that the mRNA levels were not significantly disturbed in TMEM165-deficient cells. We also showed that overexpression of CS elongating enzymes CHSY1 and CHSY2 did not rescue the elongation of CS-GAG chains using either decorin or 4MU-xyloside as substrates, thus confirming that defect in GAG synthesis was not due to lack of expression of the polymerizing enzymes. Supplying cells with xylose and galactose monosaccharides did not overcome the blockage in the polymerization process. In the other hand, Golgi glycosyltransferases use UDP-sugars as a donor substrate and require Mn^{2+} at their catalytic site to be fully active. Deficiency of Mn^{2+} results in birth defects including abnormal or poor bone formation and susceptibility to seizures [23–25]**.** Mutations in SLC39A8 a plasma membrane protein able to transport Mn^{2+} are characterized by low blood levels of Mn^{2+} associated with reduced activity of the β-1,4galactosyltransferase and Mn superoxide dismutase (MnSOD) leading to congenital disorders of glycosylation type 2N (CDG2N) with multiple signs including delayed development, dwarfism, profound psychomotor retardation, and hearing loss [26,27]. Remarkably, we found that Mn^{2+} supplementation increases the size of CS-attached decorin and HS-attached syndecan 4 in TMEM165-knockout cells and therefore support the notion that Mn^{2+} restores polymerization of CS-GAG and HS-GAG chains in TMEM165-deficient cells. These findings revealed that TMEM165 plays an essential role in the synthesis of PGs by regulating homeostasis of Mn^{2+} in the Golgi compartment. Indeed, elongation process of GAG chains takes place in the Golgi compartment and Mn^{2+} is required for full activity of GAG polymerizing enzymes. We can therefore hypothesize that GAG chains are

aborted because of lack of sufficient pool of the cofactor Mn^{2+} in the Golgi necessary for the synthesis of normal GAG chains. In line with this, we clearly showed that decorin produced in TMEM165-knockout cells is sensitive to degradation by chondroitinase ABC indicating that CS-GAG chains are elongated but to small extent, compared to wild-type cells. How Mn^{2+} supplementation rescue GAG chains elongation is not known, however we previously showed that the rescue of Golgi *N*-glycosylation defects in TMEM165-deficient cells by extracellular Mn^{2+} involves a transit across the ER compartment and the activity of thapsigargin and cyclopiazonic acid-sensitive pumps, probably the SERCA pumps [28].

Noteworthy that GDT1, a yeast ortholog of TMEM165 has been shown to be involved in Ca^{2+} homeostasis [29]. Increased phosphorylation of CaMkIIα in TMEM165-knockout ATDC5 cells and in TMEM165-deficient fibroblasts form CDG patient suggests that intracellular Ca^{2+} level is increased in TMEM165-mutant cells. These data indicate that TMEM165 is involved in the regulation of the homeostasis of Ca^{2+} in addition to that of Mn^{2+}.

Analysis of BMP and TGF-β signaling pathways revealed that they are functionally impaired in TMEM165-deficient cells. TGF-βs and BMPs play an important role in several stages of chondrogenesis. It has been reported that TGF-β inhibits the terminal differentiation of chondrocytes in high-density chondrocyte pellets or long bone cultures *in vitro* [30]. We found that TMEM165 deficiency led to down regulation of TGF-β signaling associated with downregulation of TGF-β receptor, TGFβRII and upregulation of TGF-β antagonist, asporin. We showed that the TGF-β signaling was activated when the cells were exogenously treated with TGF-β1 but at lower extent compared to wild-type cells, indicating that both basal and inducible TGF-β signaling activation is impaired in TMEM-165-deficient cells, this may be due to the downregulation of TGFβRII receptor but not only. Indeed, asporin has been shown to suppress TGF-β signaling by direct binding of the cytokine in the ECM, thus preventing its interaction with the receptor. Interestingly, our study clearly showed that TMEM165 deficiency

resulted in significant upregulation of asporin protein expression, suggesting a role in downregulation of both basal and inducible activation of TGF-β/Smad signaling pathway in TMEM165-deficient cells. TGF-β activates Smad2 and Smad3 through binding to TGFβRII receptor and recruitment of ALK5 receptor (TGFβRI) [31]**.** Noteworthy, mice lacking TGFβRII or ALK5 in chondrocytes exhibit skeletal defectsand inhibition of TGFβ signaling induces chondrocyte hypertrophy [13]**.**

We have analyzed the BMP signaling pathway and found that phospho-Smad1,5,9 was upregulated in TMEM165-deficient cells, compared to normal cells, indicating that this pathway is activated in mutant cells. Investigation of the mechanisms involved revealed that the BMP receptors BMPR2 and BMPR1B are upregulated in mutant cells. In addition to that, expression of *NOG* gene, a BMP antagonist is downregulated in TMEM165-deficient cells which may account for upregulation of BMP/Smad1,5,9 signaling. Noteworthy, BMP regulates longitudinal growth and excessive BMP signaling has been shown to accelerate chondrogenesis and chondrocyte differentiation [14,32,33]. Brachydactylies type 2 (BDB2) is a *NOG* mutation characterised by absence of terminal structures of the toes and digits due to excessive BMP signaling [34]. Mutations in *NOG* cause inability of the antagonist to bind BMP or heparin and to sequester BMPs in ECM which results in excessive BMP signaling [35,36] **.**

The increased levels of hypertrophic marker Ihh and osteocalcin in TMEM165-knockout prechondrocyte ATDC5 cells during differentiation process may lead to early hypertrophy of chondrocytes. Overexpression of Ihh induces early chondrocyte hypertrophy and ossification during chondrogenesis. It has been suggested that TGFβ inhibits hypertrophy induced by Ihh [37]. Our study has shown that TGF-β signaling is downregulated and Ihh is upregulated in TMEM165-mutant ATDC5 cells, suggesting accelerated chondrocyte hypertrophy that may lead to early ossification and defects in skeletal development.

Our findings indicate that TMEM165 deficiency causes abnormalities in PG synthesis and aberrant signaling that resulted in early chondrocyte maturation. PGs and their GAG chains are key components of the ECM and are involved in the organization and function of the matrix. Alterations in the structure of GAG chains may induce profound changes in the organization and function of the ECM and hence in cell-matrix interactions and signaling leading to defects in endochondral ossification process.

Materials and Methods

Cell culture and treatments

ATDC5 cells (Riken cell, Tsukubai, Japan) and HEK293 cells (ATCC, LGC Standards, France) were cultured in DMEM-F12 complete medium (2 mM glutamine, 100 μg/ml streptomycin, 100 IU/ml penicillin and 5% (v/v) foetal bovine serum for ATDC5 cells and 10% (v/v) for HEK293) at 37°C in a humidified atmosphere supplemented with 5% CO_2. Cells were seeded onto six-well plates at 2×10^5 cells/well and allowed to attach overnight in standard culture conditions. For treatment with growth factors, ATDC5 cells were cultured in DMEM F12 complete medium until reaching 80% confluency then the medium was replaced with DMEM-(F12 without FBS and containing 1 ng/ml of TGF-β1 (R&D Systems, Minneapolis, MN USA) or vehicle (0.1% BSA in PBS) for 1h. Cells were then washed twice with PBS and stored at -80°C prior to protein or gene expression analyses. For chondrogenic differentiation, ATDC5 cells were seeded in 12 well/plate at 4×10^4 cells/well and cultured in DMEM-F12 complete medium containing 50 mg/ml human transferrin and 3×10^{-8} M sodium selenite (Sigma, Saint Louis, MO) until confluency (day 0), then chondrogenesis was induced by addition of 100 mg/ml of human insulin (Sigma, Saint Louis, MO) in the culture medium. The medium was replaced every day for 7 days (Day 7). Cells were washed twice with PBS and stored at -80°C prior to protein or gene expression analyses.

Gene expression analysis

Total RNA from cells was extracted using TRIzol (Lifetech, Carlsbad, CA) and purified with RNeasy kit (Qiagen, Hilden, Germany) according to manufacturer's instructions. The reverse transcription was performed using 500 ng of total RNA from each sample with iScript Ready to use cDNA supermix (BIO-RAD, Hercules, CA). Quantitative PCR was performed with iTaq™ Universal SYBER Green Supermix kit (BIO-RAD, Hercules, CA) using StepOnePlus™ Real-Time PCR Systems (Applied Biosystems, Foster city, CA). Primer sequences are listed in Table S1.

Metabolic labeling of GAG chains

Metabolic labeling of GAG chains of PGs was carried out using [^{35}S]-sulfate incorporation method as described by [38]. Briefly, subconfleunt ATDC5 cells grown in 6-well culture plate were radiolabeled with 10 µCi/ml of [^{35}S]-sulfate (Perkin Elmer, Courtabœuf, France) overnight. Then, conditioned culture medium was collected, digested with papain (1mg/ml) and [^{35}S]-labeled GAGs were precipitated by cetylpyridinium chloride (CPC) as described by [39]. When GAG chains were primed by 4MU-Xyl, cells were cultured in the presence of 10 µCi/ml of [^{35}S]-sulfate and 100 µM of 4MU-Xyl overnight and radiolabeled GAG chains were directly precipitated from conditioned medium by CPC. The CPC precipitated radiolabeled GAGs were separated by SDS-PAGE on a 4-20% Tris/Glycine gel. The gel was dried and exposed to autoradiography film.

To measure the rate of sulfate incorporation into GAG chains of PGs, ATDC5 cells were radiolabeled with 10 µCi/ml of [^{35}S]-sulfate for 6 h then, conditioned culture medium was collected and digested with papain (1mg/ml). [^{35}S]-labeled GAG chains were precipitated by CPC dissolved in solvable and mixed in scintillation fluid (Perkin Elmer, MA, USA). The

radioactivity associated with GAGs was measured by liquid scintillation counting (Packard, Rungis, France).

Indirect immunofluorescence staining

The ATDC5 cells were grown on glass coverslips and fixed with 4% (w/v) paraformaldehyde in PBS for 20 min. Cells were permeabilized by treatment with 0.1% (w/v) Triton X-100/PBS solution for 4 min. After extensive washing in 0.2% (w/v) fish skin gelatin in PBS, cells were then incubated with primary antibodies anti-TMEM165 (1:100, Sigma, Saint Louis, MO) for 20 min. Cells were washed several times in 0.2% (w/v) fish skin gelatin in PBS and incubated with secondary antibodies coupled with Alexa Fluor 488 (ThermoFisher, France) for 20 min. Cells were washed with 0.2% (w/v) fish skin gelatin in PBS and incubated with primary antibodies anti-GM130 (1:100, Sigma, Saint Louis, MO) for 20 min. Cover slips were then washed several times in 0.2% (w/v) fish skin gelatin in PBS and incubated with secondary antibodies coupled with Alexa Fluor 555 for 20 min. Cells were washed with PBS and nuclei were stained with Hoechst/PBS solutions then coverslips were mounted with Moviol (National Diagnostics, U.K.) containing 1% propylgallate (Sigma, Saint Louis, MO). Digital images were captured with an inverted microscope Lieca DMI3000 B (Leica Microsystems, Germany).

CRISPR/Cas9 mutation of TMEM165 gene

Sense 5'**CACC**GCTATAACCGGCTGACTGTGC3' and antisense 5'**AAAC**GCACAGTCAG CCGGTTATAGC3' oligonucleotides (1 μg) containing 20 bp sequence (underlined) targeting TMEM165 exon 2 and cohesive ends (bold) with the vector were annealed in annealing buffer (60 mM Tris-HCl, pH7.5; 500 mM NaCl; 60 mM $MgCl_2$; 10 mM DTT) and ligated into BbsI sites of pUC57-attbU6 sgRNA vector. This vector is a basic vector with U6 promoters and improved Cas9 binding sites. 1 μg of pUC57-TMEM165, 100 ng of SVneo vector (that confer

resistance to geneticin) and 1 μg of pSpCas-9 vector were used to transfect ATDC5 cells grown at 80% confluency in six wells/plate, using Lipofectamine 2000© (Invitrogen, Carlsbad, CA) according to the instructions of the supplier. 24 h after transfection, the medium was replaced by medium containing 0.2 mg/ml geneticin sulfate and cells were cultured for 48 h before trypsinized and cloning by serial dilution in 96 wells/plate. Several clones were obtained and amplified in six wells/plates and analyzed for the presence of mutations in the targeted sequence by PCR amplification and sequencing of the genomic DNA flanking the targeted region.

Plasmids

Chsy1, Chsy2, Decorin and HA-syndecan 4 cDNAs were generated by PCR and cloned into EcoRI and BamHI or SmaI and PstI sites of pCMV empty vector (Stratagene, Valencia, CA). Decorin-S34A mutant was generated by site directed mutagenesis using QuikChange XLII (Agilent, CA, USA) according to manufacturer's instructions.

Transfection

Cells were seeded in 6-well culture plate until 80% confluency and transfected with 1 μg of either pCMV-Decorin, pCMV-HA-Syndecan 4, pCMV-Decorin-S34A, pCMV-Myc-Chsy1, pCMV-HA-Chsy2 or pCMV-empty vector using lipofectamine 2000 transfection reagent (Invitrogen, Carlsbad, CA) according to manufacturer's instructions. Expression of decorin in culture medium and of syndecan 4 in cell lysate was analyzed at 48 h post-transfection by Western blotting.

TGF-β and BMP luciferase reporter activity assays

p(CAGA)12-luc and pGL3-BRE-Luc Wild-type and TMEM165-knockout ATDC5 cells were plated onto twenty-four-well plates and grown to 80% confluency. Cells were transfected with

500 ng of p(CAGA)12-luc and pGL3-BRE-Luc promoter constructs, respectively along with 25 ng of pRL-TK vector (Promega, Madison, WI) using. Twenty-four hours after transfection, Firefly and Renilla luciferase activities in cells of each well were measured with the Dual-Luciferase Assay System (Promega) using a Berthold (Bad Wildbad, Germany) luminometer. Luciferase activities were normalized to pRL-TK vector activity.

Western Blotting

Total protein from cells was extracted using RIPA buffer (150 mM NaCl, 50 mM Tris-HCl, pH 7.5, 1% deoxycholate, 0.1% SDS, 1% Triton X-100) supplemented with protease and phosphatase inhibitors (Roche Diagnostics, Indianapolis, IN, USA). Cell lysates were sonicated on ice and protein concentration of the samples was determined by the Bradford method. Proteins (50 μg/lane) were separated on 10% SDS-PAGE gels, transferred to a PVDF membrane (Millipore, Eschborn, Germany), and subsequently blocked in PBS-Tween 20 containing 5% nonfat milk or 5% BSA. Membranes were then incubated overnight with primary antibodies directed against TMEM165 (diluted 1:1000, Sigma, Saint Louis MO), decorin (diluted 1:1000, R&D, Mineapolis, MN), HA (diluted 1:1000, Biolegend, San Diego, CA), Myc, Smad2, pSmad2, Smad1, pSmad1,5,9, CaMKIIα, pCaMKIIα, p44/42 MAPK, phospho-p44/42, β-actin, (diluted 1:1000; Cell signaling, Danvers, USA), asporin (diluted 1:1000, Sigma, Saint Louis MO), TGFβR2 or BMPR2 (diluted 1:1000, GenTex, Zeeland, MI) followed by incubation with horseradish peroxidase-conjugated secondary antibodies (diluted 1:2000, Cell signaling). Antibodies were diluted in 5% BSA/0.01% tween 20 in PBS. The blots were then developed using Clarity Western ECL substrate (BIO-RAD, Hercules, CA) according to the instructions of the manufacturer.

Data Analysis and Statistical Procedures

Each experiment was repeated at least three times independently. Quantitative data were expressed as mean ± S.D. Statistical analysis was performed with an unpaired two-tailed Student's t-test, and effects were considered statistically significant at $*P<0.05$. One representative immunoblot of three independent experiments was shown in results.

Affiliation

UMR7365 CNRS-University of Lorraine, Biopôle, Faculty of Medicine, Vandoeuvre-lès-Nancy, France

UMR8576 CNRS-University of Lille, Lille, France.

Acknowledgements

This work was supported by the Agence Nationale de la Recherche (ANR: Solv-CDG), S.K. was supported by Pakistan Higher Education Commission fellowship.

Conflict of Interest. The authors declare no competing financial interests.

References

1 Varki A. Biological roles of oligosaccharides: all of the theories are correct. *Glycobiology* 1993; **3**: 97–130.

2 Sharon N, Lis H. Carbohydrates in Cell Recognition. *Sci Am* 1993; **268**: 82–89.

3 Demaegd D, Foulquier F, Colinet AS, Gremillon L, Legrand D, Mariot P *et al.* Newly characterized Golgi-localized family of proteins is involved in calcium and pH homeostasis in yeast and human cells. *Proc Natl Acad Sci U S A* 2013; **110**: 6859–6864.

4 Foulquier F, Amyere M, Jaeken J, Zeevaert R, Schollen E, Race V *et al.* TMEM165 deficiency causes a congenital disorder of glycosylation. *Am J Hum Genet* 2012; **91**: 15–26.

5 Snyder NA, Stefan CP, Soroudi CT, Kim A, Evangelista C, Cunningham KW. H+ and Pi byproducts of glycosylation affect Ca2+ homeostasis and are retrieved from the Golgi complex by homologs of TMEM165 and XPR1. *G3 Genes, Genomes, Genet* 2017; **7**: 3913–3924.

6 Potelle S, Morelle W, Dulary E, Duvet S, Vicogne D, Spriet C *et al.* Glycosylation abnormalities in Gdt1p/TMEM165 deficient cells result from a defect in Golgi manganese homeostasis. *Hum Mol Genet* 2016; **25**: 1489–1500.

7 Domowicz MS, Cortes M, Henry JG, Schwartz NB. Aggrecan modulation of growth plate morphogenesis. *Dev Biol* 2009; **329**: 242–257.

8 Hilton MJ, Gutiérrez L, Martinez DA, Wells DE. EXT1 regulates chondrocyte proliferation and differentiation during endochondral bone development. *Bone* 2005; **36**: 379–386.

9 Watanabe Y, Takeuchi K, Higa Onaga S, Sato M, Tsujita M, Abe M *et al.* Chondroitin sulfate N-acetylgalactosaminyltransferase-1 is required for normal cartilage development. *Biochem J* 2010; **432**: 47–55.

10 Wilson DG, Phamluong K, Lin WY, Barck K, Carano RAD, Diehl L *et al.* Chondroitin sulfate synthase 1 (Chsy1) is required for bone development and digit patterning. *Dev Biol* 2012; **363**: 413–425.

11 Yada T, Gotoh M, Sato T, Shionyu M, Go M, Kaseyama H *et al.* Chondroitin Sulfate

Synthase-2. *J Biol Chem* 2003; **278**: 30235–30247.

12 Yada T, Sato T, Kaseyama H, Gotoh M, Iwasaki H, Kikuchi N *et al.* Chondroitin Sulfate Synthase-3. *J Biol Chem* 2003; **278**: 39711–39725.

13 Wu M, Chen G, Li Y-P. TGF-β and BMP signaling in osteoblast, skeletal development, and bone formation, homeostasis and disease. *Bone Res* 2016; **4**: 16009.

14 Salazar VS, Gamer LW, Rosen V. BMP signalling in skeletal development, disease and repair. *Nat Rev Endocrinol* 2016; **12**: 203–221.

15 Couchman JR. Transmembrane Signaling Proteoglycans. *Annu Rev Cell Dev Biol* 2010; **26**: 89–114.

16 Manon-Jensen T, Itoh Y, Couchman JR. Proteoglycans in health and disease: The multiple roles of syndecan shedding. FEBS J. 2010; **277**: 3876–3889.

17 Gesslbauer B, Theuer M, Schweiger D, Adage T, Kungl AJ. New targets for glycosaminoglycans and glycosaminoglycans as novel targets. Expert Rev. Proteomics. 2013; **10**: 77–95.

18 McCormick C, Leduc Y, Martindale D, Mattison K, Esford L, Dyer A *et al.* The putative tumour suppressor EXT1 alters the expression of cell-surface heparan sulfate. *Nat Genet* 1998; **19**: 158–161.

19 Mizumoto S, Ikegawa S, Sugahara K. Human genetic disorders caused by mutations in genes encoding biosynthetic enzymes for sulfated glycosaminoglycans. *J Biol Chem* 2013; **288**: 10953–10961.

20 Okajima T, Fukumoto S, Furukawa K, Urano T, Furukawa K. Molecular Basis for the Progeroid Variant of Ehlers-Danlos Syndrome. *J Biol Chem* 1999; **274**: 28841–28844.

21 Baasanjav S, Al-Gazali L, Hashiguchi T, Mizumoto S, Fischer B, Horn D *et al.* Faulty Initiation of Proteoglycan Synthesis Causes Cardiac and Joint Defects. *Am J Hum Genet* 2011; **89**: 15–27.

22 Bammens R, Mehta N, Race V, Foulquier F, Jaeken J, Tiemeyer M *et al.* Abnormal cartilage development and altered N-glycosylation in Tmem165-deficient zebrafish mirrors the phenotypes associated with TMEM165-CDG. *Glycobiology* 2015; **25**: 669–682.

23 Milatovic D, Gupta RC, Yin Z, Zaja-Milatovic S, Aschner M. Manganese. In:

Reproductive and Developmental Toxicology. Elsevier, 2017, pp 567–581.

24 Aschner M, Shanker G, Erikson K, Yang J, Mutkus LA. The Uptake of Manganese in Brain Endothelial Cultures. *Neurotoxicology* 2002; **23**: 165–168.

25 Aschner M. Manganese: Brain transport and emerging research needs. *Environ Health Perspect* 2000; **108**: 429–432.

26 Boycott KM, Beaulieu CL, Kernohan KD, Gebril OH, Mhanni A, Chudley AE *et al.* Autosomal-Recessive Intellectual Disability with Cerebellar Atrophy Syndrome Caused by Mutation of the Manganese and Zinc Transporter Gene SLC39A8. *Am J Hum Genet* 2015; **97**: 886–893.

27 Park JH, Hogrebe M, Grüneberg M, DuChesne I, von der Heiden AL, Reunert J *et al.* SLC39A8 Deficiency: A Disorder of Manganese Transport and Glycosylation. *Am J Hum Genet* 2015; **97**: 894–903.

28 Houdou M, Lebredonchel E, Garat A, Duvet S, Legrand D, Decool V *et al.* Involvement of thapsigargin- And cyclopiazonic acid-sensitive pumps in the rescue of TMEM165-associated glycosylation defects by Mn2+. *FASEB J* 2019; **33**: 2669–2679.

29 Colinet AS, Sengottaiyan P, Deschamps A, Colsoul ML, Thines L, Demaegd D *et al.* Yeast Gdt1 is a Golgi-localized calcium transporter required for stress-induced calcium signaling and protein glycosylation. *Sci Rep* 2016; **6**. doi:10.1038/srep24282.

30 Ballock RT, Heydemann A, Wakefield LM, Flanders KC, Roberts AB, Sporn MB. TGF-β1 Prevents Hypertrophy of Epiphyseal Chondrocytes: Regulation of Gene Expression for Cartilage Matrix Proteins and Metalloproteases. *Dev Biol* 1993; **158**: 414–429.

31 Derynck R, Zhang YE. Smad-dependent and Smad-independent pathways in TGF-β family signalling. *Nature* 2003; **425**: 577–584.

32 Freire-Maia N, Maia NA, Pacheco CNA. Mohr-Wriedt (A_2) Brachydactyly. *Hum Hered* 1980; **30**: 225–231.

33 Dathe K, Kjaer KW, Brehm A, Meinecke P, Nürnberg P, Neto JC *et al.* Duplications Involving a Conserved Regulatory Element Downstream of BMP2 Are Associated with Brachydactyly Type A2. *Am J Hum Genet* 2009; **84**: 483–492.

34 Lehmann K, Seemann P, Silan F, Goecke TO, Irgang S, Kjaer KW *et al.* A New

Subtype of Brachydactyly Type B Caused by Point Mutations in the Bone Morphogenetic Protein Antagonist NOGGIN. *Am J Hum Genet* 2007; **81**: 388–396.

35 Pang X, Wang Z, Chai Y, Chen H, Li L, Sun L *et al.* A Novel Missense Mutation of NOG Interferes With the Dimerization of NOG and Causes Proximal Symphalangism Syndrome in a Chinese Family. *Ann Otol Rhinol Laryngol* 2015; **124**: 745–751.

36 Masuda S, Namba K, Mutai H, Usui S, Miyanaga Y, Kaneko H *et al.* A mutation in the heparin-binding site of noggin as a novel mechanism of proximal symphalangism and conductive hearing loss. *Biochem Biophys Res Commun* 2014; **447**: 496–502.

37 Chen L, Liu G, Li W, Wu X. Chondrogenic differentiation of bone marrow-derived mesenchymal stem cells following transfection with Indian hedgehog and sonic hedgehog using a rotary cell culture system. *Cell Mol Biol Lett* 2019; **24**: 1–16.

38 de Vries BJ, van den Berg WB, Vitters E, van de Putte LBA. Quantitation of glycosaminoglycan metabolism in anatomically intact articular cartilage of the mouse patella: in vitro and in vivo studies with 35S-sulfate, 3H-glucosamine, and 3H-acetate. *Rheumatol Int* 1986; **6**: 273–281.

39 Bronson RE, Bertolami CN, Siebert EP. Modulation of Fibroblast Growth and Glycosaminoglycan Synthesis by Interleukin-1. *Coll Relat Res* 1987; **7**: 323–332.

Legends

Figure 1: CRISPR/Cas9 knockdown of TMEM165: (a) Alignment of TMEM165 targeted sequence from wild-type and mutant ATDC5 cells. **(b)**. Detection of TMEM165 in cell lysates from wild-type and TMEM165-knockout ATDC5 cells (G1B2, G1B3, G1B4 and G1B5) using anti-TMEM165 specific antibodies. β-actin was used as loading control (n=3). (**c**) Immunofluorescence analysis of the expression of TMEM165 in ATDC5 control and TMEM165-knockout cells using antibodies against TMEM165 (green). GM130 (red) was used as a Golgi marker. The nucleus was stained with DAPI (blue). Digital images were captured with an inverted microscope, Leica DM13000.

Figure 2: GAG chain elongation is impaired in TMEM165-deficient cells: **(a)** PG anabolism evaluation in wild-type and TMEM165-knockout ATDC5 cells by measurement of the incorporation rate of [^{35}S]-sulfate into the GAG chains**. (b)** SDS-PAGE and autoradiography analysis of neosynthesized radiolabelled PG-GAG chains in wild-type and TMEM165-knockout ATDC5 cells. **(c)** Detection of decorin in conditioned medium of wild-type and TMEM165-knockout ATDC5 cells and **(d)** in wild-type and TMEM165-knockout HEK293 cells. **(e)** Detection of decorin S34A mutant lacking GAG chains in conditioned medium of wild-type and mutant ATDC5 cells**. (f)** SDS-PAGE and autoradiography analysis of neosynthesized radiolabelled GAG chains primed with 4MU-Xyl in wild-type and TMEM165-knockout ATDC5 cells**. (g)** Analysis of the sensitivity to degradation by chondroitinase ABC of GAG chains of decorin in conditioned medium of wild-type and TMEM165-knockout ATDC5 cells. **(h)** Detection of HA-syndecan 4 in cell lysates of wild-type and TMEM165-knockout ATDC5 cells transfected with HA-syndecan-4 expression vector. β-actin was used as loading control. **(i)** Immunofluorescence analysis of cell surface HS GAG chains using anti-HS specific antibodies (green) and of the expression of TMEM165 (red) in wild-type and

TMEM165-knockout ATDC5 cells. The nucleus was stained with DAPI (blue). Digital images were captured with an inverted microscope, Leica DM13000. **(j)** Fold changes of CS polymerizing enzymes CHSY1 and CHSY2, and HS polymerizing enzymes EXT1 and EXT2 in TMEM165-knockout ATDC5 cells normalized to wild-type ATDC5 cells and **(k)** in TMEM165-deficient fibroblasts normalized to fibroblast control cells**.** qPCR values were normalized for the housekeeping gene ribosomal protein S29 and are expressed as the relative expression compared with control. Data are expressed as mean ±S.D. Statistical analysis was performed with an unpaired Student's t test (*$p<0.05$; **$p<0.01$). One representative blot of three independent experiments is shown.

Figure 3: Expression of CS polymerizing enzymes or supplementation with monosaccharides did not overcome GAG elongation defects in TMEM165-deficient cells: **(a)** Detection of decorin in conditioned medium of wild-type and mutant ATDC5 cells transfected with empty vector, Myc-tagged CHSY1, HA-tagged CHSY2 or Myc-tagged CHSY1 and HA-tagged CHSY2 along with decorin expression vector. **(b)** Detection of CHSY1 and **(c)** of CHSY2 in wild-type and TMEM165-knockout ATDC5 cells. β-actin was used as loading control. **(d)** Detection of decorin in conditioned medium of wild-type and TMEM165-mutant ATDC5 cells transfected with decorin expression vector and grown in the presence or absence of xylose (1 mM) and galactose (1 mM). One representative blot of three independent experiments is shown.

Figure 4: Manganese supplementation rescue GAG elongation in TMEM165-deficient cells: **(a)** Detection of decorin in conditioned medium of wild-type and TMEM165-knockout ATDC5 cells transfected with the expression vector for decorin or **(b)** decorin S34A mutant and grown in the presence or absence of $MnCl_2$ (1 µM). **(c)** Detection of HA-tagged syndecan

4 in cell lysates of wild-type and TMEM165-knockout ATDC5 cells transfected with HA-tagged syndecan 4 expression vector and grown in the presence or absence of $MnCl_2$ (1 µM). β-actin was used as loading control. **(d**) SDS-PAGE and autoradiography of [^{35}S]-sulfate radiolabelled GAG chains primed with 4MU-Xyl in wild-type and TMEM165-mutant ATDC5 cells grown in the presence or absence of $MnCl_2$ (1 µM). One representative blot of three independent experiments is shown.

Figure 5: Phospho-CaMKIIα is activated TMEM165-deicient cells: **(a)** Immunoblot analysis of phosphor-CaMkIIα (pCaMkIIα) phosphorylation in cell lysate of wild-type and TMEM165-knockout ATDC5 cells and **(b)** in cell lysate of normal fibroblasts and TMEM165-deficient fibroblasts from CDG patients, using specific antiphospho-CaMkIIα and anti-CaMkIIα antibodies. β-actin was used as loading control (n=3).

Figure 6: TGF-β signaling pathway is impaired in TMEM165-deficient cells. (a) Detection of phosphorylated Smad2 (pSmad2) and total Smad2 (Smad2) in cell lysates from wild-type and TMEM165-knockout ATDC5 cells. **(b)** Fold changes of serpine expression in TMEM165-knockout cells normalized to wild-type ATDC5 cells. **(c)** Fold changes of TGF-β reporter activity in TMEM165-knockout cells normalized to wild-type ATDC5. **(d)** Detection of phosphorylated Smad2 (pSmad2) and total Smad2 in cell lysates from control and TMEM165-defiient CDG patient fibroblast cells. **(e)** Fold changes of serpine expression in TMEM165-deficient fibroblasts normalized to normal fibroblast cells. **(f)** Detection of p-Smad2 in cell lysates from wild-type and TMEM165-knockout ATDC5 cells and **(g)** from normal and TMEM165-deficient CDG patient fibroblast cells treated or not with TGFβ1 (1ng/ml) for 1 hour. **(h)** Fold changes of TGFβR1 and TGFβR2 expression in TMEM165-knockout ATDC5 cells normalized to wild-type ATDC5 cells. (**i**) Detection of TGFβR2 in cell lysates from wild-

type and TMEM165-mutant ATDC5. (**j**) Fold changes of TGFβR1 and TGFβR2 expression in TMEM165-deficient fibroblasts from CDG patient normalized to normal fibroblast cells. **(k)** Detection of TGFβR2 in cell lysates from normal fibroblasts and TMEM165-deficient CDG patient fibroblast cells. (**l**) Fold changes of asporin expression in TMEM165-knockout cells normalized to wild-type ATDC5 cells and in TMEM165-deficient fibroblast cells normalized to normal fibroblast cells. **(m)** Detection of asporin in conditioned medium of wild-type and TMEM165-knockout ATDC5 cells and of normal fibroblasts and TMEM165-deficient CDG patient fibrobast cells. β-actin was used as loading control. qPCR values were normalized for the housekeeping gene ribosomal protein S29 and are expressed as the relative expression compared with control. Data are expressed as mean ±S.D. Statistical analysis was performed with an unpaired Student's t test (*$p<0.05$; **$p<0.01$). One representative blot of three independent experiments is shown.

Figure 7: BMP signaling is activated in TMEM165-deficient cells. **(a)** Detection of phosphorylated Smad1, 5, 9 (pSmad1,5,9) and total Smad in cell lysates from wild-type and TMEM165-mutant ATDC5 cells and **(b)** from normal fibroblasts and TMEM165-deficient CDG patient fibroblast cells. **(c)** Fold changes of Id1 expression in TMEM165-knockout cells normalized to wild-type ATDC5 cells. **(d)** Fold changes of BMP reporter activity in TMEM165-knockout cells normalized to wild-type ATDC5 cells. **(e)** Fold changes of BMPR1A, BMPR1B and BMPR2 expression in TMEM165-knockout cells normalized to wild-type ATDC5 cells. **(f)** Detection of BMPR2 in cell lysates of wild-type and TMEM165-knockout ATDC5 cells. β-actin was used as loading control. **(g)** Fold changes of BMPR1A, BMPR1B and BMPR2 expression in TMEM165-deficient fibroblasts normalized to normal fibroblast cells. **(h)** Detection of BMPR2 in cell lysates of normal fibroblasts and TMEM165-deficient CDG patient fibroblast cells. β-actin was used as loading control. **(i)** Fold changes of

Noggin expression in TMEM165-knockout ATDC5 cells normalized to wild-type ATDC5 cells and **(j)** in TMEM165-deficient CDG patient fibroblasts normalized to normal fibroblast cells. qPCR values were normalized for the housekeeping gene ribosomal protein S29 and are expressed as the relative expression compared with control. Data are expressed as mean ± S.D. Statistical analysis was performed with an unpaired Student's t test (*$p<0.05$; **$p<0.01$).

Figure 8: Cell proliferation is increased TMEM165-deicient cells: **(a)** Fold changes in proliferation of TMEM165-knockout cells normalized to wild-type ATDC5 cells and of TMEM165-deficeint fibroblasts normalized to normal fibroblast control. **(b**) Detection of phosphorylated ERK1/2 (pERK1/2) and total ERK1/2 (ERK1/2) in cell lysates of wild-type and TMEM165-knockout ATDC5 and in cell lysates of normal fibroblasts and TMEM165-deficient CDG patient fibroblast cells. β-actin was used as loading control. One representative blot of three independent experiments is shown.

Figure 9: Early hypertrophic differentiation of TMEM165-deficient ATDC5 cells: **(a)** Fold changes of chondrogenic markers expression in wild-type ATDC5 cells and TMEM165-knockout cells. RT-qPCR analysis of the mRNA levels of chondrogenic markers SOX9, Col2A and Aggrecan, and **(b)** of hypertrophic markers IHH-Indian hedgehog and OCN-osteocalcin. qPCR values were normalized for the housekeeping gene ribosomal protein S29 and are expressed as the relative expression compared with control. Data are expressed as mean ± S.D. Statistical analysis was performed with an unpaired Student's t test (*$p<0.05$; **$p<0.01$).

Abstract

Congenital Disorders of Glycosylation (CDG) is a group of human genetic disorders with defects in biosynthesis (glycosylation) of glycoproteins. Recent studies have discovered TMEM 165 as a novel protein deficient in CDG patients presenting bone abnormalities, suggesting a role of TMEM 165 in chondrogenesis and skeletal development. Proteoglycans (PGs) play a key role in several biological processes including chondrocytes maturation, growth plate development and intracellular signaling. Alterations in the synthesis of PGs may contribute to skeletal defects observed in TMEM 165-deficient CDG patients. To determine the link, if any, between TMEM165 deficiency and the synthesis of PGs, and to study the molecular mechanisms involved, we generated TMEM165 knock-out pre-chondrogenic ATDC5 cells using CRISPR/Cas9 technique. Interestingly, we showed that the knockdown of TMEM165 in ATDC5 cells resulted in profound defects in the synthesis of PGs and mainly impaired polymerization of both heparin-sulfate and chondroitin-sulfate glycosaminoglycan chains. Furthermore, we found that these defects can be overcome by supplying the cells with Mn^{2+}. Similar results were observed in fibroblast cells from TMEM165-deficient CDG patient. These data suggest that TMEM165 is involved in the regulation of the homeostasis of Mn^{2+} which is used as a co-factor of Golgi glycosyltransferases and required for full enzyme activity. On the other hand, PGs play a key role in the regulation of TGFβ and BMP signaling. Given that these pathways regulate chondrogenesis and skeletal development their integrity was evaluated in TMEM 165-deficient ATDC5 cells and fibroblast from CDG patients. We demonstrated that TMEM165-deficiency functionally impairs TGFβ and BMP signaling pathways in both ATDC5 cells and human fibroblasts, suggesting a role in skeletal abnormalities observed in TMEM165-deficeint CDG patients. In addition, *in vitro* differentiation study of ATDC5 cells revealed that loss of TMEM165 expression promotes differentiation of ATDC5 cells towards hypertrophy, a process which may lead to premature chondrocyte maturation and to dwarfism observed in TMEM165-deficient CDG patients.

Keywords: TMEM165, congenital disorders of glycosylation, chondrocytes, proteoglycans, skeletal development.

Résumé

Les troubles congénitaux de la glycosylation (CDG) sont un groupe de troubles génétiques lié aux anomalies de glycosylation des glycoprotéines. Des études récentes ont identifié TMEM165 comme étant une nouvelle protéine déficiente chez les patients CDG présentant des anomalies ostéoarticulaires importantes, suggérant un rôle de TMEM165 dans la chondrogénèse et le développement squelettique. D'autre part, les protéoglycanes (PGs) jouent un rôle clé dans plusieurs processus biologiques, notamment la maturation chondrocytaire, le développement de la plaque de croissance et la signalisation cellulaire. Afin de déterminer s'il existe un lien potentiel entre le déficit en TMEM165 et la synthèse des PGs et identifier les mécanismes moléculaires impliqués, nous avons invalidé le gène TMEM165 dans les cellules pré-chondrocytaires ATDC5 en utilisant la technique CRISPR/Cas9. De façon intéressante, nous avons montré que l'invalidation du gène TMEM165 entraîne des anomalies de synthèse des PGs et principalement un déficit de polymérisation des chaînes de glycosaminoglycanes de type héparine-sulfate et chondroïtine-sulfate. De plus, nous avons montré que ces anomalies de synthèse peuvent être palliées par la supplémentation des cellules en ions Mn2+. Des résultats similaires ont été obtenus dans les fibroblastes de patient déficient en TMEM165. Ceci suggère que TMEM165 est impliqué dans la régulation de l'homéostasie du Mn2+, co-facteur requis pour une activité optimale des glycosyltransférases dans le Golgi. D'autre part, les PGs jouent un rôle clé dans la régulation de la signalisation du TGFβ et de la BMP. Étant donné que ces voies régulent la chondrogénèse et le développement squelettique, leur intégrité a été évaluée dans les cellules ATDC5 déficientes en TMEM 165 et les fibroblastes de patients CDG. Les résultats obtenus ont permis de montrer que la déficience en TMEM165 perturbe le fonctionnement des voies de signalisation du TGFβ et de la BMP dans les cellules ATDC5 et les fibroblastes humains mutés, suggérant un rôle dans les anomalies squelettiques observées chez les patients CDG déficients en TMEM165. De plus, l'étude de la différenciation in vitro des cellules ATDC5 a permis de révéler que la déficience en TMEM165 accélère la différenciation des cellules ATDC5 vers l'hypertrophie, un processus qui peut conduire à la maturation précoce des chondrocytes et au nanisme observé chez les patients CDG déficients en TMEM165.

Mots clés : TMEM165, troubles congénitaux de la glycosylation, chondrocytes, protéoglycanes, développement ostéoarticulaire